Anti-inflammatory and Anti-proliferative Diterpenes from *Croton stellatopilosus* Ohba

Charoenwong Premprasert

A Thesis Submitted in Fulfillment of the Requirements for the Degree of Doctor of Philosophy in Pharmaceutical Sciences

Prince of Songkla University

2019

Copyright of Prince of Songkla University

Anti-inflammatory and Anti-proliferative Diterpenes from *Croton stellatopilosus* Ohba

Charoenwong Premprasert

A Thesis Submitted in Fulfillment of the Requirements for the Degree of Doctor of Philosophy in Pharmaceutical Sciences

Prince of Songkla University

2019

Copyright of Prince of Songkla University

Thesis Title Anti-inflammatory and Anti-proliferative Diterpenes from *Croton stellatopilosus* Ohba

Author Mr. Charoenwong Premprasert

Major **Program** Pharmaceutical Sciences

Major Advisor

.....

(Assoc. Prof. Dr. Juraithip Wungsintaweekul)

Co-advisor

.....

(Assoc. Prof. Dr. Supinya Tewtrakul)

Examining Committee :

.....Chairperson

(Prof. Dr. Kittisak Likhitwitayawuid)

.....Committee

(Assoc. Prof. Dr. Juraithip Wungsintaweekul)

.....Committee

(Assoc. Prof. Dr. Supinya Tewtrakul)

.....Committee

(Asst. Prof. Dr. Sukanya Dej-adisai)

The Graduate School, Prince of Songkla University, has approved this thesis as fulfillment of the requirements for the Doctor of Philosophy Degree in Pharmaceutical Sciences.

.....

(Prof. Dr. Damrongsak Faroongsarng)

Dean of Graduate School

This is to certify that the work here submitted is the result of the candidate's own investigations. Due acknowledgement has been made of any assistance received.

……..Signature

(Assoc. Prof. Dr. Juraithip Wungsintaweekul)

Major Advisor

……..Signature

(Assoc. Prof. Dr. Supinya Tewtrakul)

Co-advisor

……..Signature

(Mr. Charoenwong Premprasert)

Candidate

I hereby certify that this work has not been accepted in substance for any degree, and is not being currently submitted in candidature for any degree.

.....Signature

(Mr. Charoenwong Premprasert)

Candidate

ชื่อวิทยานิพนธ์	สารไดเทอร์ปีนที่มีฤทธิ์ต้านอักเสบและยับยั้งการเจริญของเซลล์จากเปล้าน้อย
ผู้เขียน	นาย เจริญวงค์ เปรมประเสริฐ
สาขาวิชา	เภสัชศาสตร์
ปีการศึกษา	2561

บทคัดย่อ

สารอะไซคลิกไดเทอร์ปีนจำนวน 1 ชนิด (เปลาโนทอล) และสารไซคลิกไดเทอร์ปีนจำนวน 3 ชนิด (เปลานอล เอ, เปลานอล อี และเปลานอล เอฟ) แยกได้จากใบและลำต้นเปล้าน้อย เทคนิคทางสเปคโตรสโคปี เช่น UV, IR, MS, ^{1}H-NMR และ ^{13}C-NMR ถูกนำมาใช้ในการศึกษาคุณลักษณะทางกายภาพและตรวจหาโครงสร้างของสารทั้งสี่ชนิด

ในการศึกษาศักยภาพของสารเปลานอล เอ ในการเป็นสารต้านอักเสบ ทำในเซลล์แมคโครฟาจ RAW264.7 ที่ผ่านการเหนี่ยวนำให้อักเสบด้วยสารไลโปโพลีแซคคาไลด์ ผลการทดลองพบว่าสารเปลานอล เอ มีฤทธิ์ยับยั้งการหลั่งไนตริกออกไซด์มีค่าความเข้มข้นของสารที่ยับยั้งที่ 50 เปอร์เซนต์ หรือ IC_{50} ที่ 11.69 ไมโครโมลาร์ เมื่อทดสอบความเป็นพิษต่อเซลล์โดยการย้อมด้วยสาร MTT พบว่าสารเปลานอล เอ มีความเป็นพิษต่อเซลล์ ที่ความเข้มข้นมากกว่า 30 ไมโครโมลาร์ และเมื่อศึกษาผลของเปลานอล เอ ต่อยีนที่เกี่ยวข้องกับกระบวนการอักเสบสองชนิด คือ อินดิวซิเบิล ไนตริกออกไซด์ ซินเทส และไซโคลออกซิจีเนส-2 ด้วยวิธี qRT-PCR ผลการทดลองสรุปได้ว่าสารเปลานอล เอ ยับยั้งการสร้างไนตริกออกไซด์ และมีคุณสมบัติต้านอักเสบโดยการยับยั้งการแสดงออกของยีนทั้งสองชนิด

นำสารไดเทอร์ปีนทั้ง 4 ชนิด คือ เปลาโนทอล, เปลานอล เอ, เปลานอล อี และ เปลานอล เอฟ มาศึกษาฤทธิ์ยับยั้งการแบ่งตัวของเซลล์มะเร็งที่แยกได้จากมนุษย์ ได้แก่ เซลล์ HeLa, HT-29, MCF-7 และ KB ด้วยวิธีการย้อมด้วยสาร MTT ผลการทดลองพบว่าสารเปลาโนทอล, เปลานอล เอ, และเปลานอล อี มีความเป็นพิษต่อเซลล์และยับยั้งการแบ่งตัวของเซลล์ที่ทดสอบทั้ง 4 ชนิด มีค่า

IC_{50} ช่วงระหว่าง 60-80 ไมโครโมลาร์ ในขณะที่สารเปลานอล เอฟ ไม่มีความเป็นพิษต่อเซลล์ และเมื่อทดสอบสารทั้ง 4 ชนิดในเซลล์ปกติชนิดจิงไจวอล ไฟโปรบลาส ไม่พบความเป็นพิษต่อเซลล์ที่ความเข้มข้นมากกว่า 100 ไมโครโมลาร์ และเมื่อศึกษาผลของไดเทอร์ปีนต่อวงจรการแบ่งตัวของเซลล์ พบว่าสารเปลาโนทอล ที่ความเข้มข้น 75 ไมโครโมลาร์ มีผลต่อการแบ่งตัวของเซลล์ในระยะ G0/G1 ของเซลล์ HeLa ระยะ S ของเซลล์ MCF-7 และระยะ G2/M ของเซลล์ HT-29 และเซลล์ KB สำหรับสารเปลานอล เอ ที่ความเข้มข้น 75 ไมโครโมลาร์ มีผลต่อเซลล์ในระยะ G2/M ในเซลล์ HeLa, HT-29 และ KB และระยะ S ใน MCF-7 ส่วนสารเปลานอล อี มีผลต่อการแบ่งเซลล์ของเซลล์ในระยะ G2/M ในเซลล์ทดสอบทุกชนิด และเมื่อประเมินผลของสารไดเทอร์ปีนต่อโปรแกรมการตายของเซลล์ หรืออะพอพโตซีส โดยการย้อมด้วยสาร annexin-V/7-AAD และตรวจวัดด้วยโฟลไซโตมิเตอร์ ผลการทดสอบพบว่าสารเปลาโนทอล, เปลานอล เอ และเปลานอล อี เหนี่ยวนำให้เซลล์ตายในทุกชนิดของเซลล์ที่ทดสอบ นอกจากนี้ยังพบว่าสารเปลานอล อี สามารถเหนี่ยวนำให้เซลล์ตายได้ดีกว่าสารเปลาโนทอล และเปลานอล เอ ตามลำดับ

ต่อมาศึกษาผลของสารเปลาโนทอล และสารเปลานอล อี ต่อระดับการแสดงออกของยีนที่เกี่ยวข้องกับการตายของเซลล์ ได้แก่ *TNF-*α, *BCL-2*, *BAK* และ *BAX* ด้วยวิธี qRT-PCR ที่ความเข้มข้นของสารเปลาโนทอล 50 ไมโครโมลาร์ และ 75 ไมโครโมลาร์ สารเปลาโนทอลยับยั้งยีน *TNF-*α และ *BCL-2* แต่ไม่มีผลต่อยีน *BAK* และ *BAX* ในเซลล์ชนิด HeLa, HT-29 และ MCF-7 แต่ในเซลล์ชนิด KB สารเปลาโนทอลสามารถยับยั้งการแสดงออกของยีนทั้ง 4 ชนิด เมื่อคำนวณอัตราส่วนการแสดงออกของยีน *BCL-2* และ *BAX* ที่บ่งบอกดัชนีของการทำให้เซลล์ตาย พบว่าอัตราส่วนของยีนดังกล่าวมีระดับการแสดงออกที่ลดลงในทุกชนิดของเซลล์ที่ทดสอบ ซึ่งแสดงให้เห็นว่าสารเปลาโนทอลมีกลไกยับยั้งการแบ่งตัวของเซลล์ผ่านกลไกโปรแกรมการตายของเซลล์โดยยับยั้งยีนที่เกี่ยวข้องในกระบวนการส่งสัญญาณการตาย ส่วนสารเปลานอล อี ไม่มีผลต่อระดับการแสดงออกของยีนทั้ง 4 ชนิดในเซลล์ชนิด HeLa, HT-29 และ KB แต่กลับยับยั้งยีนทั้ง 4 ชนิดในเซลล์ชนิด MCF-7 แสดงให้เห็นว่าสารเปลานอล อี มีกลไกการยับยั้งการแบ่งตัวของเซลล์แตกต่างจากสารเปลาโนทอล และเมื่อทดสอบผลของสารเปลานอล อี ต่อเอนไซม์คาสเปสชนิด -3, -8, และ -9 ในเซลล์ชนิด MCF-7 กลับพบว่าสารเปลานอล อี กระตุ้นการทำงานของเอนไซม์คาสเปส -3, -8 และ -

9 เป็น 2.67, 6.33 และ 5.33 เท่าตามลำดับเมื่อเทียบกับกลุ่มควบคุม จึงสรุปว่ากลไกการทำให้เซลล์ตายของสารเปลานอล อี ผ่านการกระตุ้นการทำงานของเอนไซม์คาสเปสทั้ง 3 ชนิด

จากผลการทดลองทั้งหมด สรุปได้ว่าสารเปลานอล เอ มีฤทธิ์ต้านอักเสบในเซลล์ RAW264.7 โดยยับยั้งยีนที่เกี่ยวข้องกับการอักเสบ *iNOS* และ *COX-2* โดยมีกลไกยับยั้งการอักเสบเช่นเดียวกับสารเปลาโนทอลและเปลานอล เอฟ การศึกษานี้ยังได้แสดงให้เห็นว่าสารไดเทอร์ปีนที่ทดสอบคือ สารเปลาโนทอล, เปลานอล เอ และเปลานอลอี มีแนวโน้มยับยั้งการแบ่งตัวของเซลล์ในเซลล์มะเร็งที่ทดสอบทั้ง 4 ชนิด ผลการทดลองสรุปได้ว่าสารเปลาโนทอล และเปลานอล อี มีคุณสมบัติยับยั้งการแบ่งตัวของเซลล์โดยเหนี่ยวนำให้เกิดเซลล์ตายหรืออะพอพโตซีส แสดงให้เห็นว่าสารทั้งสองชนิดมีแนวโน้มที่จะถูกพัฒนาไปเป็นยาต้านมะเร็งต่อไป

Thesis Title	Anti-inflammatory and anti-proliferative diterpenes from *Croton stellatopilosus* Ohba
Author	Mr. Charoenwong Premprasert
Major Program	Pharmaceutical Sciences
Academic Year	2018

ABSTRACT

One acyclic diterpene [plaunotol] and three cyclic diterpenes [plaunol A, plaunol E and plaunol F] were isolated from leaves and stems of *Croton stellatopilosus* Ohba [Euphorbiaceae]. Their physical properties and structures were determined by means of UV, IR, MS, ^{1}H-NMR and ^{13}C-NMR spectroscopies.

Anti-inflammatory potential using cell-based assay in lipopolysaccharide-induced murine macrophage RAW264.7 cells of plaunol A was evaluated. It exhibited inhibitory activity on nitric oxide (NO) production with an IC_{50} of 11.69 μM. The MTT assay indicated the cytotoxic effect at concentration $>$ 30 μM of plaunol A. Transcription profile analysis of inducible nitric oxide synthase (*iNOS*) and cyclooxygenase-2 (*COX-2*) genes in the RAW264.7 cells using qRT-PCR technique revealed that plaunol A inhibited the NO production by suppressing the *iNOS* and *COX-2* mRNAs.

Anti-proliferative activity of plaunotol, plaunol A, plaunol E and plaunol F against the four human cancer cells including HeLa, HT-29, MCF-7 and KB cells was investigated using the MTT assay. Plaunotol, plaunol A and plaunol E exhibited the cytotoxicity in types of cancer cells with the IC_{50} ranging from 60-80 μM while plaunol F did not. No cytotoxic effect in human gingival fibroblast (HGF) cells (normal cell) was observed at concentration > 100 μM. Determination the effect of diterpenes on cell cycle was performed using Muse™ cell cycle reagent. At concentration

of plaunotol 75 μM induced the cell cycle arrest at G0/G1 phase of HeLa, S phase of MCF-7 and G2/M phase of HT-29 and KB cells. At concentration of 75 μM plaunol A induced the cell cycle arrest at G2/M phase in HeLa, HT-29 and KB cells and S phase in MCF-7, while plaunol E did at G2/M phase in all types of cells. These results suggested that plaunotol, plaunol A and plaunol E performed moderate cytotoxic effect by causing cell cycle arrest during cell division. Potential on apoptosis of diterpenes using double staining of Muse™ annexin-V/7-AAD following flow cytometry was investigated. At concentrations of 75 μM and 150 μM, plaunotol, plaunol A and plaunol E caused apoptosis in all types of cancer cells. The results suggested that plaunol E has higher potency on apoptosis than plaunotol and plaunol A, respectively.

Effect of plaunotol and plaunol E on apoptotic-associated genes such as *TNF-α*, *BCL-2*, *BAK* and *BAX* using qRT-PCR was determined. Plaunotol at concentrations of 50 μM and 75 μM suppressed *TNF-α* and *BCL-2*, but not *BAK* and *BAX* genes in HeLa, HT-29 and MCF-7 cells. Plaunotol inhibited all genes mRNA in KB cells. The ratio of *BCL-2/BAX* that indicted the involvement of those genes on apoptosis, revealed the mechanism of plaunotol. The reduction of ratio observed in all types of cells. This result indicated plaunotol performed apoptosis via death signaling and mitochondrial dependent pathway. Plaunol E has no effect on *TNF-α*, *BCL-2*, *BAK* and *BAX* mRNA levels in HeLa, HT-29 and KB cells. In contrast, it suppressed the genes expressions in MCF-7. Effect of plaunol E on caspase-3, -8 and -9 in MCF-7 was investigated. It enhanced caspase-3, -8 and -9 with 2.67, 6.33 and 5.33 fold, respectively. Thus, plaunol E caused apoptosis by activation of caspases.

In conclusion, plaunol A performed anti-inflammatory activity by suppressed *iNOS* and *COX-2* genes in RAW264.7 cells in the similar manner of plaunotol and plaunol F. The present study illustrated the potential of plaunotol, plaunol A and plaunol E on anti-proliferative activity in four types of human cancer cell lines. The results suggested that plaunotol and plaunol E have affected on apoptosis induction and they exhibited a potential for further anti-cancer development.

ACKNOWLEDGEMENTS

There are many people that I would like to thank for supports during my Ph.D. study.

First of all, I wish to express my deepest and grateful thanks to Associate Professor Dr. Juraithip Wungsintaweekul, my advisor and Associate Professor Dr. Supinya Tewtrakul, my co-advisor for the opportunity to return to Pharmaceutical Sciences in Ph. D. I also thank for their helpful guidance, suggestion and encouragement throughout the course. My sincere thanks are expressed to Associate Professor Dr. Anuchit Plubrukarn, for his advice about the structure elucidation.

This research would not have been successful without the support from the Department of Pharmacognosy and Pharmaceutical Botany, Department of Pharmaceutical Chemistry, Pharmaceutical Laboratory Service Center (PLSC), Faculty of Pharmaceutical Sciences, and Scientific Equipment Center (SEC), Prince of Songkla University.

I have a special thanks to Mr. Anan Chaikitwattana from Tipco Biotech Co., Ltd., for kindly support Plaunoi samples and Dr.Nachanun Sirimangkalakitti for the optical rotation measurement at Chulalongkorn University.

I would like to thank a financial support by grants from the Thailand Research Fund through Golden Jubilee PHD Program (Grant No. PHD/071/2553). Grants from the Prince of Songkla University, the Government Annual Budget (Grant No. PHA580237S) and the Graduate School are also acknowledged.

Finally, I also appreciate the mortal support from my family, especially my parents and my best friends, who always are there for me, when I have some questions and some problems. I deeply thank to their encouragements to finally get where I am today.

Good times become good memories; Bad times become good lesson……...Thank you all.

Charoenwong Premprasert

CONTENTS

CONTENTS (CONTINUED)

CONTENTS (CONTINUED)

CONTENTS (CONTINUED)

CONTENTS (CONTINUED)

Page

LIST OF TABLES

LIST OF FIGURES

LIST OF FIGURES (CONTINUED)

LIST OF SCHEMES

LIST OF ABBREVIATIONS AND SYMBOLS

7-AAD	7-Aminoactinomycin D
ANOVA	Analysis of variance
BAX	BCL-2-associated X protein
BAK	BCL-2 homologous antagonist/killer
BCL-2	B-cell lymphoma-2
bp	Base pair
br	Broad signals for NMR spectrum
BSA	Bovine serum albumin
CAPE	Caffeic phenethyl ester
cDNA	Complementary deoxyribonucleic acid
cm	Centimeter
COX	Cyclooxygenase
COSY	Correlation spectroscopy
C_T	Threshold cycle
Cq	Cycle of quantification/qualification
cyt c	Cytochrome c
DEPT	Distortion less enhancement by polarization transfer
DNA	Deoxyribonucleic acid
dNTP	Deoxynucleotide triphosphate
DMEM	Dulbecco's Modified Eagle's Medium
DMSO	Dimethyl sulfoxide
DTT	Dithiothreitol
EDTA	Ethylenediaminetetraacetic acid

LIST OF ABBREVIATIONS AND SYMBOLS (CONTINUED)

EIMS	Electron-impact mass spectroscopy
FBS	Fetal bovine serum
EtBr	Ethidium bromide
g, kg, mg	Gram, kilogram, milligram
GAPDH	Glyceraldehyde-3-phosphate dehydrogenase
GC content	Guanine-cytosine content
HMBC	Heteronuclear multiple bond correlation
HMQC	Heteronuclear multiple-quantum coherence
IC_{50}	50% inhibitory concentration
IDM	Indomethacin
iNOS	Inducible nitric oxide synthase
IR	Infrared
J	Coupling constant (for signal of NMR)
l, ml	Liter, milliliter
L-NA	L-nitroarginine
LPS	Lipopolysaccharide
M, mM	Molar, millimolar of solution
MTT	3-(4,5-Dimethyl-2-thiazolyl)-2, 5-diphenyl-2H-tetrazolium bromide
m/z	Mass-over-charge ratio
mRNA	Messenger ribonucleic acid
MS	Mass spectroscopy
N.	Normality of solution
NCBI	National Center Biotechnology Information
NCI	National Cancer Institute

LIST OF ABBREVIATIONS AND SYMBOLS (CONTINUED)

NMR	Nuclear magnetic resonance
OD	Optical density
p	*p*-value (for statistical)
PBS	Phosphate buffer saline
PCR	Polymerase chain reaction
PI	Propidium iodide
PS	Phosphatidyl serine
pH	Potential of hydrogen (-log hydrogen concentration)
qRT-PCR	Quantitative real-time polymerase chain reaction
RNA	Ribonucleic acid
RQ	Relative quantitation
rpm	Round per minute
RPMI	Roswell Park Memorial Institute
s, d, t, m	Singlet, doublet, triplet, multiplet (The signal for NMR spectrum)
S.D.	Standard deviation
SDS	Sodium dodecyl sulfate
s, min, h	Second, minute, hour
S.E.M.	Standard error of mean
TAE	Tris-Acetate-EDTA
TNF-α	Tumor necrosis factor-α
T_m	Melting temperature
TLC	Thin layer chromatography
UV-VIS	Ultraviolet-visible

LIST OF ABBREVIATIONS AND SYMBOLS (CONTINUED)

v/v	Volume by volume
w/v	Weight by volume
w/w	Weight by weight
WHO	World health organization
Δ	Delta
ΔRn	Fluorescence signal with baseline subtracted
δ	Chemical shift in ppm
γ_{max}	Maximum wavelength
ν	Wave number
°C	Degree of Celsius
µl	Microliter
µM	Micromolar
%	Percentage
×g	Relative centrifugal force (RCF)

CHAPTER 1

INTRODUCTION

1.1 Background and rationale

Croton stellatopilosus Ohba is locally known as plaunoi (เปล้าน้อย) in Thai and it is a tropical plant belongs to family of Euphorbiaceae. Plaunoi is formerly known as *C. sublyratus* Kurz (Esser and Chayamarit, 2001). For the traditional used, several parts such as stem, bark, leaf and flower have been used as an antihelminthic for treatment of skin diseases (Ponglux, *et al*., 1987). Additionally, *C. stellatopilosus* has been reported various purposes such as stomachic, anthelminthic, digestant and tranquilizer when combined together with plauyai (*C. oblongifolius* Roxb.) that has been used for lymphatic and tumor (Bunyapraphatsara, 1989). Since 1978, plaunoi has been studied on phytochemical investigation by Ogiso and his co-workers and they have found a major compound was named as plaunotol (Ogiso *et al*., 1978). Plaunotol was isolated from acetone extract of stems and was further demonstrated on *in vivo* experiments for anti-peptic ulcer activity such as anti-shay ulcer activity in rat and reserpine-induced in mice (Ogiso *et al*., 1978). Additionally, the structure of plaunotol was proposed to acyclic diterpene alcohol and was identified to be (*E*, *Z*, *E*)-7-hydroxymethyl-3,11,15-trimethyl-2,6,10,14-hexadecatetraen-1-ol as an IUPAC name (Ogiso *et al*., 1978). Due to the chemical constituents, not only plaunotol has been isolated from *C. stellatopilosus*, but also several diterpenes were isolated including furanoditerpene lactone (clerodane type) diterpenes were named as plaunol A, plaunol B, plaunol C, plaunol D and plaunol E (Kitazawa *et al*., 1979; Kitazawa *et al*., 1980) and plaunol F (Takahashi *et al*., 1983). Other diterpenes were labdane type, ent-13α-hydroxy-13-epimanool and kaurane type, ent-16β, 17-dihydroxykaurane (Kitazawa and Ogiso, 1981). Furthermore, derivatives of plaunotol are also isolated from plaunoi; 18-hydroxygeranylgeraniol ester A-F (Kitazawa *et al*., 1982).

As mention earlier, plaunotol has been isolated and evaluated for anti-shay ulcer activity since 1978. Plaunotol was successfully registered to World Health Organization (WHO) under the name of "CS-684" and was further manufactured in the form of a soft gelatin capsule combining with corn oil under a trade name of Kelnac™(Daiichi Sankyo Co., Ltd., Tokyo, Japan) (Ogiso *et al*., 1985). The pharmacological activities of plaunotol were widely investigated for gastroprotective activity (Ogiso *et al*., 1985; Ushiyama *et al*., 1987; Shiratori *et al*., 1993), antibacterial activity (Koga *et al*., 1996; Koga *et al*., 1998; Sasaki *et al*., 2007), anti-inflammatory activity (Murakami *et al*., 1999; Takagi *et al*., 2000; Fu *et al*., 2005; Premprasert *et al*., 2013), anticancer activity (Kawai *et al*., 2005; Yamada *et al*., 2007; Yoshikawa *et al*., 2009) and wound healing activity (Khovidhunvit *et al*., 2011). Its pharmacokinetic was studied and reported in both animal and human models (Ogiso *et al*., 1985). The safety of administered plaunotol and partially purified was evaluated in animal model and revealed that they can be used as anti-gastric ulcer with safety in acute-, subchronic- and chronic-toxicities experiments (Ogiso *et al*., 1985; Chaotham *et al*., 2013). It is quite clear that plaunotol is appropriate to develop and ready to use in clinic. However, the several diterpenes from plaunoi have been rarely reported about biological and pharmacological activities. The plaunol derivatives such as plaunol A-E have been only evaluated on anti-shay ulcer activity. Their results showed that plaunol B, C, D and E exhibited the inhibitory activity with less potency than plaunotol. In contrast, plaunol A did not (Kitazawa *et al*., 1979; Kitazawa *et al*., 1980).

Recently, plaunotol, plaunol E and plaunol F have been evaluated on anti-inflammatory activity. These results indicated that diterpene compounds showed effectiveness against NO production on LPS-induced-RAW264.7 macrophage cells. Beside experiments, the cytotoxicity also determined and these results suggested that diterpenes from plaunoi showed cytotoxic effect in RAW264.7 cells. Therefore diterpenes from *C.stellatopilosus* was proposed to inhibit the growth of cancer cells (Premprasert *et al*., 2013).

Cancer is continuously remaining a main problem that causes people morbidity and mortality around the world. Cancer is the uncontrolled cells developing from the normal cells (Cooper 2000). The cancer regulation can be controlled by cell proliferation and cell death. Both processes are crucial role in the animal cells development and homeostasis (Zhivotosky and Orrenius, 2010). For cell proliferation, the cells normally undergo to the cell cycle progression for cell dividing and cell growth. These process is mainly classified into four phase following G0/G1 phase (resting stage), G1 phase (before DNA synthesis), S phase (during DNA synthesis) and G2/M (cell dividing), respectively (Duronio and Xiong, 2013). Cell death as known as programmed cell death is the reserved mechanism in the multicellular organisms for removes the unwanted cells (Pucci *et al*., 2000).

Apoptosis is one type of programmed cell death and it is the important process that cells use to commit suicide themselves (Pucci *et al*., 2000). In the fundamental, cells undergo to apoptosis have morphological change including cell shrinkage nuclear chromatin condensation, and DNA fragmentation. During apoptosis, cells also have biochemical changes in the plasma membrane, especially the change of phosphatidylserine (PS), (Hacker, 2000). PS is normally located in the inner leaflet of plasma membrane and it is located to outer of plasma membrane after cells are going to apoptosis (Bratton *et al*., 1997).

Focusing to apoptosis pathways as shown in Fig. 1.1, cells basically use at least two pathways including death signaling/NF-κB (extrinsic) and mitochondrial dependent (intrinsic) pathways. Both pathways can activate the pro-caspase into activated caspase. The extrinsic pathway is regulated by the extracellular ligand such as tumor necrosis factor (TNF) and it activates to caspase-8 (Ashkenzi and Dixit 1998). In contrast, intrinsic pathway is occurred in mitochondrion that is triggered by intermolecular such as stressed cells (Parrish *et al*., 2013). This pathway involves the releasing of cytochrome complex (cyt c). The cyt c binds to apoptotic activating factor-1 (Apaf-1) to assembly of a heptameric Apaf-1 apoptosome (Yuan and Akey, 2013). Then, the assembly of Apaf-1 apoptosome activates caspase-9 activation (Hill *et al*., 2004). Additionally, the

caspase-8 and caspase-9 generating from both pathways activate caspase-3 and cells undergo to apoptosis (Albert *et al*, 2000; Jain *et al*., 2013).

Consideration on apoptotic pathways, both pathways normally is controlled by the members of BCL-2 (B-cell lymphoma-2) family regulator proteins (Cory and Adam, 2002). The regulator proteins can be classified into two groups following pro-apoptotic and anti-apoptotic regulators. Pro-apoptotic regulators induce the releasing of the cyt c and then promote apoptosis, BAX (BCL-2-associated X protein) and BAK (BCL-2 homologous antagonist/killer) for example. In the contrast, anti-apoptotic regulator such as BCL-2 inhibits the enhancing of apoptosis by inhibiting the releasing of cyt c or blocking BAX translocation (Albert *et al*, 2000; Schuler and Green, 2001).

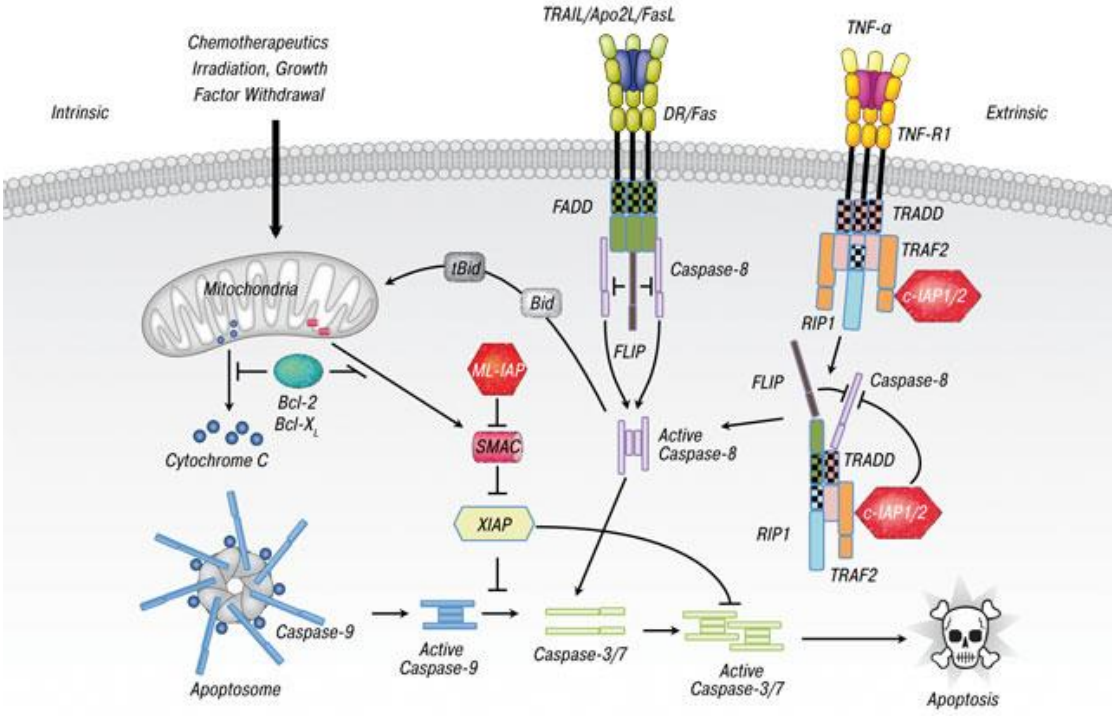

Figure 1.1 The intrinsic and extrinsic apoptotic pathways (Almagro and Vucic, 2012).

Consideration to cancer, the number of cancer cases is projected by WHO and the information about world cancer statistics for the most common cancers was estimated to rise from 14 million cases to 24 million cases in 2035 (Stewart and Chistopher, 2014). The most common cancers are diagnosed such as lung (13.0% of total cancers), breast (11.9%), colorectum (9.7%), cervix uteri (3.7%) and oral cavity (2.1%). This incident rates of cancers also found in Thailand (Imsamran, *et al*., 2015). Interestingly, the several types of cancer cells are generally developed from normal cells and cancer cells are common characteristic such as abnormal signal transduction resulting to over of cell proliferation, lack of apoptosis or programmed cell death, tissue invasion and metastasis permitting spread of cancer and angiogenesis leading for enhance blood supply of tumor (Cooper, 2000; Sonnenshein and Soto, 2013). In fact, the cell proliferation and cell death is balance in a normal cell. However, this balance also changes in uncontrolled cell. According to hallmark of cancers, more than 50% of that cells lack of tumor suppressor P53 and inhibit apoptotic pathways, so these effects to the result of uncontrolled cell proliferation (Zilfou and Lowe, 2009; Rivlin *et al*., 2011). These evidences suggested that the number of cancer cells is controlled by apoptosis and cell cycle progression.

The natural product deriving from plants, organism and marine has an important role as an alternative medicine, nowadays. Anti-cancer drugs such as paclitaxel, vincristine, vinblastine, vindesine, vinorelbine, etoposide, topotecan, irinotecan and etc., are from plants and these drugs have been isolated and evaluated on anti-cancer activity. Furthermore, these drugs have also approved by FDA. Up to date, the anti-cancer substance both from natural sources and synthesis have been discovered and approved since 1981. Among of these drugs, half of them are either from natural sources or its derivatives (Newman and Cragg, 2014).

With an attempt to conduct a research on *C. stellatopilosus*, plaunotol and others cyclic diterpenes have not been evaluated on anti-proliferative activity in human cancer cell lines including human breast carcinoma cell line (MCF-7), human cervical carcinoma cell line (KB), human cervix adenocarcinoma cell line (HeLa) and human colon adenocarcinoma (HT-29) and the

mechanisms including cell cycle and apoptotic effects of these compounds also have not been reported so far. In the present study, diterpenes are isolated and purified from *C. stellatopilosus* leaves and stems using chromatography. Anti-proliferative activity, four cancer cell lines are assessed using MTT assay, whereas human gingival cell line (HGF) is used as a normal cell line. As we interest in anticancer activity via cell cycle and apoptosis, the effects of diterpenes on cell cycle and apoptotic cells are determined. Due to apoptotic pathways, either induction or inhibition of apoptotic-associated genes and caspase activity are investigated using qRT-PCR and colorimetric method, respectively. Furthermore, anti-inflammatory activity is evaluated by using cell based assay. The inhibitory activity on nitric oxide (NO) production when LPS (lipopolysaccharide)-induced RAW 264.7 macrophage cells is investigated using Griess assay. The mRNA expression of *iNOS* and *COX-2* are investigated.

1.2 Objectives

(1) To isolate and elucidate the structures of diterpenes from *C. stellatopilosus*.

(2) To evaluate anti-proliferative activity of diterpenes in human cancer cell lines and their mechanisms on cell cycle and apoptosis.

(3) To evaluate an anti-inflammatory activity of diterpene in macrophage RAW264.7 cells and the mechanism on inflammatory mediators.

1.3 Signaling pathway-associated cancer

The signal transduction is a basic mechanism about cell communication. The cell is communicated such as cell-cell interaction and cell-environment interaction by which sending and receiving intermolecular signals. The signal transduction as known as cell signaling, a cell is highly responsive to the specific molecules including physical, chemical, protein, hormone, growth factor, and neurotransmitter to other cells (Lodish *et al*., 2000) so as to changes in its immediate environment and goals to cell behavior (metabolism, movement, proliferation and development, death) (Gehringer, 2010).

Cells originally have a transmembrane protein that is attached on the cell surface so called cell-surface receptor (Albert *et al*., 2002). The extracellular signaling molecule (ligand) binds to the membrane receptor, so signaling cascade is activated. Thus, the signaling cascade can eventually trigger to cell behavior or cell characteristic changes. The overview of mechanism of transduction signal can be simplified as followings;

1) Reception: it is the first step; the ligand binds to a cell-surface receptor.

2) Transduction: after ligand binding to cell receptor, then its signal changes or transforms to chemical transduced form as called as secondary messenger such as cAMP, ion channel (calcium, sodium, chloride ion). The secondary messenger can be activated their enzymes and may be triggered a series of signaling molecules.

3) Response: the transducer deriving from ligand-receptor binding can be amplified and its signal responds to cell behavior (Berg *et al*., 2002).

The epidermal growth factor (EGF) as a signaling molecule is an example for illustrating the key component of signal transduction mechanism during cell division (Cooper, 2000). In cell biology, cells normally have to growth and development by cell cycle process. This process depends on the cell-cell interaction and nutrients. When the cell undergo to cell cycle process, the initial signaling molecule is called EGF, binds to epidermal growth factor receptor (EGFR). Then EGF-EGFR binding activates its receptor using by phosphorylation. The phosphorylated receptor

further conjugates with growth factor receptor-bound protein 2 (GRB2). GRB2 as an adaptor protein is associated in cell communication. A complex structure is also further triggered to downstream signaling such as mitogen-activated protein kinase (MAPK) (Seshacharyulu *et al*., 2012). Due to MAPK, a protein kinase is attached to the phosphate group of the transcription factor myelocytomatosis oncogene (*MYC*). *MYC* is a family of regulatory genes (an associated gene in controlling the expression) and proto-oncogene (a gene has effect to cause cancer) that code for transcription factors. The protein encoded by this gene is a multifunctional, nuclear phosphoprotein that plays a role in cell cycle progression, apoptosis and cellular transformation (Sloan and Ayer, 2010.). A Principle of signal transduction shows key components is illustrated in Fig. 1.2.

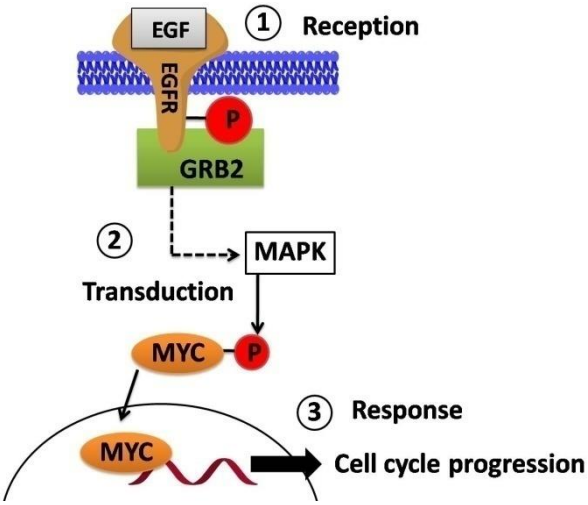

EGF: epidermal growth factor EGFR: epidermal growth factor receptor

GRB2: growth factor receptor-bound protein 2 MAPK: mitogen-actived protein kinase

MYC: myelocytomatosis oncogene

Figure 1.2 A principle of signal transduction (adapted from Molecular biology of the cell, Albert *et al*., 2002).

As mentioned earlier (Fig.1.2), it is the simply mechanism of signal transduction. However, in fact, cells have many signals to activate a specific receptor and these cells also different responses (Martin, 2003). Beside the human cancer pathways, at least nine pathways associated with cancer cells including;

(1) Tumor Growth Factor beta (TGF-β) signaling pathway (Neuzillet *et al*., 2015)

(2) Wnt signaling pathway (Zhan *et al*., 2017)

(3) G-protein-coupled receptor (GPCR) signaling pathway (Bar-Shavit *et al*., 2016)

(4) Ras signaling pathway (Fernandez-Medarde and Santos, 2011)

(5) Akt signaling pathway (Mayer and Arteaga, 2016)

(6) Death receptor and Nuclear factor kappa B (NF-κB) signaling pathway (Xia *et al*., 2014)

(7) Notch signaling pathway (Yuan *et al*., 2015)

(8) Hedgehog signaling pathway (Hanna and Shevde, 2016)

(9) Cell cycle signaling pathway (Chao *et al*., 2008)

There is a category of signal transduction associated protein, which possessed cell to cell using cell surface receptor. However, in the present study, we consider on anti-inflammatory effect, apoptosis, and cell cycle mechanisms. Therefore, two signaling cascades including Death receptor and NF-κB signaling pathway and Cell cycle signaling pathways, are further described. Following the Death receptor and NF-κB signaling pathway, it plays on inflammatory response and also programmed cells death, in particular apoptosis and necrosis (Balkwill, 2009; Colotta, 2009). Due to cell cycle progression is an important role in cell growth and development, and cell dividing (Coffman, 2004). The cell is basically proved the morphological characteristics such as cell size and the cell is also proved intermolecular components such as proteins, nuclear DNA and growth factors by checkpoint during cell cycle process (Morgan, 2007). Furthermore, the balance between live cells and death cells is also controlled by cell cycle signaling pathway.

1.3.1 Inflammatory signaling cascades

The inflammation process is a biological response to harmful stimuli such as pathogens (bacteria and virus) as well as foreign materials such as chemical and cytokines (Rosenberg and Gallin, 2003). Following by immune systems, the inflammatory response can be occurred in two types (Janeway *et al*., 2001). For innate immunity is a non specific defense mechanism to response antigens. The immunocytes such as macrophages and neutrophils are the first line and the main mechanisms including phagocytosis, release of inflammatory mediators, and activation of complement system proteins as well as cytokines and chemokines synthesis are occurred to activate to pathogen elimination and tissue injury. Whereas, adaptive immunity is second line after macrophages and neutrophils activation and it is specific immunological system (Janeway *et al*., 2001). The immunocytes such as lymphocyte T-cell and B-cell are activated to defense and response pathogen and tissue injury using by specific receptors. Therefore to mediating innate immune system, the immunocytes imply releases the pro-inflammatory mediators including cytokines such as interleukins (ILs), tumor necrosis factor (TNF), interferon gamma (IFN-γ), and granulocyte-macrophage colony stimulating factor (Abbas *et al*., 1997). Moreover, the reactive oxygen species (ROS) such as NO, super oxide (O_2^-), and etc, plays crucial role on innate immunological system (Mittal *et al*., 2014). These pro-inflammatory mediators are predominately released by cells of immunological system and it also associated transduction signaling cascades (Death receptor and NF-κB signaling pathways), Morgan and Liu, 2011.

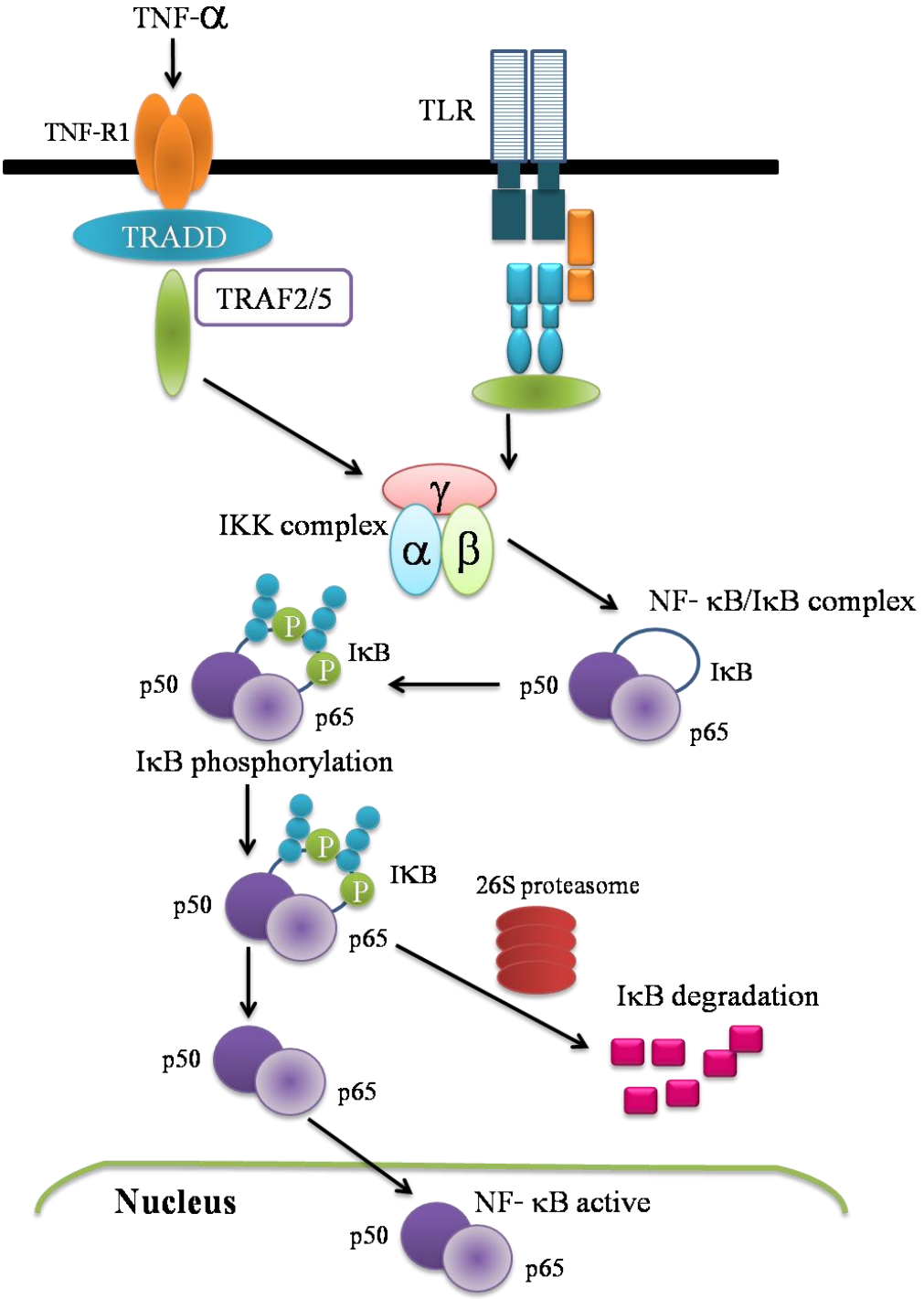

Figure 1.3 The NF-κB activation causes by TNF-α and toll like receptors. Activation of NF-κB initiates with stimulation of TNFR1 and TLR leading to activation of IKK complex and translocation of NF-κB to nucleus inducing gene transcription (Lodish *et al*., 2008).

Considering to death receptor and NF-κB signaling pathways (Fig. 1.3), the NF-κB is a nuclear factor kappa light chain enhancer of activated B-cell and it is a protein complex, which controls transcription of nuclear DNA. The NF-κB is often found in animal cells and it is further regulated on immunological system that responses to infection. The NF-κB activation is triggered by an extracellular signal, inflammatory cytokines (TNF-α and IL-1), mitogens, bacterial products and oxidative stress) for an example, leading to the recruitment of adaptor proteins and activating of IKK complex to inhibitory proteins IκB (Hayden and Ghosh, 2008). The phosphorylated IκB and degradation of IκB allow the active NF-κB to translocate to nucleus inducing specific gene transcription (Fig. 1.3). However, an incorrect regulation contributes to various diseases and problems such as septic shock, acute inflammation, viral replication and malignancies (Baeuerle and Henkel, 1994; Siebenlist *et al*., 1994; Hoesel and Schmid, 2013). As shown in Fig 1.4, there are two different pathway lead to the activation of NF-κB including canonical (classical) pathway and non canonical (alternative) pathway (Hayden and Ghosh, 2008; Vallabhapurapu and Karin, 2009; Sun, 2011). In non canonical pathway or alternative pathway, the receptor binding leads to the activation of NF-κB-inducing kinase (NIK) that phosphorylates and activates IκB kinase (IKK) complex. IKK-α homodimer is activated and results in the processing of the phosphorylation of IκB domain of P100 leading to liberation of p52/RelB (Sun, 2011). Whereas, the canonical or classical pathway the ligand such as TNF-α, IL-1 binds to a receptor and activation of tool-like receptors (TLRs) leads to recruitment and activation an IKK complex (IKK-α, β, γ). In the regulatory step, the catalytic kinase subunits of IKK-α and IKK- β and the IKK-γ regulatory subunit (as known as NF-κB essential modulator, NEMO) are activated by IKK-mediated phosphorylation of IκB leading proteasomal IκB degradation (Zandi *et al*., 1997; Yamaoka *et al*., 1998). The active NF-κB transcription factor subunit translocates to the nucleus and activates the transcription of target genes (Oeckinghaus and Ghosh, 2009; Christian *et al*., 2016).

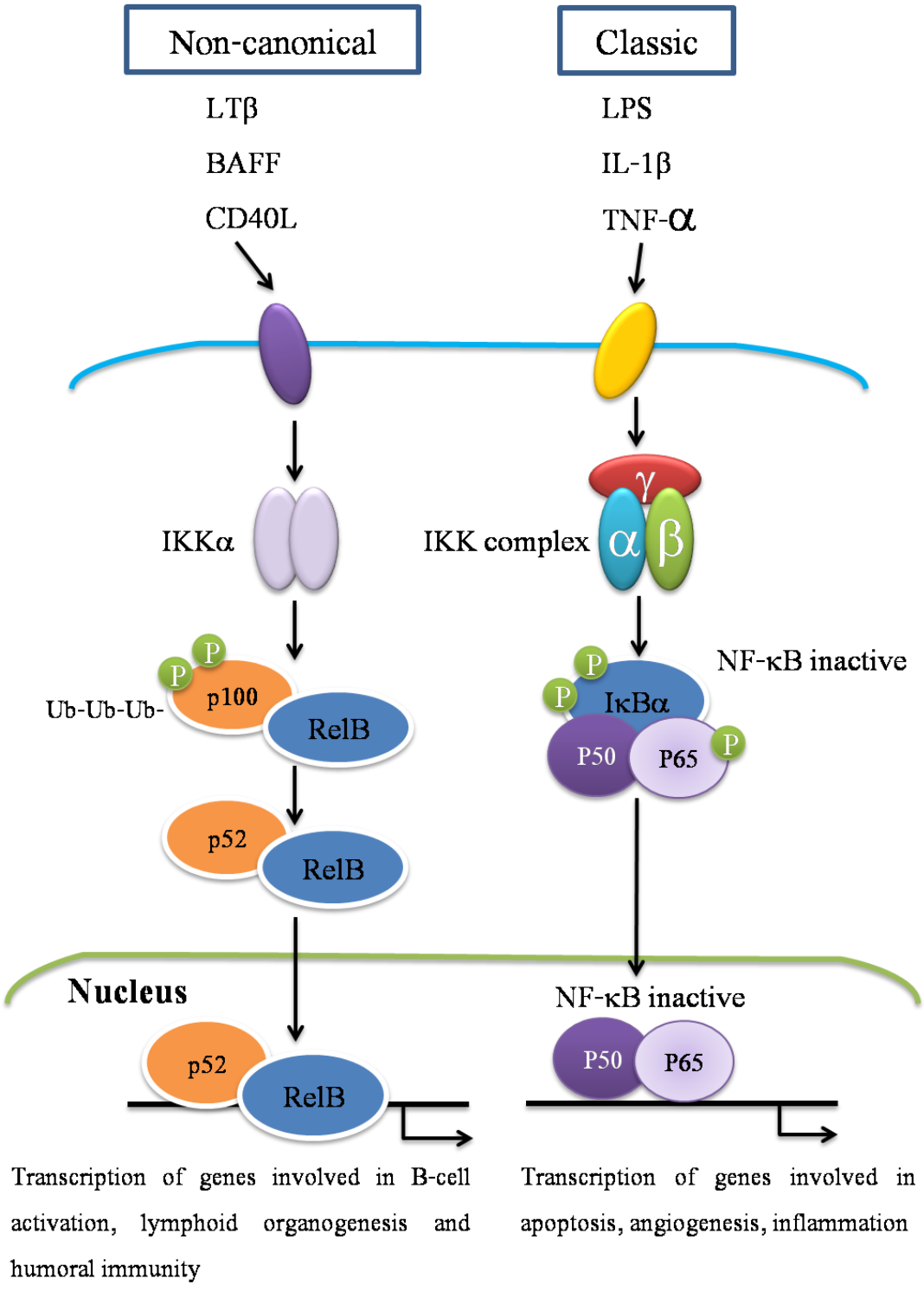

Figure 1.4 Classical (canonical) and alternative (non-canonical) NF-κB pathways (de las Heras and Hortelano, 2009).

Beside, tool like receptors (TLRs) are important receptors in the innate immune system and they are often found in immune cells, macrophage cells for example (Janssens and Beyaert, 2003). It is the plasma bound receptor and it locates on plasma. Because TRLs initiate the nucleus to transcription of mRNA and then translation to proteins by ribosomal RNA in cytoplasm, and the translated proteins lead to recognized to the cells, so the activating of TRLs is an initial process for initiates and promotes immune response (Troutman *et al*., 2012). TLR family consists of 10 members (TLR1 - TLR10) in human and 12 members (TLR1-TLR9, TLR11-TLR13) in mouse (Kawasaki and Kawai, 2014). These receptors recognize different transcription factors (Shcheblyakov *et al*., 2010). TLRs are also recognized by different foreign antigen. However, TRL-11 is not function in human, but it is recognized in mouse (Hatai *et al*., 2016). Among these TLRs, TLR4 recognizes lipopolysaccharide (LPS), which is found in gram negative bacteria and it will forms a dimer with another TLR4 during recognized TLR ligand (TRL4) (Park and Lee, 2013). The activation of TLRs initiates a cascade of transduction signaling pathway and it essentially activates certain transcription factors such as Activating protein-1 (AP-1), interferon regulatory factor (IRF) and NF-κB (Iwannaszko and Kimmel, 2015). These transcription factors are mainly activated by TLRs. For the transcription factor of AP-1, it activates protein-1 and it will essentially lead to different proliferation and even apoptosis (Shaulian and Karin, 2001). IRF as a transcription factor activates an interferon (IFN) protein in the nucleus. The IFN protein is essential protein for defense mechanism in immune system (Ikushima *et al*., 2013). The NF-κB is also transcription factor and it is mostly described on immune system and it is further associated with various diseases. The NF-κB transcription factor also activates gene and DNA as same as AP-1 and IRF, leading to transcribed pro-inflammatory cytokine such as TNF-α, IL-1β, IL-18 (Iwannaszko and Kimmel, 2015) The pro-inflammatory cytokines such as IL-1β and IL-18 are activated macrophage and other cells to enhance immune response and are triggered lymphocyte to chemotaxis (Duque and Descoteaux, 2014). For the TNF-α, it induces cells to enhance immune response as a main function, and it also induces cell undergoing apoptosis by binding onto death receptor

(Bhattacharyya *et al*., 2010). The IFN-γ is produced when there is the viral infection and it signals to other cells about that specific virus and promote the cells to enhance their defense (Perez-Rodriguez *et al*., 2009). Finally to understanding of inflammatory transcription factors in inflammatory signaling pathway whether their mediators either up-stream or down-stream signaling pathway can be guided the researchers to investigate anti-inflammatory effects. Additionally, NF-κB an ubiquitous transcription factor is the most important regulators of immune system and inflammatory response and it also regulates the transcription of a number of genes associated in other pathways, programmed cell death (apoptosis), cell adhesion, cell proliferation, cellular stress response and tissue remodeling, for instances. Pro-inflammatory mediators also associated to other signaling pathways, in particular cell cycle and apoptosis (Reuter *et al*., 2010).

1.3.2 Apoptotic signaling cascades

Apoptosis has been found since 1972 (Kerr *et al*., 1972). Apoptosis is well-known as a pathway of cell death and it is a one of terminal programmed cell death (Robertson *et al*., 2009). This biological mechanism is induced by a tightly regulated suicide program. Apoptosis associates either the physical conditions or the pathological conditions (Elmore, 2007). The physical conditions are embryogenesis, involution of hormone dependent tissue (menstruation, menopause and weaning), loss of cells in proliferating cell populations (bone marrow, thymus), removal of self reactive lymphocytes, and death of inflammatory cells after their functions are over. The pathological conditions are injured cells which cannot be repaired (the damage of DNA, the misfiled of protein accumulation, viral infections, duct obstructions) (Elmore, 2007). Apoptosis has an important role in cell morphological characteristic and cell developments (Hacker, 2000). Apoptosis is most important player on cysteine-dependent, aspartate-directed and proteases so called as caspases (Hengartner, 2000). Focusing caspases activation, the initiator caspases such as caspase-2, -8, -9, and caspase-10 and the executioner caspases such as caspase-3, -6, and caspase-7, these caspases are associated in apoptotic signaling pathways (Chen and Wang, 2002; Mcllwain *et al*., 2013). All caspases (both initiator and executioner) are inactive form, so called pro-caspases. Beside apoptosis mechanisms, the initiator caspases are activated by extrinsic or intrinsic pathways. The executioner caspases are activated by initiator caspases (Man and Kanneganti, 2016).

The ability of cancer cells to avoid apoptosis or programmed cell death and it continue to proliferation. This is one of the hallmarks of cancer and is a major focus of cancer therapy development (Sonnenshein and Soto, 2013). Regarding the signaling mechanism of apoptosis, apoptosis essentially extends over three steps including initiation, execution and phagocytosis (Bateman and Carr, 2009). Among these step the initiation step is an important and it can be initiated by two different mechanisms depending on whether the initiating signals from inside or outside the cells. Initiation step in intrinsic pathway, the most frequent signal that activates intrinsic initiation are irreparable and irreversible DNA lesion. The lesion of DNA leads to the activation of

ATM protein that is able to activate the tumor suppressor protein P53 and also leads to many other proteins (Zio *et al*., 2013). In addition, P53 is able to active the protein BAK and BAK protein locates on the outer membrane of mitochondria (Veseva and Moll, 2009). The other molecules such as calcium ions and protons, which are commonly located in the inner membrane region or locates between inner and outer of the mitochondria, may leak into the cytosol. One of these molecules is the protein cytochrome C. In the cytosol, cytochrome C binds to Apaf and may then associated with inactive form pro-caspase-9 (Rodriguez and Lazebnik, 1999). As a consequence, the inhibiting domain of the pro-caspase is hydrolyzed and dissociated from the protease. Following these mechanisms, caspase-9 becomes active form and active caspase-9 is able to cleave additional caspases and destroys other proteins. In this way, caspase-9 initiates the caspase cascades, this cascade denotes a stepwise cascade of proteases that cleave and thus activate each other. The concentration of active proteases in the cell increases rapidly leading to the destruction of many different proteins.

As mentioned earlier, apoptosis is generally triggered by two pathways including intrinsic pathway and extrinsic pathway (Albert *et al*., 2000). Intrinsic pathway is associated mitochondrial pathway and also called mitochondrial dependent pathway. The initial process is induced by the release of cytochrome C, which normally locates in mitochondria. During apoptosis, the cytochrome C is released into cytoplasm and then combines with a protein, which is called apoptosis activating factor-1 (Apaf-1). The combination between cytochrome C and Apaf-1 leads to apoptosome formation and procaspase-9 activation. Thus, the intrinsic pathway is regulated by the cytochrome C release. The regulation of apoptosis is basically regulated by *BCL-2* family of gene that locates on chromosome-18 (Sienko *et al*., 2008). *BCL-2* family genes, which are pro-apoptotic genes and anti-apoptotic genes, are important genes to control the releasing of cytochrome C in mitochondrial that leads to apoptosis. Pro- apoptotic genes regulates apoptosis through such as *BAX*, *BAK*, *BCL-XS* and anti-apoptotic *BCL-2*, *BCL-XL*, *Mcl-1* prevent leakage of cytochrome C (Cooper, 2000).

The initiation of extrinsic pathway, it is caused by extracellular signals (Ashkenazi and Dixit, 1998). A common extrinsic factor that initiates apoptosis is TNF-α, which is secreted by many cells like T-killer cells. Such cells can induce apoptosis in cells that are no longer required or dangerous from the organism, for instance tumor cells. TNF-α binds to the TNF-receptor at the outer membrane of the cell surface, and cell subsequently called death domain in the cytoplasmic site. After the receptor is activated, the specific cytoplasmic proteins then bind into their own death domain. Due to TNF receptor, the fist protein that binds to the cytosolic part of the receptor is the TNF-receptor associated protein with death domain (TRADD). As a result, the protein bounds associated protein with death domain which recruits pro-caspase-8. Pro-caspase-8 is able to auto catalyze the hydrolysis of its inhibiting segments leading to active caspase-8 which disassociates from the receptor and is then able to initiate the caspase cascades (Cooper, 2000).

Due to execution cleavage of the cytoskeleton, caspase-3 also cleaves many other proteins such as proteins of the cytoskeleton, so these cells lose its structure. Other proteins cause the cell to collapse into vesicles so called apoptotic blebs. The apoptotic blebs mostly contain mitochondria and also portions of the nucleus including DNA. These components allow energy to be maintained and new proteins are synthesized. The rapid breakup of the cell and of the formed vesicles is avoided preventing an inflammatory reaction in the surrounding tissue. The phagocytosis is the final step for apoptosis, the various processes of the execution phase lead to significant modification of the structure and composition of the outer membrane of cell and apoptotic blabs. Based on the modified membrane structure, the phagocytes like macrophages can recognize the blebs in the cytosol. During phagocytosis, the apoptotic blebs fuse with lysosome that is organelles containing enzymes. Finally the apoptotic blebs are destroyed (Nunez *et al*., 1998; Pellegrini *et al*., 2008).

Following to execution-cleavage of DNA, this is important steps of the execution phase are the cleavage of DNA and the cleavage of the cytoskeleton. In the normal cells, the nuclear DNA is complex to an inhibitor and is activated after initiation and activation of the caspase cascade. The caspase-3 is able to cleave this inhibitor. Then the activated DNA is cleaved DNA cleavage site.

Its results are located at regular intervals of 180 base pairs in between histone proteins of nucleosomes, which protect the DNA against DNA cleavage (Hosid and Ioshikhes, 2014).

In summary, the signaling mechanism of apoptosis, apoptosis essentially extends over three steps including initiation, execution and phagocytosis. The initiation step is triggered by extrinsic pathway that associates with death receptors (Fas and TNF) and activates to caspase-8, and also initiated by intrinsic pathway that involves with the releases of cytochrome C in mitochondrial and actives caspase-9. The initiator caspases (such as caspase-8 and caspase-9) consequently recruits to executioner caspases, especially caspase-3. The caspase-3 is one of executioner caspases that has an important role of apoptosis. Caspase-3 often cleaves the nuclear DNA and it also cleaves the cytoskeleton (Pellegrini *et al*., 2008; White *et al*., 2015).

Interestingly, to development novel molecules derived natural sources for cancer treatment, which promote apoptosis by targeting apoptotic mechanisms, so the regulation of apoptotic pathways including extrinsic and intrinsic signaling pathway are firstly considered. Based on the knowledge of apoptotic signaling pathways, the pro-apoptotic mediators such as Fas and TNF-α (extrinsic pathway) and BAX, BAK and BCL-XS (intrinsic pathway), and anti-apoptotic mediators such as BCL-2 and BCL-XL (intrinsic pathway). Furthermore, the activation of caspases, both initiator caspases (caspase-2, -8, -9, and caspase-10) and execution caspases (caspase-3, -6 and caspase-7) are also involved in apoptotic mechanisms. These executioner caspases leads to nuclear DAN breakdown by endonuclease activation and it also leads to breakdown cytoskeleton, so resulting into apoptotic blebs. These cell fragments are formed and are continuously destroyed by phagocytes. These cleavages of nuclear DNA and cell structures and apoptotic blebs elimination not affect on inflammatory system. In addition, other apoptotic mediators also associated this process such as PARP (Cooper, 2000; Albert *et al*., 2002; Pellegrini *et al*., 2008; White *et al*., 2015). Considering apoptotic mechanisms exists for activation of apoptosis, the understanding of the apoptotic mechanism behind tumor cell proliferation is considered by different regulated-apoptotic genes.

1.3.3 Cell cycle signaling cascades

Cell is building block of life that contained many organelles to function in our bodies. Cell is successive cell divisions in cell's cycles (Albert *et al*., 2000). In this re-production process, cells must replicate their allotment of DNA to division, so that each daughter cell will receives the same DNA content as the parent. Cells increase the component (growth) and divide through cell cycle. Due to cell cycle, cells duplicate the DNA before cell dividing and the cell cycle compose of four phases: G1 phase, S phase, G2 phase and M phase or mitosis. This cell's cycles beginning with the G1 phase, cell is growing and preparing to replicate the DNA. Then enter to S or synthesis phase, the cell starts the DNA synthesis. At the end of S phase, the cellular proteins which necessary for two daughter, cells are synthesized and duplicated through the G2 phase. Finally, the cell is divided into two identical daughter cells in M or mitosis phase. After completion of mitosis, cell can then gets into G1 again and go along the cell cycle, or get into latent or resting period or G-zero. The length of these phases may vary between different cell types that are actively in the process of cell division. Typical time spans in which the cell is engaged in each of the phases of the cell cycle are 12 hours for G1, 6 hours for S phase, 4 hours for G2, and 0.5 hour for mitosis (Hardin and Bertoni, 2015).

The regulation of the cell cycle, each individual phase is controlled by an order set of events during movement from one phase to another. A unique combination of cyclins and cyclin dependent kinases (CDKs) is the most prominent molecule associated in the cell cycle control (Pines, 1995). These regulatory proteins belonging to CDKs family activate kinase and then phosphorylate specific target proteins, leading to cell proliferation and cell dividing. However, a breakdown in the regulation of this cycle can induce to uncontrolled cell growth and tumor formation. In cancer cell, defects in many molecules that control the cell cycle are commonly involved regulated protein such as cellular tumor protein 53 (p53), CDK inhibitors (such as p15, p16, p18, p19, p21 and p27), retinoblastoma protein (Rb), ataxia telangiectasia mutated (ATM) and autologous tumor killer

(ATK) (Malumbres and Barbacid, 2009; Choi *et al*., 2016). According to these molecules, they act to remain the cell cycle process until damaged DNA is repaired and they also associated programmed cell death, so called apoptosis (Baychelier and Vieillard, 2013).

Furthermore, the regulation of cells is also controlled by time stamp of cells; commonly called checkpoints (Barnum and O'Connell, 2014). Therefore the cell cycle is monitored by the timing and condition of cell cycle events depending on cell cycle checkpoints that guide cells either proliferation or termination (Fig 1.5). On cell cycle checkpoints, there are three time stamps (checkpoints) including (1) G1/S checkpoint, it locates between G1-phase to S-phase, (2) G2/M checkpoint, it locates between G2-phase to M-phase and (3) cell division checkpoint, or spindle assembly checkpoint or M checkpoint, it locates on M-phase during the chromosome attachment to spindle fiber, which occurs between metaphase and anaphase, respectively (Albert *et al*., 2000; Barnum and O'Connell, 2014). In each of those checkpoints the cell will check whether certain things inside the cells are correct or not. If the component inside that cell is correct, that cell can then undergoing on cell cycle process and will divide. If that cell is not correct, cell will not proceeds and stops cell division. Additionally, the checkpoints at which the cell cycle can be arrested if the previous event is not been completed.

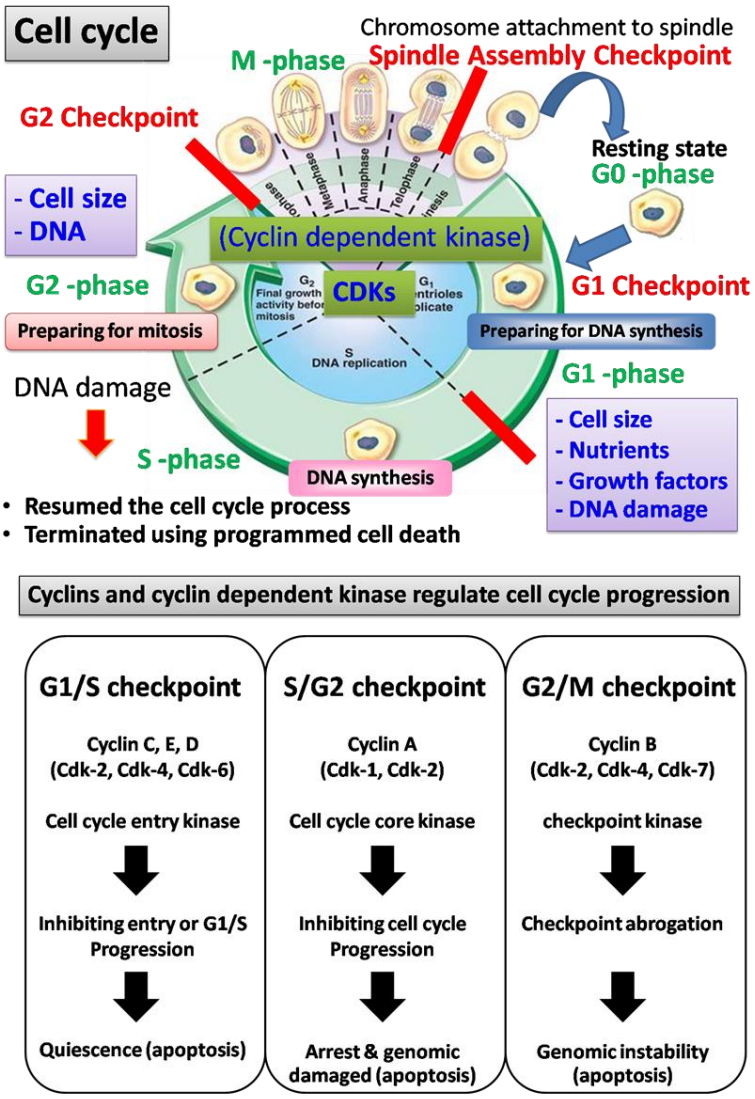

Figure 1.5 Cell cycle checkpoint associated cell cycle progression and apoptosis (adapted from Albert *et al*., 2000).

As shown in Fig. 1.5, during cell cycle, the nucleus and cytoplasm ratio (N/C) is changes (Murphy and Michael, 2013) and the dynamic changes in gene expression as a function of cell cycle progression are regulated by specific CDK activities. These variations in gene expression levels control the accumulation of several cyclins and thereby regulate CDK activity (Bertoli *et al*., 2013). The primary G1/S cell cycle checkpoint controls the commitment of eukaryotic cells to transition

through the G1 phase to enter into the DNA synthesis S phase. Two cell cycle kinase complexes, CDK4/6-Cyclin D and CDK2-Cyclin E, work in concert to relieve inhibition of a dynamic transcription complex that contains the Rb and E2F. G2/M checkpoint as a DNA damage checkpoint during DNA replication, it further proves the DNA synthesis processes and prevents the cell from entering mitosis (M-phase) with genomic DNA damage. The G2/M DNA damage checkpoint involves the activity of the Cyclin B-cdc2 (CDK1) complex. The M-checkpoint as a mitotic spindle checkpoint during cell dividing progression maintains genome stability by delaying cell division until accurate chromosome segregation can be guaranteed. It then checks the location of the corrective chromosomal DNA whether it attaches to the spindle fiber is correctly or not (Lara-Gonzalez *et al*., 2012; Bertoli *et al*., 2013).

In summary, the cell cycle depending DNA replication and segregation to two daughter cells. During cell cycle, it is regulated by cell cycle checkpoints and these checkpoints are associated a complex series of cyclins and CDKs, so the cell cycle able to either proliferate or terminate (Malumbres and Barbacid, 2001). The terminated program generally triggered through apoptosis. Therefore, the cell does not enter to the cell cycle, so the cell can be repaired the cell cycle. If the process cannot be resumed the cell must be promoted to cell cycle arrest and be promised suicide itself that normally mediated by apoptosis.

In the case of cancers, almost cancer cells normally lack of apoptosis resulting in uncontrolled cells proliferation and growth (Sonnensheinand Soto, 2013). In anti-cancer drug development, a new strategy for cancer treatment is firstly involved cell cycle and apoptosis. Therefore researches of anti-cancer substances that are derived from natural source, chemical, or whatever often are considered by cell cycle and also triggered by apoptosis. An approval evident of a link between cell cycle progression and apoptosis has been studied by morphological and biochemical changes during cell cycle and apoptosis corresponding to cell cycle arrest and apoptotic cells (Alenzi, 2005). The cell cycle and apoptotic regulators also have been studied such as several cyclins and CDKs (for cell cycle) and P53, RB, BCL-2 family regulator proteins and

TNF-α (for apoptosis mediators), respectively. Various target molecules that effect to cancer cells and it showed strong effect. However, the enormous published article about cytotoxic, anti-cancer, anti-proliferative and apoptotic activities have been found, but rarely found about their mechanisms.

1.4 Drugs derived from natural sources

The natural sources including micro-organism, plant, and animal are the source of lead compounds for drug and development. Up to date, many categories of the secondary metabolites derived natural products have been investigated, terpenoids, flavonoids, alkaloids and others, for instance. The several compounds obtained from natural product have been reported on several biological and pharmaceutical activities since 1930. Interestingly, the researchers have been published their articles about natural product as a source of new drugs and they collected the data since 1930 until 2014 (Newman and Cragg, 2014). Due to approved drugs, these drugs have many categories such as biological macromolecule, unaltered natural source, botanical source, natural derivative, semi-synthesis and chemical synthesis. These drugs also exhibit several activities, for example anti-bacterial, anti-fungal, analgesic, anti-histamine, anti-inflammatory, immunostimulant, immunosuppressant, and anti-cancer activities. Even though, the several chemical constituents are worldwide discovered and these chemical constituents also showed high potency on several biological and pharmacological activities as well as safety and side effects during clinical trials, a little of candidate drugs were further approved as new drug. However, the phytochemical investigation, high throughput screening as well as animal experiments are also important in the process of drug discovery. The extended knowledge about chemistry and mechanism also guide the researchers to either develop a new drug or make them to understand new strategies for treatments of various diseases (Newman and Cragg, 2014).

1.4.1 Approved anti-inflammatory drugs

A total number of anti-inflammatory drugs have been discovered with 57 substances since 1970 to 2014. The anti-inflammatory drugs about 27% of total drugs (14 drugs) have been found and these candidate drugs are derived from natural products (Newman and Cragg, 2014). Therefore, there are some medicinal plants and their compounds have been evaluated on anti-inflammatory activity through cell based assay and in vivo experiments.

Focusing on anti-inflammatory activity and its mechanisms, several anti-inflammatory model has been used for evaluated such as LPS-induced NO production, neutrophil activation, reactive oxygen species determination, and inflammatory mediated active protein kinase (AKT) and nuclear factor kappa B (NF-κB) signaling pathways. The inflammatory mediated signaling pathways are cannabinoid CB1 receptor (CB1R), human synovials PLA2, phospholipase A2 (PLA-2), 5-lipoxygenase (5-LOX), cyclooxygenase (COX), calcium channel, AKT, and p38, for examples.

Salvinorin A as a hallucigenic substance has been reported on anti-inflammatory effect though LPS-stimulated murine macrophage and its results showed anti-inflammatory effect of salvinorin A associated with κ-Opioid Receptor (KOR) and cannaninoid CB1 receptor (Aviello *et al*., 2011). The study of (12S)-6α-acetoxy-4 α, 18-epoxy-12-hydroxy-19-tigloyloxy-*neo*-clerod-13-en-15, 16-olide and ajugalide D on LPS-induced NO production in murine microglial BV-2 cells indicated that both compounds showed an inflammatory activity with an IC_{50} values 28.6±2.6 and 43.5±4.7 mM, respectively (Guo *et al*., 2012). The anti-inflammatory activity also evaluated using LPS and TNF-γ activated macrophage-like cell line J774.1 and the inhibitory effect on NO production was investigated after treatment with four clerodanes including tinospin A, 12- EPI-tinospin A, tinospinoside B, and tinospinoside. These compounds showed inhibitory activities of NO production with the IC_{50} values of 162, 182, 290, and 218 μM, respectively (Li *et al*., 2012). On inhibitory activities against human sPLA2 (a 14 kDa secretory enzyme PLA-2) and 5-LOX, two clerodanes including E-isolinaridial (EI) and E-isolinaridial methyl ketone derivative showed

highly potent activity with an IC_{50} of 0.20 and 0.49 μM, respectively (Benrezzouk *et al*., 1999). Furthermore the compound 16-hydroxycleroda-3, 13(14) E-dien-15-oic acid (PL3S) as a clerodane was established anti-inflammatory function in human neutrophils. This result suggested that the suppressive effects of PL3S on human neutrophil respiratory burst and degranulation are at least partly mediated by inhibition of calcium, AKT, and p38 signaling pathways (Chang, *et al*., 2008).The compound 3β,4β:15,16-diepoxy-13(16),14-clerodadiene and tysapathone showed an inhibitory effect on NO production in LPS-stimulated RAW 264.7 cells with an IC_{50} value was 20.1 and 11.6 μM, respectively (Harinantenaina *et al*., 2006).

1.4.2 Approved anti-cancer drugs

Consideration about the anti-cancer drugs, they described that the total 174 substances were approved and these substances were also classified. As shown in Fig 1.6, about33 (20%) of biological macromolecules (B), 17 (10%) of unaltered natural products (N), 1 (1%) of botanical drug (mixture substances, NB), 38 (22%) of the derivative from natural products (ND), 37 (22%) of semi synthetic substance and mimic substances using natural product as a pharmacophore (S* and S*/NM), and 43 (25%) of chemical synthesis (S* and S*/NM), respectively. According to these results, it indicated that half of all anti-cancer substances are derived from natural sources. Among the approval anti-cancer drugs, taxanes (paclitaxel and docetaxel), vinca alkaloids (vinblastine, vincristine, vindesine, vinorelbine), podophyllotoxin and derivative (etoposide, teniposide), camptothecin and its derivatives (topotecan, irinotecan), anthracyclines (doxorubicin, daunorubicin, epirubicin, idarubicin) derived plant source are mostly mentioned and these drug are also accepted for cancer treatment rather than others. The approval drugs were summarized in Table 1.1 (Newman and Cragg, 2014).

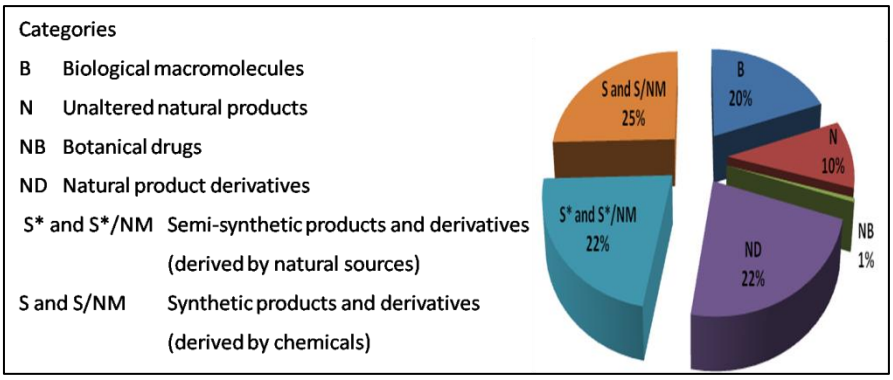

Figure 1.6 Approved anti-cancer drug since 1970 to 2014 (Newman and Cragg, 2014).

Table 1.1 Approved anti-cancer drugs used for cancer treatments and their mechanisms (Payne and Miles, 2008).

Types	Substances	Mode of action	Anti-cancer drug
Taxanes	Main action; these drugs attach on β-sub unit of tubulin in microtubule and its effects inhibit function of microtubules (cell cycle arrest G2/M) and direct activation of apoptotic pathways.		
	(1) Paclitaxel	Mitotic spindle poisons	Taxol , Anzatax
	(2) Docetaxel		Taxotere
Vinca alkaloids	Main action; these drugs attach on β-sub unit of tubulin in microtubule and its effects inhibit function of microtubules.		
	(1) Vinblastine	Mitotic spindle poisons	Vinblastine
	(2) Vincristine		Vincristine Rx
	(3) Vinorelbine		Navelbine
Topoisomerase inhibitors	Main action; these drugs inhibit topoisomerase during DNA synthesis leading to terminate cell cycle (cell arrests at S/G2 phase) and induce apoptosis.		
	(1) Doxorubicin	Inhibits topoisomerase II	Doxorubicin ,
	(2) Liposomal doxorubicin	Inhibits topoisomerase II	Adriblastina Caelyx , Lipo-Dox
	(3) Epirubicin	Inhibits topoisomerase II	Farmorubicin
	(4) Etoposide	Inhibits topoisomerase II	Fytosid
	(5) Idarubicin	Inhibits topoisomerase II	Zavedos
	(6) Irotecan	Inhibits topoisomerase I	Campto
	(7) Topotecan	Inhibits topoisomerase I	Hycamtin

1.5 Diterpenes

Diterpene is a chemical structure that normally consists of 20 carbon atoms and its structure is generally derived by isoprene unit as a building block (5 carbon atoms), which is formed either isopentenyl pyrophosphate (IPP) or dimethylallyl pyrophosphate (DMAPP). Therefore the chemical structure of diterpenes is composed by four isoprene units (Harborne *et al*., 1999). According to chemical structure, the diterpenes substances have been found from several plants, animals and marine organisms (Li, *et al*., 2016). A variety of the composed structures of diterpenes are worldwide found and their structures are depended on chemistry and enzymatic reaction in a variety of natural sources. The simply structures and complex structures are also classified by chemical structures (Breitmaier, 2006). The simply structures are derived from either IPP or DMPP and their structures normally linked by head to tail or head to tail, forming to acyclic structures so called acyclic diterpenes (Talapatra and Talapatra, 2015). Whereas the modified or complex structure of diterpenes are formed by different types of cyclization reaction and these structures are consequently associated with enzymes. Therefore, the diterpene structures can be classified by the membered-rings and chemical structures that are composed in the assemble structure following acyclic structures, monocyclic diterpenes, bicyclic diterpenes, tricyclic diterpenes, tetracyclic diterpnes, cembranes and cyclocembranes, prenyl sesquiterpenes, and ginkgolides, respectively.

1.5.1 Anti-inflammatory activity

The traditional medicinal plants have been used for anti-inflammatory substances since long time ago. These plants have been used as a traditional medicine remedy for inflammatory conditions that are concurred by classical signs including fevers, pain, analgesic and arthritis. Many metabolites from either primary metabolites or secondary metabolites are derived by natural sources. The substances exert anti-inflammatory effects are terpenoids, flavonoids, phenolic compounds, and their derivates.

The researching of natural product based on phytochemistry, semi-synthesis, biological activity and pharmacological activity has been rapidly continued since the secondary metabolite currently occurring natural sources play on biological system. Regarding the inflammatory effects of secondary metabolite derived natural product, many published reports are found from international data base, nowadays. Furthermore, many compounds act as anti-inflammatory agent such as the pure anti-inflammatory substances and plant extracts, which are isolated and purified from natural product. One of the most important families of natural compounds known for their medical value is the terpenoids (de las Heras and Hortelano, 2009). Terpenoids are the largest and most widespread group of secondary metabolites. As shown in Table 1.2, the diterpenes derived natural origins such as plant and marine sources, which exert anti-inflammatory potency, have been studied using various anti-inflammatory models.

The potency of natural diterpenes as well as modified diterpenes to reduce inflammatory effects has been evaluated in the past year. Most of anti-inflammatory studies on diterpenes have been considered on NF-κB signaling pathway (de las Heras and Hortelano, 2009). Actually, NF-κB as a common target in the action of these compounds annotates their anti-inflammatory and immunomodulatory responses. The molecular basis of anti-inflammatory effects of diterpenes involved in NF-κB activation provides many steps for specific inhibition of NF-κB activity including (a) inhibiting the activation of IKK complex (such as hispanole derivatives, hypoestoxide, tanshinone IIA, foliol and linearol), (b) targeting the proteasomal degradation of NF-κB

translocation to nucleus (such as andalusol and inflexinol) and (c) interfering the NF-κB translocation to nucleus or NF-κB binding to DNA (such as andrographolide, oridonin, ponicidin kamebakaurin, triptolide and inflexinol). Several diterpenes as an anti-inflammatory substance from natural sources associated in NF-κB signaling cascades are summarized in Table 1.2.

Table 1.2 Anti-inflammatory substances derived natural sources.

Sources	Types	Substances	Mode of action	References
Acanthopanax koreanum	Pimaranes	Acanthoic acid and its derivatives	- a potent anti-inflammatory and anti-fibrosis effects by inhibiting IL-1 and TNF-α production - inhibit TNF-α mediated IL-8 production by blocking in both the MAPK (inhibiting P38, JNK1/2, ERK1/2 activation) and NF-κB (inhibiting IκB degradation, NF-κB transcription translocation and NF-κB/DNA binding) pathways in HT-29 cells -inhibit pro-inflammatory cytokines such as IL-1β, IL-6 and TNF-α in PBMC and RAW264.7 cells and the anti-inflammatory effect by inhibiting NF-κB-activated cytokine production	Kang *et al*., 1996; Lam *et al*., 2003; Kim *et al*., 2004; Chao *et al*., 2005

Table 1.2 (Continued)

Sources	Types	Substances	Mode of action	References
Andrographis paniculata	Labdanes	Andrographolide	- Inhibit TNF-α and IL-12 in LPS-induced macrophages - Inhibit NF-κB activation through covalent modification of reduced cysteine 62 of p50	Xia *et al*., 2004; Qin *et al*., 2006
Annona glabra	Kauranes	Three *ent*-kuarane diterpenes	- exhibit the inhibitory of NO production with IC_{50} 0.01 – 0.32 µM	Nhiem *et al*., 2015
Axinell sp.(sponge)	Amphilectene	Cycloamphilectenes (1-6)	- reduce NO production with IC_{50} 0.1-4.3 µM - inhibit iNOS expression without affecting COX-2 expression - act as NF-κB inhibitor	Lucas *et al*., 2003
Ballota hispanica Neck ex Nym. (*B. hirsuta* Benth.)	Labdanes	Hispanolone-derived landanes	- exhibit anti-inflammatory activities by inhibition of NO, PGE_2 and TNF-α production with IC_{50} 1 – 10 µM in LPS-induced RAW264.7 cells - Inhibit iNOS and COX-2 expression	Savona *et al*., 1978; Girón *et al*., 2008

Table 1.2 (Continued)

Sources	Types	Substances	Mode of action	References
			-inhibit IKK activity and inhibition of the nuclear translocation of NF-κB	
Biota orientalis	Labdanes	Pinusolide 15-methoxypinusolidic acid	- inhibit NO production and iNOS expression, independent on MAPK and NF-κB in LPS-induced BV2 cells - suppress TNF-α, IL-6 and COX-2 - not affect to NF-κB signaling pathway (the degradation of IκBα and the translocation of NF-κB) - not affect to MAPK signaling pathway (P38 MAPK, ERK(1-2) and SAPK/JNK)	Choi *et al*., 2008
Croton tonkinensis	Kauranes	Four *ent*-kuarane diterpenes	- inhibited LPS-induced NF-κB activation in murine macrophage RAW264.7	Giang *et al*., 2003

Table 1.2 (Continued)

Sources	Types	Substances	Mode of action	References
Dodonaea polyandra	Clerodanes	polyandric acid A	- inhibit pro-inflammatory cytokine production and other inflammatory mediators *in vitro* and *in vivo*	Simpson *et al*., 2014
Dodonaea viscosa	Clerodanes	Hautriwaic acid	- reduce pro-inflammatory cytokines IL-1β, IL-6 and TNF-α in the joint by kaolin /carrageenan-induced monoarthritis model	Salinas-Sánchez *et al*., 2015
Eurphobia peplus	Puplanes	Pupluanone	-act as anti-inflammatory agent in carragenan-rat paw edema - reduce the NO, PGE_2, and TNF-α production via suppressing the expression of iNOS, COX-2 and TNF-α mRNA through down-regulation of NF-κB binding activity	Corea *et al*., 2015

Table 1.2 (Continued)

Sources	Types	Substances	Mode of action	References
Hypoestes rosea	A bicyclo [9,3,1] pentadecane	Hypoestoxide	- inhibit the pro-inflammatory mediators (IL-1β, IL-6 and TNF-α) in LPS-stimulated normal human peripheral blood mononuclear cells (PBMC) - inhibit NO production by IL-1β or IL-17 activated normal human articular chondrocyte though inhibition of IKK activity - inhibit phorbol ester-induced ear inflammation in mice	Ojo-Amaize *et al*., 2001
Isodon excisus	Kauranes	Inflexinol	- inhibit NO and suppress the expression of iNOS and COX-2 in LPS-induced RAW264.7 cells and astrocytes	Lee *et al*., 2007

Table 1.2 (Continued)

Sources	Types	Substances	Mode of action	References
			-inhibit transcriptional and DNA binding activity of NF-κB via inhibition of IκB degradation and the translocation of p50 and p65 into nucleus	
Isodon excisus	Kauranes	Inflexinol	- inhibit NO and suppress the expression of iNOS and COX-2 in LPS-induced RAW264.7 cells and astrocytes -inhibit transcriptional and DNA binding activity of NF-κB via inhibition of IκB degradation and the translocation of p50 and p65 into nucleus	Lee *et al*., 2007
Isodon japonicus	Kauranes	Kamebanin Kamabecetal Kamebakurin Excisanin A	- as a potent inhibitor of NF-κB activation by directly targeting DNA-binding of P50	Hwang *et al*., 2001; Lee *et al*., 2002

Table 1.2 (Continued)

Sources	Types	Substances	Mode of action	References
Isodon rubescens	Kauranes	Oridonin Ponicidin Xindongnin A	- a potent inhibitors of NF-κB transcription - inhibit COX-2 and iNOS and interfere with DNA-binding activity of NF-κB -have an impact on the translocation of NF-κB from the cytoplasm to nucleus without IκB-α phosphorylation and degradation	Leung *et al*., 2005
Nepeta suavis	clerodanes	Nepetolide	- exhibit anti-inflammatory effect in carrageenan-induced rat paw edema - inhibit COX-2, EPFR, LOX-2 *in silico* model	Ur Rehman *et al*., 2018
Oryza sativa L	Pimaranes	Oryzalexin A Momilactone A	- inhibit NO production and iNOS mRNA and protein expression in LPS-stimulated RAW264.7 macrophages	Cho *et al*., 2015

Table 1.2 (Continued)

Sources	Types	Substances	Mode of action	References
Rosmarinus officinalis	Abietanes	Carnosol Carnosic acid	- inhibit ERK1/2, AKT, P38, NF-κB and c-Jun in B16/F10 mouse melanoma cells -inhibit LPS-induced iNOS and NO by blocking NF-κB activation in RAW264.7 - inhibit LPS-induced P38 and ERK activation	Lo *et al*., 2002; Huang *et al*., 2005; Kuo *et al*., 2011
Sideritis linearifolia Lam	Kauranes	Foliol Linearol *ent*-Kaur-16-en-19-oic acid	- inhibit iNOS expression and TNF-α production in LPS-induced J744 macrophage cells - inhibit NF-κB and IκB kinase (IKK) activation in *in vivo* study -delay the phosphorylation of P38, ERK1/2, and MPKs in J744 cells	de Quesada *et al*., 1972; Castrillo *et al*., 2001

Table 1.2 (Continued)

Sources	Types	Substances	Mode of action	References
Siegesbackia pubescens	Kauranes	Siegeskauroic acid	- exhibit anti-inflammatory effect in animal models - inhibit the production of NO, PGE_2 and TNF-α, iNOS, COX-2 and TNF-α protein expression - down regulation of NF-κB binding activity	Park *et al*., 2007
Slideritis foetens	Labdanes	Andalusol	- Inhibit iNOS protein expression through the activation of NF-κB activation in J744 cells. - Inhibit the degradation of IκBα - Exhibit anti-inflammatory effects (*in vivo*)	Navarro *et al*., 1997; de Las Heras *et al*., 1999
Thyrsanthera suborbicularis Pierre ex Gagnep	Rosanes	15-rosadiene	- inhibit NO production via suppression of the iNOS mRNA expression in LPS-induced RAW264.7 cells	Khiev *et al*., 2011

Table 1.2 (Continued)

Sources	Types	Substances	Mode of action	References
Tripterygium wilfordii Hook F	Diterpene expoxide	Triptolide	- inhibit myeloperoxidase activity and edema of lung in mice - reduce TNF-α, IL-1β and IL-6 production in LPS-induced mice - inhibit the LPS-activated phosphorylation of Iκ α and NF-κB p65 and the expression of TLR4	Wang *et al*., 2014

1.5.2 Anti- cancer activity

The major causes of human death often associated cancers and the cancers also continue to be the first factor of death worldwide. In facts, the cancer is caused by the un-controlled cells, which depends genetic, incorrect diet and environments. The human life style has been already changed from traditional life styles, so too much immediately products and the containing products are become. Therefore the changed style may be associated to cancer development that corresponding a research of cancer. About 95% of total cancer causes are occurred by human life styles and for the cancer development may later find as long as 20-30 years (American Cancer Society, 2017). Consideration to the phenomenon of cancers, they were observed that more than 12 million cases of cancers are found and more than 7 million death cases are caused by cancers. The cancers are rapidly diagnosed on nowadays. The American Cancer Society (ACS) together with International Union Against Cancer (IUAC) estimated the case of cancers may be increased to double cases than previous year in 2030 (about 30 million cancer cases and 17 million deaths), American Cancer Society, 2017).

A history of anti-cancer substance originally derived natural sources has been discovered more than 50 years ago. The anti-cancer drug originates from plant such as paclitaxel, docetaxel vinblastine, vincristine, topotecan and irinotecan. These compounds exhibit different mechanisms and also currently use for cancer treatment. Even though, the effective-approved anti-cancer drugs obtain from synthetic drugs, these drugs also have some side effects. Therefore, the development of anti-cancer drug that are obtained from edible plant or medicinal plant may be less side effect than synthetic drugs.

The rationale for anti-cancer study is considered by anti-proliferative, cytotoxic effects and its mechanisms (Table 1.3). Following preliminary screening study, enormous international reports about anti-proliferative and cytotoxic activities using MTT are currently published. The results normally exhibited as an IC_{50} of the compound that effective to various cancer cells. Among their results, the potency of anti-cancer compound as a candidate substances are found less than 1 μM to

100 μM for the pure compounds and less than 1 mg/ml to 100 mg/ml (for crude extracts and partial purified), respectively. According their results indicated that the potency of anti-cancer compounds including high, moderate, less, slightly, or whatever are various adjusted and they did not described the guideline references, however corresponding to Nation Cancer institute (NCI) 60 cancer cell screening programs, 60 cancer cell lines are further tested by natural crude drugs and compounds and 5 x 10 fold for testing concentrations are used; the high concentration with 100 μM and 150 μg/ml for an extract and compounds, respectively, so the active compounds are mostly exhibits with an IC_{50} either 1 to 100 μM or 1 to 150 μg/ml.

Besides anti-cancer and cytotoxic effects, the cell cycle arrest and programmed cell death such as apoptosis or autophagy are generally investigated. Other effects associating anti-cancer activity are also studied such as anti-antioxidant activity (the reactive oxygen species (ROS) mediated and/or pro-oxidative leading to cancer development) and anti-inflammatory activity (NF-κB signaling-mediated pro-inflammatory mediators leading cancer development). Furthermore, the effect of anti-cancer drug resist cancer cells and miscellaneous are also considered. Recently, the anti-cancer diterpenes and its derivatives that had been published in database since 2012 to 2017 were summarized and these compounds showed difference anti-cancer mechanisms (Islam, 2017). The diterpenes associated anticancer pathways with various mechanisms are shown in Fig. 1.7 and Table 1.3.

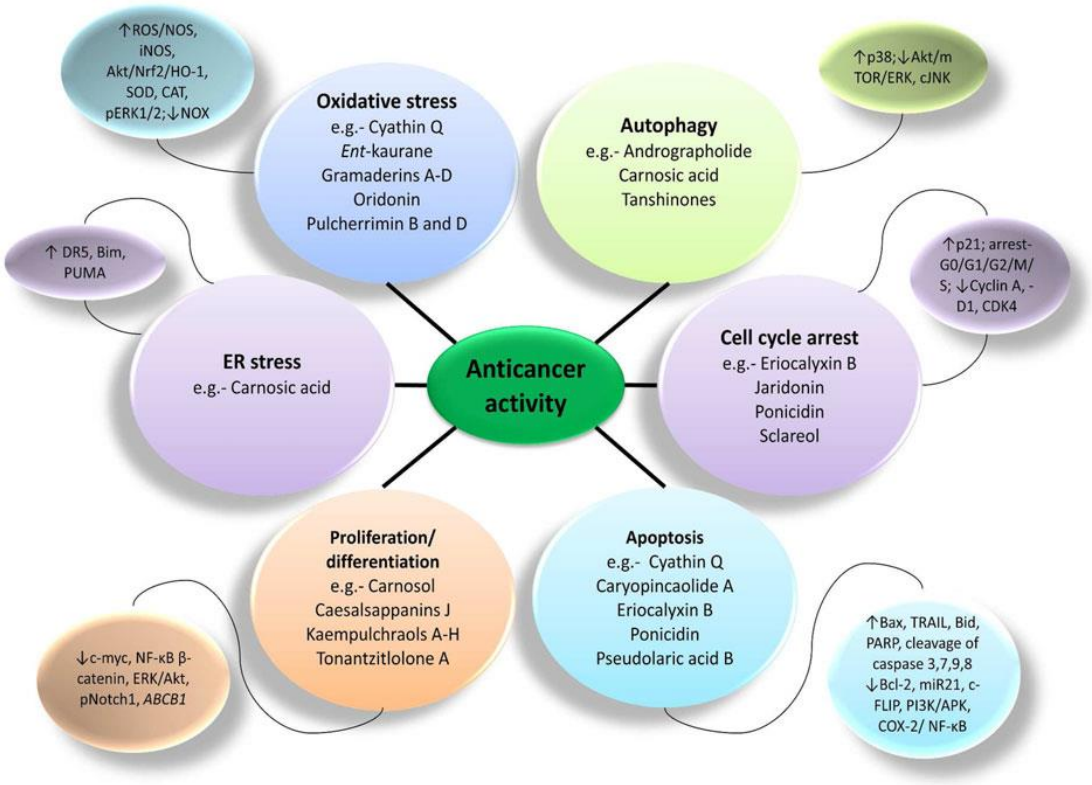

Figure 1.7 Major anti-cancer pathways of diterpenes (Islam, 2017).

Table 1.3 Several of diterpenes act as anti-cancer activity.

Sources	Compounds	Cell lines	Activities (IC_{50} and its mechanisms)	References
A. Preliminary screening study				
Acanthella cavernosa (*Sponge*)	(1-4) Cavernenes A–D (5-6) kalihinenes E-F (Formamido-diterpenes)	Human cancer cell lines (HCT-116, A549, HeLa, QGY-7701 and MDA-MB-231)	IC_{50} values in the range of 6–18 μM	Xu *et al*., 2012
Alpinia officinarum	(*Z*)-12,14-labdadien-15(16)-olide-17-oic acid	HeLa and HepG2 cancer cell lines	IC_{50} values > 50 μg/ml	Zou *et al*., 2016
Annona glabra	(1-2)Annoglabasin B, E (3) 19-norent- kaurent-4-ol-17-oic acid (ent-kauranes)	LU-1, MCF-7, SK-Mel2 and KB cancer cell lines	Cytotoxicity	Anh Hle *et al*., 2014
Aphanamixis polystachya	(1-6) Aphanamixins A–F (acyclic diterpenes)	HepG2, AGS, MCF-7 and A-549 cancer cell lines	IC_{50} values > 10 μM.	Zhang *et al*., 2014

Table 1.3 (Continued)

Sources	Compounds	Cell lines	Activities (IC_{50} and its mechanisms)	References
Aphanamixis polystachya	(1-4) Aphanaperoxides E–H	HepG2, A549, AGS and MCF-7 cancer cell lines	IC_{50} values > 20 µM	Wu *et al*., 2013
Caesalpinia minax	(1-5) Caesalmins N–Q	Three human cancer cell lines	IC_{50} values 45.4 to 78.1 µM	Li *et al*., 2016
Caesalpinia minax	(1-2) Caesalpinolide F and G	Human colon (HCT-8) and breast (MCF-7) cancer cell lines	IC_{50} values 78.4 to 62.3 µg/ml	Ma *et al*., 2013
Caesalpinia minax	(1-8) Caesalminaxins A–L (cassanes) Caesalminaxin H and D	HepG-2, K562, HeLa and Du145 cells	IC_{50}values 9.2 to > 50 µM	Zheng *et al*., 2013

Table 1.3 (Continued)

Sources	Compounds	Cell lines	Activities (IC_{50} and its mechanisms)	References
Caesalpinia minax	(1-5) Neocaesalpin AA, AB, AC, AD, AE (6) 12α-methoxyl,5 α,14β-dihydroxy-1 α,6 α,7 β - triacetoxycass-13(15)-en-16,12-olide	Hela, HCT-8, HepG-2, MCF-7and A549 cancer cells	Moderate activity with IC_{50} values from 18.4 to 83.9 μM	Ma *et al*., 2012
Caesalpinia minax	Neocaesalpin MR	HeLa and colon (HCT-8) cancer cell lines	Mild activity (IC_{50} 36.8 and 45.2 μg/ml)	Ma *et al*., 2012
Caesalpinia sappan	(1-5) Caesalppans A–F	HeLa, ArT-20, KB and MCF7 cell lines	IC_{50} values 19.3 to >50.0 μM	Xu *et al*., 2016
Caesalpinia sappan	(1)Tomocinon (2-3) Tomocinol A and B (Cleistanthanes)	PANC-1 human pancreatic cancer cell line	IC_{50} values 34.7 to 42.4 μM	Nguyen *et al*., 2013

Table 1.3 (Continued)

Sources	Compounds	Cell lines	Activities (IC_{50} and its mechanisms)	References
Cespitularia sp. *(soft coral)*	Alcyonolide and other five diterpenes	HCT 116 cells	IC_{50} values 5.85 and 91.4 µM	Roy *et al*., 2012
Cladiella sp.	(1-5)Cladieunicellins M–Q (Eunicellins) Cladieunicellin A, C and E	Human leukaemia Molt 4 and HL60 cells	IC_{50} values 14.17 to 16.43 µM	Chen *et al*., 2014
Cladiella sp.	(1-2) Cladieunicellins K and L (eunicellins)	MOLT-4 human leukaemia	IC_{50} values 14.42 µM	Shih *et al*., 2013
Cladiella sp.	(1-5)Cladieunicellins M–Q (Eunicellins) Cladieunicellin A, C and E	Human leukaemia Molt 4 and HL60 cells	IC_{50} values 14.17 to 16.43 µM	Chen *et al*., 2014
Cladiella sp.	(1-2) Cladieunicellins K and L (eunicellins)	MOLT-4 human leukaemia	IC_{50} values 14.42 µM	Shih *et al*., 2013

Table 1.3 (Continued)

Sources	Compounds	Cell lines	Activities (IC_{50} and its mechanisms)	References
Clinopodium chinense	(1) 3β-hydroxy-12-O- β –D-glucopyranosyl-8,11,13-abietatrien-7-one	A549 and HepG-2 cancer cell lines	IC_{50} values 68.1 to 76.8 µg/ml	Zhong *et al*., 2014
Colletotrichum higginsianum	(1-2) Higginsianins A and B	Six cancer cell lines	IC_{50} values >80 µM	Cimmino *et al*., 2016
Crossopetalum gaumeri	Ten diterpenes Crossogumerin, nimbiol	HeLa and Hep-2 turmor cells, and normal Vero cells	IC_{50}values 30.1 and 22.6 µM	Miron-Lopez *et al*., 2014
Daphne genkwa	(1-4) Genkwadanes A–D (Daphnanes)	Ten human cancer cell lines	IC_{50}values < 9.56 µM	Li *et al*., 2013
Delphinium trichophorum	(1-5) Trichodelphinines A–E (diterpene alkaloids)	A549 cancer cells	IC_{50} values 12.03 to 52.79 µM	Lin *et al*., 2014

Table 1.3 (Continued)

Sources	Compounds	Cell lines	Activities (IC_{50} and its mechanisms)	References
Dictyota dichotoma	(1-2) Pachydictyols B and C	Human tumour cell lines	IC_{50} values> 30.0 µM	Abou-El-Wafa *et al*., 2013
Euphorbia connata	(1) Pentahydroxy-13(17)-epoxy-8,10 (18)-myrsinadiene (2) Tetrahydroxy-5,6-epoxy-14-oxo-jatropha-11(E)-ene	MDA-MB and MCF-7 cell lines	IC_{50} values 24.33 to 55.67 µM	Shadi *et al*., 2015
Euphorbia cyparissias	(1-2) Cyparissins A and B	A2780 cell line	Anti-cancer activity	Lanzotti *et al*., 2015
Euphorbia fischeriana	Eight ent-atisane diterpenoids (Ent-3β-hydroxyatis-16-ene-2, 14-dione)	MCF-7 cells	Anti-proliferative effect	Kuang *et al*., 2016
Euphorbia pekinensis	Pekinenin G (casbanes)	BGC-823, HT-29, MCF-7 and A549 cell lines	IC_{50} values 11.3 to 110.7 µM	Wang *et al*., 2015

Table 1.3 (Continued)

Sources	Compounds	Cell lines	Activities (IC_{50} and its mechanisms)	References
Euphorbia pekinensis	(+)-(1S)-15-hydroxy-18-Carboxycembrene (cembranes)	HeLa, PC-3, HT1080, A375-S2 and MDA231 cell lines	IC_{50} values 28.7 to 53.9 µM	Hou *et al*., 2013
Euphorbia pekinensis	Four casbane diterpenoids	MGC-803, SW620, SMMC-7721, Ketr-3, MCF7, HL60 and A549 cell lines	IC_{50}values 2.2 to 27.3 µM	Tao *et al*., 2013
Excoecaria acerifolia	(1-2) Acerifolin A and B	HL60, SMMC-7721, A549, MCF7 and SW-480 cell lines	IC_{50} values 13.01 to > 40 µM	Wu *et al*., 2013
Isodon excisoides	Six diterpenes (ent-kauranes)	HCT-116, HepG2, A2780, NCIH1650 and BGC-823 cell lines	IC_{50} values 1.09 to 8.53 µM	Dai *et al*., 2015
Jatropha gossypifolia	Abiodone	Lung cancer cells	Anti-cancer activity	Falodun *et al*., 2012

Table 1.3 (Continued)

Sources	Compounds	Cell lines	Activities (IC_{50} and its mechanisms)	References
Juniperus sabina	Sabiperones F	HL-60, A549, MCF7, HepG2 and HCT116 human cancer cell lines	Moderate activity IC_{50} values 6.37 to > 50 μM	Janar *et al*., 2012
Klyxum molle (soft coral)	(1-5) Klymollins T–X (eunicellin-based diterpenoids)	LPS-stimulated RAW 264.7 macrophage and CCRF-CEM, K562, Molt 4 and T47D cells	ED_{50} values 4.2 to16.5 μg/ml	Chang *et al*., 2014
Klyxum simplex (soft coral)	(1) Simplexins A, P-R (eunicellins)	K-562, CCRF-CEM, T47D and MOLT 4 cancer cells	ED_{50} values 2.7 to 30.3 μg/ml	Wu *et al*., 2012
Loxocalyx urticifolius	13-epiloxocalyxin E	A549 and MCF-7 cancer cell lines	IC_{50} values 22.4 μM (A549) and 47.3 μM (MCF-7)	Zhao *et al*., 2017
Malleastrum sp.	Four clerodane diterpenes	A2780 cell line	IC_{50} values 3.01 to 17.9 μM	Liu *et al*., 2015

Table 1.3 (Continued)

Sources	Compounds	Cell lines	Activities (IC_{50} and its mechanisms)	References
Molinaea retusa	(1-2) Cupacinoside and 6-de-Oacetylcupacinoside (diterpene glycosides)	A2780 human ovarian cancer cell line	IC_{50} values 9.5 to 10.9 µM	Eaton *et al*., 2013
Pleurotus eryngii	Eryngiolide A (macrocyclic diterpenes)	HeLa and HepG2 cancer cell lines	Moderate activity	Wang *et al*., 2012
Podocarpus imbricatus	(1-2) Podoimbricatin A and B	A549 and NCI-H292 cancer cell lines	IC_{50}values 9.5 to 47.8 µM	Han *et al*., 2014
Pteris henryi	Henrin A (Ent-kauranes)	KB, HCT116, MCF-7 and A549 cell lines	IC_{50} values > 20 µg/ml	Li *et al*., 2015
Rabdosia lophanthoides	Nine abietane diterpenoids	HepG2 and HCF-8 cell lines	IC_{50} values 4.68 to 9.43 µM (HepG2) and 9.12 to 13.53 µM (HCF-8)	Lin *et al*., 2016
Salvia amarissima	(1-3) Amarissinins A–C	MCF7, MDA-MB-231, HeLa, HCT-15 and HCT-116 cell lines	IC_{50} values 1.05 to19.3 µg/ml	Bautista *et al*., 2016

Table 1.3 (Continued)

Sources	Compounds	Cell lines	Activities (IC_{50} and its mechanisms)	References
Sarcophyton glaucum (*soft coral*)	(1) Sarcophytolol (2-3) sarcophytolide B and C (cembranoids)	HepG2, MCF-7 and PC-3 cells	IC_{50} values 9.3 to 25 µM	Al-Lihaibi *et al*., 2014
Scapania irrigua	(1-11) Scapairrins A–Q (labdanes)	A549, MDA-MB-231, A2780, HeLa, HT-29 and HUVEC cell lines	IC_{50} values 3.0 to >10.0 µM	Zhang *et al*., 2015
Scutellaria barbata	(1) Scutebata D (2) Scutebata S- T (neo-clerodanes)	HL-60, KB, LU-1, MCF7 and Hep-G2 cell lines	IC_{50} values10.67 to>100.10 µM	Thao do *et al*., 2014
Scutellaria coleifolia	Twenty neo-clerodane type diterpenoids	HeLa, A549, KB and MCF7 cell lines	IC_{50} values 36.2 to 82.5 µg/ml	Kurimoto *et al*., 2016

Table 1.3 (Continued)

Sources	Compounds	Cell lines	Activities (IC_{50} and its mechanisms)	References
Scutellaria strigillosa	(1-3) Scutestrigillosins A–C	HONE-1, P-388, MCF7 and HT29 cell lines	IC_{50} values 3.5 to 7.7 µM	Dai *et al*., 2016
Sinularia (soft coral)	(1-4) Numerosol A–D (cembranoids)	Numerosa P-388 (mouse lymphocytic leukaemia) cell	ED_{50} values 6.9 µM	Tseng *et al*., 2014
Sinularia leptoclados (*soft coral*)	Leptoclalin A (spatanes)	K-562 and T-47 D cell lines	IC_{50} values 12.8 and 15.4 µg/ml	Tsai *et al*., 2013
Sinularia sp. (soft coral)	Ten diterpenes	Human tumour cell lines (SF-268, MCF-7 and H460)	IC_{50} between 6.8 to 175 µM	Chen *et al*., 2012
Trigonostemon xyphophylloides	(1-3) Trigoxyphins J–N	SPC-A-1 and SGC-7901 cancer cell lines	IC_{50} values 4.08 to 5.0 µM	Yang *et al*., 2013
Vietnamese Caesalpinia sappan	Cassane diterpenes (1-8) Tomocins A–H	PANC-1 cancer cells	IC_{50} values 51 to 75 µM	Nguyen *et al*., 2016
Vitex trifolia	(1-6) Vitextrifolins A–G (Labdanes)	Human cancer cell lines (A549, HCT116, HL-60)	IC_{50} values > 5 µg/ml.	Zheng *et al*., 2013

Table 1.3 (Continued)

Sources	Compounds	Cell lines	Activities (IC_{50} and its mechanisms)	References
B. Reactive oxygen species (ROS)-mediated and/or pro-oxidative effects				
A synthetic diterpene	ent-Kaurane diterpene (DS2)	Human esophageal cancer cell (EC9706, EC109 and HEECs), Liver cell (HL-7702) lines	Mitochondria-mediated cell death associated with BAX regulation and ROS generation were observed by ent-kuaranes.	Ma *et al*., 2016
Caesalpinia pulcherrima	Thirteen diterpenes such as (1) 6β-Cinnamoyl-7 β - hydroxyvouacapen-5α-ol (2) Pulcherrin A (3-5) Pulcherrimin B-D	MCF-7, HeLa and PC-3 cell lines	These diterpenes exhibited cytotoxicity with IC_{50} values ranging from 7.02 to 36.49 μM. Pulcherrimin B and D decreased ROS generation.	Erharuyi *et al*., 2016

Table 1.3 (Continued)

Sources	Compounds	Cell lines	Activities (IC_{50} and its mechanisms)	References
Cyathus africanus	Cyathin Q (Cyathanes)	HCT116 cells	Compound increased mitochondrial ROS, downregulated BCL-2 protein and upregulated Bim protein. Compound cleaved autophagy-related protein ATG5 and caused apoptotic cell death.	He *et al*., 2016
Grangea maderaspatana	(1-4) Gramaderins A–D and other three (5-7)	(1) FMLP/CB-induced human neutrophils (2) Inhibition of ROS generation	Their activity showed IC_{50} between 4.70 – 10 μM.	Chang *et al*., 2016

Table 1.3 (Continued)

Sources	Compounds	Cell lines	Activities (IC_{50} and its mechanisms)	References
Isodon phyllostachys	Thirty two enmein-type ent-kaurane diterpenoids (enmein-type entkaurane diterpenoids)	HL-60, SMMC-7721, A-549, MCF-7 and SW-480 cell lines	These compounds reduced ROS levels and showed cytotoxicity with IC_{50} values ranging from 0.74 to 5.0 μM.	Yang *et al*., 2016
Rabdosia rubescens	Oridonin	HEp-2 cells ROS and caspase-9 dependent apoptosis	Anti-oxidative and apoptotic effects were observed by oridonin treatments.	Kang *et al*., 2015
Tinospora sagittata	4 diterpenes (clerodanes)	Six human cancer cell lines including RAW264.7	Compounds exhibited the cytotoxic effect against cancer cells and also exhibited inhibitory activities on LPS-induced NO production.	Zhang *et al*., 2016a

Table 1.3 (Continued)

Sources	Compounds	Cell lines	Activities (IC_{50} and its mechanisms)	References
C. Apoptosis, cell cycle arrest and autophagy				
Andrographis paniculata	Andrographolide	Nasopharyngeal carcinoma (NPC)	This compound induced apoptotic cells and cell cycle arrest, and down regulation of NF-κB.	Peng *et al*., 2015
Andrographis paniculata	Semi synthesis (andrographolide used as a starting material) Indolo[3,2-β]andrographolide	MCF-7, HCT116, DU145	This compound showed an anti-proliferative effect with an IC_{50} values between 1.22 and 1.85 μM. It also induced apoptosis and cell cycle arrest at S phase.	Song *et al*., 2015
Brassica oleracea var. *capitata*	chlorophyll-derived diterpenoid Phytol	Huh7 and HepG2	Compound exhibited antitumor activity via apoptosis and it effect activated caspase-9/3 and inhibited the epithelial mesenchymal transition signaling in cancer cells.	Kim *et al*., 2015

Table 1.3 (Continued)

Sources	Compounds	Cell lines	Activities (IC_{50} and its mechanisms)	References
Brassica oleracea var. *capitata*	chlorophyll-derived diterpenoid Phytol	Huh7 and HepG2	Compound exhibited antitumor activity via apoptosis and it effect activated caspase-9/3 and also inhibited the epithelial mesenchymal transition signaling in cancer cells.	Kim *et al*., 2015
Caryopteris incana	Caryopincaolide A–L (Abietanes)	Human cancer cells (Hey and A-549)	Caryopincaolide A showed a potent cytotoxic activity and induced apoptosis in Hey and A-549 cells.	Zhao *et al*., 2016
Isodon adenolomus	Ponicidin	HT29 colorectal cancer cell line	Compound induced Cell cycle arresting at G1 phase, induced apoptosis via AKT and MEK signaling pathways, and affected on caspase-3 and BAX expression.	Du *et al*., 2015

Table 1.3 (Continued)

Sources	Compounds	Cell lines	Activities (IC_{50} and its mechanisms)	References
Isodon eriocalyx	Eriocalyxin B	Human pancreatic adenocarcinoma (PANC-1,SW1990, CAPAN-1 and CAPAN-2) cell lines	- Eriocalyxin B affected on caspase-dependent apoptosis and also induced cell cycle arrest at the G2/M phase.	Li *et al*., 2012
Isodon rubescens	Jaridonin	MGC-803 cell line	This compound affected on the cell cycle regulators (ATM, Chk1, Chk2, phosphorylated Cdc2 and CDK2) and induced cell cycle arrest at G2/M phase.	Ma *et al*., 2016
Isodon xerophilus	Xerophilusin B	Esophageal squamous cell carcinoma (ESCC) cell lines	Induced G2/M cell cycle arrest and promoted apoptosis by cytochrome-C dependent pathway, activating caspase cascade, especially caspase-9 and caspase-3.	Yao *et al*., 2015

Table 1.3 (Continued)

Sources	Compounds	Cell lines	Activities (IC_{50} and its mechanisms)	References
Rabdosia rubescens (Isodon plant)	Oridonin	Uveal melanoma OCM-1 and MUM2B cell lines	Oridonin reduced cell viability and induced apoptosis, and mediated apoptosis by inhibition of Fas and activation of BCL-2 through apoptotic pathways.	Gu *et al*., 2015
Rosemarinus officinalis	Carnosic acid	HepG2 cells	This compound affected on autophagic cell death through inhibition of the Akt/mTOR pathway	Gao *et al*., 2015
Salvia miltiorrhiza Bunge.	Tanshinone IIA	CaSki, SiHa, HeLa and C33a cells	This compound induced cell cycle arrest at S phase and apoptosis.	Munagala *et al*., 2015
Salvia miltiorrhiza Bunge.	Tanshinones	Apoptosis-resistant colon cancer cells	Cytotoxicity caused by tanshinone depending autophagic cell death and p53-mediated cytotoxicity.	Hu *et al*., 2015

Table 1.3 (Continued)

Sources	Compounds	Cell lines	Activities (IC_{50} and its mechanisms)	References
Salvia miltiorrhiza Bunge.	Tanshinone IIA	Human ovarian carcinoma cells (TOV-21G, SKOV3 and OVCAR3)	This compound enhanced TRAIL and induced apoptosis by up-regulating DR5 receptors through the ROS-JNKCHOP pathway.	Chang *et al*., 2015 Lin *et al*., 2015
Salvia officinalis	Sclareol	MG63 osteosarcoma cells	Scalreol induced apoptosis, accompanied by G1-phase cell cycle arrest and loss of $\Lambda\Psi_m$	Wang *et al*., 2015
Scoparia dulcis	Scopadulciol	AGS human gastric adenocarcinoma cells	This compound triggered TRAIL-induced apoptosis.	Fuentes *et al*., 2015
Tripterygium wilfordii	Triptolide (diterpenoid triepoxides)	Human RCC cells	Compound activated TRAIL-induced apoptosis through altered TRAIL death receptor and heat shock protein expression.	Brincks *et al*., 2015

Table 1.3 (Continued)

Sources	Compounds	Cell lines	Activities (IC_{50} and its mechanisms)	References
Tripterygium wilfordii	Triptolide (diterpenoid triepoxides)	Colon cancer cell lines HCT116 and HT29	Triptolide induced cell cycle arrest at G1 phase by inhibiting E2F transcriptional regulator.	Oliveira *et al*., 2015
Tripterygium wilfordii	Tripchlorolide	A549 cells	Tripchlorolide had an effects on autophagic cell death	Chen *et al*., 2016
Vellozia kolbekii	(5R,8R,9S,13R)-halim-1,10-ene-15,16-diol (halimanes)	SF-295, MDAMB-435 and HCT-8	This compound affected on cell cycle arresting at S and G2M phases.	Silva *et al*., 2015

Table 1.3 (Continued)

Sources	Compounds	Cell lines	Activities (IC_{50} and its mechanisms)	References
D. Effects on cell proliferation and differentiation				
1,2,3-Triazole-substituted carnosic acid and Carnosol derivatives	Semi-synthesis of abietane diterpenes used Carnosic acid and carnosol as a starting material.	MRC-5, AGS, SK-MES-1 and J82 cells	Carnosoic acid γ lactones showed the most active for anti-proliferative compounds and their IC_{50} values were 39.2–48.9 μM.	Pertino *et al*., 2015
Caesalpinia sappan	Caesalsappanins A–L	A small panel of human cancer cell lines	Caesalsappanins J exhibited anti-proliferative activity against KB cell line with an IC_{50} value of 7.4 μM.	Ma *et al*., 2015
Euphorbia osyridea	2,3,5,7,8,9,14,15-octahydroxyjatropha-6(17), 11E-diene derivatives	Caov-4 and OVCAR-3 cancer cell lines (jathophanes)	Compound inhibited cell proliferation effect via apoptosis.	Ghanadian *et al*., 2015

Table 1.3 (Continued)

Sources	Compounds	Cell lines	Activities (IC_{50} and its mechanisms)	References
Euphorbia piscatoria	Four diterpenes	L5178Y mouse T lymphoma; human MDR gastric, pancreatic and colon cell lines	Their compound exhibited an anti-proliferative effect (IC_{50} values between 39.51 to 66.02 μM)	Reis *et al*., 2014
Kaempferia pulchra	Kaempulchraols A–H	A549, HeLa, PANC-1, PSN-1, MDA-MB-231 and TIG-3 cell lines	These compounds showed anti-proliferative and anticancer activity.	Win *et al*., 2015
Pseudolarix kaempferi	Pseudolaric acid B	HeLa cells	A compound inhibited cell proliferation and induced apoptosis via Akt-dependent pathway.	Li and Hong, 2015
Pseudolarix kaempferi	Pseudolaric acid B	MDR gastric cancer cell line	This compound inhibited cell proliferation, induced apoptosis, circumvented MDR and increased the sensitivity of chemotherapeutic	Yu *et al*., 2015

Table 1.3 (Continued)

Sources	Compounds	Cell lines	Activities (IC_{50} and its mechanisms)	References
			agents in vitro by down-regulating the expression of P-gp and COX-2	
Rabdosia rubescens	Oridonin	HCT-116 and LoVo cells	Inhibited cell proliferation and induced apoptosis	Yang *et al*., 2015
Salvia miltiorrhiza	Tanshinone IIA	Acute promyelocytic leukaemia (APL) cells	Compound inhibited proliferation and further triggered apoptosis.	Zhang *et al*., 2016
Salvia przewalskii	Crypotanshinone	DU145 prostate cancer cells	A compound inhibited cell proliferation and induced apoptosis via PI3K/AKT signaling pathway.	Yao *et al*., 2015
Stillingia sanguinolenta	Tonantzitlolone A and its synthetic enantiomers		Compounds exhibited moderate anti-proliferative effect by cytostatic activity and induction of monoastral spindle formation in cell	Pfeffer *et al*., 2016

Table 1.3 (Continued)

Sources	Compounds	Cell lines	Activities (IC_{50} and its mechanisms)	References
E. Effects on drug-resistant cancer cells				
Euphorbia exigua	Three jatrophane diterpenes	L5178 mouse lymphoma cells	Diterpenes significant affected on MDR reversing activity.	Rédei *et al*., 2015
Euphorbia lathyris	Lathyrol diterpene	Multidrug-resistant MCF-7/ADR cells	Compound showed MDR reversal activity.	Jiao *et al*., 2015
Euphorbia sororia	Jatrophane diterpenoid ester	KBv200 cells	Compound showed strong MDR-reversal activity at 10 μM.	Lu *et al*., 2014
Euphorbia sp.	Six diterpenes	LoVo and doxorubicin-resistant LoVo/ Dx cells	Diterpenes reduced cytotoxicity and showed a high potency of anti-MDR.	Wiśniewski *et al*., 2016

Table 1.3 (Continued)

Sources	Compounds	Cell lines	Activities (IC_{50} and its mechanisms)	References
F. Miscellaneous effects				
Acanthopanax koreanum	Acanthoic acid	B16 melanoma cells	Compound inhibited melanin biosynthesis through down-regulation of microphthalmia-associated transcription factor.	Yoon *et al*., 2013
Andrographis paniculata	Andrographolide	Esophageal (ECA109) cancer cell	Compound exhibited anti-proliferative effect and their effect increased in Caspase3/BAX protein, while decrease in BCL-2/NF-κB expression.	Wang *et al*., 2016
Andrographis paniculata	Andrographolide 10 mg/kg	Hepatoma cancer cells	Compound decreased VEGFD expression via inducing c-Fos protein.	Ji *et al*., 2015

Table 1.3 (Continued)

Sources	Compounds	Cell lines	Activities (IC_{50} and its mechanisms)	References
Andrographis paniculata	Andrographolide and analogues	Various cell lines	Compounds showed difference of their mechanisms.	Mishra *et al*., 2015
Casearia grewiifolia	Two clerodane diterpenoids	Human KB, HepG-2, LU-1 and MCF-7 cancer cells	These compounds showed significant selective inhibition against cancer cells	Nguyen *et al*., 2015
Coffee beans	Cafestol	Human renal carcinoma Caki cells	Compound enhanced ABT-737 sensitivity in cancer therapy. Down-regulation of Mcl-1 expression and up regulation of Bim expression mediated cytotoxic effect.	Woo *et al*., 2014
Euphorbia dendroides	Jatrophanes	Colorectal multidrug resistant (MDR) cells (DLD1-TxR)	Compound strongly inhibited P-gp, higher than R(+)-verapamil and tariquidar.	Jadranin *et al*., 2013

Table 1.3 (Continued)

Sources	Compounds	Cell lines	Activities (IC_{50} and its mechanisms)	References
Ginkgo biloba	Ginkgolide A	N2a cell lines	Compound affected on phosphorylation of PI3K and Akt.	Chen *et al*., 2012
Jatropha curcas Linn	Phorbol ester (tigliane family of diterpenes)	P4E6, LNCaP and PC3	Compounds showed tumor genesis effect.	Schmitt *et al*., 2014
Oridonin	Jesridonin structural modification of Oridonin	EC109 cell line and on tumour xenografts in mice	Compound showed antitumor activity.	Wang *et al*., 2015
Plectranthus excisus	A diterpene		Compound increased the expression of p53 and Cdk1A, while decreased in Cdk2.	Liu *et al*., 2015
Rhizophora stylosa	Rhizovarins A–F	HL-60 and A-549 cell lines	Compounds showed an antitumor activity.	Gao *et al*., 2016
Rosemary extracts	Carnosic acid, carnosol and rosmanol	Varieties of cell line	These compound exhibited anticancer effect.	Petiwala and Johnson, 2015

Table 1.3 (Continued)

Sources	Compounds	Cell lines	Activities (IC_{50} and its mechanisms)	References
Rosmarinus officinalis	Carnosic acid and carnosol	HT-29 colon cancer cells	Nrf2-mediated anti-cancer activity is caused by these compounds.	Valdés *et al*., 2017
Sacrophyton species (soft coral)	Cembranoids (soft	Various cancer cells	Cembranoid showed anticancer effect.	Cheng *et al*., 2014
Salvia carnosa	Carnosol	PNT2 and B16F10 cell lines	Compound showed anti-cancer activity and it also activated melanogenesis.	Alcaraz *et al*., 2013
Salvia cavaleriei	11α, 12 α –epoxyleukamenin E	Normal human colon mucosal epithelial cells	Compound exhibited an anticancer activity and its effect triggered on Wnt signaling pathway.	Ye *et al*., 2015
Salvia miltiorrhizae	Tanshinone I	HCT116 and SW480 cells	Compound affected on ERK1/2 and cyclin D1 that further mediated cytotoxic effect.	Kim *et al*., 2015

Table 1.3 (Continued)

Sources	Compounds	Cell lines	Activities (IC_{50} and its mechanisms)	References
Salvia miltiorrhizae	Tanshinone IIA	Drosophila melanogaster	Compound induced the expression of Cx43 and Cx26.	Jiang *et al*., 2015
Tinospora crispa	Crispene E (clerodanes)	STAT3-dependent MDA-MB 231breast cancer cell line	Compound selectively inhibited STAT3 expression and affected cyclin D1, Fascin and BCL-2	Mantaj *et al*., 2015

1.6 *Croton* species

Croton is members of plants belonging to subfamily of Crotonoideae of Euphorbiaceae. Plants belong to genus croton are discovered more than 1,300 species and there are extensive angiosperms. According to the botanical description of Crotons, Crotons are described following; deciduous shrubs or small trees, variously stellate-hairy or with lepidote scales, stipules minute, leaves alternate; blades with 2 glands at base. The flowers of plants are monoecious, dioecious or a combination of both, inflorescence racemose, usually terminal; flowers 5-merous, males with small disk glands, stamens 5-30; females often with vestigial petals; ovary 3-locular. About 800 species or more than are widespread distributed in the tropical and sub-tropical regions including Africa and America and it slightly less than 100 species in Asia. In Thailand has been found 30 species (Salatino *et al*., 2007; Welzen, 2010; Flora of Thailand).

The chemistry of *Croton* species is various types of secondary metabolites. Terpenoid compounds are mainly found as a major component found in Crotonoideae and Euphorbiaceae. Different types of terpenes are predominantly discovered including diterpenoids, which normally belong to phytanes (acyclic diterpenes), cyclophytanes and its derivatives such as cembranoid, clerodane, neoclerodane, halimane, isopimarane, kaurane, secokaurane, labdane, phorbol and trachylobane skeletal types, pentacyclic tri-terpenoids or steroids. Other types of secondary metabolites are also found in *croton* species, mono- and sequitepenes, alkaloids, phenolic substances including flavonoids, lignoids, proanthocyanidins, for instances.

About the biological and pharmacological activities of *Croton* species, since there are consisted a variety of compounds that are metabolized by its own, so there are several components and further active on several activity such as anti-lipidemic, wound healing, anti-gastric ulcer, anti-diarrheic, immunodulary, anti-bacterial, anti-fungal, anti-viral, anti-malarial, anti-mutagenic, mutagenic, anti-oxidant, myorelaxant, anti-spasmodic, anti-hypertensive, anti-cancer, anti-inflammatory, anti-nociceptive activities, etc (Salatino *et al*., 2007).

Focusing *Croton* species in Thailand, there has been found 30 species and some species has been investigated on phytochemical, biological and pharmacological studies. Numbers of *Croton* species locate in Thailand and their activities are also summarized (Table 1.4).

Table 1.4 Chemical constituents and their activities of *Croton* species (Thailand).

Species	Type of compounds	Chemical constituents	Activities	References
1) *Croton acutifolius*	-	-	(1) Ethnobotanical study	Khuankaew *et al*., 2014
2) *Croton argyratus*				
Leaves			(1) Anti-plasmodial activity The growth of Inhibition = 60	Noor Rain *et al*., 2007
			(1) Anti-plasmodial activity (2) Brine shrimp toxicity assay (2) Cytotoxicity assays	Horgen *et al*., 2001
3) *Croton bonplandianus*				
Leaves	Acetone extract		(1) Cytotoxic (2) Pro-apoptotic activities against lung cancer (A549)	Bhavana*et al*., 2016

Table 1.4 (Continued)

Species	Type of compounds	Chemical constituents	Activities	References
Aerials	Essential oil	(1) β-caryophyllene (16.7%) (2) germacrene D (14.7%) (3) borneol (8.3%) (4) Z- β-damascenone (6.0%) (5) isobornyl acetate (6.2%) (6) α-humulene (6.1%) (7) germacrene A (5.2%) (8) caryophyllene oxide (4.5%) (9) sesquiterpene hydrocarbons (60.1%)	(1) Analysis using GC-MS	Joshi, 2014

Table 1.4 (Continued)

Species	Type of compounds	Chemical constituents	Activities	References
4) *Croton cascarilloides*				
Stems	Crotofolanes	(1-6) crotocascarins L-Q		Kawakami *et al*., 2016
	Nor-crotofolanes	(7) neocrotocascarin		
Leaves	crotofolanes and	(1-3) crotocascarins I-K		Kawakami *et al*., 2015
	nor-crotofolanes	(4) crotocascarin γ		
Stems	crotofolane and	(1-8) crotocascarins A-H		Kawakami *et al*., 2013
	nor-crotofolanes	(9) crotocascarins α		
		(10) crotocascarins β		
Stems	Megastigmane	(1-7) crotonionosides A–G,		Kawakami *et al*., 2010
	glycosides	(8-9) dendranthemosides A- B		
		(10) citroside A		

Table 1.4 (Continued)

Species	Type of compounds	Chemical constituents	Activities	References
5) *Croton caudatus*				
	Halimanes, Eudesmanes, Tiglianes	(1) ent-15,16-epoxyhalim-5(10),13(16),14-trien-18- carboxylic acid (2) margocin (3) pomiferin D (4) pomiferin E (5) 15-hydroxy-7-oxoabieta-8,11,13-triene, 5-epieudesm-4(15)-ene-1β,6β-diol (6) crotusins A-C	(1) cytotoxicity	Chen *et al*., 2016
Leaves	Extract	-	(1) Protective effect	Dey *et al*., 2015

Table 1.4 (Continued)

Species	Type of compounds	Chemical constituents	Activities	References
Twigs and leaves	Abietanes	(1) crotontomentosin A (2-5) crotontomentosins B-E	(1) Cytotoxicity	Song *et al*., 2015
Stems	Flavonones	(1) Crotoncaudatin 3,5,6,7,8,3',4'-heptamethoxyflavone (2) tangeretin (3) nobiletin (4) 5,6,7,4'-tetramethoxy-flavone (5) sinensetin (6) kaempferol (7) tiliroside (8) kaempferol-3-O-rutinoside (9) rutin		Zou *et al*., 2010
6)*Croton columnaris*	-	-	-	-

Table 1.4 (Continued)

Species	Type of compounds	Chemical constituents	Activities	References
7) *Croton crassifolius*				
Roots		Penduliflaworosin	(1) Angiogenic Effect via VEGF Receptor-2 Signaling Pathway	Liang *et al*., 2017
Roots	Clerodanes	(1-3) crassifolius A-C	(1) Cytotoxicity (2) Apoptosis mechanisms	Tian *et al*., 2017
Roots	Diterpenoids	(1-8) crassins A-H	(1) Cytotoxicity	Yuan *et al*., 2017
Roots	Patchoulane-type sesquiterpenoid glycoside	(1-6) 1 new and 6 known	(1) Cytotoxic activities	Yuan *et al*., 2017
Roots	Pyran-2-one derivative	(1) crotonpyrone C	(1) Anti-angiogenic activity	Huang *et al*., 2016
Roots	Diterpnes	(1-6) crassifolin J-O	(1) Anti-angiogenic activity	Wang *et al*., 2016

Table 1.4 (Continued)

Species	Type of compounds	Chemical constituents	Activities	References
Roots	Clerodanes	(1-3) cracrosons A–C	(1) Cytotoxicity	Qiu *et al*., 2016
		(4) crassifolin		
		(5-6) crassifolin H-I		
		(7-8) crassifolin A-B		
		(9) isoteufin		
		(10) teucvidin		
		(11) teucvin		
		(12) chettaphanin I		
		(13) (12S)-15,16-epoxy-6β-methyoxy-19-norneoclerodane-4,13(16),14-triene-18,6α,20,12-diolide		
		(14) cyperenol		
		(15) cyperenoic acid		

Table 1.4 (Continued)

Species	Type of compounds	Chemical constituents	Activities	References
		(16) acetyl aleuritolic acid (17) lupeol		
Roots	Sesquiterpenes	(1) cyperenoic acid (2) 8-hydroxy-α-guaiene (3) (+)-guaia-l(10),ll-dien-9-one	(1) Anti-angiogenic activity and its mechanisms.	Huang *et al*., 2015
Roots	Norclerodanes			Zhang *et al*., 2015
Roots	Clerodanes	(1) chettaphanin I (2) Penduliflaworosin (3) 1,4-methano-3-benzoxepin-2(1H)-one (4) Isoteucvin (5) teucvin		Hu *et al*., 2012

Table 1.4 (Continued)

Species	Type of compounds	Chemical constituents	Activities	References
Roots	Clerodanes	(1-7) clerodane diterpenes 1 -7 (2) spiro[furan-3-(2H),1'(2'H)-naphthalene]-5'-carboxylic acid	(1) Antiviral activity against herpes simplex virus type 1 (HSV-1)	Wang *et al*., 2012
Roots	Ethanol extract		Anti-nociceptive Anti-inflammatory effects	Zhao *et al*., 2012
Roots	Sesquiterpene acid	(1) cyperenoic acid (2) acetylaleuritolic acid (3) chettaphanin-I (4) β-amyrin	(1) Cytotoxicity	Boonyarathanakornkit *et al*.,1988
8) *Croton decalvatus*	-	-	-	-
9) *Croton delpyi*	-	-	-	-
10) *Croton griffithii*	-	-	-	-

Table 1.4 (Continued)

Species	Type of compounds	Chemical constituents	Activities	References
11) *Croton hirtus*				
Roots	the bis-nor dolabradane dolabradanes kauranes cyclopropakauranes hirtusanes germacradiene esters			Fuentes *et al*., 2004
12) *Croton hutchinsonianus*				
Branches		(1) 3'-(4"-hydroxy-3",5"-dimethoxyphenyl)-propyl benzoate) (2) 3'-(4"-hydroxyphenyl)-propyl benzoate	COX-1, COX-2 inhibitors and antifungal agents	Athikomkulchai *et al*., 2006

Table 1.4 (Continued)

Species	Type of compounds	Chemical constituents	Activities	References
		(3) 3'-(4"-hydroxy-3"-methoxyphenyl)-propyl benzoate (4) poilaneic acid (5) farnesyl acetone (6) 4-hydroxybenzaldehyde		
13) *Croton kerrii*				
14) *Croton kongensis*				
	Nor-lignan	kongensin A	(1) Anti-necroptosis (2) Apoptosis induction -	Li *et al*., 2016

Table 1.4 (Continued)

Species	Type of compounds	Chemical constituents	Activities	References
Twigs and leaves	Diterpenes	(1) 4 β-hydroxy-3-oxo-ent-kaur-16-ene (2) 8S-(-)-8-(4-hydroxy-3-methoxybenzoyl)-dihydrofuran-8(8'H)-one (3) ent-7α,14β-dihydroxykaur-16-en-15-one (4) ent-18-acetoxy-7a,14βdihydroxykaur-16-en-15-one (5) (1R,5R,6S)-6-(4-hydroxy-3-methoxypheyl)-3,7-dioxabicyclo[3.3.0]octan-2-one (6) pinoresinol (7) matairesinol		Sun *et al*., 2014

Table 1.4 (Continued)

Species	Type of compounds	Chemical constituents	Activities	References
	secokaurane diterpenes	(1) ent-8,9-seco-7α,11 β-diacetoxykaura-8(14),16-dien-9,15-dione, (2) ent-8,9-seco-8,14-epoxy-7α-hydroxy-11 β-acetoxy-16-kauren-9,15-dione, (3) ent-8,9-seco-7α-hydroxy-11 β-acetoxykaura-8(14),16-dien-9,15-dione (4) ent-7 β-hydroxy-15-oxokaur-16-en-18-yl acetate	(1) Antimycobacterial activity (2) Antimalarial activity (3) Cytotoxicity	Thongtan *et al*., 2003

Table 1.4 (Continued)

Species	Type of compounds	Chemical constituents	Activities	References
15) *Croton kongkandanus*	-	-	-	-
16) *Croton krabas*	-	-	-	-
17) *Croton lachnocarpus*				
Roots	Triterpenoid saponin	(1) saponin, 3-O-β-D-xylopyranosyl spathodic acid (2) myriaboric acid (3) 3 β-acetyl-erythrodiol (4) 3 β-acetyl-oleanoic acid (5) (24S)-24-ethylcholesta-3β,5α,6β-triol	(1) Cytotoxic activity	Pan *et al*., 2014
18) *Croton longissimus*	-	-	-	-
19) *Croton mekongensis*	-	-	-	-

Table 1.4 (Continued)

Species	Type of compounds	Chemical constituents	Activities	References
20) *Croton oblongifolius*	Primaranes	Oblongifoliol	(1) Cytotoxic acitity	Rao *et al*., 1968; Aiyar and Seshadri, 1970; Suwancharoen *et al*, 2010
		deoxyoblongifoliol		
		Oblongifolic acid		
		Acanthoic acid		
	Cembranoids	Crotocembraneic acid		Roengsumran *et al*., 1997; Podhom *et al*., 2007
		Neo-crotocembranic acid		
		Furanocembranoid 1-4		
	Labdanes	(1) Labda-7,12 (*E*), 14 triene	(1) Cytotoxic acitity	Roengsumran *et al*., 1998; Roengsumran *et al*., 2000; Roengsumran *et al*., 2002; Roengsumran *et al*., 2001
		(2) Labda-7,12 (*E*), 14 triene-17 al		
		(3) Labda-7,12 (*E*), 14 triene-17 ol		
		(4) Labda-7,12 (*E*), 14 triene-17 oic acid		
		(5) 2-acetoxy-3-hydroxy-labda-8 (17), 12 (*E*)-14-triene		
		(6))3-acetoxy-3-hydroxy-labda-8 (17),		

Table 1.4 (Continued)

Species	Type of compounds	Chemical constituents	Activities	References
		12 (*E*)-14-triene (7) 2,3-dihydroxy-labda-8 (17), 12 (*E*)-14-triene, (8) Nedrorellol		
	Kauranes	(-)-ent-kuar-16-en-19-oic acid	(1) Inhibitory of Na+, K+ - ATPase activty	Ngamrojnavanich *et al*., 2003
	furoclerodanes	(1) Croblongifolin (2) Crovatin (3) 3,4,15,16-diepoxy-cleroda-13(16),14 diene-12,17-olide	(1) Cytotoxic acitity	Roengsumran *et al*., 2001; Roengsumran *et al*., 2011
	halimanes	(1) Crotohalimaneic acid (2) Crotohalimoneic acid (3) 12-benzoylxycrotohalimaneic acid	(1) Cytotoxic acitity	Roengsumran *et al*., 2003
	Other types -Trisubstituted furan	(1) 3(3′-methoxy-5′-phenylfuran-2′-yl)propan-1-ol	(1) Cytotoxic acitity	Roengsumran *et al*., 2011

Table 1.4 (Continued)

Species	Type of compounds	Chemical constituents	Activities	References
21) *Croton phuquocensis*	-	-	-	-
22) *Croton poilanei*	-	-	-	-
23) *Croton poomae*	-	-	-	-
24) *Croton robustus*				
Stem barks		(1) trachyloban-19-oic acid (2) trachyloban-19-ol and poilaneic acid	(1) Cytotoxic activity against gastric carcinoma and colon carcinoma	Ngamrojnavanich *et al*., 2003
25) *Croton roxburghii*				
Barks	Extract		(1) Anti-steroidogenic activity	Gupta *et al*., 2004
Barks and leaves	Extract (aqueous and alcoholic)		(1) Antibacterial activity	Panda *et al*., 2010

Table 1.4 (Continued)

Species	Type of compounds	Chemical constituents	Activities	References
Barks	Acetone, ethanol, methanol and water extracts		(1) Antibacterial (2) Antioxidant activities	Rath *et al*., 2011
Barks	Essential oil	(1) α-pinene (2) β-pinene (3)α-phellandrene	(1) Repellent activity against mosquitoes	Vongsombath *et al*., 2012
26) *Croton sepalinus*	-	-	-	-

Table 1.4 (Continued)

Species	Type of compounds	Chemical constituents	Activities	References
27) *Croton stellatopilosus* (*Croton sublyratus*)	Acyclic diterpenes	- Plaunotol (18-hydroxyl-geranylgeraniol) - Ester derivatives of GGOH (Ester A, B, C, D, E and F)	(1) Anti-peptic ulcer activity and gastric protection (2) Anti-bacterial activity (3) Anti-inflammatory activity (4) Anti-cancer activity and apoptosis (DLD-1) (5) wound healing activity (6) Pharmacokinetic study and safety	Ogiso *et al*., 1978;Kitazawa *et al*., 1982; Ogiso *et al*., 1985; Ushiyama *et al*., 1987; Shiratori *et al*., 1993; Koga *et al*., 1996; Koga *et al*., 1998; Murakami *et al*., 1999; Takagi *et al*., 2000; Wallace and Ma, 2001;Fu *et al*., 2005; Kawai *et al*., 2005; Sasaki *et al*., 2007; Yamada *et al*., 2007; Yoshikawa *et al*., 2009; Khovidhunvit *et al*.,2011; Premprasert *et al*., 2013; Chaotham *et al*., 2013

Table 1.4 (Continued)

Species	Type of compounds	Chemical constituents	Activities	References
	Furano clerodanes	- Plaunol derivatives (Plaunol A, B, C, D, E and F)	(1) Anti-shay ulcer activity (2) Anti-inflammatory activity (plaunol E and F)	Kitazawa *et al*., 1980; Takahashi *et al*., 1983; Kitazawa *et al*., 1979; Kitazawa *et al*., 1980; Premprasert *et al*., 2013
	Kauranes	ent-16β, 17-dihydroxykaurane		Kitazawa and Ogiso, 1981
	Labdanes	ent-13α-hydroxy-13-epimanool		Kitazawa and Ogiso, 1981
28) *Croton thorelii*	-	-	-	-
29) *Croton tiglium*				
Twigs and leaves	phorbol esters		(1) Cytotoxic activity	Jiang *et al*., 2017
Seeds	Extracts (methanol)		(1) Proliferation and apoptosis	Li *et al*., 2016
Stems, leaves, seeds	Ethanol extracts		antidermatophytic activities	Lin *et al*., 2016

Table 1.4 (Continued)

Species	Type of compounds	Chemical constituents	Activities	References
Leaves	tigliane diterpenes	(1-5) Compound (6) 12-O-tiglylphorbol-13-acetate (7) crotignoid F (8) phorbol	(1) Antitubercular activity (2) Cytotoxic activity	Zhao *et al*., 2016
Branches and leaves	phorbol diesters	(1) 20-deoxy-20-oxophorbol 12-tiglate 13-(2-methyl)butyrate. (2) 12-O-acetylphorbol-13-Isobutyrate (3) 12-O-benzoylphorbol-13-(2-methyl)butyrate (4) 12-O-tiglyl-7-oxo-5-ene-phorbol-13-(2 methylbutyrate)	(1) Cytotoxic activity (2) Anti-inflammatory activity	Wang *et al*., 2015

Table 1.4 (Continued)

Species	Type of compounds	Chemical constituents	Activities	References
		(5) 13-O-(2-metyl) butyryl-4-deoxy-4a-phorbol. (6) 12-O-tiglylporbol-13-propionate (7) 12-O-tiglylphorbol-13-isobutyrate (8) 12-O-tiglylphorbol-13-(2-methyl)butyrate (9) tiglin A		
Seeds	Phorbol diester	(1) 12-O-(2-methyl)butyrylphorbol-13-tiglate. (2) 12-O-tiglylphorbol-13-propionate (3)13-O-acetylphorbol-20-oleate. (4) 13-O-acetyl-4-deoxy-4α-phorbol-20-linoleate	(1) Cytotoxicity	Zhang *et al*., 2013

Table 1.4 (Continued)

Species	Type of compounds	Chemical constituents	Activities	References
		(5) 13-O-acetyl-4-deoxy-4 α-phorbol-20-oleate (6) 12-O-tiglyl-4-deoxy-4 α-phorbol-13-decanoate. (7)12-O-tiglyl-4-deoxy-4α-phorbol-13-phenylacetate (8) 12-O-tiglyl-4-deoxy-4α-phorbol-13-(2-methyl)butyrate (9) 12-O-tiglylphorbol-13-isobutyrate (10) 12-O-tetradecanoylphorbol-13-acetate, (11) 12-O-hexadecanoylphorbol-13-acetate		

Table 1.4 (Continued)

Species	Type of compounds	Chemical constituents	Activities	References
		(12) 12-O-tiglylphorbol-13-(2-methyl)-butyrate (13) 12-O-acetylphorbol-13-decanoate (14) 12-O-(2-methyl)-butyrylphorbol-13-isobutyrate, (15) 12-O-acetylphorbol-13-dodecanoate (16) 13-O-acetylphorbol-20-linoleate (17) 12-O-(2-methyl)-butyrylphorbol-13-dodecanoate, (18) 12-O-tiglyl-4-deoxy-4α-phorbol-13-acetate, (19) 12-O-tiglyl-4-deoxy-4 α -phorbol-13-isobutyrate		

Table 1.4 (Continued)

Species	Type of compounds	Chemical constituents	Activities	References
Stems and barks		(1) crotocaudin	(1) Toxicity	Yadav and Singh, 2010
Leaves	pyrazine derivative	(1) crotonine	(2) Analgesic activity	Wu *et al*., 2007
Seeds	Phorbol diesters	(1) 13-O-acetylphorbol-20-(9Z, 12Z-octadecadieno-ate). (2) 13-O-tigloylphorbol-20-(9Z,12Z-octadecadienoate). (3) 12-O-acetylphorbol-13-tigliate. (4) 12-O-decanoylphorbol-13-(2-methylbuty-rate) (5) 12-O-tigloylphorbol-13-(2-methylbutyrate) (6) 12-O-acetylphorbol-13-decanoate,	(1) Anti-HIV-1	El-Mekkawy *et al*., 2000

Table 1.4 (Continued)

Species	Type of compounds	Chemical constituents	Activities	References
		(7) 12-O-(2-methylbutyryl)-phorbol-13-dode-canoate (8) 12-O tetradecanoylphorbol-13-acetate (TPA)		
Seeds	Phorbol diester	(1)13-O-Acetylphorbol-20-linoleate (2) 13-O-Tigloylphorbol-20-linoleate (3) 12-O-Acetylphorbol-13-tiglite (4) 12-O-Decanoylphorbol-13-(2-methylbutyrate) (5) 12-O-tigloylphorbol-13-(2-methylbutyrate) (6) 12-O-Acetylphorbol-13-decanoate	(1) Anti-HIV-1	El-Mekkawy *et al*., 1999

Table 1.4 (Continued)

Species	Type of compounds	Chemical constituents	Activities	References
		(7) 12-O-(2-Methyl butyroyl)phorbol-13-dodecanoate (8) 12-O-tetradecanoylphorbol-13-acetate		
Croton oil Seeds	Croton oil Proteins	(1) phorbol 12-tiglate 13-decanoate (1-3) Crotin I-III	(1) Antileukemic activity (1)Toxicity	Kupchan *et al*., 1976 Stirpe *et al*., 1976
29) *Croton wallichii*	-	-	-	-
30) *Croton santisukii*	-	-	-	-

CHAPTER 2

RESEARCH METHODOLOGY

2.1 Plant materials

The mature leaves and stems of *C. stellatopilosus* Ohba were collected from Klong whale, PrachuapKhiri Khan, Thailand. These materials were kindly supplied from Tipco Foods (Thailand) Public Co. Ltd. A voucher specimen of this plant was deposited in the Herbarium Royal Forest Department in Bangkok, Thailand (No. 21867). The leaves and stems were collected, chopped, sliced into small pieces and dried at 50 °C for overnight. Then, the dried materials were ground into powder using a mechanical grinder.

2.2 Chemicals, reagents and solutions

2.2.1 General chemicals

For phytochemical study, chemical solvents were used either analytical or commercial grades. For commercial grade, solvents were distilled prior to use. The chemicals including acetone, chloroform, dichloromethane, 95% absolute ethanol, ethyl acetate, glacial acetic acid, hexane, hydrochloric acid (37% w/w) and methanol were purchased from Lab-Scan Asia Co. Ltd., (Bangkok, Thailand). Anisaldehyde was obtained from Fluka, Buchs, Switzerland and sulfuric acid was obtained from J.T. Baker, New Jersey, USA. The chromatography, silica gel 60 (SiO_2 60, 230-400 mesh) and TLC plate (silica gel GF-254) were from Merck, Darmstadt, Germany. The silica gel (VertiFlash™ Silica 60A, 40-63 μm) was purchased from vertical chromatography Co. Ltd., (Nonthaburi, Thailand).

2.2.2 Culture media and chemicals for cell culture

Roswell Park Memorial Institute 1640 medium (RPMI 1640) and Dulbecco's Modified Eagle's Medium (DMEM) were from Gibco BRL, California, USA.

For cultured medium and phosphate buffer, all chemicals were analytical grade including sodium bicarbonate ($NaHCO_3$), anhydrous disodium phosphate (Na_2HPO_4), monopotassium phosphate (KH_2PO_4), potassium chloride (KCl) and sodium chloride (NaCl). The supplements in culture medium including fetal bovine serum (FBS) from Gibco BRL, California, USA and the antibiotic drug as a penicillin G (100 unit/ml) plus streptomycin (100 μg/ml) were from Invitrogen®, California, USA.

Trypsin-ethylenediaminetetraacetic acid (trypsin-EDTA) used for trypsinization was purchased from Gibco BRL, California, USA. The chemicals were biotechnological grade including dimethyl sulfoxide (DMSO) and trypan blue, and the reagents including 3-(4,5-dimethyl-2-thiazolyl)-2, 5-diphenyl-2H-tetrazolium bromide (MTT), lipopolysaccharide (LPS) from *Escherichia coli* O55:B5 L4005 (purified by trichloroacetic acid (TCA) extraction) and bovine serum albumin (BSA), were purchased from Sigma-Aldrich, Missouri, USA.

2.2.3 Extraction kits and test kits

β-mercaptoethanol was from Sigma, Missouri, USA. Total RNA Mini kit (blood and cultured cell) used for total RNA extraction was obtained from Geneid Biotech Ltd., New Taipei, Taiwan. One Step SYBR®PrimeScript™ RT-PCR Kit II (perfect Real Time) used for cDNA synthesis and gene amplification was purchased from TaKaRa, Shiga, Japan. Total protein concentration was determined by protein-dye binding method using Bio-Rad Protein assay (Bio-Rad Laboratories, California, USA). Caspase-3, -8,-9 proteolytic activities in cell lysates were determined by colorimetric assay using ApoTarget™ Caspase colorimetric protease assay sample kit, purchased from Invitrogen™, California, USA. For apoptotic detection and cell cycle analysis,

Muse™ Annexin-V ɛt Dead cell reagent and Muse™ cell cycle reagents were purchased form Merck, Darmstadt, Germany. The kit components were summarized in Table 2.1.

Table 2.1 Kit components.

Kits	Components
Total RNA Mini kit (Blood and cultured cell)	- RBC Lysis Buffer (contains detergent and chaotropic salt) - RB Buffer (contains chaotropic salt) - W1 Buffer and Wash Buffer - RNase-free Water - RB Columns and collection tubes
One Step SYBR®PrimeScript™ RT-PCR Kit II (perfect Real Time)	- 2X One Step SYBR RT-PCR Buffer (contains dNTP mixture, Mg^{2+} and SYBR Green I) - PrimeScript 1 step Enzyme Mix 2 (PrimeScriptRTase, RNase Inhibitor, and TaKaRa Ex Taq*HS*.) - RNase Free dH_2O - 50x ROX Reference Dye (for Applied Biosystems 7300 Real-Time PCR System)
Muse™ Annexin-V εt Dead cell kit	- Muse™ Annexin-V εt Dead cell reagent (contains Annexin-V and 7-amino actinomycin D (7-AAD) fluorescence dyes and sodium azide)
Muse™ cell cycle kit	- Muse™ cell cycle reagent (contains propidium iodide (PI) and fluorescence dyes and sodium azide)
Bio-Rad Protein assay	- Protein assay dye reagent (contains Coomassie®Brilliant Blue G-250 dye, phosphoric acid and methanol)
ApoTarget™ Caspase Colorimetric Protease Assay Sampler Kit	- Cell Lysis Buffer (includes Tris buffered saline containing detergent) - 2x Reaction Buffer (contains buffered saline, glycerol and detergent) - Caspase substrate (contains 4 mM of synthetic peptides conjugated to the chromophore, *p*NA (*p*-nitroanilide), in DMSO; Caspase-3 (DEVD-*p*NA), Caspase-8 (IETD-*p*NA) and Caspase-9 (LEHD-*p*NA). - DTT (contains 1 M dithiothreitol)

2.2.4 Authentic standards

The positive substances using for anti-inflammatory activity, caffeic acid phenetylester (CAPE) and indomethacin (IDM) were from Sigma, Missouri, USA and L-nitroarginine (L-NA) was from Gibco BRL, California, USA. For anti-cancer drug, the paclitaxel (Paclitaxel injection USP, Intaxel®) was purchased from Fresenius Kabi (Thailand) Ltd. Bangkok, Thailand.

2.2.5 Other solutions and preparation

Solution	Preparation
Ethidium bromide solution	Ethidium bromide (10 µl) was mixed in 100 ml of distilled water. Handle with care.
Loading buffer	Contained sodium dodecyl sulfate (SDS) (1% w/v), glycerol (50% v/v) and bromophenol blue (0.05% w/v)
Tris-Acetate-EDTA (TAE) buffer, 50x	The 50x TAE buffer composed of tris base (121 g), EDTA trisodium (19.7 g), glacial acetic acid (35 ml). All components were dissolved with distilled water; pH was adjusted with 1 N HCl to 8.0. The volume was adjusted to 500 ml with distilled water.
10x Phosphate buffer saline (PBS)	NaCl (80.0 g), NaH_2PO_4 (11.6 g), KCl (2.0 g) and KH_2PO_4 (2.0 g) were dissolved and adjusted the volume to 1 L in distilled water. The solution was sterilized by autoclave.
Bradford reagent	The Dye Reagent concentrate (Bio-Rad Protein assay) was prepared by diluting with deionized water (1:4). The solution was further filtered and kept at room temperature for 2 weeks.

Solution	Preparation
1% RPMI-1640 medium	RPMI powder (10.4 g) was dissolved with distilled water to a final volume of 1 L. $NaHCO_3$ (2.0 g) was added, pH was adjusted to 7 with 1 N NaOH or 1 N HCl. RPMI medium (900 ml) was mixed with fetal calf serum (90 ml) and antibiotics (10 ml; composed of penicillin G (100 U/ml), streptomycin (100 µg/ml). The RPMI medium was sterilized through 0.22 µm filter membrane under vacuum.
2% DMEM medium	DMEM powder (10.2 g) was dissolved with distilled water to a final volume of 1 L. $NaHCO_3$(3.2 g) was added, pH was adjusted to 7 with 1 N NaOH or 1 N HCl. RPMI medium (900 ml) was mixed with fetal calf serum (80 ml) and antibiotics (20 ml; composed of penicillin G (100 U/ml), streptomycin(100 µg/ml). The RPMI medium was sterilized through 0.22 µm filter membrane under vacuum.
Griess reagent	Solution A: sulfanilamide (1.0 g) was dissolved with 100 ml sterile water (1% v/v). Solution B: *N*-1-naphthalenediamine (0.1 g) was prepared in 100 ml of sterile water containing 5% H_3PO_4 (0.1% v/v). Then 50 ml of solution A was mixed with 50 ml of solution B (1:1). The homogenous solution was kept at 4° C until used.

Solution	Preparation
lipopolysaccharide (LPS)	The LPS (2.5 mg) was dissolved in RPMI medium to final volume of 50 ml, (LPS 50 µg/ml).
MTT solution (5 µg/ml)	MTT (200 mg) was dissolved with PBS to final volume of 40 ml.
0.04 M HCl in isopropanol	1 N HCl was prepared in distilled water. 20 ml of 1 N HCl was mixed with 480 ml of isopropanol and the prepared solution was stirred to homogenous solution.

2.3 Cell lines

Cells including murine macrophage-like RAW264.7 (RAW264.7) cells, human breast carcinoma cell line (MCF-7; CLS No. 300273), human cervical carcinoma cell line (KB, CLS No. 300446), human cervix adenocarcinoma (HeLa, CLS No. 300194), and human colon adenocarcinoma (HT-29, CLS No. 300215) were obtained from the Cell Line Service, Heidelberg, Germany and human gingival fibroblast cell line was kindly provided by the Faculty of Dentistry, Prince of Songkla University. It can be noted that the origin of KB cell is controversial argument. Misidentification of KB is described as shown in the appendices (Gey *et al*., 1952; Eagle, 1955; Vaughan *et al*., 2017).

2.4 Primers

Primers used in this study were designed based on the NCBI database (www. ncbi. nih. nlm. gov). Primers for *iNOS*, *COX-2* and endogenous *GADPH* genes were designed from mouse; *Mus musculus* (Premprasert et al., 2013), (Table 2.2). Apoptotic-associated genes including *TNF-*α, *BCL-2*, *BAX* and *BAK*, and *GADPH* as an endogenous were designed. All genes were designed from Human; *Homo sapiens*. Primer 3 free online software was used. The oligonucleotide encoding interested genes (Table 2.3) was purchased from Eurofin MWG Operon (http://www.operon.com/technical/pcr_primer_design.aspx). According to this guideline for

primer design, both the percentage of base guanine and cytosine base content (GC content about 40 - 60%) and melting temperature (T_m) of amplicon (about 60-65°C) were set. All primers using for qRT-PCR are shown in Table 2.2 and Table 2.3.

Table 2.2 *Mus musculus* primers used in qRT-PCR study.

Name	Accession no.[a] (location)	Sequence ($5' \rightarrow 3'$)	Product size (bp)
iNOS F	M84373.1	ACT TGG ATC AGG AAC CTG AA	580
iNOS R	(3002-3581)	CCT TTT TTG CCC CAT AGG AA	
COX-1F	AK160886.1	CCC ACC AGT TCT TCA AGA CC	269
COX-1R	(679-947)	AAG CAA CCC AAA CAC CTC C	
COX-2F	NM011198.3	TCT ACA ACA ACT CCA TCC TCC	244
COX-2R	(1281-1524)	GCA GCC ATT TCC TTC TCT C	
GAPDH F	NM008084.2	AAG CCC ATC ACC ATC TTC C	302
GAPDH R	(258-559)	TCC ACA ATG CCA AAG TTG TC	

[a] Accession No. from http://www.ncbi.nlm.nih.gov/

Table 2.3 Primers of *Homo sapiens* apoptotic primers used in qRT-PCR study.

Name	Accession No. [a] (location)	Sequences ($5' \rightarrow 3'$)	Product size (bp)
TNF-α (F)	NM_000594.3	TGCTTGTTCCTCAGCCTCTTCTC	201
TNF- α (R)	(263-463)	AGGGTTTGCTACAACATGGGC T	
BCL-2 (F)	NM_000633.2	CCTGTGGATGACTGAGTACCTG	130
BCL-2 (R)	(1015-1144)	CAGAGACAGCCAGGAGAAATCA	
BAX (F)	NM_001291428.1	GAGAGGTCTTTTTCCGAGTGGC	106
BAX (R)	(335-440)	GCCTTGAGCACCAGTTTGCTG	
BAK (F)	NM_001188.3	GGGTCTATGTTCCCCAGGATTC	160
BAK (R)	(1366-1525)	GAGCAGGGGTAGAGTTGAGCA	
GAPDH (F)	NM_001256799.2	ACCCACTCCTCCACCTTTGAC	180
GAPDH (R)	(1066-1245)	TCCTCTTGTGCTCTTGCTGG	

[a] Accession No. from http://www.ncbi.nlm.nih.gov/

2.5 Equipments

Autoclave	Model HA-3D (Hirayama, Japan)
Balance	Ohaus (New Jersey, USA); Avery Berkel (Ohio, USA), Sartorius TE 3102S (Goettingen, Germany); Precisa (Dietikon (Switzerland)
Centrifuge	Microcentrifuge: Denver instrument company (New York, USA); high speed centrifuge: Kubota 5922 (Tokyo, Japan)
CO_2 chamber	Shel lab (Oregon, USA)
Electrophoresis	Mupidα Mini Electrophoresis System (Tokyo, Japan)
Gene amplification	TaKaRa PCR Thermal Cycler Dice Version III Model TP600 (Shiga, Japan)
Hot air oven	Memmert (Schwabach, Germany)
Incubator	Thermomixer comfort (Eppendorf, Germany)
IR spectrophotometer	JASCO IR-810, Japan Spectroscopic (Tokyo, Japan)
Laminar air flow cabinet	Ultrasafe 48, Faster (Milan, Italy)
NMR	Varian® Unity Inova 500 spectrometer (California, USA)
Mass spectrometer	Thermo Finnigan MAT 95XL (Massachusetts, USA)
Micropipettes	Socorex: 0.1-2.0 µl, 2-20 µl, 20-200 µl, 100-1000 µl (Ecublens, Switzerland)
Microplate reader	Biotek Power, BioTek Instruments, Inc (Vermont, USA)
Microplate	96-well, Nunc (Roskilde, Denmark)
Microscope	Olympus, CK2 model, Olympus optical Co. Ltd. (Tokyo, Japan)
Microwave oven	LG (Bangkok, Thailand)
pH meter	Eutech instruments, Cyber Scan 510 (Nijkerk, Netherlands)
Real-time PCR ABI7300	Real-time PCR system (California**,** USA) and used Sequence Detection Software version 1.4 (SDS V. 1.4)

Refrigerator	Sanden Intercool (4°C), (SingBuri, Thailand); Whirlpool (-20°C), (Bangkok, Thailand); Deep freezer (-80°C), Forma Scientific (Ohio, USA)
UV-cabinet II	for 254, 366 nm, CAMAG (North Carolina, USA)
UV-VIS spectrophotometer	Genesis-6, Thermo scientific (Massachusetts,USA)
Vortex	MS 1 mini shaker, IKA Co., Ltd. (Petaling Jaya, Malaysia)
Water bath	Memmert (Schwabach, Germany)

2.6 General experimental procedures

2.6.1 Thin-layer chromatography (TLC)

Adsorbents:	The TLC plate for routine work was pre-coated TLC plate of silica gel 60 F-254 from Merck, Darmstadt, Germany.
Layer thickness:	250 µm
Technique:	one way, ascending, 5.0-6.5 cm or as appropriate
Temperature:	laboratory temperature (30°-35 °C)
Detection:	(1) ultraviolet light at wavelength 254, 366 nm (2) anisaldehyde/H_2SO_4 spray reagent

Anisaldehyde/H_2SO_4 spray reagent:

p-Anisaldehyde (3.5 ml) was mixed with glacial acetic acid (15 ml). Methanol (350 ml) was added. Finally, 50 ml of concentrated sulfuric acid (H_2SO_4) was cautiously mixed. The reagent was kept at 4 °C until used.

2.6.2 Column chromatography

Adsorbents:	Silica gel (SiO_2 60, 230-400 mesh) from Merck, Darmstadt, Germany.
Packing:	(1) adsorbent poured as a suspension into the column (2) vacuum chromatography
Addition of sample:	Crude extract was dissolved in the small volume of solvent and gently placed on top of the column.
Technique:	Open column chromatography using gravity or flash column chromatography using low pressure (1-2 bar)
Solvent:	hexane, chloroform, dichloromethane, ethyl acetate and methanol

Examination of elute: The fractions were spotted on TLC plate. TLC plate was examined by quenching spot when using UV light at wavelength 254 nm and 366 nm and it was further detected with anisaldehyde/H_2SO_4 spray reagent.

2.6.3 Spectroscopy

2.6.3.1 Ultraviolet-visible (UV-vis) absorption spectra were recorded (200 to 800 nm with a Genesys^{TM}6 spectrophotometer. (Sample was dissolved with appropriate solvents at a concentration between 0.1 to 0.6 mM)

2.6.3.2 Infrared (IR) spectra were obtained on IR spectrometer at the wave number (ν) ranging from 400 to 4000 cm^{-1}. A mixture of sample and potassium bromide (KBr) crystal was prepared using disc technique at the Department of Pharmaceutical Chemistry, PSU.

2.6.3.3 Nuclear magnetic resonance (NMR) spectra were obtained from Fourier transform NMR, Varian® Unity Inova 500 spectrometer (Scientific Equipment Center (SEC), Prince of Songkla University, Thailand. The sample about 2-10 mg was dissolved in the suitable solvents (NMR grade). The chemical shifts were reported in ppm scale, using tetramethylsilane (TMS) as internal standard for further references. The NMR (500 MHz) indicate chloroform-*d* ($CDCl_3$); δ_H 7.25 and δ_C 77.0 ppm; acetone-d_6 (C_3D_6O); δ_H 2.05 and δ_C 206.7 and 29.9 ppm; dimethyl sulfoxide (DMSO)-d_6 (C_2D_6OS); δ_H 2.50 and δ_C 39.5 as operating solvents.

2.6.3.4 Mass spectrometry (MS), the spectra was obtained from Thermo Finnigan MAT 95 XT (Scientific Equipment Center (SEC), Prince of Songkla University, Thailand. The sample was prepared in appropriate solvents and was analyzed by electron-impact-mass spectrometry (EI-MS) or electron-spaying-mass spectrometry (ESI-MS) technique.

2.6.4 Cell culture

2.6.4.1 Cell lines were maintained in appropriated medium. Cells were manipulated in a CO_2 incubator. Incubator is normally set to 37 °C, 95% relative humidity and a CO_2 level of 5%. After 3-5 days, cells were continuously grown to monolayer cells and cells were then sub-cultured by trypsinization technique.

2.6.4.2 Trypsinization technique, monolayer cells presenting 80-90% confluence were chosen and then cells were washed twice with 1x PBS. Cells were incubated in CO_2 incubator with 0.25% w/v trypsin-EDTA for 3-10 min. The reaction for trypsinization was further stopped by using cultured medium. Trypsin-EDTA was discarded after centrifugation at 500 ×g for 5 min, cells were re-suspended in cultured medium and cells were either cultured or were harvested.

2.6.5 qRT-PCR study

2.6.5.1 Isolation of total RNA

Total RNA was isolated from both untreated and treated cells using a Total RNA Mini Kit (Geneaid®, New Taipei City, Taiwan). According to the manufacturer's protocol, cells pellet was chilled on ice. Then the cells pellet was gently re-suspended by pipette with RBC Lysis Buffer (100 µl). The mixture was transferred to 1.5 ml micro-centrifuged tube. After that 400 µl of RB Buffer and 4 µl of β-mercaptoethanol were added and vigorously re-suspended to prepared solution. The mixture was further incubated at room temperature for 5 min. Then obtained RNA was pre-purified using ice cold 70% v/v ethanol in water (500 µl), and the solution was mixed by pipette as much as possible for break up any precipitate and remove some impurities such as proteins. The mixture (500 µl, each) was transferred to RB spin column in a 2 ml collection tube and was centrifuged

14,000 × g for 1 min and the flow-through was discarded. The RB column was placed in the new 2 ml collection tube and RB column was incubated with 50 µl of DNase I in DNase free water (0.2 U/µl) for 15 min at room temperature. After that, the absorbed RB column was added with 400 µl of RW1 and was centrifuged at 14,000 × g for 30 min, and then the flow-through was discarded. The Wash Buffer containing ethanol (600 µl) was added into RB column. The column was centrifuged at 14,000 × g for 30 min and the flow-through was discarded. The RB column was dried under centrifugation and was placed to new 1.5 ml centrifuge tube. Then the total RNA, which was absorbed on the dried-column matrix, was incubated with RNase free water (50 µl) for 1 min. After standing, the total RNA was eluted by centrifuged at 14,000 × g for 1 min. Finally, the total RNA was obtained and the amount of total RNA was determined from an OD at 260 nm. For the purity of obtained total RNA was considered by a ratio of OD_{260}/OD_{280}. Furthermore, the isolated total RNA was checked an intact RNA by agarose gel electrophoresis. Briefly, the total RNA was separated using 1% (w/v) agarose gel in TAE 1X buffer for 30 min (100 volt). During gel electrophoresis, the total RNA was separated by the different molecular weight and then the separated-band of RNA together with DNA marker (100 -1,000 bp) were stained with ethidium bromide. The isolated RNA was kept at -80ºC until further used for qRT-PCR step.

2.6.5.2 qRT-PCR

Subsequently, the total RNA (from 2.6.5.1) was used as a template for qRT-PCR using a One Step SYBR®PrimeScript™ RT-PCR kit II (Perfect Real Time, Takara, Japan). Quantitative RT-PCR (qRT-PCR) was performed by the ABI Prism® 7300 Fast Real-Time PCR system (California, USA). According to the manual construction for one step PCR kit, the obtained mRNA from total RNA was firstly synthesized by reverse transcription using with PrimeScript reverse transcriptase and specific primer to a first strand complementary DNA (1^{st} cDNA). Then the 1^{st} cDNA was continuously synthesized to the 2^{nd} cDNA and then further used as a DNA template for PCR reaction. The cDNA was amplified by polymerase enzyme (*TaKaRa Ex taq* HS) and specific

primer. The complete DNA was sequentially continued by PCR cycles including heat denaturation, primer annealing and DNA extension. Finally, the amplified DNA was further detected using fluorescence that produced during the primer annealing and DNA polymerase steps by interaction between the adding DNA intercalator (SYBR® Green) and double strand DNA. Herein, this bounding fluorescence with double strand DNA was monitored during real time PCR. The PCR result was displayed by amplification plot (Δ Rn VS cycle of amplification), Fig. 2.1. Additionally, genes expressions of treated sample were analyzed and *GAPDH* was used as an endogenous gene. For the relative expression results, the threshold cycle was calculated when the control group was calibrator.

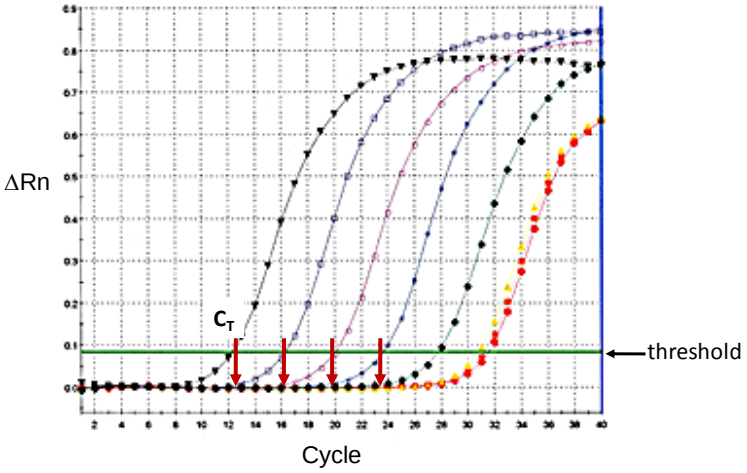

Figure 2.1 Amplification plot.

In qRT-PCR study, the PCR reaction was carried out in a final volume of 20 µL (Table 2.4). The PCR reaction system containing forward and reverse specific primers, 2x one step RT-PCR buffer IV, reference ROX dye, the total RNA (used as a template), Primescript 1 step enzyme mix II and RNase free water. The PCR cycling was carried out by 4 stages; stage 1-2 was reverse transcription step (42 °C, 5 min and 5°C, 5 sec) for 1 cycle, stage 3 was PCR reaction (initial denaturation step at 95°C for 5 sec followed by 60°C, 31 sec for 40 cycles), and stage 4 was dissociation step (95°C for 15 sec, 60 °C for 1 min and 95°C for 15 sec), respectively.

Table 2.4 The PCR components using for mRNA expressions.

PCR components	Volume	Final concentration
(1) 2x one step RT-PCR buffer IV	10 µl	1x
(2) Primescript 1 step enzyme mix II	0.8 µl	
(3) ROX dye (50x)	0.4 µl	1x
(4) 10 µM of Forward primer	0.8 µl	0.4 µM
(5) 10 µM of Reverse primer	0.8 µl	0.4 µM
(6) Total RNA (equivalent to 20 ng)	varied	
(7) RNase free water	To final volume	
Total	20 µl	

2.6.6 Agarose gel electrophoresis

Agarose D-1 Low EEO was from the Research Organics, Ohio, USA and DNA ladder (100 bp + 1.5 kb) was purchased from Sib-enzyme, Novosibirsk, Russia. In this study, 1% w/v the agarose gel electrophoresis was used for checking the intact RNA and product size of DNA. The general procedure following;

Pouring: Agarose gel powder (0.8 g) was mixed with 1x TAE buffer in a microwaveable container. Microwave for 3-5 min (approximately), until agarose gel is completely melted (cautiously, this prepared solution do not over boil). Standing until this solution cool down to about 50 °C, it was poured in to a gel tray together with comb. Agarose gel was put at room temperature (25° C) for 30-40 min, and then it has completely solidified.

Loading: The gel box was filled with running buffer (1x TAE) and this buffer was covered the gel. Then sample and DNA ladder (100 bp + 1.5 kb) were separately mixed with loading dye and it were carefully loaded into the additional well of the prepared gel.

Running: The gel was run at 100 volt for 30 min.

Staining: Gel was carefully transferred into a container that filled with running buffer (1x TAE) containing EtBr or SYBR green. Gel was stained for 15 min and then gel was de-stained with water for 5 min.

Detection: The stained gel was visualized by UV transmission at 312 nm.

2.7 Phytochemical and chromatographic procedures

In this study, the extraction and isolation from *C. stellatopilosus* was followed by the routine extraction procedures including maceration, liquid-liquid extraction or partition and chromatography, respectively. Then obtained fractions were chosen and were further purified using various chromatographic techniques such as vacuum column chromatography (flash column chromatography) and opened column chromatography. Absorbents such as silica gel, Sephadex LH-20, Diaion HP-20 and RP-18 were used. Spectrometry such as UV, IR, NMR and MS were used to evaluate the structure of compound.

2.7.1 Preparation of crude extracts from leaves

10 kg of the dried leaves powder from *C. stellatopilosus* (LCS) was macerated at room temperature for three days with methanol (15 l, 3 times). After filtration, the filtrate were pooled and concentrated under reduced pressure using by a rotary evaporator until dryness. The dry mass of crude methanol extract (LCSME) (1713 g; 17.13 % w/w) was obtained. Then the methanol extract was further separated using liquid-liquid extraction and chromatography.

The crude methanol extract (LCSME 950.2 g) was dissolved in methanol until the solution was dissolved and then the distilled water was added to adjust to 80% v/v methanol in water. After that, the mixture was partitioned with the ascending polarity solvents including hexane, dichloromethane (CH_2Cl_2) and ethyl acetate (EtOAc), consecutively, (500 ml x 3 times each). The solutions, which obtained from each step were pooled and then evaporated under reduced pressure. Finally, hexane fraction (174.61 g, 18.38 %w/w) CH_2Cl_2fraction (194.68 g, 20.49 %w/w), EtOAc fraction (101.61 g, 10.69% w/w) and also the residue from polar fraction (88.32 g, 9.29 %w/w) were obtained and all fractions were kept at 4 °C until used (Fig. 2.2).

Conduct to the objective of our study, four diterpenes from *C. stellatopilosus* including plaunotol, plaunol A, plaunol E and plaunol F were obtained from crude methanol extract and CH_2Cl_2 fractions. Three flavonoids including apigenin-8-C-glycoside (vitexin), luteolin-7-O-

β-D-glucoside and luteolin-4′-O-glucoside and, and two phytosterols including β-sitosterol and β-sitosterol-D-glycoside were obtained from study. The procedure of their isolation was described as followings;

From methanol extract

Firstly, the methanol extract (LCSME 50 g) from *C. stellatopilosus* leaves (from 2.7.1) was pre-purified using by the vacuum column chromatography. The silica gel for chromatography (362 g) was packed into sintered glass funnel (13 cm × 4 cm). The methanol extract was dissolved with methanol and then mixing with silica gel (42 g). After removing chemical solvent until dryness by vacuum, the dried methanol extract, which was absorbed on silica gel was obtained and was loaded on the top of sintered glass column. This column was covered with filter paper to protect the uneven surface of packed silica by eluting solvent, which may aggravate from Eddy diffusion and was eluted by difference solvents including hexane, CH_2Cl_2, EtOAc and methanol by ascending polarity to afford fractions (200 ml, of each). Finally the collected fractions were separately spotted on TLC plate and the developed by mobile phase. The expected compound was visualized under UV cabinet at both wavelengths (254 and 366 nm) and this TLC plate also was sprayed with anisaldehyde/H_2SO_4 reagent. The collected fractions, which showed a similar pattern obtaining by TLC plates were pooled and evaporated to dryness. In addition, four pooled fractions were obtained from vacuum chromatography as followed; Isolation scheme is shown in Fig. 2.2.

- Fraction 1-13 were combined and assigned as fraction 5F-1 (10 g).
- Fraction 14-19 were combined and assigned as fraction 5F-2(5 g). This fraction was re-crystallization with mixing solvent between CH_2Cl_2 and methanol in a ratio 3:1 to yield a white crystal; CSBS (10 mg, 0.02 % w/w from methanol extracts).
- Fraction 20-43 were combined and assigned as fraction 5F-3 (12 g). This fraction was isolated and was purified using opened column chromatography

(5 cm x 40 cm) that was eluted with chloroform and EtOAc (4:1) to afford a yellow oil; CSPNT (800 mg, 1.6% w/w of methanol extracts).

- Fraction 44-56 were combined and assigned as fraction 5F-4 (7 g). This fraction then was re-crystallization with $CH_2Cl_2$and methanol in a ratio 3:1 to yield a white amorphous powder; CSBDG (12 mg, 0.02 % w/w from methanol extracts).

From dichloromethane extract

The isolation and purification procedure using vacuum chromatography were described in brief. CH_2Cl_2 fraction approximately 103.7 g (LCSD) was dissolved in chloroform and blended with silica gel, and gently placed on the top of silica gel sintered glass column (12.5 cm × 4 cm). This column was eluted with hexane, CH_2Cl_2, EtOAc and methanol (500 ml, 2 times) following the increasing polarity in a ratio 20:80, 50:50, and 80:20, respectively. During chromatography, the obtained fractions were collected and were pooled as guided with TLC. Then the pooled fractions were further evaporated to dryness under reduced pressure to give the five fractions (1F1 -1F5).

Fraction 1F3 was continued re-crystallization with chloroform: hexane (3:1) to give a white amorphous solid; CSA1. Fraction 1F4 was also continued re-crystallization with EtOAc: acetone (3:1) to obtain a white amorphous powder: CSA2. The yielding of CSA1 and CSA2 were 144.9 mg (0.13 %w/w of CH_2Cl_2extract) and 17.9 mg (0.019 % of CH_2Cl_2extract), respectively.

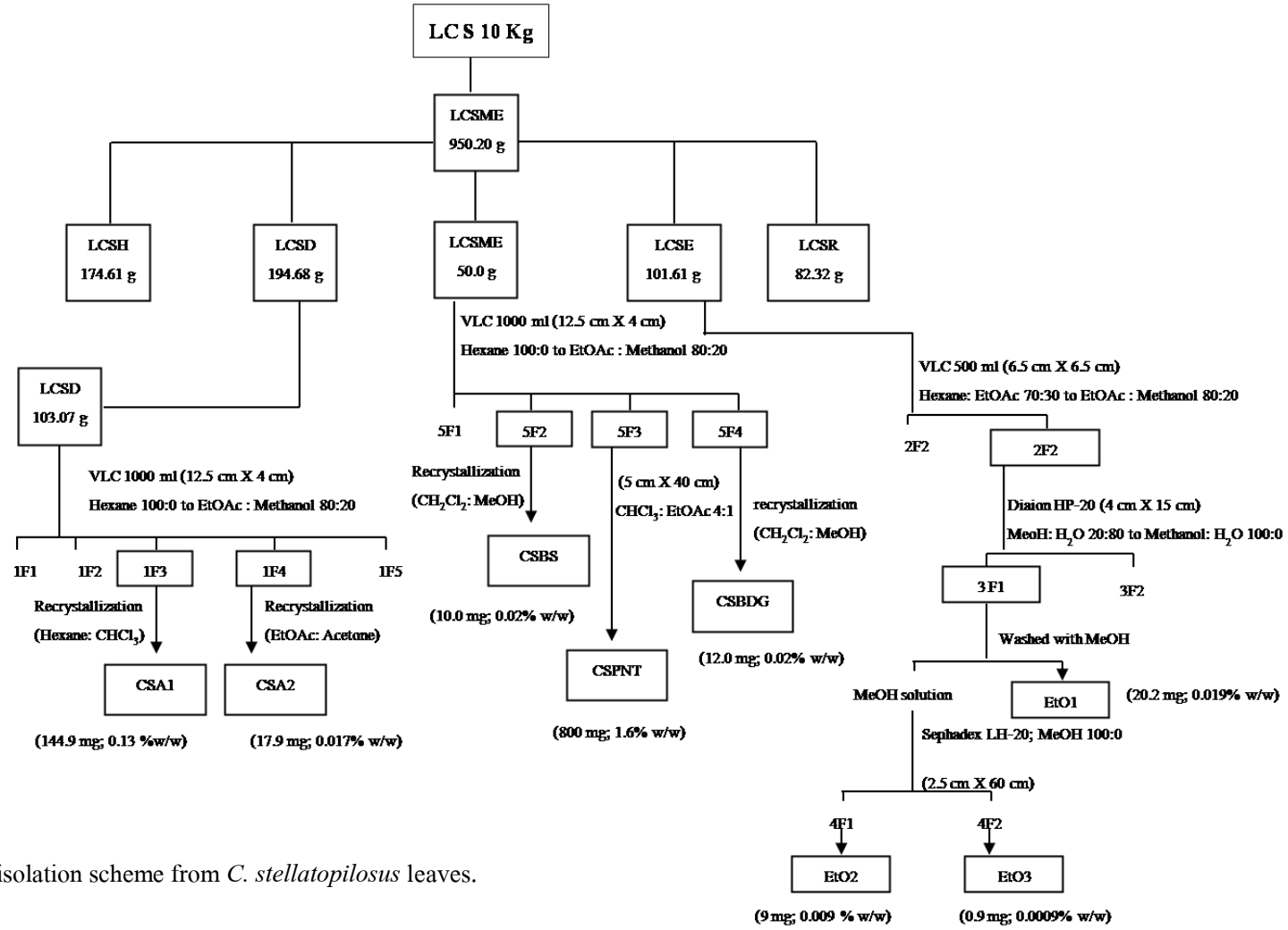

Figure 2.2 The isolation scheme from *C. stellatopilosus* leaves.

From ethyl acetate extract

The 101.61 g of EtOAc fraction (LCSE) was selected for further isolation using diaion HP-20. Briefly, diaion HP-20 (61 g) was packed into opened-column (4 cm × 15 cm), and then the diaion HP-20 was washed with methanol before use. The diaion HP-20 was equilibrated with water (200 ml, 3 times). The EtOAc fraction was dissolved with 320 ml of 80% v/v methanol in water. The column was firstly eluted with water, and then was eluted by a various ratios between methanol and water (20:80, 40:60, 60:40, 80:20 and 100:0; 200 ml, of each, 3 times), consecutively. Finally, five fractions (3F-1 to 3F-5) were collected and were separately spotted on TLC, and then this fraction was further pooled. Three fractions were obtained as following;

- Fractions 1-3 were combined and assigned as fraction 3F-1 (1.3 g). 3F-1 fraction containing a yellow amorphous solid was washed with methanol to remove other impurity. The EtO-1 was 20.2 mg (0.019 %w/w of EtOAc fraction).
- Fractions 3-6 were combined and assigned as fraction 3F-2(3.1g). This residue fraction was dissolved with the methanol and then was separated using sephadex LH-20. During size exclusion column chromatography, the sephadex LH-20 was packed with methanol in to the column (2.5 cm × 60 cm). The residue fraction was also dissolved with methanol in a small volume and was placed on top of packed column. The column was set and was eluted with methanol. The fractions were collected (10 ml, of each) and were pooled after TLC as guided similar pattern. Finally, EtO-2 (9 mg, 0.009 % w/w of EtOAc fraction) and EtO-3 (0.9 mg, 0.0009 %w/w of EtOAc fraction) were obtained.
- Fractions 7-20 were combined and marked as a residue fraction.

2.7.2 Preparation of crude extracts from stems

The phytochemical constituents study was continuously isolated from the stem of *C. stellatopilosus* (SCS). As shown in Fig. 2.3, the stem powder (5 kg) was macerated in methanol at room temperature for three days (3 times) and filtered. The filtrate was collected and concentrated under reduced pressure to give methanol extract (470.28 g, 9.73 %w/w). The methanol extract was kept at 4°C.

During partition procedures, the methanol extract was dissolved with 80% (v/v) methanol in water and was consecutively partitioned with hexane, CH_2Cl_2, and EtOAc to afford the hexane (72.36g; 15.36% w/w), CH_2Cl_2 (78.97; 16.79% w/w), EtOAc (49.36g; 10.49% w/w) and methanol residue fractions (265.06g; 56.36% w/w) respectively.

Furthermore, the CH_2Cl_2 fraction was selected for isolation by silica gel column chromatography (using a glass column 12 cm × 37 cm). The CH_2Cl_2 fraction (SCSD 78.97g) was blended with silica gel, and the mixed sample was then put on the top of packed silica gel. The column was eluted with isocratic solution (CH_2Cl_2: MeOH (95:5)). The fractions were collected and were pooled. Three fractions (6F-1 to 6F-3) were collected. Fraction 6F-3 was re-crystallizedin hexane and acetone mixture (3:1) to give CSA3 (12.9 mg; 0.016% w/w). The isolation procedures of *C. stellatopilosus* stems were illustrated in Fig. 2.3. Besides, CSA1 and CSA2 were also obtainedfrom this column chromatography followed by re-crystallization.

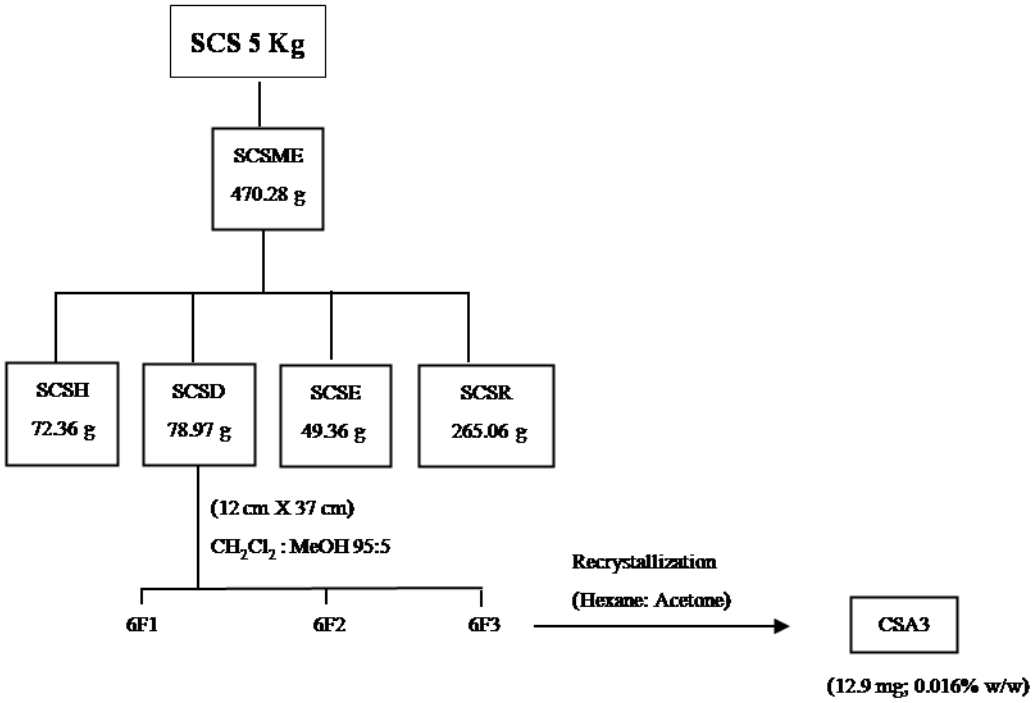

Figure 2.3 The isolation scheme from *C. stellatopilosus* stems.

2.8 Biological evaluation using cell based assay and qRT-PCR

Four diterpene compounds including plaunotol, plaunol A, plaunol E and plaunol F were evaluated for the anti-inflammatory and anti-proliferative activities. The anti-proliferative activity was assessed on the human cancer cell lines including HeLa, HT-29, KB and MCF-7 and human normal cell lines (HGF). Apoptotic potential was evaluated including cell cycle analysis and apoptosis. The transcription profile of apoptotic associated genes such as *TNF-*α, *BAX*, *BCL-2* and *BAK* were also studied by qRT-PCR. For the anti-inflammatory activity, the inhibitory of NO production in RAW 264.7 macrophage cells was carried out. Consideration of anti-inflammatory effect, the *iNOS* and *COX-2* transcription profiles were analyzed by qRT-PCR.

2.8.1 Anti-proliferative and apoptotic activities

2.8.1.1 Human cell lines culture

Anti-proliferative activity was investigated in four human cancer cell lines and human normal cell line (2.3). Cells were routinely maintained in DMEM medium and were incubated at 37 °C, 5% CO_2, 95% relative humidity. The cells manipulation, subculture using trypsinization reaction, and cells count using trypan blue technique were presented in this experiment.

2.8.1.2 Treatment of the cells

Four compounds including plaunotol, plaunol A, plaunol E and plaunol F were prepared in DMSO. After the cells were grown at 80-90 % confluence, cells were washed with PBS and were trypsinized with 0.25% w/v trypsin-EDTA. Cells pellet was obtained by centrifugation at 500 ×g for 5 min and was re-suspended into fresh DMEM medium. Both cancer and normal cells were prepared at 5×10^5 cell/ml. The cells suspension was separately seeded into 96-well plate (5×10^3 cells/well) and these cells were maintained at 37 °C, 5% CO_2 for 24 h, for adherence.

After 24 h, cells were continued to study. The compound was separately exposed to the cell following various treatments. For the screening of anti-proliferative activity and cytotoxicity, the final concentrations of sample treatments were at 0, 3, 10, 30 and 100 µM, respectively. For positive control, the paclitaxel was used and the final concentrations were investigated at 0, 0.01, 0.1 and 1 µM, respectively. The treated cells were continuous incubated in CO_2 incubator at 37 °C, 5% CO_2 for 48 h.

2.8.1.3 MTT assay

Cells were incubated in a presence of target compound for 48 h (2.8.1.2). After that, 100 µl of the supernatant was combined together with 10 µl of MTT (5 mg/ml in PBS) and cells were then incubated at 37 °C for 3 h. The formazan crystal is delivered by the reduction of tetrazolium salt, which is caused by the dehydrogenase or reductase and it is used for detection of cell proliferation and toxicity. The insoluble precipitate product was dissolved using 0.04 N HCl in isopropanol. The decolorized solution was measured at 570 nm using micro-plate reader.

According to these results, the OD data was recorded and the IC_{50} was calculated using Microsoft office (Excel). All data was expressed as mean ± S.E.M (n=3 individual experiment). The anti-proliferative activity was considered by the percentage of cytotoxicity when compared with untreated cells (control group).

2.8.1.4 Cell cycle analysis

Four cancer cell lines including HeLa, HT-29, KB and MCF-7 were seeded in to 6-wells plate at 5×10^5 cells/well. Then cells were incubated for 24 h at 37 °C, 5% CO_2. Cells were separately exposed to compounds (plaunotol, plaunol A and plaunol E) at various concentrations for 48 h. The concentrations of plaunotol were 0, 25, 50, 75 and 100 µM and the concentrations of plaunol A and plaunol E were 75 and 150 µM. After 48 h, cells were harvested by 0.25% of trypsin-EDTA (1 ml/well) and then the detached cells were further centrifuged at 500×g for 5 min. The supernatant

was carefully removed, and the cell-pellet was re-suspended with PBS for cells cleaning (1 ml each, 2 times). Cells were re-suspended again with 70% v/v ethanol in water for cell fixation and these cells were stored at -20 °C for overnight. The next day, cells were thawed on ice, and then cells were centrifuged at 500 ×g for 5 min. After that a supernatant was carefully discarded, the fixed cells were rinsed by PBS. Cells were again centrifuged and supernatant was discarded. 200 µl of Muse™ cell cycle reagent (Merck, Darmstadt, Germany) was added into cells pellet and then mixed to homogeneous solution. After standing at room temperature for 20 min under the dark condition, the stained cells were analyzed by Muse™ cell analyzer (Merck, Darmstadt, Germany) and data were analyzed using Muse 1.4 software.

During cell cycle using flow cytometry, these cells were separated by distribution of DNA level in a heterogeneous population of cells including G0/G1 phase, S phase and G2/M phase, respectively. Therefore, the result was expressed mean ± S.D (n=3) and also showed as the DNA histogram.

2.8.1.5 Annexin-V/7-AAD detection

To evaluate the apoptotic activity of diterpenes including plaunotol, plaunol A and plaunol E. Annexin-V and 7-AAD double staining was used in this study. Briefly, HeLa, HT-29, KB and MCF-7 cancer cell lines (5×10^5 cells/well) were cultured in 6-well plate at 37 ºC, 5% CO_2 for 24 h and then cell were treated with diterpenes at a various concentrations (0, 75 and 150 µM). Paclitaxel at 1 µM was used as a positive control. After exposure for 48 h, cells were washed with PBS (1 ml, 2 times) and cells were trypsinized with 0.25 % trypsin-EDTA. Then centrifugation at 500 ×g for 5 min, both trypsin-EDTA and cultured medium were discarded. Cell pellet was re-suspended in 100 µl of the fresh DMEM media containing 1% FBS. 100 µl of Muse™ Annexin V εt Dead cell reagent (Merck, Darmstadt, Germany) was added and the mixture was incubated for 20 min at room temperature, under dark condition. Finally, the stained cells were analyzed by flow cytometer using Muse™ cell analyzer (Merck, Darmstadt, Germany).

The data was analyzed using Muse™ 1.4 software. During apoptosis detection using flow cytometry, cells were distributed into four quadrants, in which based on the biochemical changes including live cells (Q1), early apoptotic cells (Q2), late apoptotic cell (Q3) and dead cells (Q4), receptivity. The data of these cells were recorded the relative number of apoptotic cell (%) as mean ± S.D. (n=3) and also represented as Annexin-V/7-AAD dot plots.

2.8.1.6 Determination of apoptotic-associated gene expressions

Treatment of cells

HeLa, HT-29, KB and MCF-7 cancer cells (5×10^5 cells/well) were maintained in 6-well plate and were induced with different concentrations of diterpenes depending on each experiments (0, 75 and 150 μM) for 48 h for apoptosis induction. The control cells were cultured in 0.2% DMSO. Paclitaxel at 1 μM was used as positive control. After incubation, cultured medium and compounds were removed. Cells were rinsed with PBS (1 ml, 2 times) and were then harvested by trypsinization using 0.25% w/v trypsin-EDTA. After that, the detached cells were removed and placed into a new 50 ml centrifuged tube. Cells were then centrifuged at 500 ×g for 5 min. The supernatant was discarded and cell pellet was washed with PBS (1 ml, 2 times). Cells were centrifuged and the PBS was further removed. Finally, cell pellet was again centrifuged and then using the pipette tip to removed solution. Dried pellet was kept at -80 ºC until further total RNA extraction.

Isolation of total RNA

The total RNA was extracted from cell lines using Total RNA Mini Kit (Geneaid®, New Taipei City, Taiwan). According to the manufacturer's protocol (2.6.5.1), the total RNA was obtained and was kept at -80 °C for qRT-PCR.

qRT-PCR

The apoptotic associated genes including *TNF-α*, *BCL-2*, *BAX* and *BAK* were amplified by qRT-PCR using PCR system ABI 7300. The nucleotide sequences of specific primers are shown in Table 2.3. The PCR components performed with one-step PCR system, the 20 ng total RNA was added together with other components including PrimeScripRTase and *TaKaRa Ex Tag* HS, primers (0.8 µl, each), 2x buffer (10 µl) and ROX dye (0.4 µl). Then PCR reaction was adjusted to final volume (20 µl) with RNA free water (Table 2.4). The amplified DNA was analyzed by the intercalated SYBR Green I fluorescence bound to double strand DNA in real time PCR system. Finally, the amplification plot was obtained and the threshold was set at 0.2 for using RQ calculation. The threshold cycle (C_T) was subtracted by *GAPDH* as endogenous gene and then calculated by comparative C_T method when control group as a calibrator. The transcription profile of target genes was compared with untreated cell. The RQ value was expressed as mean ± S.D (n = 3).

$$\Delta C_T \text{ value} = [C_T \text{ of target gene} - C_T \text{ of endogenous GAPDH}] \quad (1)$$

$$\Delta\Delta C_T \text{ value} = [\Delta C_T \text{ of target gene} - \Delta C_T \text{ of calibrator}] \quad (2)$$

$$\text{Relative quantitation (RQ)} = 2^{-\Delta\Delta C_T} \quad (3)$$

2.8.1.7 Caspase activity

Focusing on caspase activity in MCF-7 cells after treatment with plaunol E was investigated. Caspase colorimetric protease assay sample kit (Apotarget; invitrogen, Frederick, MD) was used.

Treatment of cells

MCF-7 cell line 5×10^6 cells were chosen and were seeded into cultured flask. The culture was incubated at 37 °C, 5% CO_2. After 24 h, cells were treated with plaunol E at 50 µM to induce apoptosis for 48 h. Cells were harvested by trypsinization using 0.25% w/v trypsin-EDTA (1 ml) and cells were then centrifuged at 500 ×g for 5 min. After discard the supernatant, cells were washed with PBS (2 ml, 2 times) to remove the remaining cultured medium and cells were then stored at -80 °C.

Protein extraction

All procedures were performed at 4 °C. Cell pellet was thawed and was digested with chilled cell lysis buffer (50 µl). Cell was re-suspended and then incubated on ice for 10 min. After that, the mixture was centrifuged at 10,000 ×g for 1 min. The supernatant or cytosol extract was transferred into 1 ml micro-centrifuge tube.

Determination of total protein

The protein assay modified from Bradford, 1976. Total protein of the cytosol extract was determined using Bradford assay (Bio-Rad Protein assay, California, USA). Standard curve of albumin bovine serum (BSA) was prepared at a various concentrations including 0.1, 0.08, 0.06, 0.04, 0.02 and 0.01 mg/ml, respectively. The Bradford reaction was performed in 96-well plate. The sample was prepared in deionized water (10 µl), followed by 200 µl of Bradford reagent. The mixture was incubated at room temperature for 5 min. The protein dye complex was determined by

micro-plate reader at 595 nm (Scheme 2.1). The OD was plotted against BSA concentrations using Microsoft office (Excel) and the linear regression was generated. The amount of protein that presented in each sample was calculated by equivalent to BSA standard curve. The protein content was expressed as mean ± S.D (n = 3).

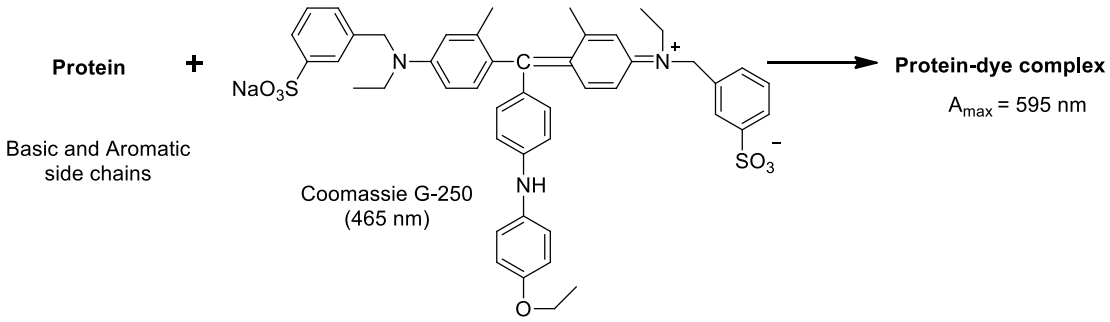

Scheme 2.1 Bradford assay (Thermo scientific pierce protein assay technical handbook, Thermo Fisher Scientific Inc. 2010).

Caspase activity

After the amount of protein was obtained, the cytosol extract was calculated equivalent to 100 µg protein and was further mixed with 50 µl of 2x Reaction buffer containing 10 mM DTT. After that, 5 µl of the synthetic peptide conjugated with *p*-nitroanilide (*p*-NA) as a substrate including DEVD-*p*NA (caspase-3), IETD-*p*NA (caspase-8), and LEHD-*p*NA (caspase-9) was separately added. The mixture was incubated at 37 °C, for 2 h (in the dark condition). The optical density was measured at 405 nm. The fold-increase in caspase-3, -8 and caspase-9 activity was calculated by direct comparison to the level of the untreated cells (mean ± S.D, n = 3).

2.8.2 Anti-inflammatory activity

2.8.2.1 RAW 264.7 cell line culture

The frozen cells were kept in 5% (v/v) DMSO and were preserved at -80 °C. These cells were taken and were thawed at room temperature. After thawing, the DMSO was removed by centrifugation at 500 ×g for 5 min. Then the cells pellet was harvested and mixed with fresh completed RPMI medium (10 ml). The homogenized cells were seeded into cultured flask and cells were cultured in CO_2 incubator under 37 °C, 95% of relative humidity and 5% CO_2. After 3-4 days, the monolayer cells were grown at nearly 80-90 % confluence. Cells were trypsinized using 0.25% w/v trypsin-EDTA (2 ml) for 5 min. Fresh medium (2 ml) was added to stop the reaction. The mixture was then transferred to 50 ml centrifuge tube and centrifuged. Discard supernatant, the pellet was re-suspended in RPMI medium. Cell was ready for further experiment.

2.8.2.2 Treatment of RAW 264.7 cells

Trypan blue (0.04% in PBS; 20 µl) was added to the 20 µl cells from 2.8.2.1. Cells were counted using hemocytometer. Cells were adjusted with RPMI medium to a final concentration of 5×10^6 cells/ml.

For evaluation of NO inhibitory activity, 100 µl of cells solution was seeded into 96-well plate and these cells were incubated to adherence at 37 °C for 1 h. After incubation period, the medium were removed and then 100 µl of fresh medium containing LPS (200 ng/ml) was added. Stock solution of a sample was prepared in DMSO. Sample solution was then diluted with RPMI to obtain final concentrations of 3, 10, 30 and 100 µM, respectively. 100 µl of sample solution was added into cells and incubated at 37 °C for 24 h. Groups of treatments are shown in Table 2.5. CAPE, IDM and L-NA were used as positive controls. Cells without LPS and standard drug were used as negative controls.

Table 2.5 The treatment group for anti-inflammatory activity.

Treatments	RAW 264.7 cells	LPS	RPMI	Sample/positive drug
Normal/blank of control	+	-	+	-
Control	+	+	+	-
Sample/ positive	+	+	+	+

Note: with (+), without (-); n = 3

2.8.2.3 Griess assay and MTT assay

Griess assay is used to determine amount of NO in the cells. NO is an unstable endogenous gas releasing from macrophage after LPS-induced inflammation. NO is changed to nitrite (NO_2^-) by enzymatic reaction on mitochondria. Griess assay is performed as shown in Scheme 2.2. The treated cells (2.8.2.2) were incubated for 24 h. After incubation, 100 µl of the supernatant was transferred to the new 96-well plate. 100 µl of Griess reagent was added. The mixture was determined for absorbance at 570 nm.

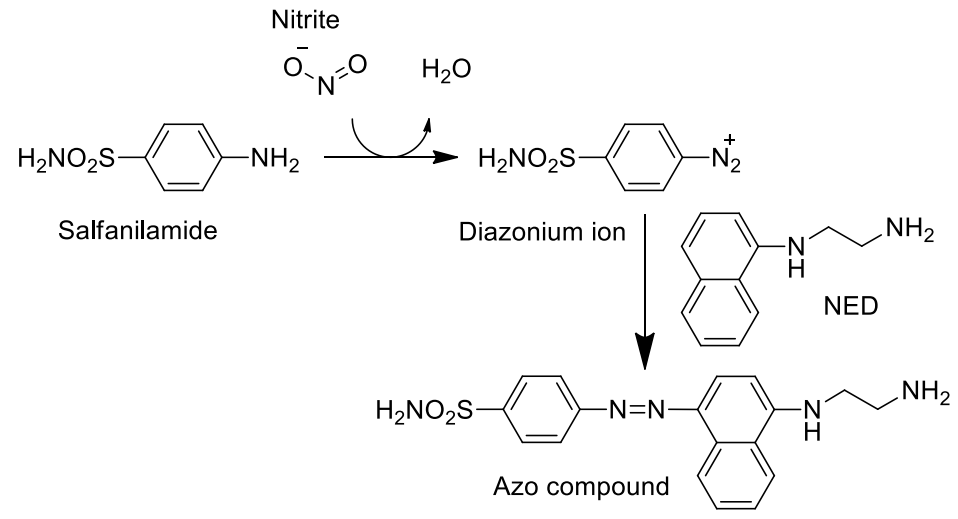

NED : N--napthylethylenediamine dihydrochloride

Scheme 2.2 Griess reaction (modified from Technical Bulletin, Promega Corporation, USA).

In addition, the adherence cells were checked for cell viability. For the cytotoxicity using MTT assay (Scheme 2.3), adherence cells were incubated with 10 µl of MTT reagent (5 mg/ml) at 37 °C for 3 h. Then the MTT reagent was discarded. The formazan product was mixed with 0.04 N HCl in isopropanol. The solution was measured at 570 nm.

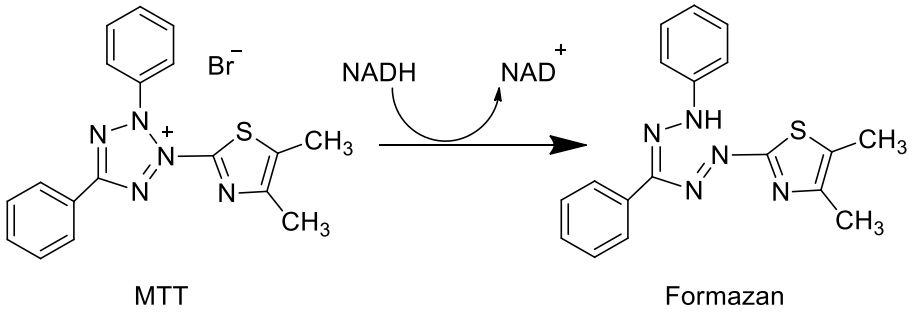

Scheme 2.3 MTT assay (Animal cell culture: a practical approach; Master, 2000).

The OD data after Griess and MTT assay were calculated using Microsoft Excel. For NO assay, the % inhibition of NO production was calculated as shown in following equations. Then either linear regression or non-linear regression was plotted between the percentages of inhibitory effect (%) against concentrations of sample (µM). The regression was chosen using the correlation coefficient (R^2) that closed to 1. Finally, the inhibitory concentration at 50 % of every treatment was considered. The cytotoxicity using MTT assay, the OD was set following the OD of sample group was less than 80 % of that in the control group was judged the test compound to be cytotoxic. The data was represented by mean ± S.E.M (n=3).

$$\% \text{ inhibition of NO} = \frac{[(\text{control} - \text{blank of control}) - (\text{sample} - \text{blank of sample})]}{[(\text{control} - \text{blank of control})]} \times 100$$

2.8.2.4 Determination of *iNOS* and *COX-2* expressions

Genes expressions of *iNOS* and *COX-2* were determined using quantitative real-time (qRT)-PCR.

Treatment of RAW264.7 cells

Macrophage RAW 264.7 cells were sub-cultured and were placed in to 6-well plate (1×10^6 cells/well). These cells were incubated for 24 h and then cells were separately treated including normal, control, sample, and also positive group. Sample was prepared at various concentrations in DMSO and the solution was added cells to a final concentration of 0, 3, 10, and 30 µM, respectively. The treated cells were incubated at 37 °C, 5% CO_2 for 20 h.

After incubation, the cultured medium was removed and cells were washed with PBS (3 ml. 2 times). Then, the freshly RPMI (1.5 ml) was added to cells and then cells were scrapped by cell scrapper. The suspension of treated cells was collected into 1.8 ml micro-centrifuge tube and was kept at ice-box.

Isolation of total RNA

Total RNA was isolated from the untreated and treated cells using a Total RNA Mini Kit (Geneaid®, New Taipei City, Taiwan). According to the manufacturer's protocol (2.6.5.1), the total RNA was obtained. The isolated RNA was kept at -80ºC until further used for qRT-PCR step.

qRT-PCR

Subsequently, 20 ng of total RNA was used as a template for qRT-PCR using a One Step SYBR®PrimeScript™ RT-PCR kit II (Perfect Real Time, Takara, Japan). Quantitative RT-PCR (qRT-PCR) was performed by the ABI Prism® 7300 Fast Real-Time PCR system (California, USA). PCR reaction was performed (2.5.6.2); the amplification plot of target genes was then obtained. The quantification cycle (Cq) value was obtained and the relative gene expression and %

gene inhibition were then calculated by ΔΔCq method as shown below when using *GAPDH* as endogenous gene and control group as a calibrator (mean ± S.D., n = 3).

ΔΔCq equation followings;

$$\Delta Cq = \Delta Cq\,[\text{target gene}] - \Delta Cq\,[\text{GAPDH}] \quad (1)$$

$$\Delta Cq \text{ expression} = 2^{-\Delta Cq} \quad (2)$$

$$\Delta\Delta Cq \text{ expression} = \frac{\text{Mean } \Delta Cq \text{ expression of target gene}}{\text{Mean } \Delta Cq \text{ expression of calibator}} \quad (3)$$

$$\%\text{ gene inhibition} = [1 - \Delta\Delta Cq] \times 100 \quad (4)$$

2.9 Statistical analysis

All data at each concentration for each sample including the inhibitory of NO production and MTT assay were expressed as mean ± standard error of the mean (S.E.M.) of three determinations from individual experiment (n= 3). These data was plot against concentration and the IC_{50} value was then calculated by Microsoft excel program. Data for cell cycle analysis and Annexin-V/7AAD detecting apoptosis were expressed on the percentage (mean ± standard deviation (S.D.), n= 3. For qRT-PCR, the RQ value showed as mean ± S.D, (n = 3). The caspase activity was expressed to fold of control (mean ± S.D., n = 3). In this study, the statistical analysis of all data was used one-way analysis of variance (ANOVA), followed by Dunnett's test (compared with untreated group) and the significance was set at $p < 0.05$.

CHAPTER 3

RESULTS

3.1 Phytochemical study

Herein, the dried leaves and stems of *C. stellatopilosus* were used as materials for isolation of diterpenes. The crude extract was obtained from maceration. Using chromatographic methods, four diterpenes were isolated and designated as CSPNT, CSA1, CSA2 and CSA3. Furthermore, three flavonoids and phytosterols were also isolated and designated as EtO-1, EtO-2, EtO-3, CSBS and CSBSDG. These compounds were analyzed using spectroscopy and their structures werefurther elucidated and identified. The isolation schemes of compounds from *C. stellatopilosus* is summarized in Fig. 3.1

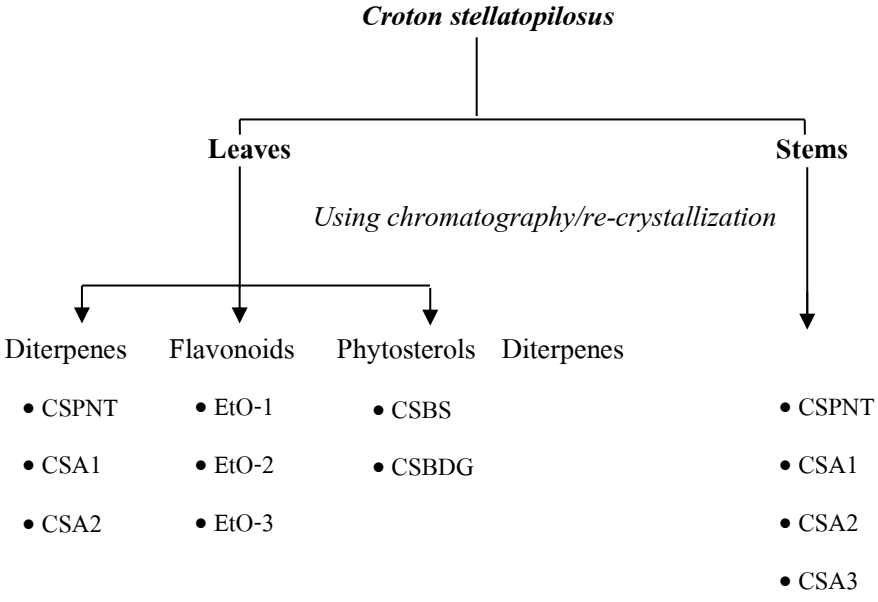

Figure 3.1 The isolation scheme of compounds from *C. stellatopilosus*.

3.1.1 Identification of CSPNT as plaunotol

Compound CSPNT was obtained by column chromatography with chloroform: EtOAc (3:1). A yield of CSPNT was 800 mg (1.6% w/w of LCSME).

Characteristic	pale yellow oil, soluble in hexane, dichloromethane, chloroform and methanol
Molecular weight (g/mol)	306
UVλmax (nm)	290
IR absorption (νmax cm^{-1})	3300, 1665, 1440, 1380 and 1000
1D-NMR	in $CDCl_3$ (Table 3.1)
^{1}H-NMR (500 MHz)	δ: 4.07 (2H, d, J = 7.1 Hz, H-1), 5.35 (1H, m, H-2), 2.02 (2H, m, H-4), 2.16 (2H, m, H-5), 5.22 (1H, m, H-6), 2.10 (2H, m, H-8), 1.90-2.20 (2H, m, H-9), 5.06 (1H, m, H-10), 2.02 (2H, m, H-12), 1.95 (2H, m, H-13), 5.09 (1H, m, H-14), 1.64 (3H, s, H-16), 1.64 (3H, s, H-17), 4.05 (2H, s, H-18), 1.60 (3H, s, H-19), 1.60 (3H, s, H-20)
^{13}C-NMR (125 MHz)	δ: 59.8 (CH_2, C-1), 124.2 (CH, C-2), 138.9 (C, C-3), 39.2 (CH_2, C-4), 25.8 (CH_2, C-5), 127.4 (CH, C-6), 138.8 (C, C-7), 38.4 (CH_2, C-8), 26.7 (CH_2, C-9), 123.9 (CH, C-10), 131.3 (C, C-11), 39.6 (CH_2, C-12), 26.6 (CH_2, C-13), 124.0 (CH, C-14), 135.3 (C, C-15), 15.6 (CH_3, C-16), 16.4 (CH_3, C-17), 58.9 (CH_2, C-18), 17.6 (CH_3, C-19), 15.9 (CH_3, C-20)

Compound CSPNT was obtained as an oil from the hexane extract. Its IR spectrum, showed hydroxyl and olefin absorption bands at 3300 cm^{-1} (O-H) and 1665 cm^{-1} (C=C), respectively. Other signals at 1440, 1250 and 100 cm^{-1}were also found and indicated as aliphatic hydrocarbon absorption (C-H). The molecular weight of CSPNT was analyzed using ESI-MS and its spectrum indicated the molecular ion peak appeared at m/z 306. Based on spectral data, the ^{1}H-NMR showed the signal of 34 protons, and ^{13}C-NMR showed the signals of 20 carbons, corresponding four methyl (CH_3 = 4), eight ethylene (CH_2 =8) and four methane (CH =4) from DEPT 90 and DEPT 135 experiments. Other signals were further indicated as four quaternary carbon (C =4). Moreover, the two signals of hydroxyl functional group connecting methylene were further proposed at δ 4.05 and 4.07, respectively. These spectral data indicated that the molecular formula of CSPNT was deduced to be $C_{20}H_{34}O_2$. The double bond equivalent (D.B.E.) in this molecule showed the unsaturated bond of four, so that its structure further related to four of olefin.

The ^{13}C-NMR spectrum showed four olefinic carbons at δ 124.2 (CH, C-2), 127.4 (CH, C-6), 123.9 (CH, C-10) and 124.0 (CH, C-14), respectively, therefore these signals were corresponding for four unsaturated degree, which related with molecular formula. Herein, compound CSPNT was indicated as an acyclic diterpene alcohol. The ^{1}H-NMR spectrum showed four olefinic protons including δ 5.35 (1H, m, H-2), 5.22 (1H, m, H-6), 5.02 (1H, m, H-10) and 5.39 (1H, m, H-14), and together with four protons attached to the oxygenated methylene carbons at δ 4.07 (2H, d, J = 7.1 Hz, H-1) and 4.05 (2H, s, H-18). Its structure also exhibited four singlets of vinyl methyl groups at δ1.64 (6H, s, H-15, H-16) and 1.60 (6H, s, H-19, H-20). Furthermore, these fragments of partial structure were connected with six signals of aliphatic methylene at δ 2.02 (2H, m, H-4), 2.16 (2H, m, H-5), 2.10 (2H, m, H-8), 1.90-2.20 (2H, m, H-9), (2H, m, H-12), 1.95 (2H, m, H-13) using COSY, HMQC and HMBC spectral data (Table 3.1). In addition, by comparison of its spectral data with previous reports, the CSPNT was identified as plaunotol (Ogiso *et al*., 1978; Premprasert *et al*., 2013).

The ^{1}H and ^{13}C-NMR of CSPNT are summarized in Table 3.1 and the partial structures that related to plaunotol structure are shown in Fig 3.2.

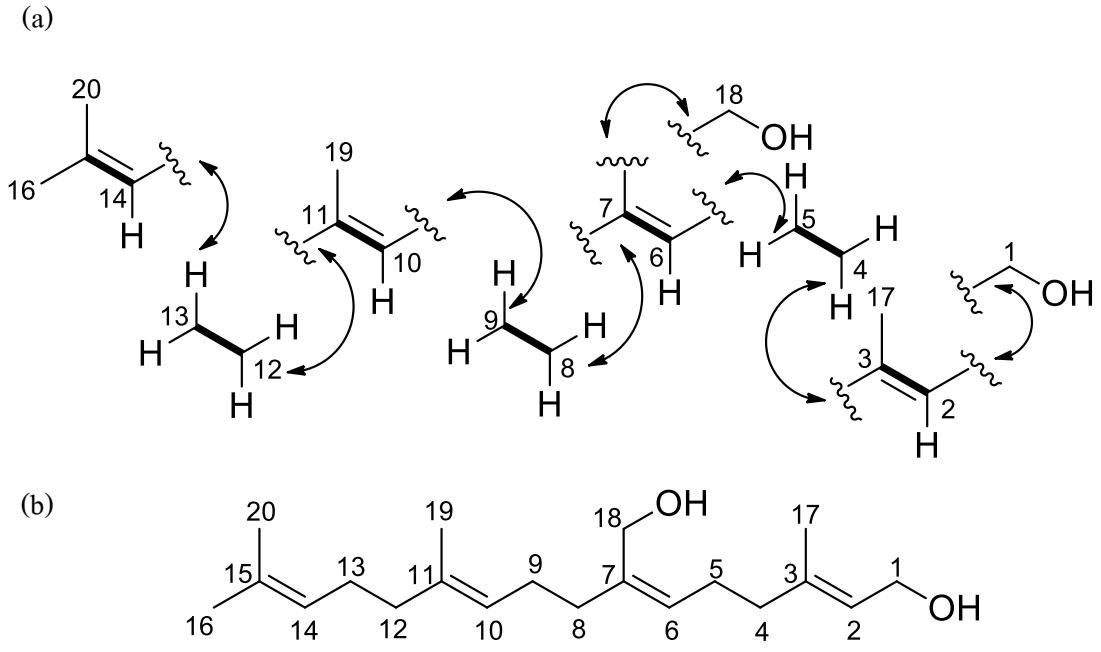

Figure 3.2 The partial structures (a) and the structure of CSPNT as plaunotol (b).

Table 3.1 ^{1}H and ^{13}C-NMR of CSPNT (500 MHz for ^{1}H; $CDCl_3$).

Carbon position	CSPNT		References (Ogiso *et al*., 1978)	(Premprasert *et al.,* 2013)	
	^{1}H-	^{13}C-	^{1}H	^{1}H-	^{13}C-
1	4.07 (d; *J* = 7.1)	59.8 (CH_2)	3.97 (d)	4.07 (d; *J* = 7.1)	59.8 (CH_2)
2	5.35 (m)	124.2 (CH)	5.30 (t)	5.35 (m)	124.2 (CH)
3		138.9 (C)			138.9 (C)
4	2.02 (m)	39.2 (CH_2)	1.9-2.3 (m)	2.02 (m)	39.2 (CH_2)
5	2.16 (m)	25.8 (CH_2)	1.9-2.3 (m)	2.16 (m)	25.8 (CH_2)
6	5.22 (m)	127.4 (CH)	5.14 (t)	5.22 (m)	127.4 (CH)
7		138.8 (C)			138.8 (C)
8	2.10 (m)	34.8 (CH_2)	2.01(m)	2.10 (m)	34.8 (CH_2)
9	1.9-2.2(m)	26.7 (CH_2)		1.9-2.2(m)	26.7 (CH_2)
10	5.06 (m)	123.9 (CH)	5.05 (m)	5.06 (m)	123.9 (CH)
11		131.3 (C)			131.3 (C)
12	2.02 (m)	39.6 (CH_2)		2.02 (m)	39.6 (CH_2)
13	1.95 (m)	26.6 (CH_2)	1.95 (m)	1.95 (m)	26.6 (CH_2)
14	5.09 (m)	124.0 (CH)	5.05 (m)	5.09 (m)	124.0 (CH)
15		135.3 (C)			135.3 (C)
16	1.64 (s)	25.6 (CH_3)	1.66 (s)	1.64 (s)	25.6 (CH_3)
17	1.64 (s)	16.4 (CH_3)	1.67 (s)	1.64 (s)	16.4 (CH_3)
18	4.05 (s)	58.9 (CH_2)	3.94 (s)	4.05 (s)	58.9 (CH_2)
19	1.60 (s)	17.6 (CH_3)	1.58 (s)	1.60 (s)	17.6 (CH_3)
20	1.60 (s)	15.9 (CH_3)	1.58 (s)	1.60 (s)	15.9 (CH_3)

3.1.2 Identification of CSA1 as plaunol F

After re-crystallization with hexane and chloroform (3:1), colorless compound (CSA1) was obtained to a yield 144.9 mg (0.13% w/w of dichloromethane fraction).

Characteristic	colorless crystal, soluble in dichloromethane, chloroform and acetone
Molecular weight (g/mol)	340
UV λmax (nm)	290
IR absorption (νmax cm^{-1})	3140, 1760, 1640, 1500, 900, 880
1D-NMR	in $CDCl_3$ (Table 3.2)
^{1}H-NMR (500 MHz)	δ: 1.41(1H, m, H-1), 1.79 (1H, m, H-1), 2.23 (1H, m, H-2), 2.46 (1H, m, H-2), 6.70 (1H, dd, *J* = 7.6, 2.2 Hz, H-3), 1.54 (1H, dddd, *J* = 13.2, 10.5, 2.7, 2.7, H-6), 2.13 (1H, ddd, *J* = 13.4, 9.5, 7.1), 2.42 (1H, m, H-7), 2.56 (1H, m, H-7), 2.20 (1H, m, H-10), 2.60 (1H, dd, *J* = 13.7, 6.4 Hz, H-11), 2.75 (1H, dd, *J* = 13.7, 8.5 Hz, H-11), 5.52 (1H, dd, *J* = 8.5, 6.6 Hz, H-12), 6.35 (1H, d, *J* = 0.97 Hz, H-14), 7.40 (1H, d, *J* = 1.95 Hz, H-15), 7.40 (1H, d, *J* = 1.95 Hz, H-16), 4.81 (1H, d, *J* = 0.90 Hz, H-17), 5.03 (1H, d, *J* =1.2 Hz, H-17), 4.24 (1H, dd, *J* = 9.9,2.2 Hz, H-19), 4.29 (1H, d, *J* = 9.0 Hz, H-19)
^{13}C-NMR (125 MHz)	δ: 21.5 (CH_2, C-1), 26.6 (CH_2, C-2), 133.7 (CH, C-3), 137.2 (C, C-4), 44.1 (C, C-5), 32.6 (CH_2, C-6), 27.9 (CH_2, C-7), 147.4 (C, C-8), 53.5 (C, C-9), 49.0 (CH, C-10), 43.8 (CH_2, C-11), 71.6 (CH, C-12), 124.8 (C, C-13), 108.5 (CH, C-14), 144.1 (CH, C-15),

140.1 (CH, C-16), 113.4 (CH_2, C-17), 169.5 (C=O, C-18), 73.5 (CH_2, C-19), 176.7 (C=O, C-20)

The molecular formula of CSA1 was $C_{20}H_{20}O_5$, determined by EI-MS and its molecular ion peak at m/e 340. The IR spectrum of this compound contained an intensive band for γ-lactone at 1760 cm^{-1}, which corresponded to two lactone carbonyl carbons at δ 169.5 (C-18) and 176.7 (C-20) on ^{13}C-NMR (fragment A). The IR absorption band at 3140, 1500 and 900 cm^{-1} proved the presence of β-mono substitute furan ring (fragment B). The protons and carbons of the furan ring later could be exhibited in the NMR spectrum at δ 6.35 (1H, d, J = 0.97 Hz, H-14), 7.40 (1H, d, J = 1.95 Hz, H-14) and 7.40 (1H, d, J = 1.95 Hz, H-14) for ^{1}H-NMR, and at δ 108.5 (C-14), 144.1 (C-15) and 140.1 (C-16). The olefin moiety was found at 1640 and 880 cm^{-1} and its functional group also exhibited on ^{1}H and ^{13}C- NMR, which showed at δ 6.70 (1H, dd, *J* = 7.6, 2.2 Hz, H-3) for 1H, and δ 133.7 (C-3) for ^{13}C, respectively (fragment C). Its structure also found one signal of vinyl methylene functional group, its signals showed at δ 5.03 (1H, J = 1.2 Hz, H-17) and 4.81 (1H, d, *J* = 0.9 Hz, H-17); fragment D. As shown in Fig. 3.3, all fragments (A-D) were connected using COSY and HMQC spectral data to give proposed partial structures. According to the molecular formula, it was equivalent to the unsaturated degrees of eleven, which referred three unsaturated degrees of furan ring, two of carbonyl lactones, one of olefin, one of vinyl methylene, and proposed four rings. Therefore this structure was estimated as pentacyclic clerodane-type diterpene. The interpretation on HMBC spectrum, its spectrum guided that the obtained partial structures were further linked with quaternary carbons at C-4, C-6, C-10, and C-19 to C-5; C-8, C-10, C-11, and C-20 to C-9, and the furan ring was connected to oxygenated methane carbon at C-12. Finally, all spectral data was interpreted by comparison with previously published report and the CSA1 structure was identified as plaunol F (plaunolide) (Takahashi *et al*., 1983, Premprasert *et al*., 2013).

The ^{1}H and ^{13}C-NMR of CSA1 are summarized in Table 3.2 and the partial structures that related to plaunol F structure are shown in Fig. 3.3.

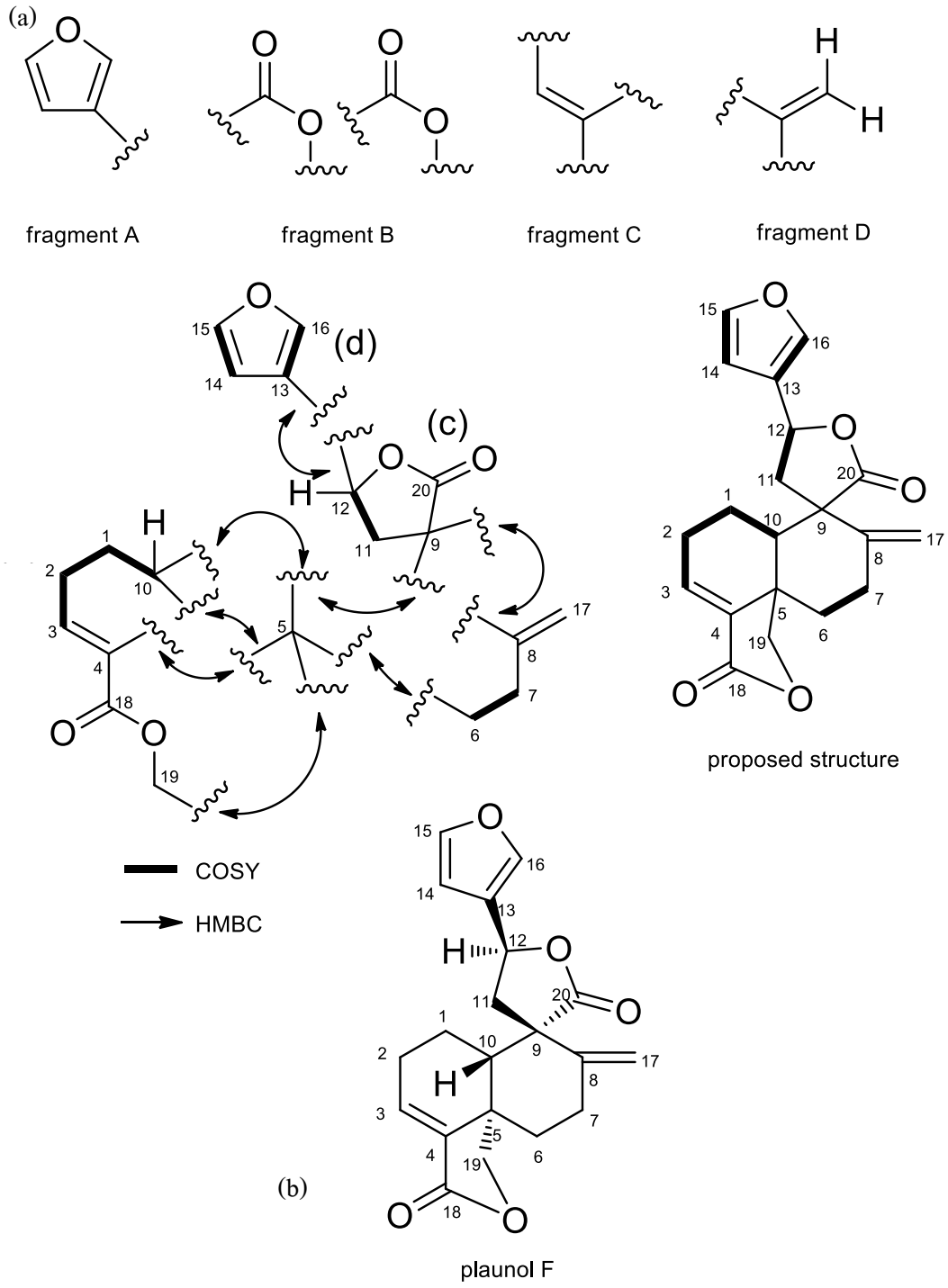

Figure 3.3 The partial structures (a) and the structure of CSA1 as plaunol F (b).

Table 3.2 ^{1}H and ^{13}C-NMR of CSA1 (500 MHz for ^{1}H; $CDCl_3$).

Carbon position	CSA1		References		
			(Takahashi *et al*., 1983)	(Premprasert *et al*., 2013)	
	^{1}H-	^{13}C-	^{1}H	^{1}H-	^{13}C-
1	1.41 (m) 1.79 (m)	21.5 (CH_2)		1.40 (m) 1.80 (m)	21.5 (CH_2)
2	2.23 (m) 2.46 (m)	26.6 (CH_2)		2.21 (m) 2.48 (m)	26.5 (CH_2)
3	6.70 (dd, 7.6, 2.2)	133.7 (CH)	6.64 (1H, dd, 7.4)	6.70 (dd, 7.6, 2.2)	133.7 (CH)
4		137.2 (C)			137.2 (C)
5		44.1 (C)			44.1 (C)
6	1.54 (dddd, 13.2,10.5,2.7,2.7) 2.13 (ddd,13.4,9.5,7.1)	32.6 (CH_2)		1.53 (dddd, 13.2,10.5,2.7,2.7) 2.13 (ddd,13.2,9.3,6.8)	32.6 (CH_2)
7	2.42 (m) 2.56 (m)	27.9 (CH_2)		2.44 (m) 2.58 (m)	27.9 (CH_2)
8		147.4 (C)			147.4 (C)
9		53.5 (C)			53.5 (C)
10	2.20 (m)	49.0 (CH)		2.19 (m)	48.9 (CH)
11	2.60 (dd, 13.7, 6.4) 2.75 (dd, 13.7, 8.5)	43.8 (CH_2)		2.60 (dd, 13.7,6.6) 2.75 (dd, 13.7, 8.5)	43.7 (CH_2)
12	5.52 (dd, 8.5, 6.6)	71.6 (CH)	5.69 (1H, dd, 7.0, 8.0)	5.52 (dd, 8.5, 6.6)	71.6 (CH)
13		124.8 (C)			124.8 (C)
14	6.35 (d, 0.97)	108.5 (CH)	6.50 (1H, m)	6.35 (d, 0.98)	108.5 (CH)
15	7.40 (d, 1.95)	144.1(CH)	7.56 (1H, m)	7.40 (d, 1.95)	144.1 (CH)
16	7.40 (d, 1.95)	140.1(CH)	7.64 (1H, m)	7.40 (d, 1.95)	140.0 (CH)
17	4.81 (d, 0.90) 5.03 (d, 1.2)	113.4 (CH_2)	4.82 (1H, br s,) 5.06 (1H, d, 2.0)	4.80 (d, 0.5) 5.02 (d, 1.5)	113.4 (CH_2)

Table 3.2 (Continued)

Carbon position	CSA1		References (Takahashi *et al*., 1983)		(Premprasert *et al*., 2013)
	^{1}H-	^{13}C-	^{1}H	^{13}C-	^{1}H-
18		169.5 (CO)			169.5 (CO)
19	4.24 (dd, 9.0, 2.2) 4.29 (d, 9.0)	73.5 (CH_2)	4.22 (1H, d, 9.0) 4.15 (1H, d, 9.0)	4.23 (dd, 9.0, 2.2) 4.30 (d, 9.0)	73.5 (CH_2)
20		176.7 (CO)			176.7 (CO)

3.1.3 Identification of CSA2 as plaunol E

After re-crystallization with EtOAc : acetone (3:1), amorphous compound (CSA2) was obtained to a yield 17.9 mg (0.017% w/w of dichloromethane fraction).

Characteristic	colorless amorphous crystal, soluble in acetone, ethyl acetate and methanol
Molecular weight (g/mol)	314
UV λmax (nm)	290
IR absorption (νmax cm^{-1})	3420, 3140, 1750, 1720, 1645, 1500, 880
1D-NMR	in acetone-d_6 (Table 3.3)
^{1}H-NMR (500 MHz)	δ: 2.23 (1H, m, H-1), 3.18 (1H, m, H-1), 4.66 (1H, m, H-2), 6.68 (1H, d, *J* =2.2 Hz, H-3), 4.68 (1H, dd, *J* = 12.0, 6.1 Hz, H-6), 2.45 (1H, dd, *J* = 13.4, 6.1 Hz, H-7), 2.82 (1H, dd, *J* =13.4, 6.1 Hz, H-7), 2.04 (1H, m, H-10), 1.97 (1H, dd, *J* = 15.6, 1.9 Hz, H-11), 2.07 (1H, dd, *J*= 15.6, 10.2 Hz, H-11), 5.95 (1H, dd, *J* = 10.0, 1.8 Hz, H-12), 6.43 (1H, m, H-14), 7.49 (1H, m, H-15), 7.49 (1H, m, H-16), 5.07 (1H, d, *J* = 2.2 Hz, H-17), 5.40 (1H, d, *J* = 2.4 Hz, H-17), 3.31 (1H, dd, *J* = 11.0, 1.4 Hz, H-19), 4.01 (1H, d, *J* =11.0 Hz, H-19), 4.75 (1H, d, *J* = 3.9 Hz, H-20), 2.01 (3H, s, H-22), 4.50 (1H, d, J =4.9 Hz, OH-2), 5.57 (1H, d, *J* =3.9 Hz, OH-20)
^{13}C-NMR (125 MHz)	δ:30.0 (CH_2, C-1), 64.7 (CH, C-2), 141.9 (CH, C-3), 133.0 (C, C-4), 41.0 (C, C-5), 81.3 (CH, C-6), 38.3 (CH_2, C-7), 148.3 (C, C-8), 46.5 (C, C-9), 32.6 (CH, C-10), 39.4 (CH_2, C-11), 66.4 (CH, C-12), 128.1 (C, C-13), 109.6 (CH, C-14), 144.3 (CH, C-15),

140.3 (CH, C-16), 115.5 (CH_2, C-17), 169.1 (C=O, C-18), 62.7 (CH_2, C-19), 101.3 (CH, C-20), 170.9 (C, C-21), 21.3 (CH_3, C-22)

^{1}H-NMR and ^{13}C-NMR suggested that compound was furano clerodane-type diterpene as same as plaunol F, which was mentioned above. The structure elucidation of compound CSA2 was established as followed. Its IR spectrum showed the vibration signals including O-H stretching at 3420 cm^{-1}, two signals of C=O stretching at 1750 and 1720 cm^{-1} and C= C stretching at 1645 cm^{-1}. These IR spectral data indicated that CSA2 composed hydroxyl group, two carbonyl carbons and olefin moiety, respectively. The IR spectrum also found at 3140, 1500 and 880 cm^{-1} and its data was further indicated as β-mono-substituted furan structure. The ^{1}H-NMR signal showed the three protons signals for β-mono substituted furan ring at δ7.49 (2H, m, H-15, H-16), which were exhibited for two protons on α-position and at δ 6.43 (1H, m, H-14), which was exhibited on β-position, one signal for olefin functional group at δ 6.68 (1H, d, J = 2.2 Hz, H-3), two signals for exo-methylene moiety at δ 5.07 (1H, d, J = 2.2 Hz, H-17) and 5.40 (1H, d, J = 2.4 Hz, H-17) and one signal for methyl group at δ 2.01 (3H, s, H-22). The other signals for 15 protons were exhibited on ^{1}H-NMR and its protons were further elucidated as aliphatic hydrocarbon. For ^{13}C-NMR signal showed two signals for quaternary carbon at δ 169.1 (C-18) and 170.9 (C-21), four signals for β-mono substituted furan ring at δ 128.1 (C, C-13), 109.6 (CH, C-14), 144.3 (CH, C-15) and 140.3 (CH-16), two signals for olefinic carbon at δ 141.9 (CH, C-3) and 133.0 (C, C-4), two signals for exo-methylene at δ 148.3 (C, C-8) and 115.5 (CH2, C-17), five oxygenated carbon at δ 64.7 (C-2), 81.3 (C-6), 66.4 (C-12), 62.7 (C-19) and 101.3 (C-20) and one signal for methyl at δ 21.3 (CH3, C-22) and other carbon signals for 6 carbons showed at aliphatic carbon signal following δ 30.0 (C-1), 41.0 (C-5), 38.3 (C-7), 46.5 (C-9), 32.6 (C-10), 39.4 (C-11), respectively. Due to ^{1}H and ^{13}C-NMR, the proposed molecular formula of CSA2 was $C_{22}H_{24}O_8$corresponding the molecular ion peak at m/e 416. The unsaturated degree of its molecular formula established on 10, so the

functionality of this compound was composed two carbonyl, four olefin and four-membered rings. The structure of CSA2 was similar to plaunol F, however the breakage of lactone ring at C-9 and the formation bridge were occurred on CSA2. The carbon-carbon connection of CSA2 structure was relied on 2D-NMR such as COSY, HMQC and HMBC. Finally, the expected functional groups were linked by aliphatic carbon and all spectral data was compared with previous report and CSA2 was then identified as plaunol E (Kitazawa *et al*., 1980; Premprasert *et al*., 2013). The ^{1}H and ^{13}C-NMR of CSA2 are summarized in Table 3.3 and the partial structures that related to plaunol E structure are shown in Fig 3.4.

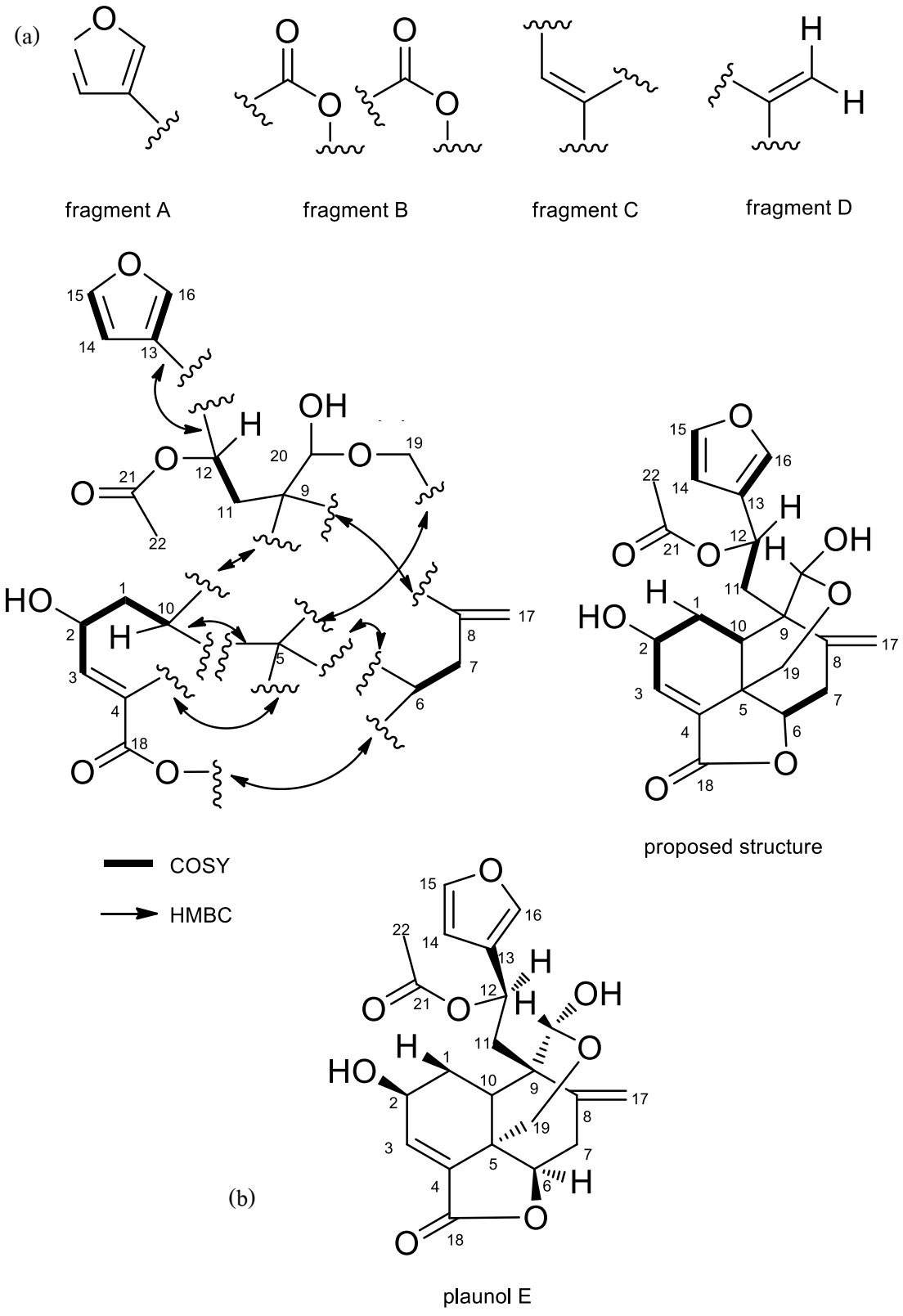

Figure 3.4 The partial structures (a) and the structure of CSA2 as plaunol E (b).

Table 3.3 ^{1}H and ^{13}C-NMR of CSA2 (500 MHz for ^{1}H; C_3D_6O).

Carbon position	CSA2		References		
			(Kitazawa *et al.,* 1980)	(Premprasert *et al*., 2013)	
	^{1}H-	^{13}C-	^{1}H	^{1}H-	^{13}C-
1	2.23 (m) 3.18 (m)	30.0 (CH_2)		2.25 (m) 3.20 (m)	30.0 (CH_2)
2	4.66 (m)	64.7 (CH)	4.67 (m)	4.67 (m)	64.7 (CH)
3	6.68 (d, 2.2)	141.9 (CH)	6.68 (d, 2.5)	6.68 (d, 2.3)	141.9 (CH)
4		133.0 (C)			132.9 (C)
5		41.0 (C)			40.9 (C)
6	4.68 (dd, 12.0, 6.1)	81.3 (CH)	4.68 (dd, 11.5, 6.2)	4.68 (dd, 11.9, 6.2)	81.3 (CH)
7	2.45 (dd,13.4, 6.1) 2.82 (dd,13.4, 6.1)	38.3 (CH_2)	2.83 (dd, 13.5, 6.2) 2.45 (ddd, 13.5, 11.5, 2.0)	2.45 (dd,13.5, 6.2) 2.83 (dd,13.3, 6.2)	38.3 (CH_2)
8		148.3 (C)			148.2 (C)
9		46.5 (C)			46.4 (C)
10	2.04 (m)	32.6 (CH)	2.03 (m)	2.03 (m)	32.6 (CH)
11	1.97 (dd, 15.6, 1.9) 2.70 (dd, 15.6, 10.2)	39.4 (CH_2)	1.97 (dd, 15.5, 2.0) 2.72 (dd, 15.5, 10.0)	1.97 (dd, 15.8, 1.8) 2.72 (dd, 15.8, 10.0)	39.3 (CH_2)
12	5.95 (dd, 10.0, 1.8)	66.4 (CH)	5.92 (dd, 10.0, 2.0)	5.95 (dd, 10.0, 1.8)	66.3 (CH)
13		128.1 (C)			128.0 (C)
14	6.43 (m)	109.6 (CH)	6.68 (m)	6.42 (m)	109.5 (CH)
15	7.49 (m)	144.3 (CH)	7.49 (m)	7.48 (m)	144.2 (CH)
16	7.49 (m)	140.3 (CH)	7.49 (m)	7.48 (m)	140.3 (CH)
17	5.07 (d, 2.2) 5.40 (d, 2.4)	115.5 (CH_2)	5.06 (d, 2.0) 5.40 (d, 2.0)	5.06 (d, 2.3) 5.40 (d, 2.3)	115.5 (CH_2)
18		169.1 (C)			169.1 (C)
19	3.31 (dd, 11.0, 1.4) 4.01 (d, 11.0)	62.7 (CH_2)	3.31 (dd,11.0, 1.5) 4.01 (d, 11.0)	3.31 (dd, 11.0, 1.4) 4.01 (d, 11.0)	62.6 (CH_2)

Table 3.3 (Continued)

Carbon position	CSA2		References		
			(Kitazawa *et al.,* 1980)	(Premprasert *et al*., 2013)	
	^{1}H-	^{13}C-	^{1}H	^{1}H-	^{13}C-
20	4.75 (d, 3.9)	101.3 (CH)	4.76 (d, 4.0)	4.76 (d, 3.6)	101.3 (CH)
21		170.9 (C)			170.8 (C)
22	2.01 (3H, s)	21.3 (CH_3)	2.01 (3H, s)	2.01 (3H, s)	21.3 (CH_3)
OH-2	4.50 (OH, d, 4.9)		4.40 (OH, d, 5.0)	4.50 (OH, d, 5.0)	
OH-20	5.57 (OH, d, 3.9)		5.49 (OH, d, 4.0)	5.57 (OH, d, 3.9)	

3.1.4 Identification of CSA3 as plaunol A

After re-crystallization using hexane: acetone (3:1), CSA3 12.9 mg (0.016% w/w) was afforded.

Characteristic	white amorphous crystal
Molecular weight (g/mol)	356
UV λmax (nm)	290
IR absorption (νmax cm^{-1})	3300, 1665, 1440, 1380 and 1000
Optical rotation	$[\alpha]_D^{20}$: -45.9° (c = 0.1, acetone)
1D-NMR	in acetone-d_6 (Table 3.4 and Figure 3.6-3.7)
^{1}H-NMR (500 MHz)	δ: 2.16, 2.40 (2H, m, H-1), 2.50, 2.65 (2H, m, H-2), 6.76 (1H, dd, *J* = 4.9, 2.7 Hz, H-3), 4.97 (1H, dd, *J*= 12.4, 5.9 Hz, H-6), 2.83 (1H, dd, *J* = 14.0, 5.9 Hz, H-7), 2.54 (1H, dd, *J* = 13.4, 6.1 Hz, H-7), 2.10 (1H, m, H-10), 2.53 (1H, dd, *J* = 13.5, 7.8 Hz, H-11), 2.34 (1H, dd, *J* = 13.4, 8.3 Hz, H-11), 5.15 (1H, t, *J*= 8.1, H-12), 6.53 (1H, m, H-14), 7.54 (1H, m, H-15), 7.59 (1H, m, H-16), 5.24 (1H, d, *J* = 2.4 Hz, H-17), 5.19 (1H, d, *J* = 2.7 Hz, H-17), 5.47 (1H, d, *J* = 4.9 Hz, H-19), 5.02 (1H, s (br), H-20), 6.16 (1H, d, *J* = 4.6 Hz, OH-19)
^{13}C-NMR (125 MHz)	δ: 19.4 (CH_2, C-1), 25.9 (CH_2,C-2), 138.1 (CH, C-3), 132.7 (C, C-4), 40.9 (C, C-5), 75.2 (CH, C-6), 37.1 (CH_2, C-7), 146.0 (C, C-8), 48.7 (C, C-9), 38.72 (CH, C-10), 40.9 (CH_2, C-11), 70.6 (CH, C-12), 129.4 (C, C-13), 109.6 (CH, C-14), 144.7 (CH, C-15), 140.0 (CH, C-16), 113.2 (CH_2, C-17), 169.4 (CO, C-18), 92.6 (CH, C-19), 109.9 (CH, C-20).

DEPT 90	δ: 138.1 (CH, C-3), 75.2 (CH, C-6), 38.72 (CH, C-10), 70.6 (CH, C-12), 109.6 (CH, C-14), 144.7 (CH, C-15), 140.0 (CH, C-16), 92.6 (CH, C-19), 109.9 (CH, C-20)
DEPT 135	positive phase; δ 138.1 (CH, C-3), 75.2 (CH, C-6), 38.72 (CH, C-10), 70.6 (CH, C-12), 109.6 (CH, C-14), 144.7 (CH, C-15), 140.0 (CH, C-16), 92.6 (CH, C-19), 109.9 (CH, C-20) and negative phase; δ 19.4 (CH_2, C-1), 25.9 (CH_2,C-2), 37.1 (CH_2, C-7), (CH_2, C-17)
2D-NMR	COSY, HMQC and HMBC in acetone-d_6 (Table 3.4 and Figure 3.8)

For the assignment of the ^{1}H- and ^{13}C-NMR spectra of compound CSA3, a combination between one-dimensional (1D) such as ^{1}H-, ^{13}C- and DEPT experiments and two-dimensional (2D) such as COSY, HMQC and HMBC were carried out for confirming the relative stereochemistry and evaluating the structure conformation of the ring system in this compound. According to this information together with the previous publish of the chemical constituents of *C. stellatopilosus* suggested that compound CSA3 had a clerodane type diterpene skeleton. Table 3.4 shows the complete structure elucidation of ^{1}H and ^{13}C-NMR spectra of a clerodane-type diterpene.

The compound CSA3 was isolated as white amorphous powder. It showed the molecular formula of $C_{20}H_{20}O_6$, as assumed from the molecular ion peak [M^+] at 356 in EIMS. Therefore, the proposed molecular formula required the double bond equivalent of eleven. According to unsaturation degree, this compound was equipped of one carbonyl, three olefins, one exocyclic double bond and six rings system. From the IR spectrum was observed the wave number followings; at 3397 cm^{-1} (O-H (stretching)) was assigned as hydroxyl functional group, 1727 cm^{-1} (C = O (stretching)) was assigned as α, β unsaturated carbonyl functional group on γ-lactone ring

system, at 2920 cm^{-1} (C-H (stretching)), 1456 cm^{-1} (C=C (stretching)) and 903 cm^{-1} were assigned as mono substitute furan moiety. For wave number at 1668 cm^{-1}(C=C (stretching)) and 872 cm^{-1} (out of plane) were shown as exomethylenefunctional group.

The ^{1}H-NMR spectrum of compound CSA3 was indicated 20 signals of proton and its spectrum showed the presence of three olefinic protons for furan moiety (δ 7.40, 2H, H-15, H-16;6.35, 1H, H-14), one olefinic proton at δ 6.70, H-3 and one olefinic proton for exocyclicmethylene at δ 5.02, H-17 and δ 4.80, H-17). As reported by ^{13}C-NMR spectrum displayed 20 carbon signals. These signals were assigned as one carbonyl carbon for a 18, 19-γ lactone ring (δ 169.5, C-18) and eight olefinic carbon including four carbons were assigned on mono substitute furan moiety (δ 144.7, C-13;109.6, C-14; 144.7, C-15), two carbons were assigned on a double bond at C-3 and C-4 (δ 138.1 and 132.7, respectively); and two carbons were assigned on exocyclic methylene that was contacted with C-8 at δ 146.0, (C-8) and 113.2 (C-17), respectively.

In addition, the information of carbon attached with hydrogen on 1D-NMR was performed using the DEPT experiment including DEPT 90° and DEPT 135°, respectively. The off-resonance decoupled spectra were obtained. For DEPT 90° spectrum of compound CSA3 showed nine methane carbons (CH) as shown on positive phase. For DEPT 135° spectrum of compound CSA3 exhibited five methylene carbons (CH_2) as shown in negative phase and this compound also did not compose the methyl group (CH_3), as shown in positive phase of DEPT 135°spectrum). In line with 1D-NMR (^{1}H-, ^{13}C-, and DEPT-) spectra suggested that the compound CSA3 was observed 20 carbon atoms including nine methines, five methylenes and six quaternary carbons, respectively.

Interpretation of 2D-NMR; the COSY spectrum showed the cross peaks in aliphatic methylene field at δ 6.53 (1H, m, H-14), 7.54 (1H, m, H-15), and 7.59 (1H, m, H-16), indicating the presence of mono-substitute furan moiety (fragment A). The COSY spectrum also showed the cross peak at δ 6.76 (1H,dd, *J*= 4.9, 2.7 Hz, H-3); 2.65 (1H, m, H-2); 2.50 (1H, m, H-2); 2.40 (1H, m, H-1); 2.16 (1H, m, H-1); 2.10 (1H, m, H-10), indicating the presence of fragment B. At δ 4.97

(1H, dd, *J* = 12.4, 5.9 Hz, H-6); 2.83 (dd, *J*= 13.4, 6.1 Hz) showed the correlation between C-6 to C-7 (fragment C). At δ 5.15 (1H, dd, *J*= 8.1, 8.1 Hz, H-12); 2.53 (1H, dd, *J*= 13.5, 7.8 Hz, H-11); 2.34 (1H, dd, *J* = 13.4, 8.3 Hz, H-11), showed the correlation between C-11 to C-12 (fragment D). Additionally, HMQC spectrum showed the correlation and led to get three partial structures (showed as fragment E – G). The ^{1}H and ^{13}C NMR of CSA3 were summarized in Table 3.4 and the partial structures were shown on Fig. 3.5.

The connection of partial structures (fragment A – G) and six quaternary carbons (δ 169.4 (C=O, C-18); 146.0 (C-8); 132.7 (C-4); 129.4 (C-13); 48.7 (C-9); 44.3 (C-5)), was assigned using HMBC spectrum. According to HMBC data, quaternary carbon C-5 connected to C-4, C-6, C-10 and C-19, C-18 as a γ lactone carbonyl (δc 169.4, C-18) connected to C-4 and C-6, C-8 connected to C-7, C-9 and C-17, C-4 connected to C-5 and γ lactone carbonyl on C-18, C-9 connected to C-10, C-11 and C-20, and C-20 connected to oxygened function at C-12 and C-19. After HMBC assignments, the partial structures were connected through six quaternary carbons and exhibited the six rings system as shown in Fig. 3.5.

Regarding to the relative configuration, the compound CSA3 was further measured the optical rotation using polarimeter and this compound showed $[\alpha]_D^{20}$: -45.9° (c = 0.1, acetone). Interestingly, by comparison the spectra of compound CSA3 with the previously published data (Kitazawa *et al*., 1980), CSA3 was elucidated and further identified as plaunol A. Thus, this is the first reported on^{13}C-, DEPT- and also 2D-NMR including COSY, HMQC and HMQC, formerly only ^{1}H-NMR was available. The spectral data are summarized and are illustrated in Table 3.4 and Fig. 3.5, respectively.

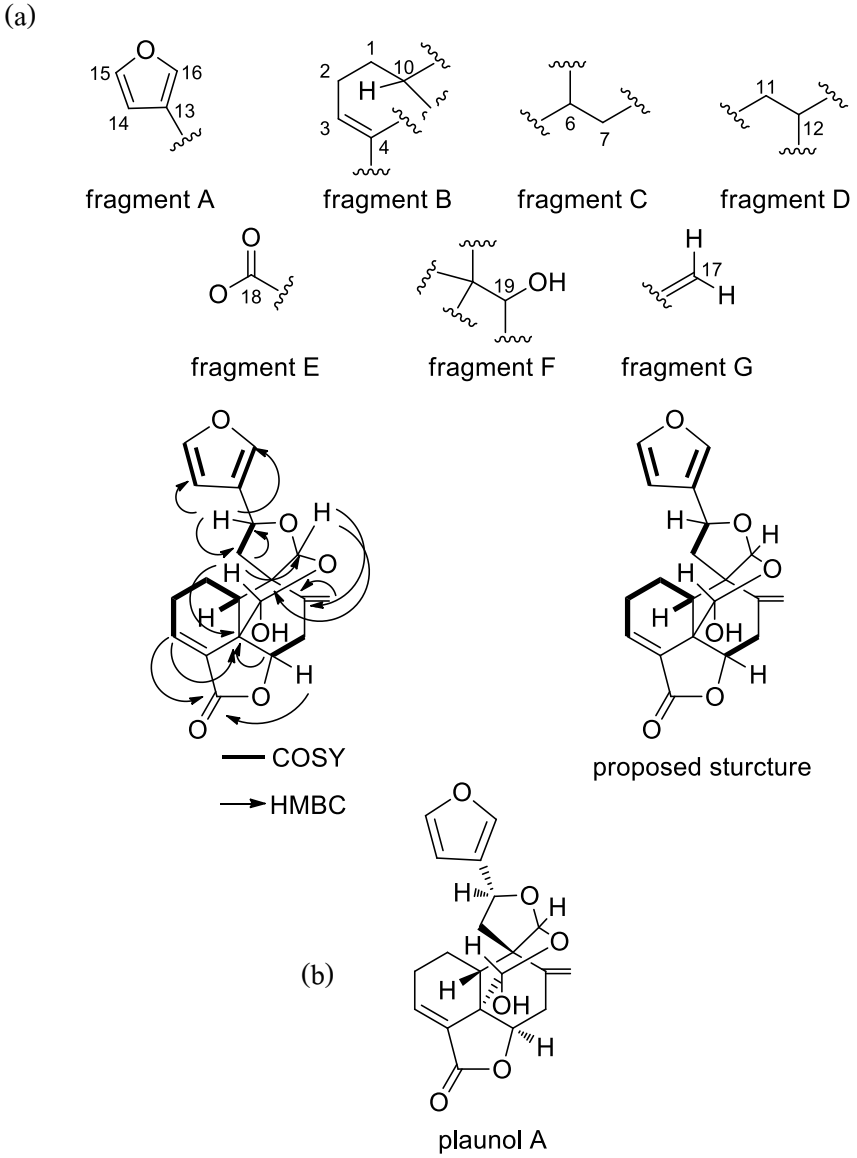

Figure 3.5 The partial structures (a) and the structure of CSA3 as plaunol A (b).

Table 3.4 ^{1}H and ^{13}C-NMR of CSA3 (500 MHz for ^{1}H; C_3H_6O).

Carbon position	CSA3			Reference (Kitazawa *et al*., 1980)
	^{1}H-	^{13}C-	HMBC	^{1}H
1	2.16 (m)	19.4 (CH_2)	H-2, H-10, H-11	
	2.40 (m)			
2	2.50 (m)	25.9 (CH_2)	H-1	
	2.65 (m)			
3	6.76 (dd, 4.9, 2.7)	138.1 (CH)	H-1, H-2	6.76 (dd, 4.0, 3.0)
4		132.7 (C)	H-2, H-7	
5		44.3 (C)	H-1, H-6, H-7, H-11, H-19, OH-19	
6	4.97 (dd, 12.4, 5.9)	75.2 (CH)	H-7, H-19	4.98 (dd, 12.0, 6.0)
7	2.83	37.1 (CH_2)	H-17	2.84
	(dd,14, 5.9)			(dd, 14.0, 6.0)
	2.54			2.40 – 2.60
	(dd,13.4, 6.1)			(ddd, 14.0, 12.0, 2.0)
8		146.0 (C)	H-7, H-11, H-17, H-20	
9		48.7 (C)	H-10, H-11, H-7, H-20, H-17	
10	2.10 (m)	38.72 (CH)	H-1, H-11, H-7	
11	2.53 (dd,13.5, 7.8)	40.9 (CH_2)	H-12	2.54 (dd, 13.5, 8.0)
	2.34 (dd,13.4, 8.3)			2.35 (dd, 13.5, 8.0)
12	5.15 (t, 8.1)	70.6 (CH)	H-11, H-20, H-16	5.15 (dt, 1.0, 8.0)
13		129.4 (C)	H-11, H-12, H-14, H-16	
14	6.53 (m)	109.6 (CH)	H-12, H-15, H-16	6.52 (m)
15	7.54 (m)	144.7 (CH)	H-14, H-16	7.53 (m)
16	7.59 (m)	140.0 (CH)	H-12, H-14, H-15	7.58 (m)
17	5.24 (d, 2.4)	113.2 (CH_2)	H-7, H-11, H-10	5.24 (d, 2.0)
	5.19 (d, 2.7)			5.19 (d, 2.0)
18		169.4 (CO)	H-3, H-6	
19	5.47 (d, 4.9)	92.6 (CH)	H-6, H-10, H-20, OH-19	5.47 (d, 4.5)
20	5.02 (br, s)	109.9 (CH)	H-7, H-10, H-17	5.03 (s)
OH-19	6.16 (OH, d; 4.6)			6.11 (OH, d, 4.5)

^{1}H-NMR

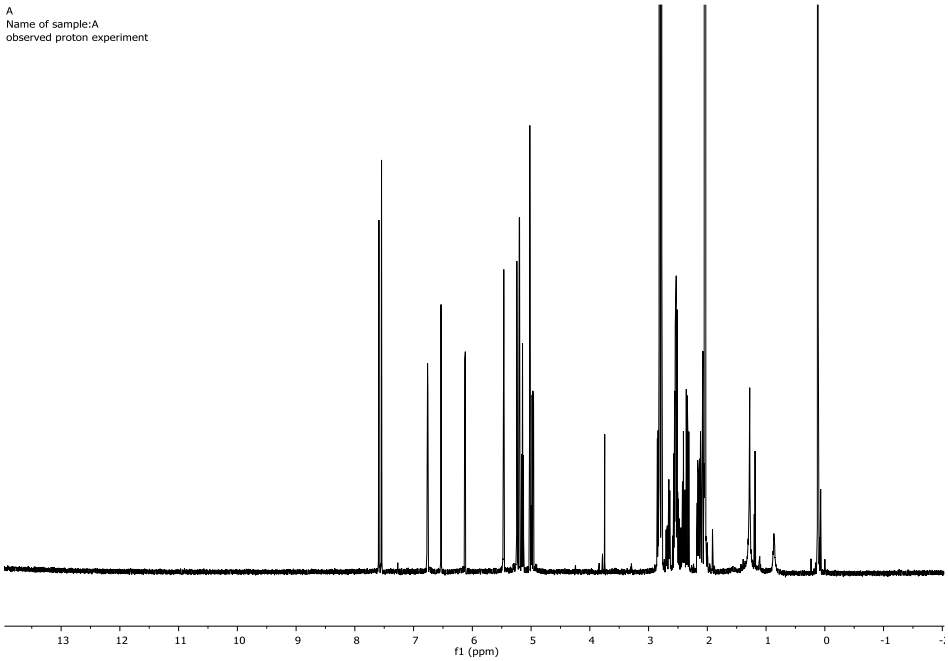

^{13}C-NMR

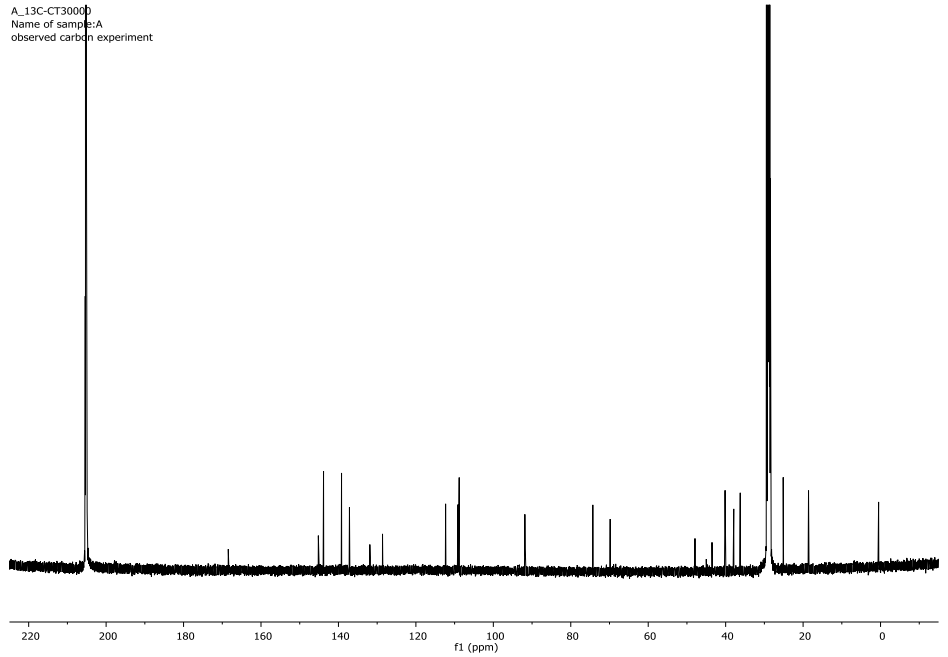

Figure 3.6 ^{1}H and ^{13}C -NMR spectrum of CSA3 (500 MHz for ^{1}H, acetone-d_6).

DEPT 90

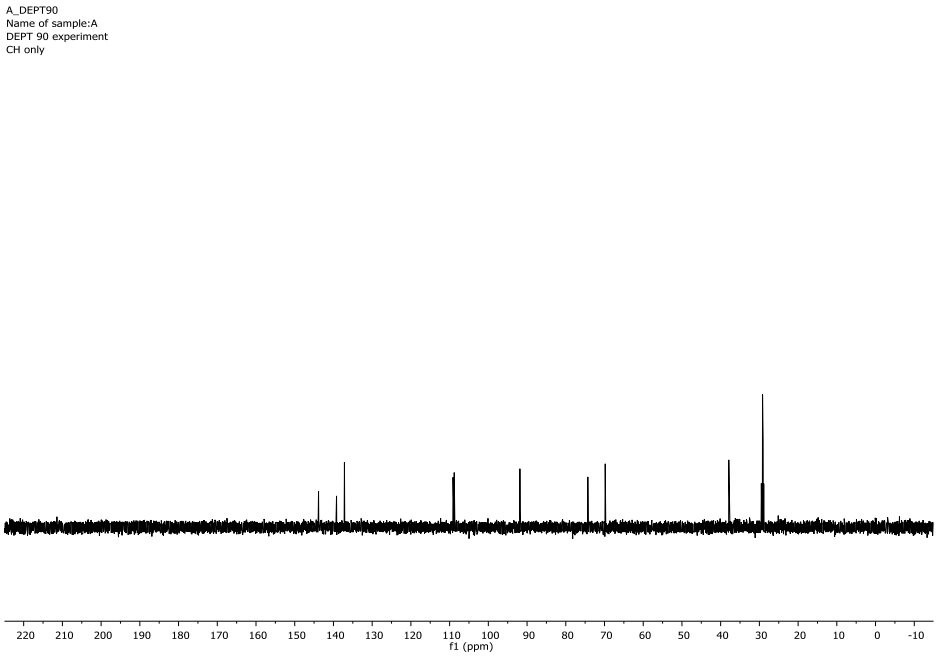

DEPT 135

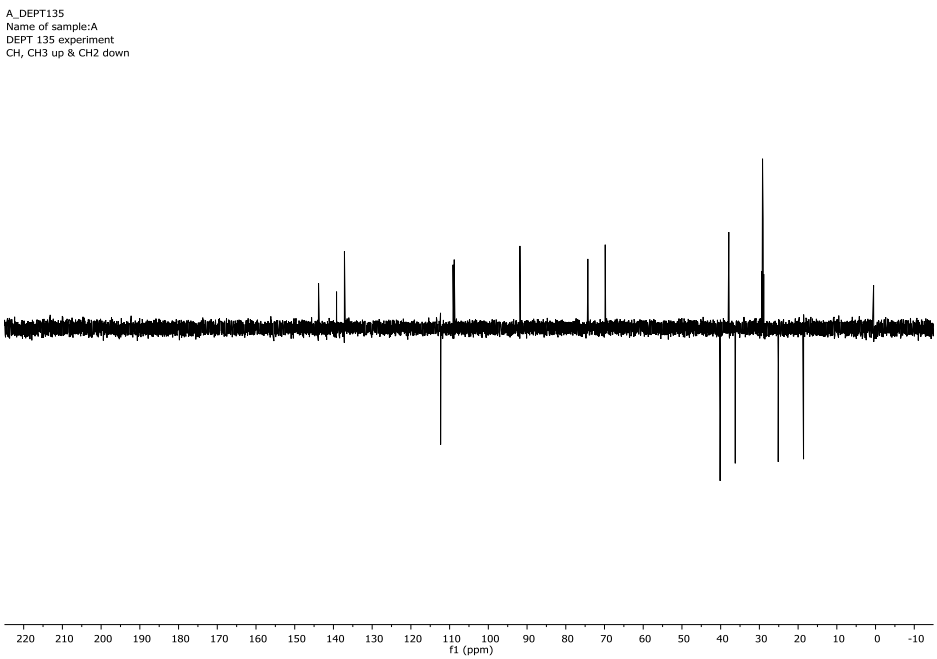

Figure 3.7 DEPT spectrum of CSA3 (500 MHz for ^{1}H, acetone-d_6).

^{1}H-^{1}H-COSY

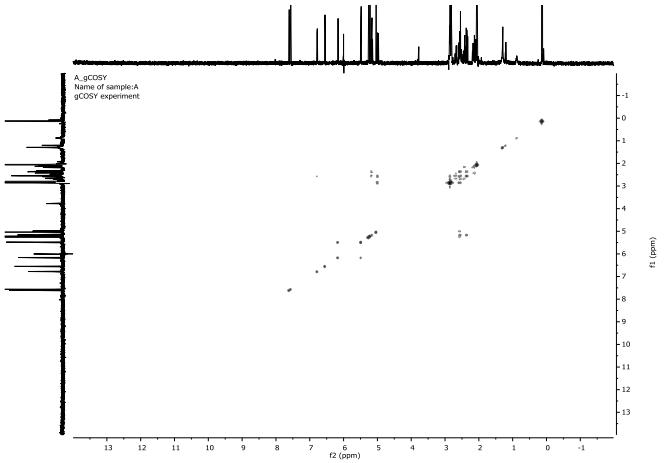

HMQC

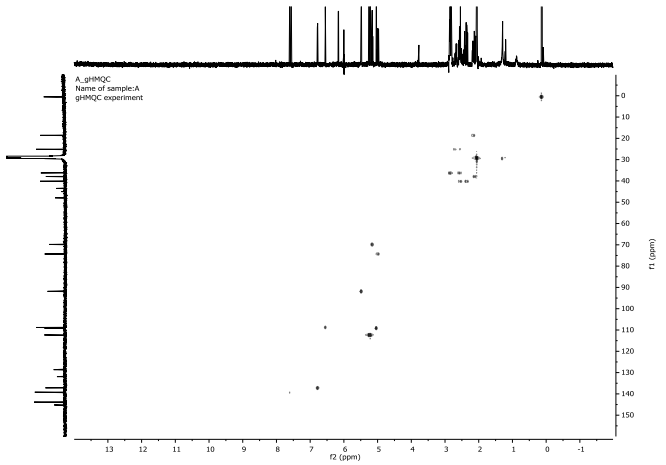

HMBC

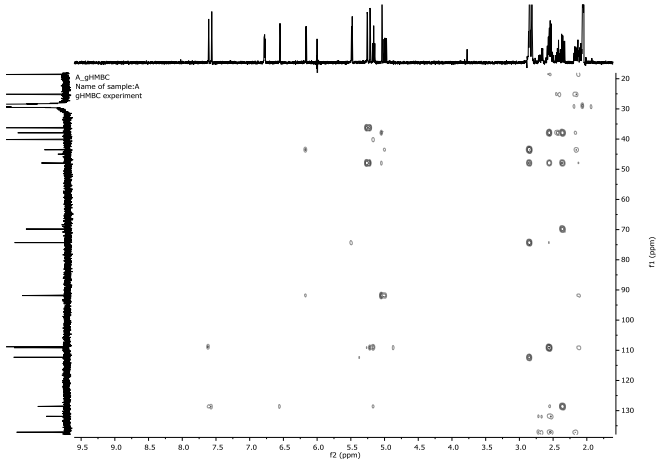

Figure 3.8 2D-NMR spectrum of CSA3 (500 MHz for ^{1}H, acetone-d_6).

3.1.5 Identification of EtO-1 as apigenin-8-C-β-D-glucoside

Characteristic	yellow powder
Molecular weight (g/mol)	432
IR absorption (νmax cm^{-1})	3476, 3819, 2923, 1678, 1559, 1460, 1370, 1280
1D-NMR	in dimethyl sulfoxide-*d*6 (C_2D_6SO) (Table 3.5)
^{1}H-NMR (500 MHz)	δ: 6.76 (1H, s, H-3), 6.27 (1H, s, H-6), 8.01 (1H, d, *J* = 8.8 Hz, H-2′), 6.88 (1H, d, *J* = 8.8 Hz, H-3′), 6.88 (1H, d, *J* = 8.8 Hz, H-5′), 8.01 (1H, d, *J* = 8.8 Hz, H-6′), Sugar region 4.68 (1H, d, *J* = 10.1, H-1′′), 3.83 – 3.24 (6H, m, H-2′′- 6′′), hydroxyl group; 13.17 (1H, br, s, OH-5), 10.32 (1H, br, s, OH-7)
^{13}C-NMR (125 MHz)	δ: 164.1 (C, C-2), 102.6 (CH, C-3), 182.2 (CO, C-4), 160.5 (C, C-5), 98.3 (CH, C-6), 162.7 (C, C-7), 104.2 (C, C-8), 156.1 (C, C-9), 104.8 (C-10), 121,7 (C, C-1′), 129.1 (CH, C-2′), 116.0 (CH, C-3′), 161.3 (C, C-4′), 116.0 (C,C-5′), 129.1 (CH,C-6′), sugar region; 73.5 (CH, C-1′′), 71.0 (CH, C-2′′), 78.8 (CH, C-3′′), 70.7 (CH, C-4′′), 82.0 (CH, C-5′′), 61.4 (CH_2, C-6′′)

Compound EtO-1 as a yellow powder was afforded from vacuum liquid chromatography eluting with gradient of mobile phase by ascending polarity (30 % EtOAc in hexane to 20% MeOH in EtOAc). Then obtained fractions from chromatography were pooled and were further purified using diaion HP-20 to afford EtO-1. Followed by NMR spectra, it was confirmed that EtO-1 was a glycosylflavone. The molecular formula of $C_{21}H_{20}O_{10}$ was analyzed using a combination of ^{1}H-NMR and ^{13}C-NMR. The ^{1}H-NMR spectrum (500 MHz, DMSO-d_6) of this compound showed two exchangeable protons that observed at δ 13.17 and 10.32, which is a characteristic of hydroxyl functional group at C-5 and C-7, respectively. Beside the coupling constants and chemical shift, the proton signals at δ 8.01 (2H, d, J = 8.8 Hz, H-2′, 6′) and 6.88 (2H, d, J =8.6 Hz, H-3′, 5), were assigned for aromatic ring (ring C). This compound also found the one aromatic signal of at δ 6.76 (1H, s, H-6); ring A and olefinic proton at δ 6.27 (1H, s, H-3); ring B, respectively. Therefore, aglycone moiety was further elucidated as apigenin. Furthermore, the sugar moiety also exhibited an anomeric at δ 4.68 (1H, d, J =10.1 Hz, H-1′′) and aliphatic protons of sugar at δ 3.83 -3.24. The ^{13}C-NMR (125 MHz, DMSO-d_6) δ: 164.1 (C-2), 102.6 (C-3), 182.2 (C-4), 160.5 (C-5), 98.3 (C-6), 162.7 (C-7), 104.2 (C-8), 156.1 (C-9), 104.8 (C-10), 121,7 (C-1′), 129.1 (C-2′), 116.0 (C-3′), 161.3 (C-4′), 116.0 (C-5′), 129.1 (C-6′), 73.5 (C-1′′), 71.0 (C-2′′), 78.8 (C-3′′), 70.7 (C-4′′), 82.0 (C-5′′), 61.4 (C-6′′). According ^{1}H signal at δ 4.68 (1H, d, J =10.1) and ^{13}C at δ 73.5 (C-1′′) as anomeric signals indicated that compound EtO-1 was C-glycosyl flavone and further elucidated this structure as apigenin-8-C-β-D-glucoside (vitexin), by NMR analysis and after comparison with its previous reports (Cuong *et al*., 2015). The ^{1}H and ^{13}C-NMR of EtO-1 are summarized in Table 3.5 and the partial structures are shown in Fig. 3.9.

(a)

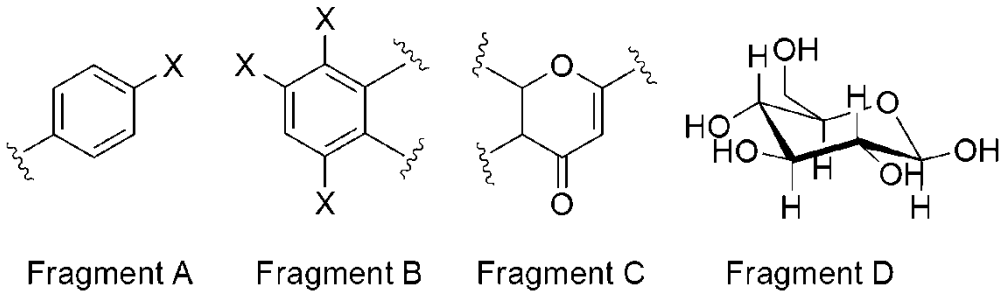

(b)

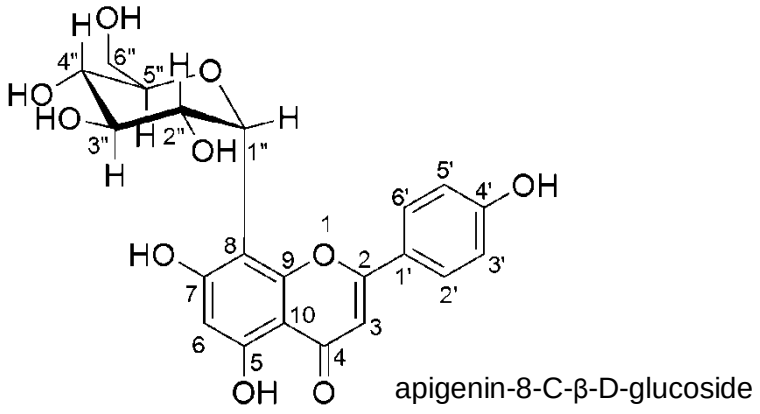

Figure 3.9 The partial structures (a) and the structure of EtO-1 as apigenin-8-C-β-D-glucoside (b).

Table 3.5 ^{1}H and ^{13}C-NMR of EtO-1 (500 MHz for ^{1}H; C_2D_6SO).

Carbon position	EtO-1		Reference (Cuong *et al.*, 2015)	
	^{1}H-	^{13}C-	^{1}H-	^{13}C-
2		164.1 (C)		163.9 (C)
3	6.76 (s)	102.6 (CH)	6.77 (s)	102.4 (CH)
4		182.2 (C)		182.0 (C)
5		160.5 (C)		160.4 (C)
6	6.27 (s)	98.3 (CH)	6.27 (s)	98.1 (CH)
7		162.7 (C)		162.7 (C)
8		104.2 (C)		104.6 (C)
9		156.1 (C)		156.0 (C)
10		104.8 (C)		104.0 (C)
1′		121.7 (C)		121.6 (C)
2′	8.01 (d; 8.8)	129.1 (CH)	8.02 (d; 8.0)	128.9 (CH)
3′	6.88 (d; 8.8)	116.0 (CH)	6.89 (d, 8.0)	115.8 (CH)
4′		161.3 (C)		161.6 (C)
5′	6.88 (d; 8.8)	116.0 (CH)	6.89 (d, 8.0)	115.8 (CH)
6′	8.01 (d; 8.8)	129.1(CH)	8.02 (d; 8.0)	128.9 (CH)
1″	4.68 (d; 10.1)	73.5 (CH)	4.69 (d; 10.0)	73.4 (CH)
2″	3.83 (m)	71.0 (CH)	3.84 (dd; 9.0,10.0)	70.8 (CH)
3″	3.26 (m)	78.8 (CH)	3.29 (m)	78.7 (CH)
4″	3.38 (m)	70.7 (CH)	3.34 (m)	70.5 (CH)
5″	3.24 (m)	82.0 (CH)	3.26 (m)	81.8 (CH)
6″	3.75 (m) 3.52 (m)	61.4 (CH_2)	3.76 (br, d; 11.0) 3.52 (dd; 5.5, 11.0)	61.3 (CH_2)
OH-5	13.17 (br,s)			
OH-7	10.32 (br,s)			

3.1.6 Identification of EtO-2 as luteolin-7-O-β-D-glucoside

Characteristic	yellow powder
Molecular weight (g/mol)	448
IR absorption (νmax cm^{-1})	3424, 1637, 1560, 1460, 1370, 1280
1D-NMR	in dimethyl sulfoxide-*d*6; C_2D_6SO (Table 3.6)
^{1}H-NMR (500 MHz)	δ: 6.73 (1H, s, H-3), 6.43 (1H, d, J = 2.2 Hz, H-6), 6.77 (1H, d, 1.95 Hz, H-8), 7.40 (1H, d, J = 2.2 Hz, H-2′), 6.88 (1H, d, J = 8.3 Hz, H-5′), 7.44 (1H, dd, J = 8.3, 2.2 Hz, H-6′), sugar region; 5.06 (1H, d, J = 7.6 Hz, H-1′′), 3.15 – 3.70 (6H, m, H-2′-H6′)
^{13}C-NMR (125 MHz)	δ: 164.6 (C, C-2), 103.3 (CH, C-3), 182.0 (CO, C-4), 161.3 (C, C-5), 99.9 (CH, C-6), 163.1 (C, C-7), 94.6 (CH, C-8), 157.1 (C, C-9), 105.5 (C, C-10), 121.5 (C, C-1′), 113.8 (CH, C-2′), 145.9 (C, C-3′), 150.1 (C, C-4′), 116.1 (CH, C-5′), 119.4 (CH, C-6′), sugar region; 101.1 (CH, C-1′′), 73.3 (CH, C-2′′), 76.5 (CH, C-3′′), 69.7 (CH, C-4′′), 77.3 (CH, C-5′′), 60.4 (CH2, C-6′′)

The compound EtO-2 as yellow amorphous powder obtained from EtOAc fraction was analyzed by ^{1}H (500 MHz) and ^{13}C (125 MHz)-NMR (dimethyl sulfoxide-*d*6; C_2D_6SO) The ^{1}H NMR spectrum showed the down field signal at aromatic regions. According to chemical shift and coupling constant, the presence at δ 7.44 (1H, dd, *J* = 8.3, 2.2 Hz, H-6′), 7.40 (1H, d, *J* = 2.2 Hz, H-2′) and 6.88 (1H, d, *J* = 8.3 Hz, H-5′) exhibited a characteristic of 1, 2, 4-trisubstituted phenyl moiety (ring C). Its spectrum also found two aromatic protons, which showed meta-coupled doublet at δ 6.43 (1H, d, *J* = 2.2 Hz, H-6), 6.77 (1H, d, 1.95 Hz, H-8), ring A. The only one singlet signal of olefinic proton was observed at C-3 and it showed at δ 6.73 (1H, s, H-3), ring A. These spectral data suggested that compound EtO-2 was luteolin as aglycone structure. Furthermore, the attributable to aliphatic region at δ 3.15 – 3.70 was proposed to sugar moiety (6H, m, H-2′-H6′). Following spectra, the anomeric proton was observed at δ 5.06 (1H, d, *J* = 7.6 Hz, H-1′′), so that the anomeric signals was indicated as β-O-glucoside moiety. The ^{13}C-NMR of EtO-2 spectrum, showed one of ketone carbonyl at δ 182.0 (C-4), two olefinic carbons at δ 164.6 (C-2) and 103.3 (C-3), four hydroxyl carbon at δ 161.3 (C-5), 163.1 (C-7), 145.9 (C-3′) and 150.1 (C-4′), and along with eight aromatic carbons at 99.9 (C-6), 94.6 (C-8), 157.1 (C-9), 105.5 (C-10), 121.5 (C-1′), 113.8 (C-2′), 116.1 (C-5′) and 119.4 (C-6′). ^{13}C-NMR of six glycoside signals (C-1′′ - C-6′′) found at δ101.1, 73.3, 76.5, 69.7, 77.3 and 60.4, respectively. By comparison with the published reports of luteolin, it was suggested that the spectral of EtO-2 was further identified as luteolin-7-O-β-D-glucoside (Gohari *et al*., 2011). The ^{1}H- and ^{13}C-NMR of EtO-2 are summarized in Table 3.6 and the partial structures are shown on Fig. 3.10.

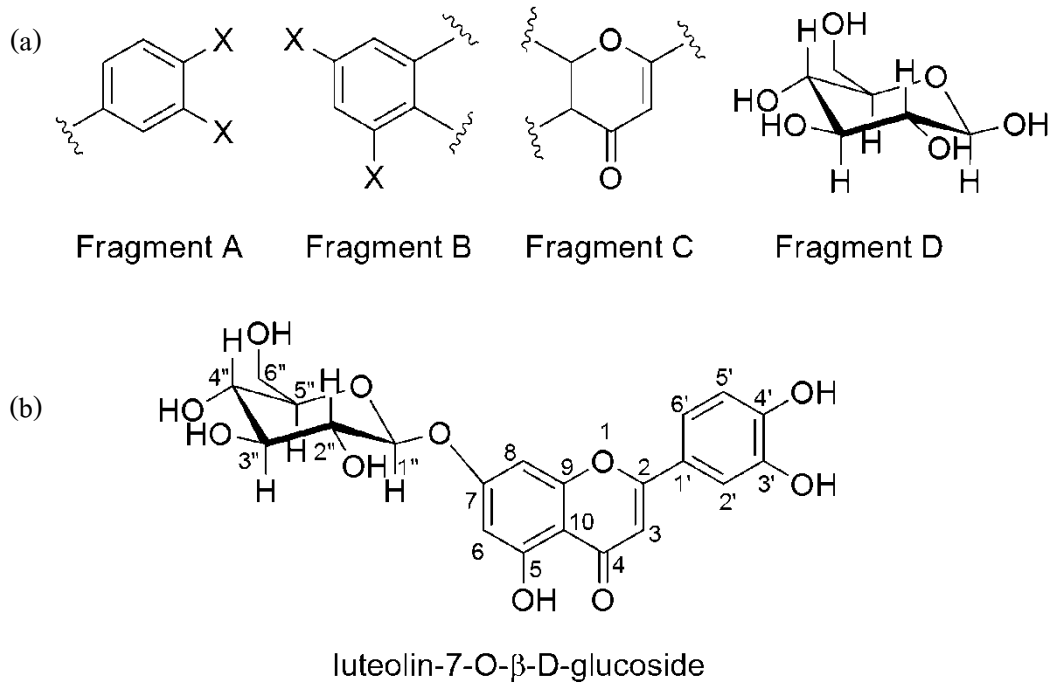

Figure 3.10 The partial structures (a) and the structure of EtO-2 as luteolin-7-O-β-D-glucoside (b).

Table 3.6 ^{1}H and ^{13}C-NMR of EtO-2 (500 MHz for ^{1}H; C_2D_6SO).

Carbon position	EtO-2		Reference (Gohari *et al*., 2011)	
	^{1}H-	^{13}C-	^{1}H-	^{13}C-
2		164.6 (C)		164.4 (C)
3	6.73 (s)	103.3 (CH)	6.72 (s)	99.8 (CH)
4		182.0 (C)		181.8 (C)
5		161.3 (C)		162.1 (C)
6	6.43 (d; 2.2 Hz)	99.9 (CH)	6.83 (d; 1.8 Hz)	95.3 (CH)
7		163.1 (C)		162.9 (C)
8	6.77 (d; 1.95 Hz)	94.6 (CH)	6.78 (d; 1.8 Hz)	95.6 (CH)
9		157.1 (C)		156.9 (C)
10		105.5 (C)		103.1 (C)
1′		121.5 (C)		121.3 (C)
2′	7.40 (d; 2.2 Hz)	113.8 (CH)	7.41 (d; 1.8 Hz)	113.5 (CH)
3′		145.9 (C)		145.7 (C)
4′		150.1 (C)		149.9 (C)
5′	6.88 (d; 8.3 Hz)	116.1 (CH)	6.88 (d; 8.3 Hz)	115.9 (CH)
6′	7.44(dd;8.3, 2.2 Hz)	119.4 (CH)	7.44 (dd; 8.5, 1.8, Hz)	119.0 (CH)
1″	5.06 (d; 7.6 Hz)	100.1 (CH)	5.07 (d; 7.3 Hz)	99.4 (CH)
2″	3.27	73.3 (CH)	3.16-3.73 (m)	73.0 (CH)
3″	3.27	76.5 (CH)	3.16-3.73 (m)	76.3 (CH)
4″	3.15	69.7 (CH)	3.16-3.73 (m)	69.5 (CH)
5″	3.45	77.3 (CH)	3.16-3.73 (m)	77.1 (CH)
6″	3.45 3.70	60.4 (CH_2)	3.16-3.73 (m)	60.5 (CH_2)

3.1.7 Identification of EtO-3 as luteolin-4′-O-β-D-glucoside

Characteristic	yellow powder
Molecular weight (g/mol)	448
1D-NMR	in methanol-*d*3; CD_3OD (Table 3.7)
^{1}H-NMR (500 MHz)	δ: 6.61 (1H, s, H-3), 6.21 (1H, d, *J* = 2.0 Hz, H-6), 6.45 (1H, d, *J* = 2.2 Hz, H-8), 7.44 (1H, d, *J* = 2.0 Hz, H-2′), 7.31 (1H, d, *J* = 8.6, H-5′), 7.45 (1H, d, *J* = 8.3, 2.2 Hz, H-6′), sugar region; 4.93 (1H, d, *J* = 7.6 Hz, H-1′′), 3.53 – 3.92 (6 H, m, H-2′′ - H-6′′)
^{13}C-NMR (125 MHz)	δ: 166.2 (C, C-2), 105.1 (CH, C-3), 183.9 (CO, C-4), 163.3 (C, C-5), 100.3 (CH, C-6), 165.6 (C, C-7), 95.1 (CH, C-8), 159.4 (C, C-9), 105.4 (C, C-10), 127.3 (C, C-1′), 114.9 (CH, C-2′), 148.7 (C, C-3′), 150.0 (C, C-4′), 118.1 (CH, C-5′), 119.9 (CH, C-6′), sugar region; 103.3 (CH, C-1′′), 74.8 (CH, C-2′′), 77.6 (CH, C-3′′), 71.3 (CH, C-4′′), 78.5 (CH, C-5′′), 62.4 (CH_2, C-6′′)

The compound EtO-3 as yellow amorphous powder obtained from EtOAc fraction was analyzed by ^{1}H (500 MHz) and ^{13}C (125 MHz)-NMR (methanol-*d*4; CD_3OD). On ^{1}H-NMR spectrum of EtO-3 detected signal of five aromatic protons including H-2′ at δ 7.44 (1H, d, *J* = 2.0 Hz), H-5′ at δ 7.31 (1H, d, *J* = 8.6 Hz, H-5′), H-6′ at δ 7.45 (1H, d, *J* = 8.3, 2.2 Hz), H-6 at δ 6.21 (1H, d, *J* = 2.0 Hz,) and H-8 at δ 6.45 (1H, d, *J* = 2.2 Hz). Detection of the singlet signal of olefinic proton was observed at δ 6.61 (1H, s, H-3). These presences indicated that EtO-3 was flavonoid structure as luteolin. On the basis on ^{13}C-NMR, five aromatic carbon at δ 100.3 (C-6), 95.1 (C-8), 114.9 (C-2′), 118.1 (C-5′) and 119.9 (C-6′) were observed. Its spectrum also found one signal of ketone carbonyl at δ 183.9 (C-4), two of olefinic carbons at δ 166.2 (C-2) and 105.1 (C-3), and four hydroxyl carbons at δ 163.3 (C-5), 165.6 (C-7), 148.7 (C-3′) and 150.0 (C-4′). These signals were connected with quaternary of aromatic carbons with C-9, C-10 and C-1′ at the δ 159.4, 105.4 and 127.3, respectively. In addition, the spectrum also detected the aliphatic signal at 60 ppm to 103 ppm and indicated as aliphatic signals of sugar moiety, which connected to luteolin. According to the ^{1}H and ^{13}C data of anomeric position were exhibited at δ 4.93 (1H, d, *J* = 7.6 Hz, H-1′′) and δ 103.3 (C-1′′). Due to observed chemical shift on both signals and the coupling constant of this compound, it was elucidated as O-glycoside of luteolin structure. After structure elucidation, all spectra were compared with literature and finally, EtO-3 structure was luteolin-4′-O-β-D-glucoside (Krenn *et al.,* 2003). The ^{1}H- and ^{13}C-NMR of EtO-3 are summarized in Table 3.7 and the partial structures are shown on Fig. 3.11.

(a)

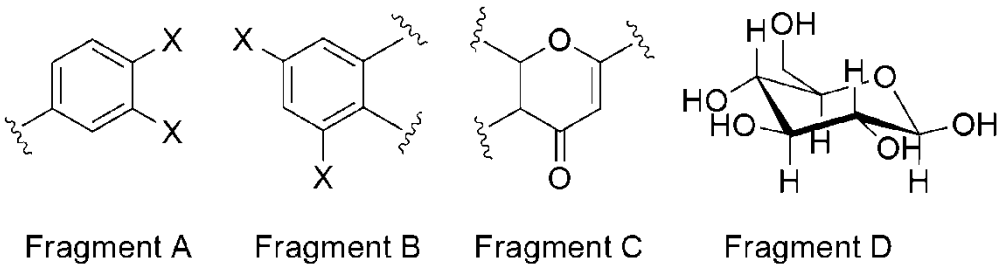

Fragment A Fragment B Fragment C Fragment D

(b)

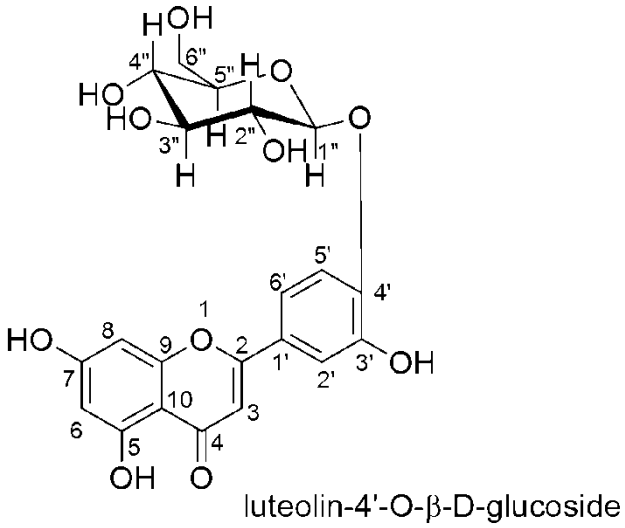

luteolin-4'-O-β-D-glucoside

Figure 3.11 The partial structures (a) and the structure of EtO-3 as luteolin-4′-O-β-D-glucoside (b).

Table 3.7 ^{1}H and ^{13}C-NMR of EtO-3 (500 MHz for ^{1}H; C_2D_6SO).

Carbon position	EtO-3		Reference (Krenn *et al.,* 2003)	
	^{1}H-	^{13}C-	^{1}H-	^{13}C-
2		166.2 (C)		166.2 (C)
3	6.61 (s)	105.1 (CH)	6.62 (s)	105.3 (CH)
4		183.9 (C)		183.7 (C)
5		163.3 (C)		163.2 (C)
6	6.21 (d; 2.0 Hz)	100.3 (CH)	6.22 (d; 2.1 Hz)	100.3 (CH)
7		165.6 (C)		165.4 (C)
8	6.45 (d; 2.2 Hz)	95.1 (CH)	6.43 (d; 2.1 Hz)	95.2 (CH)
9		159.5 (C)		159.4 (C)
10		105.4 (C)		105.4 (C)
1′		127.3 (C)		127.2 (C)
2′	7.44 (d; 2.0 Hz)	114.9 (CH)	7.45 (d; 2.4 Hz)	114.9 (CH)
3′		148.7 (C)		148.6 (C)
4′		150.0 (C)		149.9 (C)
5′	7.31 (d; 8.6 Hz)	118.1 (CH)	7.32 (d; 8.4 Hz)	117.9 (CH)
6′	7.45(d;8.3, 2.2 Hz)	119.9 (CH)	7.46 (dd; 8.4, 2.4 Hz)	119.8 (CH)
1″	4.93 (d; 7.6 Hz)	103.3 (CH)	4.95 (d; 7.5 Hz)	103.2 (CH)
2″	3.53	74.8 (CH)	3.55 (t)	74.8 (CH)
3″	3.47	77.6 (CH)	3.50 (obs)	77.5 (CH)
4″	3.42	71.3 (CH)	3.40 (t)	71.3 (CH)
5″	3.48	78.5 (CH)	3.50 (obs)	78.5 (CH)
6″	3.72 3.92	62.4 (CH_2)	3.72 (dd) 3.91 (dd)	62.4 (CH_2)

3.2 Anti-proliferative and apoptotic activities of diterpenes from *C. stellatopilosus*

3.2.1 Anti-proliferative activity

Anti-proliferative activity of diterpenes was evaluated using MTT assay. After 24 h for incubation of cancer cells including HeLa, HT-29, MCF-7 and KB cells together with various concentrations of diterpenes (plaunotol, plaunol A, plaunol E and plaunol F), treated cells were investigated for cell viability by adding the MTT solution. The formazan product was formed after 2 h and it was re-dissolved with 0.04N HCl in isopropanol. The optical density was recorded using microplate reader at 570 nm. Anti-proliferative result further considered to be toxic when the optical density of the treated sample was compared with control group. The anti-proliferative result was shown as an IC_{50} value (Table 3.8).

Table 3.8 The IC_{50} values of plaunotol, plaunol A, plaunol E and plaunol F.

Compound	IC_{50} (μM)[a]				
	HeLa	HT-29	MCF-7	KB	HGF
Plaunotol	65.47± 6.39	72.92±5.73	62.25±9.15	80.90±3.48	> 100
Plaunol A	> 100	58.16±8.24	71.22±1.07	62.66±1.78	> 100
Plaunol E	67.45± 0.39	86.25±0.00	63.39±2.64	69.47±0.99	> 100
Plaunol F	> 100	> 100	> 100	> 100	> 100
Paclitaxel	0.012 ± 0.003	0.008 ± 0.004	0.004 ± 0.002	0.001± 0.005	

[a] IC_{50} value was expressed as mean ± S.E.M, n=3.

The MTT results indicated that diterpenes including plaunotol, plaunol A and plaunol E showed slightly affected on cancer cells and the range of IC_{50} at 60 – 80 μM. Whereas plaunol F was inactive (IC_{50}> 100 μM). The paclitaxel as anti-cancer drug was used as a positive control. In addition, plaunotol, plaunol A, plaunol E and plaunol F at the same concentrations were also incubated with normal cells (HGF) for 48 h. The results suggested that all compounds did not have cytotoxicity.

3.2.2 Effects on cell cycle analysis

Regarding to cells cycle progression, a general process used for cell proliferation and dividing. The cell proliferation is defined as the increase in cell number resulting from completion of the cell cycle progression. The cell cycle is composed of four phases including sub G1 (a population of cells with a reduced DNA content), G0/G1 (resting cells contain one copy of nuclear DNA), S (cells are synthesized nuclear DNA and the nuclear DNA concentration more than one copy of nuclear DNA), and G2/M phase (cells are synthesized nuclear DNA and the nuclear DNA contain two copies of nuclear DNA), respectively. As shown in Fig. 3.12, the cellular nuclear DNA concentration changes characteristically depending on cell cycle phase during cell cycle

progression. Followed by flow cytometry, a DNA-conjugating fluorescence dyes makes it possible to determine the distribution of cell population and its result shows in DNA histogram (Fig. 3.12).

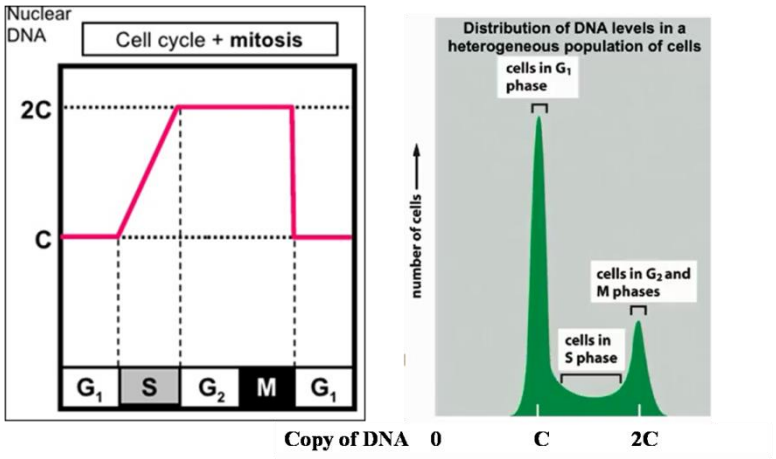

Figure 3.12 Changes of nuclear DNA concentration during the cell cycle analysis (modified from Ormerod, 2008).

In the present study, an effective compound, as shown in Table 3.8, was further investigated on cell cycle progression using flow cytometry. Therefore, plaunotol, plaunol A and plaunol E have an anti-proliferative effect on several cancer cells with an IC_{50}value ranging 60 - 80 µM and these compounds were investigated on cancer cells for cell cycle analysis. After 48 h, treated cells were analyzed using Muse™ cell cycle reagent (Merck, Darmstadt, Germany). The cell cycle results may suggest the anti-proliferative mechanism of target compounds in cancer cells.

3.2.2.1 Plaunotol

On the cell cycle analysis, plaunotol was prepared at 25, 50, 75 and 100 μM, respectively. Prepared solutions of plaunotol were further treated to cancer cells and were then incubated for 48 h. The results of plaunotol treatments were considered by DNA histogram. The percentages of cell related with copies of DNA, in which stage during cell cycle also showed when using Muse™ Analyzer. The DNA histogram of plaunotol treatments are shown in Fig. 3.13 and the relative number of cells that represented in G0/G1, S and G2/M phase of plaunotol against four cancer cells are summarized in Table 3.9.

In HeLa cells, plaunotol at dose dependent manner from 25 μM to 75 μM was slightly significantly increased the number of cells in G0/G1 phases from 58.2 ± 2.9 % to 65.7% (p<0.05) when compared with control, and it also decreased the number of cells in S phase from 19.6 ± 0.7 % to 15.3 ± 2.3 % (p< 0.05). At G2/M phase, plaunotol seemed to be not significant difference from control. To check whether cells undergo to cell cycle process, the paclitaxel was used as positive control. Herein, the number of cells was significantly increased in G2/M phase from 22 ± 2.1 % to 44.0 ± 1.4 % (p< 0.01), after treatment with paclitaxel at 1 μM when compared with control. Thus, these results suggested that plaunotol might be induced the cell cycle arrest at G0/G1 phase in HeLa cells.

In HT-29 cells, plaunotol at 25 μM to 75 μM did not affect on cell cycle. Interestingly, plaunotol at 75 μM significantly decreased the cell cycle arrest in G0/G1 from 46.54 ± 5.4% to 38.3 ± 0.2 % and cells significantly increased from 36.0 ± 4.1 % to 44.7 ± 1.2% in G2/M phase, when its results compared with control group (p < 0.01). Among these results, plaunotol at 75 μM induced cell cycle arrest on G2/M phase. The paclitaxel was significant difference from the control group and its results significantly increased the cell into G2/M phase (36.0 ± 4.1 % to 64.1 ± 3.1 %). According this study, it indicated that plaunotol can be induced cell cycle arrest at G2/M phase in HT-29 cells.

In MCF-7 cells, following dose dependent manner of plaunotol at 25 μM to 75 μM did not affected on the cell cycle progression; however, plaunotol at 100 μM significantly increased the number of cells from 144 ± 1.2 % to 42.5 ± 1.4 in S phase ($p < 0.01$). The paclitaxel also observed that it significantly increased cells in G2/M phase, when compared with control (24.0 ± 0.6 % to 70.4 ± 2.4; $p < 0.01$). Therefore, plaunotol induced cell cycle arrest at S phase in MCF-7 cells.

In the KB cells, plaunotol at 25 μM to 75 μM slightly increased the number of cells in G0/G1 phase, however at 100 μM plaunotol significantly increased from 55.7 ± 1.0 % to 69.1 ± 2.1 %, when compared with control. The paclitaxel showed significant different from control and showed cell cycle arrest on G2/M (26.7 ± 0.3 % to 90.2 ± 1.1 %; $p < 0.01$).

In our experiments indicated that plaunotol induced the cell cycle arrest on several cancer cells with the different stages during cell cycle progression including plaunotol induced G0/G1 phase in HeLa and KB cells, induced S phase in MCF-7, and it also induced G2/M phase in HT-29. Due to the cell cycle process, it can be classified into G0/G1, S and G2/M. Each stage has a check point to prove that cell has complete components such as DNA, protein and nutrient. If the cell has damaged DNA or incomplete components, it must be terminated itself. The terminated process normally linked to one of the programmed cell death (PCD), so called apoptosis.

Table 3.9 Cell cycle distribution of cancer cells after plaunotol treatments.

Cells	Treatment	Distribution of cells between cell cycle phase (%)		
		G0/G1	S	G2/M
HeLa	Control (0.2% DMSO)	58.2 ± 2.9	19.6 ± 0.7	22.2 ± 2.1
	Plaunotol 25 μM	65.2 ± 0.1*	17.1 ± 1.2	17.8 ± 1.3
	Plaunotol 50 μM	64.1 ± 2.4	17.0 ± 2.4	18.8 ± 2.1
	Plaunotol 75 μM	65.7 ± 2.3*	15.3 ± 2.3*	19.1 ± 0.8
	Plaunotol 100 μM	58.0 ± 1.8	18.1 ± 1.8	23.8 ± 0.2
	Paclitaxel 1 μM	25.8 ± 1.4**	30.1 ± 1.4**	44.0 ± 1.4**
HT-29	Control (0.2% DMSO)	46.5 ± 5.4	17.5 ± 1.6	36.0 ± 4.1
	Plaunotol 25 μM	43.0 ± 1.2	21.4 ± 3.5*	35.6 ± 4.1
	Plaunotol 50 μM	46.8 ± 1.3	17.9 ± 1.4	35.3 ± 1.1
	Plaunotol 75 μM	38.3 ± 0.2**	17.0 ± 1.1	44.7 ± 1.2**
	Plaunotol 100 μM	41.8 ± 0.7	18.6 ± 0.3	39.5 ± 0.5
	Paclitaxel 1 μM	17.2 ± 1.7**	18.6 ± 2.6	64.1 ± 3.1**
MCF-7	Control (0.2% DMSO)	61.6 ± 1.7	14.4 ± 1.2	24.0 ± 0.6
	Plaunotol 25 μM	63.1 ± 0.7	11.5 ± 0.6	25.4 ± 0.2
	Plaunotol 50 μM	62.2 ± 6.5	13.1 ± 2.5	24.7 ± 3.7
	Plaunotol 75 μM	65.0 ± 0.0	12.2 ± 0.5	17.9 ± 6.5
	Plaunotol 100 μM	31.5 ± 2.8**	42.5 ± 1.4**	26.1 ± 1.3
	Paclitaxel 1 μM	24.2 ± 0.8**	5.4 ± 1.6**	70.4 ± 2.4**
KB	Control (0.2% DMSO)	55.7 ± 1.0	17.5 ± 1.0	26.7 ± 0.3
	Plaunotol 25 μM	55.9 ± 1.3	21.8 ± 1.0	22.0 ± 0.3*
	Plaunotol 50 μM	60.6 ± 1.2*	20.6 ± 2.0	18.7 ± 0.6 **
	Plaunotol 75 μM	58.6 ± 0.8	18.1 ± 4.0	23.1 ± 3.2
	Plaunotol 100 μM	69.1 ± 2.1**	11.9 ± 1.5**	18.9 ± 2.1 **
	Paclitaxel 1 μM	5.6 ± 1.2 **	4.3 ± 0.1**	90.2 ± 1.1**

The data represented as mean ± S.D. * $p< 0.05$ and ** $p< 0.01$, were considered to indicate significant from control treatment (n =3).

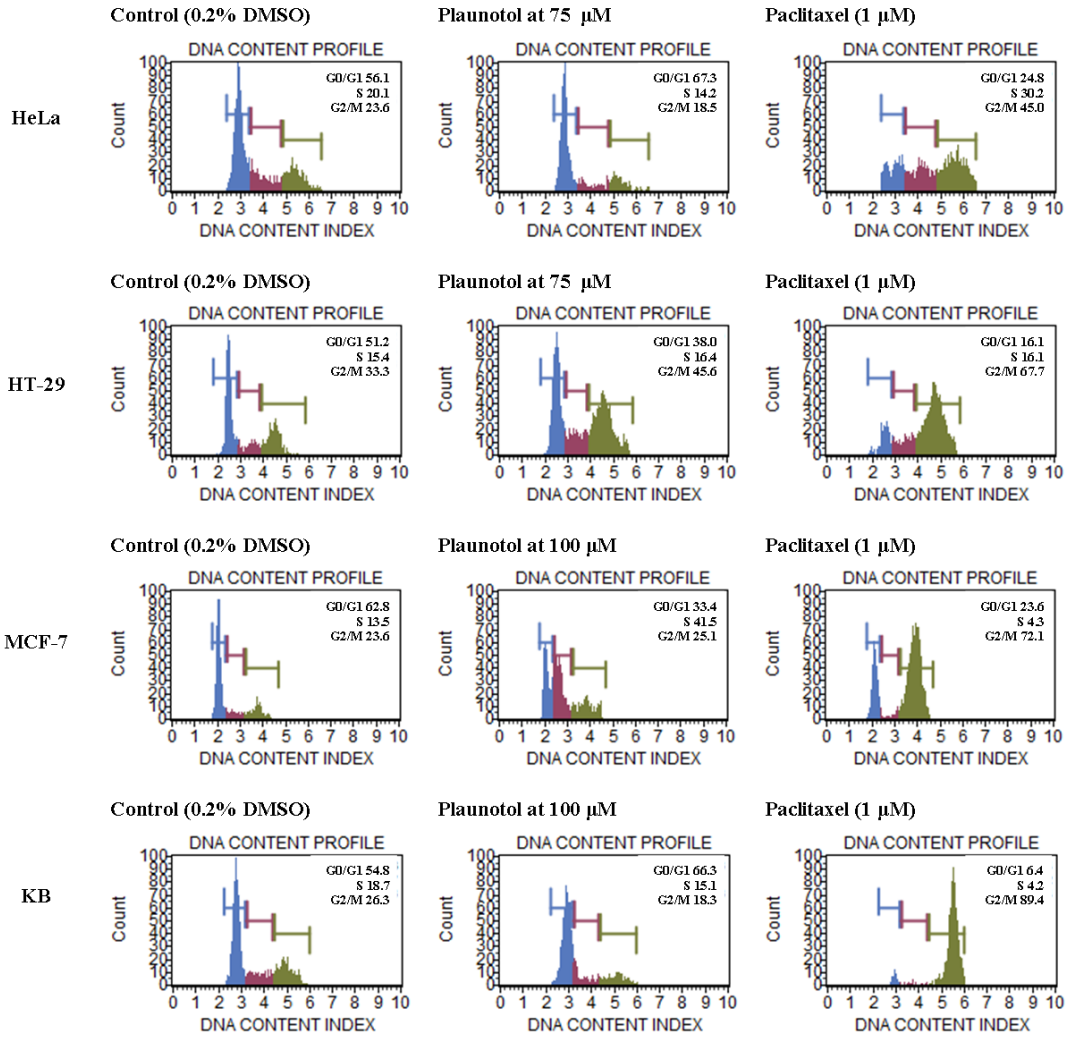

Figure 3.13 DNA histograms of cancer cell lines after 48 h plaunotol treatment.

3.2.2.2 Plaunol A

On the cell cycle analysis, plaunol A was selected and was prepared at 75 μM and 150 μM, respectively. Prepared solutions of plaunol A were further treated to cancer cells for 48 h. The results of plaunol A treatments were considered by DNA histogram (Fig. 3.14) as well as the percentages of cell related with copies of DNA during cell cycle progression (Table 3.10).

As shown in Table 3.10, plaunol A at 75 μM significantly increased G0/G1 phase and plaunol A at 150 μM significantly increased G2/M phase in HeLa cells when compared with control. As the same way, plaunol A also significantly induced G2/M arrest in HT-29 at both concentrations, whereas plaunol A did not affect in MCF-7. In KB cells, plaunol A at 75 μM significantly induced cell cycle arrest at G2/M phase, and plaunol A at 150 μM was cytotoxicity. During cell cycle experiments, we used the paclitaxel as positive drug and its results significantly induced cell cycle arrest at G2/M phase that observed in every cancer cells. From these results we can conclude that plaunol A induced the cell cycle arrest onG2/M phase in HeLa, HT-29 and KB cells, but it had no effect in MCF-7.

Table 3.10 Cell cycle distribution of cancer cells after plaunol A treatments.

Cells	Treatment	Distribution of cells between cell cycle phase (%)		
		G0/G1	S	G2/M
HeLa	Control (0.2% DMSO)	53.8 ± 1.4	24.5 ± 0.9	21.7 ± 1.9
	Plaunol A 75 μM	58.8 ± 2.8*	22.9 ± 0.8	18.2 ± 2.3
	Plaunol A 150 μM	45.1 ± 1.1**	21.7 ± 0.4**	33.2 ± 0.9**
	Paclitaxel 1 μM	15.8 ± 0.9**	27.2 ± 1.3**	57.1 ± 0.3**
HT-29	Control (0.2% DMSO)	55.0 ± 3.3	23.4 ± 5.2	21.4 ± 2.4
	Plaunol A 75 μM	53.9 ± 1.1	14.9 ± 2.4	31.1 ± 2.7*
	Plaunol A 150 μM	37.2 ± 2.0**	16.6 ± 2.0*	46.0 ± 2.4**
	Paclitaxel 1 μM	8.1 ± 2.2**	6.2 ± 1.7**	85.0 ± 4.0**
MCF-7	Control (0.2% DMSO)	58.6 ± 2.7	29.0 ± 2.4	12.1 ± 3.3
	Plaunol A 75 μM	57.7 ± 2.7	34.7 ± 2.2	6.9 ± 0.8
	Plaunol A 150 μM	57.3 ± 3.4	30.7 ± 5.9	11.9 ± 6.9
	Paclitaxel 1 μM	9.2 ± 2.1 **	15.7 ± 3.2**	75.1 ± 5.2**
KB	Control (0.2% DMSO)	55.7 ± 1.0	17.5 ± 1.0	26.7 ± 0.3
	Plaunol A 75 μM	45.2 ± 1.0**	11.3 ± 1.3**	43.5 ± 2.1**
	Plaunol A 150 μM	nd	nd	nd
	Paclitaxel 1 μM	5.6 ± 1.2**	4.3 ± 0.1**	90.2 ± 1.1**

The data represented as mean ± S.D. * $p< 0.05$ and ** $p< 0.01$, were considered to indicate significant from control treatment (n =3).

Not determined (nd); cytotoxicity was observed.

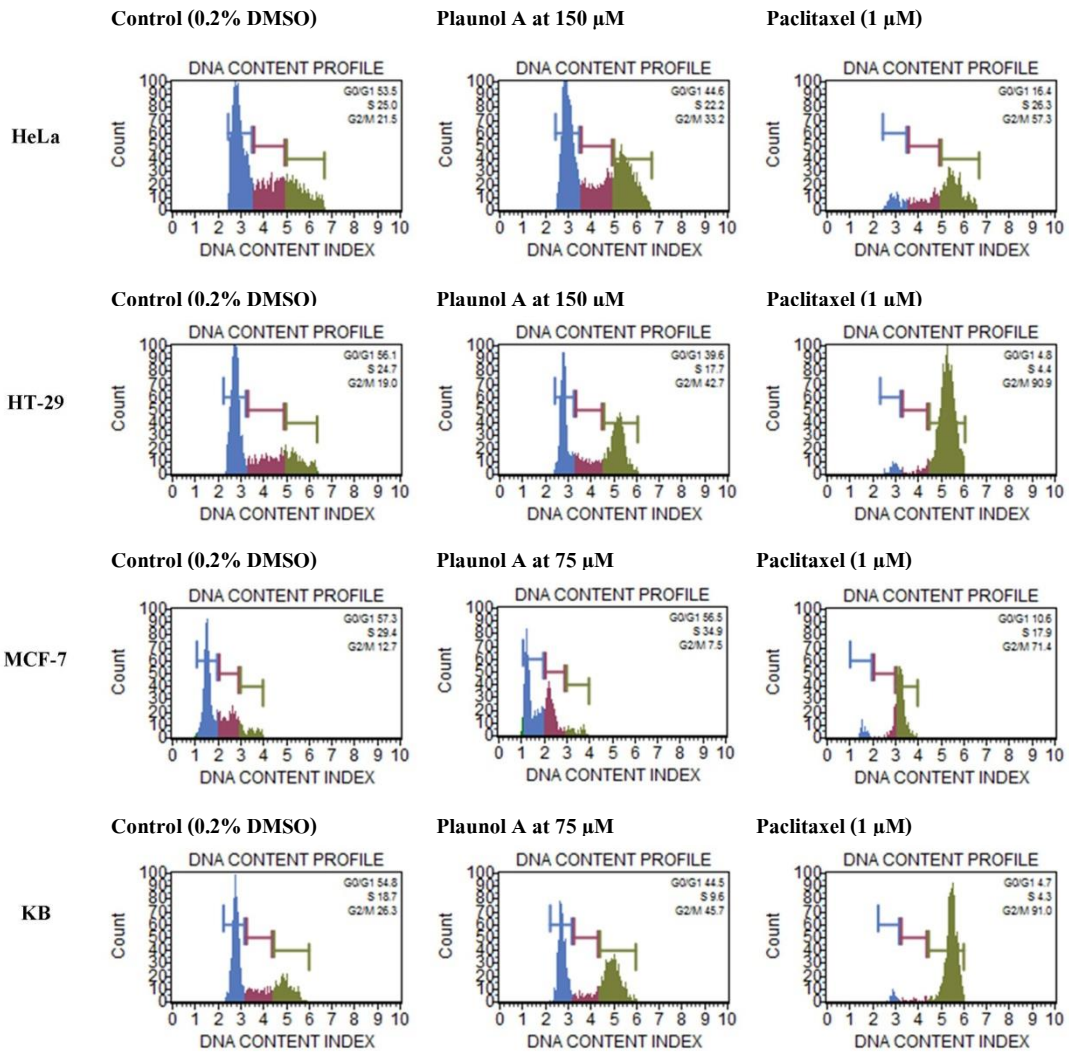

Figure 3.14 DNA histograms of cancer cell lines after 48 h plaunol A treatment.

3.2.2.3 Plaunol E

Plaunol E at 75 μM and 150 μM were chosen and were treated to cancer cells for 48 h (Table 3.11 and Figure 3.15).

In HeLa cells, plaunol E at 75 μM and 150 μM were significantly induced cell cycle arrest at G2/M phase with 31.0 ± 1.6 % and 28.8 ± 1.3 μM, respectively. These results were increased from the untreated cells, which 21.7 ± 1.9 %. As the same way, plaunol E at lower concentration did not affect on the cell cycle, however the population of cells on G2/M phase significantly increased to 41. 6 ±1.8 % from 21.4 ± 2.4 % in HT-29, 31.7 ± 4.3 % from 12.1 ± 3.3 % in MCF-7, and 46.5 ± 3.6 % from 26.7 ± 0.3 % in KB, respectively. Furthermore, the paclitaxel at 1 μM was used for positive control and its results indicated G2/M arrest with 57.1 ± 0.3 % (HeLa), 85.0 ± 4.0 (HT-29), 75.1 ± 5.2 % (MCF-7) and 90.2 ± 1.1% (KB), respectively. These results revealed that plaunol E has affected on cell cycleon G2/M phase in every cancer cell lines.

Table 3.11 Cell cycle distribution of cancer cells after plaunol E treatments.

Cells	Treatment	Distribution of cells between cell cycle phase (%)		
		G0/G1	S	G2/M
HeLa	Control (0.2% DMSO)	53.8 ± 1.4	24.5 ± 0.9	21.7 ± 1.9
	Plaunol E 75 µM	49.0 ± 1.9**	20.0 ± 1.1	31.0 ± 1.6**
	Plaunol E 150 µM	47.6 ± 1.5**	23.6 ± 0.5**	28.8 ± 1.3**
	Paclitaxel 1 µM	15.8 ± 0.9**	27.2 ± 1.3*	57.1 ± 0.3**
HT-29	Control (0.2% DMSO)	55.0 ± 3.3	23.4 ± 5.2	21.4 ± 2.4
	Plaunol E 75 µM	56.5 ± 6.6	15.8 ± 4.6	27.5 ± 5.3
	Plaunol E 150 µM	46.3 ± 4.4	11.6 ± 3.8**	41.6 ± 1.8**
	Paclitaxel 1 µM	8.1 ± 2.2**	6.2 ± 1.7**	85.0 ± 4.0**
MCF-7	Control (0.2% DMSO)	58.6 ± 2.7	29.0 ± 2.4	12.1 ± 3.3
	Plaunol E 75 µM	58.6 ± 4.9	30.3 ± 4.5	10.3 ± 1.8
	Plaunol E 150 µM	38.4 ± 1.5**	29.7 ± 2.8	31.7 ± 4.3**
	Paclitaxel 1 µM	9.2 ± 2.1 **	15.7 ± 3.2**	75.1 ± 5.2**
KB	Control (0.2% DMSO)	55.7 ± 1.0	17.5 ± 1.0	26.7 ± 0.3
	Plaunol E 75 µM	58.1 ± 2.1	12.9 ± 1.2**	28.9 ± 1.4
	Plaunol E 150 µM	43.1 ± 3.7**	10.4 ± 0.8**	46.5 ± 3.6**
	Paclitaxel 1 µM	5.6 ± 1.2**	4.3 ± 0.1**	90.2 ± 1.1**

The data represented as mean ± S.D. * $p< 0.05$ and ** $p< 0.01$, were considered to indicate significant from control treatment (n =3).

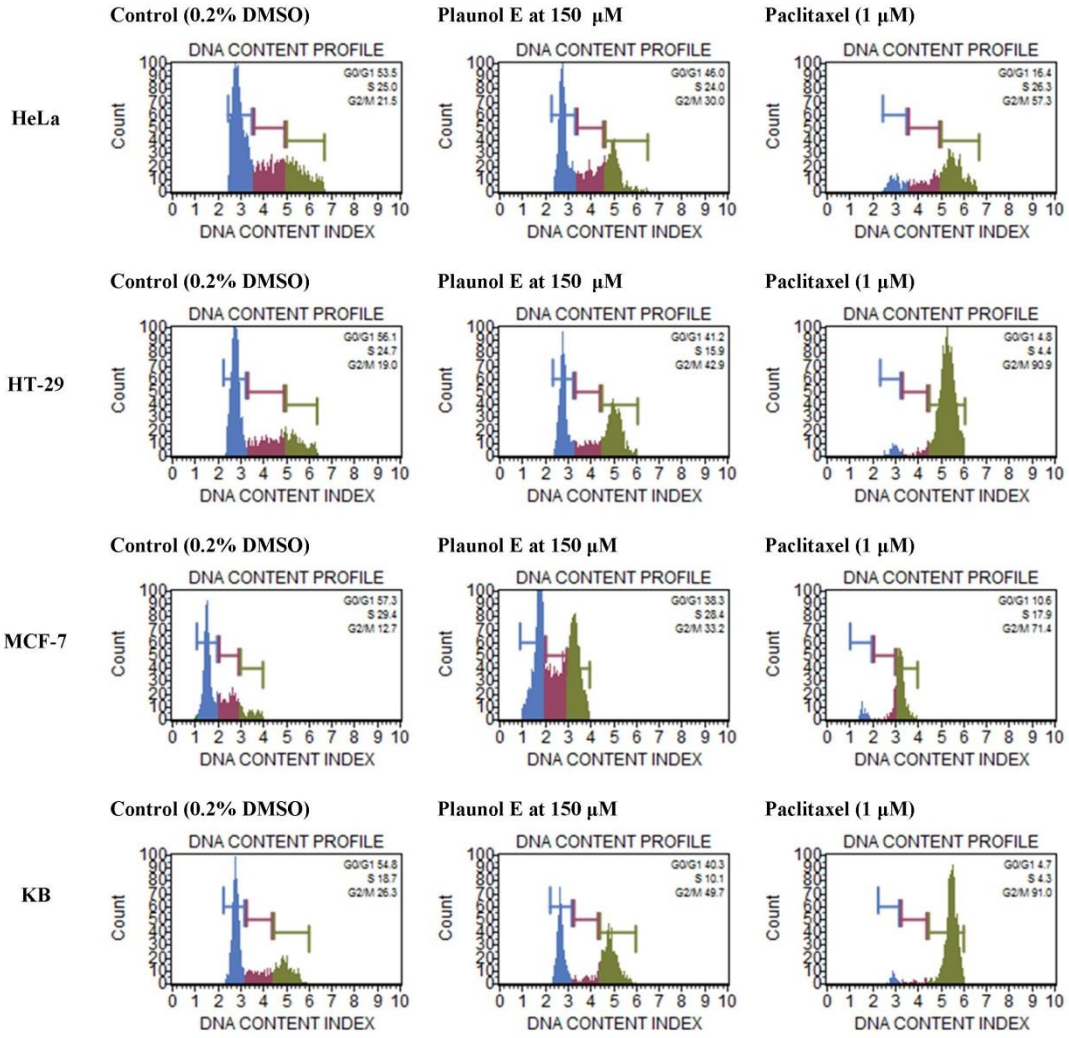

Figure 3.15 DNA histograms of cancer cell lines 48 h after plaunol E treatment.

3.2.3 Effects on apoptosis

The phosphatidylserine is generally located on inner leaflet of plasma membrane, but is can be located on outer leaflet during apoptosis. The located phosphatidylserine can be detected using annexin-V. Using double staining annexin-V/7-AAD followed by flow cytometry can be further classified cell into four groups. The cells in each group depend on the morphological and biochemical changes (Fig. 3.16). The apoptotic results were shown in annexin-7AAD dot plot. The cells population was presented in different quadrants including live cells (Q1), early apoptotic cells (Q2), late apoptotic cell (Q3) and dead cells (Q4), respectively (Fig. 3.16).

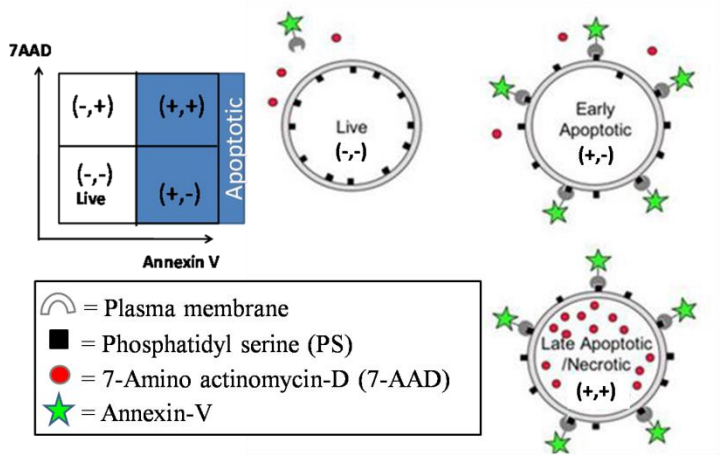

Figure 3.16 Biochemical changes during apoptosis and annexin-7AAD detection.

3.2.3.1 Plaunotol

In this study, plaunotol at 75 μM and 150 μM were prepared and were separately treated with cancer cells for 48 h. The results were expressed on scatter plot (Fig.3.17) and the relative number of apoptotic cells was expressed in percentage (Fig.3.18).

In HeLa cells, plaunotol at 75 μM showed the viable cells with 49.05 ± 4.27 %, early apoptotic cells with 40.97 ± 3.95 % and late apoptosis or dead cells with 9.99 ± 0.32 %. As the same way, plaunotol at 150 μM also showed the viable cells with 44.38 ± 1.04 %, early apoptotic cells with 46.52 ± 0.74 % and late apoptosis or dead cells with 9.11 ± 0.30 %. Whereas the cells were treated with 0.2% DMSO showed the viable cells with 96.41 ± 3.2 %, early apoptotic cells with 3.81 ± 1.86 % and late apoptosis or dead cells showed with 1.58 ± 1.17 %. These results indicated that plaunotol both 75 μM and 150 μM significantly induced early apoptotic cell from 3.81% to 40.97 ± 3.95 % and 46.52 ± 0.74 % ($p< 0.01$), respectively when compared with control group (0.2% DMSO). According these results, it indicated that plaunotol induced early apoptosis in HeLa cells.

At the same way in other cell lines, the plaunotol at both 75 μM and 150 μM was observed that it significantly decreased the viable cells and it also significantly increased early apoptotic cells, when compared with control.

In HT-29, only plaunotol at 75 μM significantly induced early apoptosis from 5.22 ± 6.43 % to 4.13 ± 1.57 % ($p< 0.01$). The plaunotol at 150 μM was cytotoxicity.

In MCF-7, plaunotol at 75 μM and 150 μM significantly induced early apoptosis from 4.13 ± 1.57 % to 85.87 ± 1.38 % and 90.31 ± 3.09 % ($p< 0.01$), respectively.

In KB cells, plaunotol at both 75 and 150 μM were slightly induced apoptotic cell from 7.14 ± 0.71 % to 14.19 ± 6.82 %and 20.32 ± 0.68 %, ($p< 0.05$) respectively.

Furthermore, the paclitaxel at 1 µM was used as a positive control and it also significantly induced apoptosis when compared with control group, the apoptotic cell with 37.94 ± 12.47 %(HeLa), 52.09 ± 5.27 % (HT-29), 51.81 ± 3.30% (MCF-7) and 17.68 ± 1.17 % (KB), respectively.

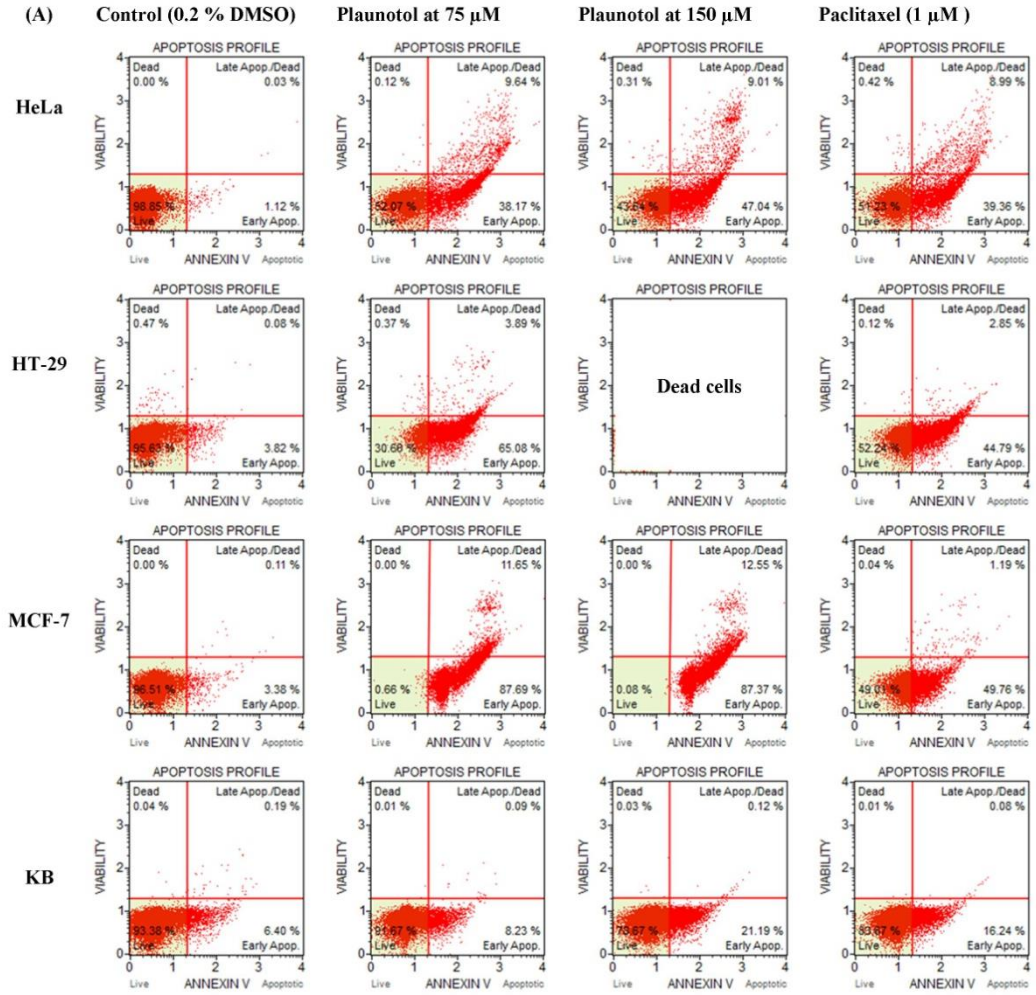

Figure 3.17 Scatter plots in each apoptotic stage of cancer cells after treatment with plaunotol, detection with annexin/7-AAD.

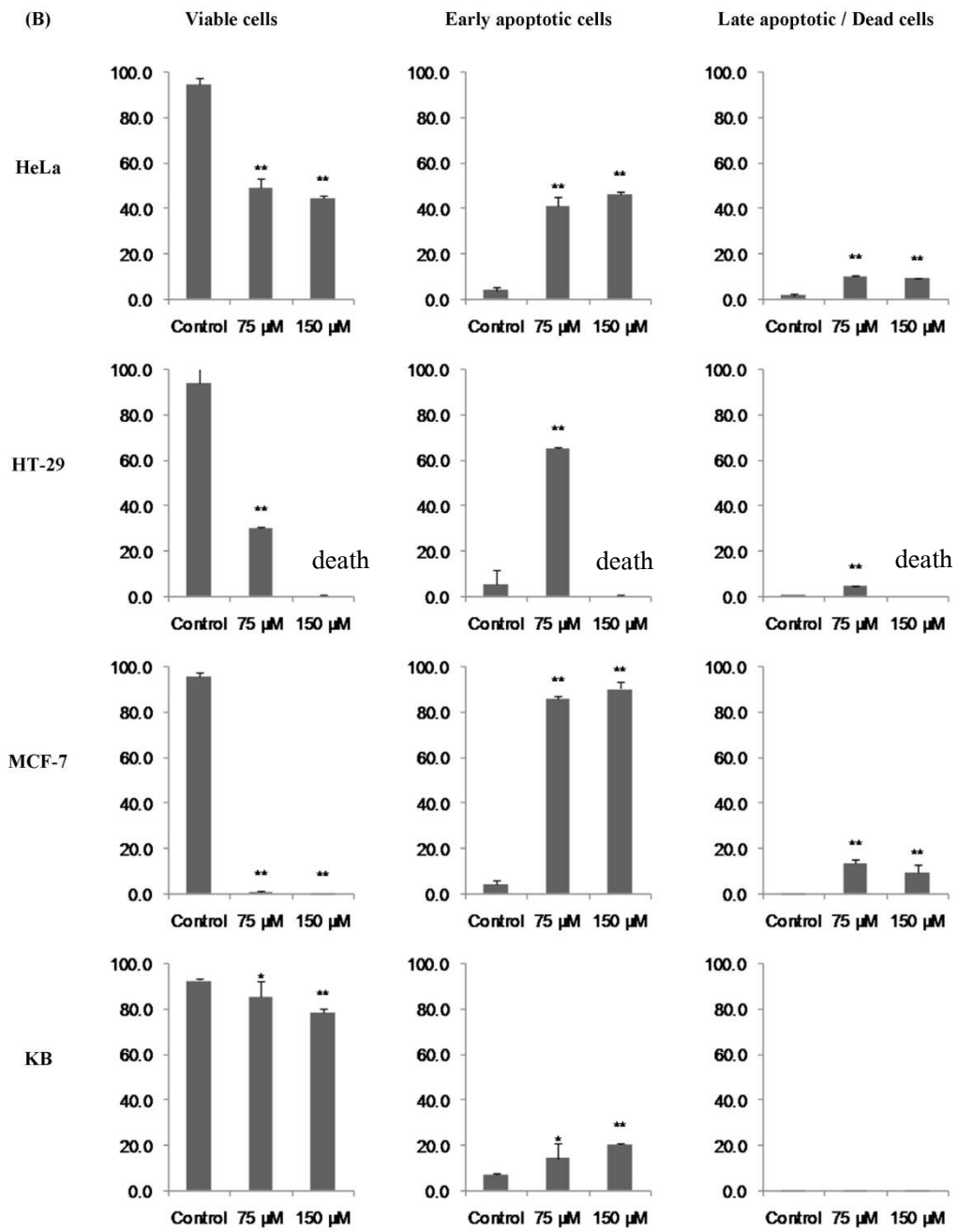

Figure 3.18 Summary of the percentage of cells number after plaunotol treatments.

The percentage of live, early apoptotic, late apoptotic and dead cells were recorded by Muse™ Analyzer.* $p< 0.05$, ** $p< 0.01$ indicates significant (one-way ANOVA followed Dunnett's test, n =3).

3.2.3.2 Plaunol A

The apoptotic result of plaunol A was interpreted the same way with plaunotol. The scatter plot and the percentages of cells in each apoptotic stages were recorded by Muse™ cell analyzer. As expressed in Fig. 3.19 and 3.20, the viable cells were more than 80% in control group including 94.61 ± 3.02 % (HeLa), 91.4 ± 6.85 % (HT-29), 95.75 ± 1.62 (MCF-7), and 92.73 ± 0.61% (KB), respectively. Interestingly, the live cells decreased after plaunol A treatments with 75 μM and 150 μM for 48 h, while early apoptotic cells significantly increased at both concentrations. Among these results, plaunol A significantly induced the highest of early apoptotic cells with 14.25 ± 5.95 % (HeLa), 53.91 ± 2.72 % (HT-29), 90.31 ± 3.09 % (MCF-7) and 20.32 ± 0.68 % (KB), respectively. The paclitaxel at 1 μM also significantly induced apoptotic cells with 37.94 ± 12.47 (HeLa), 52.09 ± 5.27 % (HT-29), 51.18 ± 3.30 % (MCF-7) 17.68 ± 1.17 % (KB), respectively. Thus, these results indicated that the effectiveness of plaunol A in HeLa and HT-29 were better than MCF-7 and KB cells.

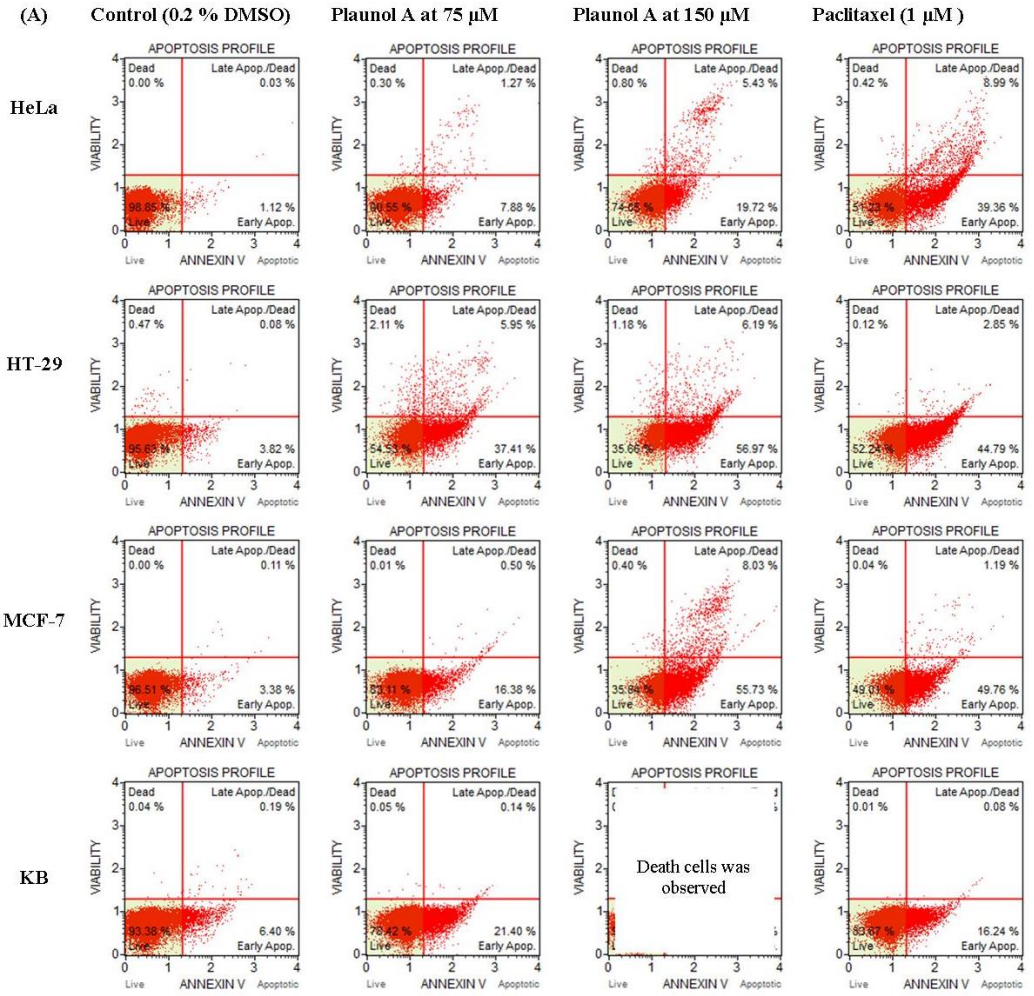

Figure 3.19 Scatter plots in each apoptotic stage of cancer cells after treatment with plaunol A, detection with annexin-V/7-AAD.

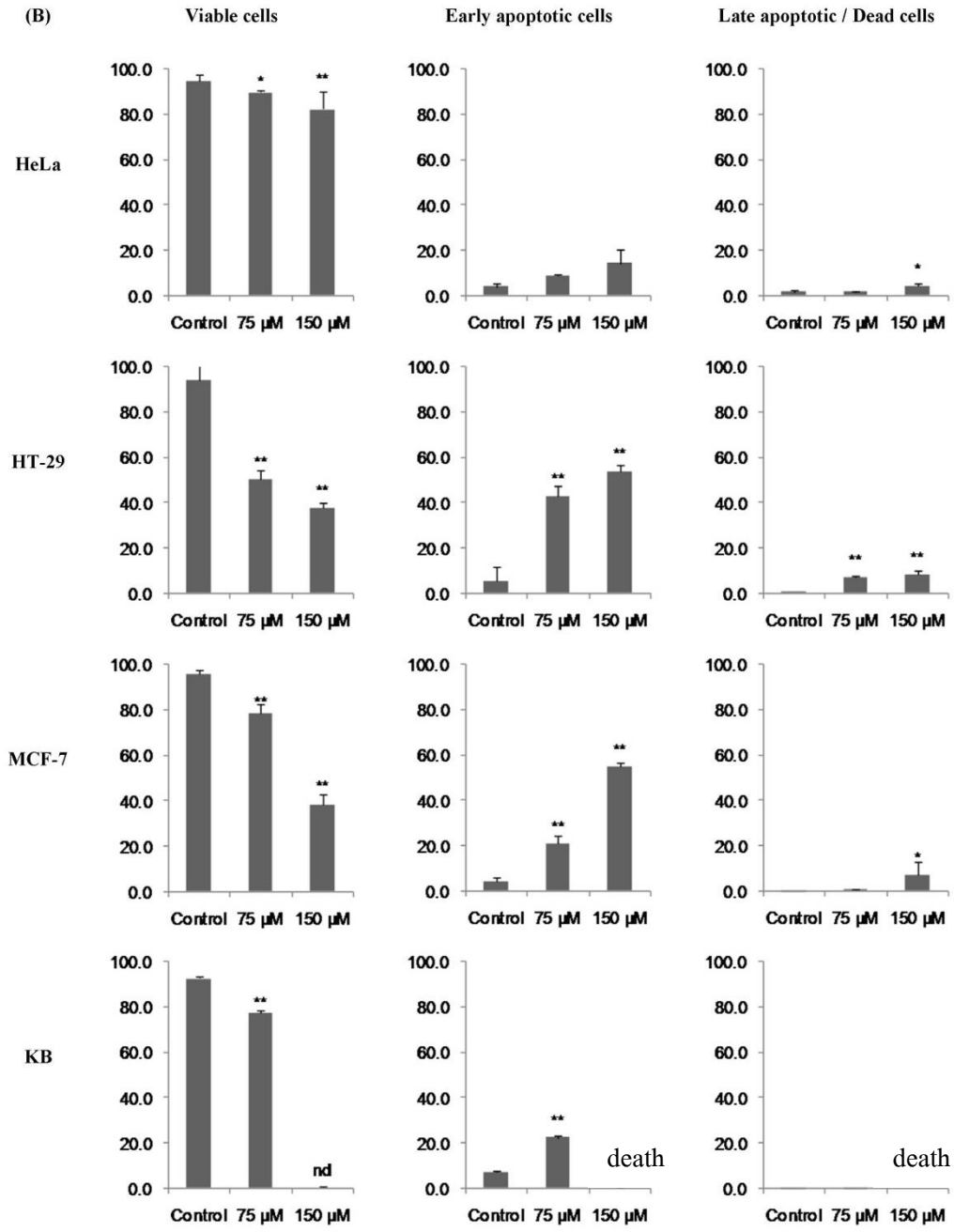

Figure 3.20 Summary of the percentage of cell number after plaunol A treatments.

The percentage of live, early apoptotic, late apoptotic and dead cells were recorded by Muse™ Analyzer.* $p< 0.05$, ** $p< 0.01$ indicates significant (one-way ANOVA followed Dunnett's test, n =3).

3.2.3.3 Plaunol E

Plaunol E was investigated on the apoptotic detection using Annexin-V/7AAD double staining. According to our experiment, plaunol E at 75 μM and 150 μM were separately treated to various cancer cells including HeLa, HT-29, MCF-7 and KB cells for 48 h. The populations of cells during apoptotic detection were expressed in scatter plot (Fig. 3.21).

In HeLa cells, plaunol E significantly induced early apoptotic cells with 82.24 ± 2.88% and 93.16 ± 1.75% when treated with plaunol E at 75 μM and 150 μM, respectively. In control group was 3.81 ±1.86%.

In HT-29 cells, plaunol E at both concentrations also significantly induced early apoptotic cells from control group, which was 5.22 ± 6.43% to 44.98 ± 4.39% and 59.93 ± 1.97% after treatment with plaunol E at 75 μM and 150 μM, respectively.

In MCF-7 cells, plaunol E at both concentrations also significantly induced early apoptotic cells from control group, which expressed as 4.13 ± 1.57% to 35.48 ± 2.05% and 59.16 ± 2.34% after treatment with plaunol E at 75 μM and 150 μM, respectively.

The effect of plaunol E also found on KB cells, but it showed lower potency than other cells. The plaunol E at 75 μM showed early apoptotic cells with 17.96 ± 0.87% and 24.39 ± 0.84 % after treatment with 150 μM of plaunol E.

During experiments, paclitaxel at 1 μM also significantly increased apoptotic cells including 37.94 ± 12.47% (HeLa), 52.09 ± 5.27% (HT-29), 51.18 ± 3.30% (MCF-7) and 17.68 ± 1.17% (KB), respectively.

According to apoptotic results, these results indicated that plaunol E can induce early apoptosis in every human cancer cells. Among these cell lines, plaunol E has an effect in HeLa, HT-29 and MCF-7 and less effect in KB cells (Fig. 3.22).

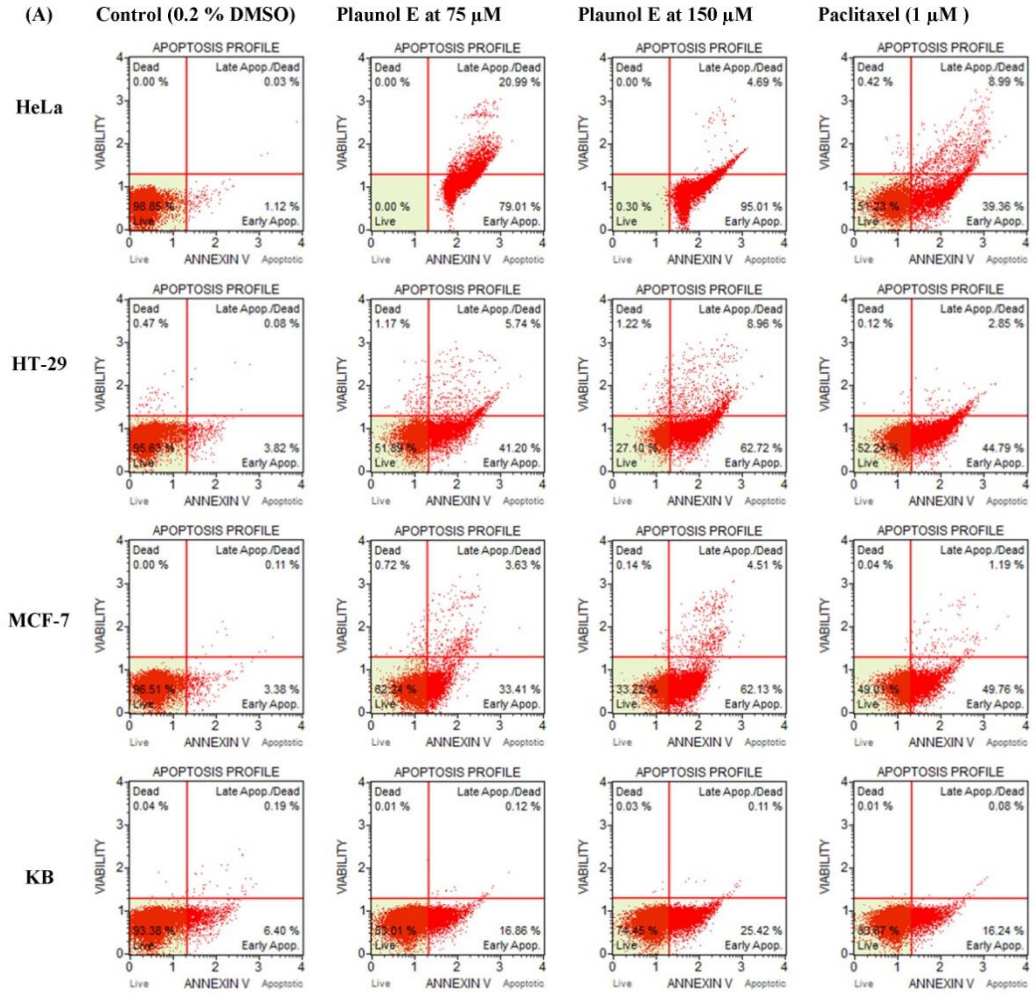

Figure 3.21 Scatter plots in each apoptotic stage of cancer cells after treatment with plaunol E, detection with annexin-V/7-AAD.

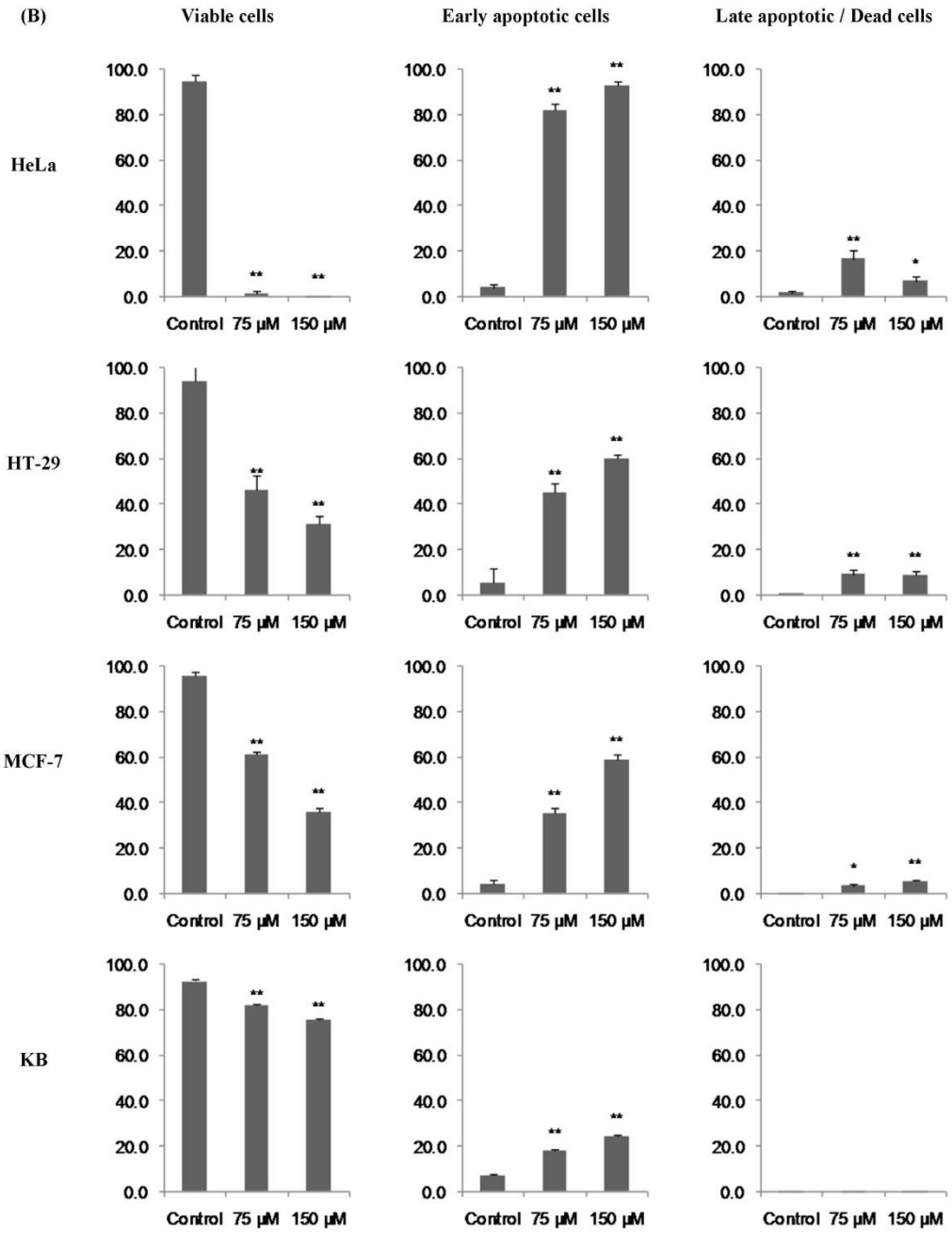

Figure 3.22 Summary of the percentage of cells number after plaunol E treatments.

The percentage of live, early apoptotic, late apoptotic and dead cells were recorded by Muse™ Analyzer.* $p< 0.05$, ** $p< 0.01$ indicates significant (one-way ANOVA followed Dunnett's test, n =3).

3.2.4 Transcription profile of apoptotic-associated genes

The mitochondria play an important role in the apoptosis of mammalian cells. The permeability of the mitochondrial membrane during apoptosis is regulated directly by the BCL-2 protein family. For mitochondria dependent apoptosis, anti-apoptotic proteins such as BCL-2 promote cell proliferation and apoptotic proteins such as BAK and BAX promote cell death. Therefore, the ratio between anti- and pro-apoptotic regulatory factors such as BCL-2/BAX can be determined either cell survival or cell death. Moreover, apoptotic cells can be active from mitochondria independent apoptotic pathway or death receptor/NF-κB signaling pathway. The signaling molecules such as TNF-α also promote cells leading to apoptosis.

Herein, the effects of plaunotol and plaunol E on the mRNAs expression of *TNF-α, BCL-2, BAK*and *BAX* genes were investigated in various cancer cells. These results may explain the mechanism of anti-proliferative activity of plaunotol and plaunol E in cancer cells. The mRNA sequences of *TNF-α, BCL-2, BAK*and *BAX* as target genes and *GAPDH* as endogenous genes from *Homo sapiens* in NCBI database provide us to design the specific primers. The mRNA level was determined by qRT-PCR.

3.2.4.1 Plaunotol

Plaunotol at 50 and 75 μM were incubated with cancer cells for 48 h. The expression profiles of plaunotol in different cancer cells were investigated using qRT-PCR. The relative quantification after calculated was expressed and was illustrated on the Fig.3.23.

During experiment, plaunotol at 50 μM and 75 μM were tested in HeLa, HT-29, MCF-7 and KB cells. In HeLa cells, the results indicated that plaunotol up-regulated on *TNF-α* and it also down-regulated on *BCL-2*, but it did not affect on *BAK* and *BAX*. The expression profiles of plaunotol results in other cells were indicated in the same way as followings;

In HT-29, plaunotol at 50 μM increased mRNA level of*TNF-α*and *BAK*, inhibited *BCL-2* and it also slightly increased *BAX*, while plaunotol at 75 μM increased *TNF-α*, inhibited *BCL-2* and it also slightly increased *BAX* and *BAK*.

In MCF-7, plaunotol at 50 μM increased *TNF-α*, *BAX* and *BAK* and it also inhibited *BCL-2*. Plaunotol at 75 μM increased *BAX* and *BAK*, but inhibited *TNF-α* and *BCL-2*.

In KB, plaunotol at both concentrations inhibited *TNF-α*, *BCL-2*, *BAX* and *BAK* at dose dependent manner.

These results of plaunotol indicated that it showed different effects in various cancer cell lines, it increased *TNF-α* in HeLa, HT-29, and MCF-7, but it also inhibited *BCL-2*. Furthermore, a key factor of apoptosis deriving mitochondrial dependent pathway is considered by a ratio between *BCL-2* and *BAX*. A high level of *BCL-2*/*BAX* ratio, it makes cells resistant to apoptosis, while a low level induces apoptosis or cell death. Comparing to these results from our study, the level of mRNA expression of *BCL-2*/*BAX* as shown in Fig. 3.24, it showed lower than untreated cells in HeLa, HT-29 and MCF-7, but did not affect in KB cells. According to our results, plaunotol increased *TNF-α* and it also inhibited *Bcl-2*/*BAX* ratio. That mean, plaunotol induced apoptosis using death receptor/NF-κB signaling and mitochondrial dependent pathways.

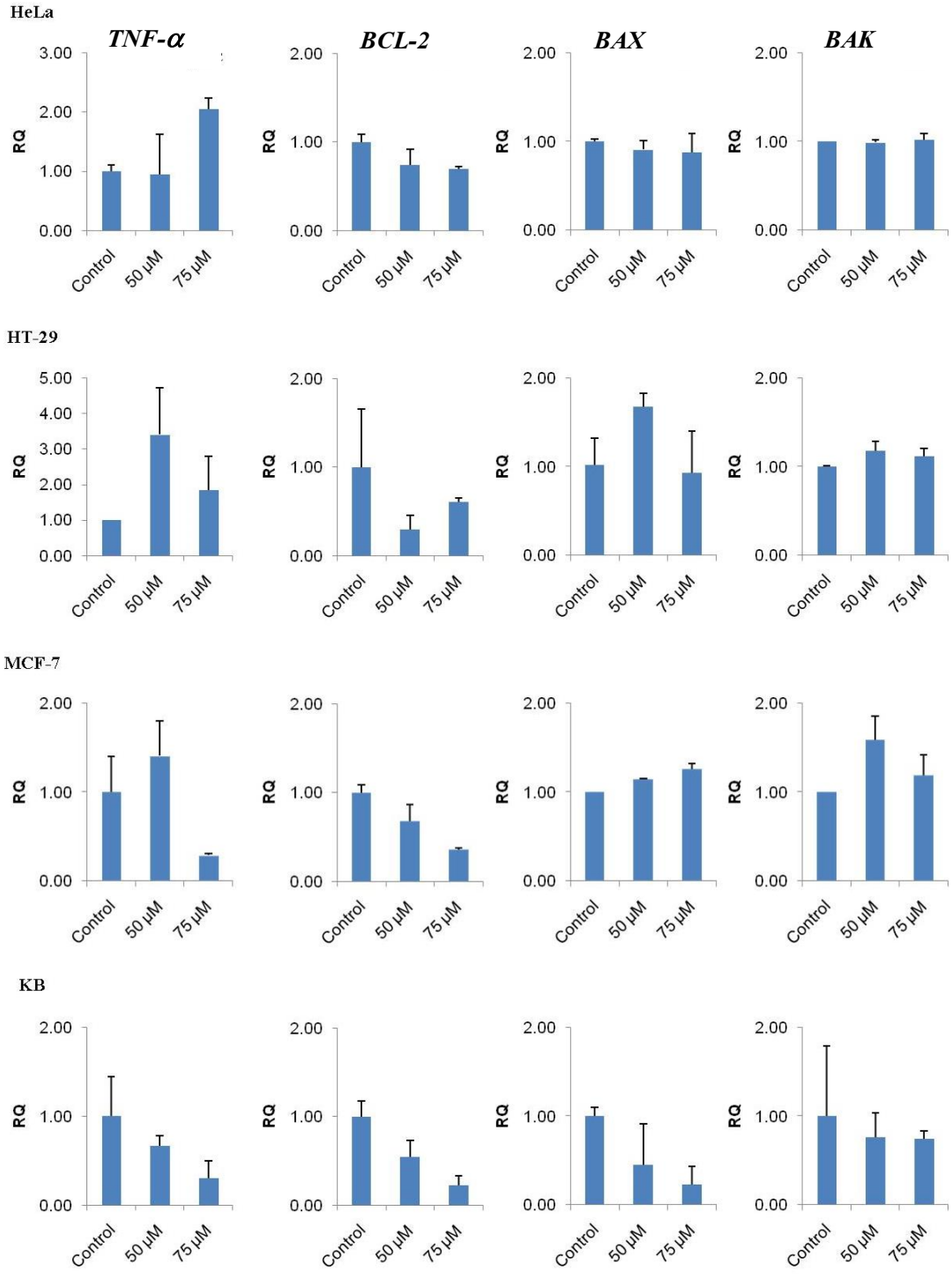

Figure 3.23 RQ of *TNF-α, BCL-2, BAX* and *BAK* of plaunotol treatment.

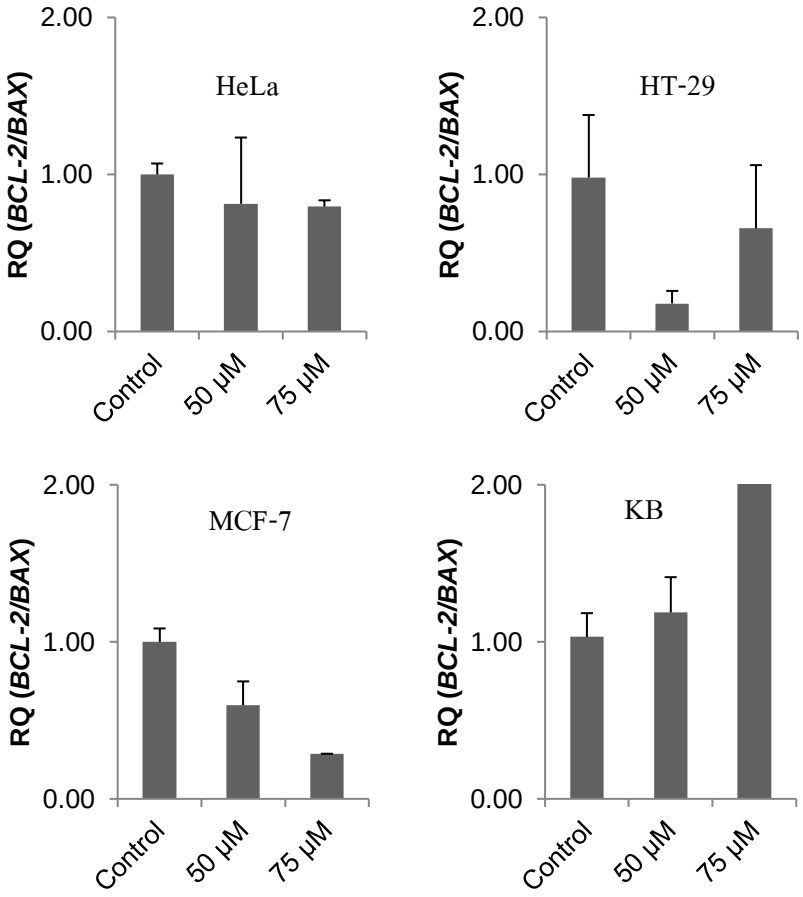

Figure 3.24 The *BCL-2/BAX* ratio of plaunotol treatment.

3.2.4.2 Plaunol E

Plaunol E was selected at 75 μM and 150 μM for treatment with cancer cells including HeLa, HT-29, MCF-7 and KB cells for 48 h. After incubation time, the treated cells were harvested and extracted for the total RNA. Total RNA with 20 ng was performed in qRT-PCR reaction and was amplified by specific primers including *TNF-α*, *BCL-2*, *BAX* and *BAK* and other components (see in chapter 2). The *GADPH* was used as an internal standard in each experiment. After qRT-PCR was finished, amplification plot was obtained. Following the threshold value was set at 0.2, and the threshold cycle (C_T) was recorded by subtracting with an endogenous *GADPH*. The relative quantification (RQ) was calculated using comparative C_T method and the result was compared with untreated cells as a calibrator. As shown in Fig. 3.25, the relative of apoptotic related genes are summarized and are illustrated. These results indicated that plaunol E at various concentrations exhibited the different transcription profiles against several cancer cells following;

In HeLa cells, plaunol E at 50 μM and 75 μM up-regulated on *TNF-α* and down-regulated on *BCL-2* at dose dependent manner, but it did not affect on *BAX* and *BAK*.

In HT-29 cells, the results of plaunol E did not affect on dose dependent manner, however, the plaunol E also showed apoptotic effects. Plaunol E at 50 μM up-regulated on TNF-α, down-regulated on *BCL-2* and it also slightly increased on *B*AX and *BAK* when compared with control. At 75 μM of plaunol E also showed up-regulation on *TNF-α*, down-regulation on *BCL-2*, and it also slightly affected on *BAX* and *BAK*.

In MCF-7 cells, the results of plaunol E showed up-regulation on *TNF-α* and down-regulation on *BCL-2* when using plaunol E at 50 μM. After increasing plaunol E to 75 μM, the *TNF-α* and *BCL-2* were decreased. Plaunol E at both concentrations slightly increased *BAX* and *BAK*.

In KB cells, the *TNF-α*, *BCL-2*, *BAX* and *BAK* expression level were decreased after plaunol E treatments at dose dependent manner.

That described above, the plaunol E at various concentrations showed different effect in various types of cancer cells. Considering to apoptotic genes, up-regulation of *TNF-*α and *BAX*, and down-regulation of *BCL-2* indicated cells undergoing to apoptosis. In line with these results, plaunol E exhibited as apoptotic agent in HeLa, HT-29 and MCF-7, but did not act as apoptotic agent on KB. Moreover, the key factor of apoptosis regulation is considered by the *BCL-2/BAX* ratio. The decreasing of *BCL-2/BAX* indicates apoptosis, whereas increasing of *BCL-2/BAX* ratio indicates anti-apoptotic (promote of cancer cells). As shown in Fig. 3.26, the results of *BCL-2/BAX* ratio obviously induced in HeLa, HT-29 and MCF-7, but decreased in KB. These results corresponded with transcription profiles of apoptotic related genes. Both of transcription profile and *BCL-2/BAX* ratio suggested that plaunol E was effective in HeLa, HT-29 and MCF-7, and these results was clearly that plaunol E did not have apoptotic effect in KB cells.

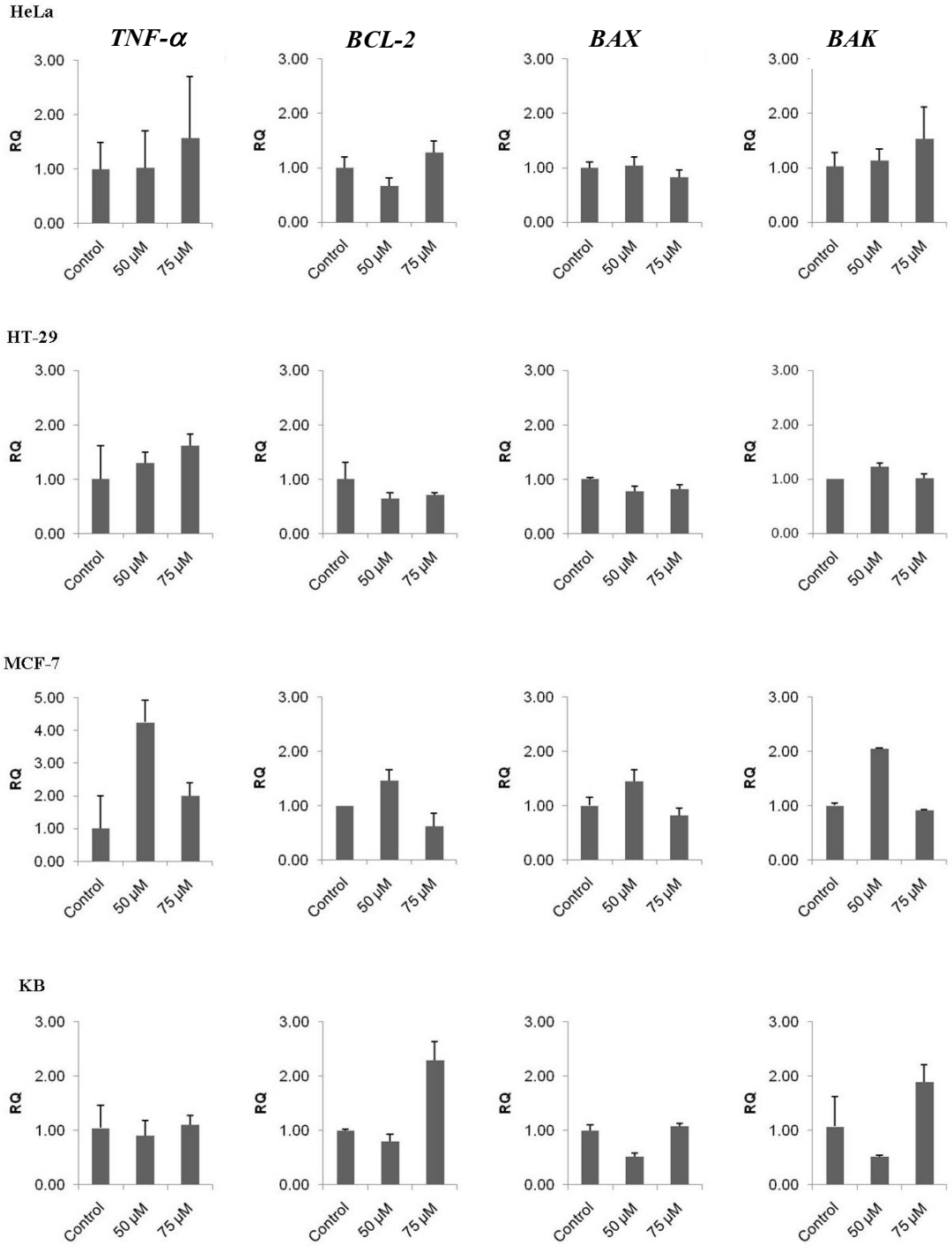

Figure 3.25 RQ of *TNF-α, BCL-2*, *BAX* and *BAK* of plaunol E treatment.

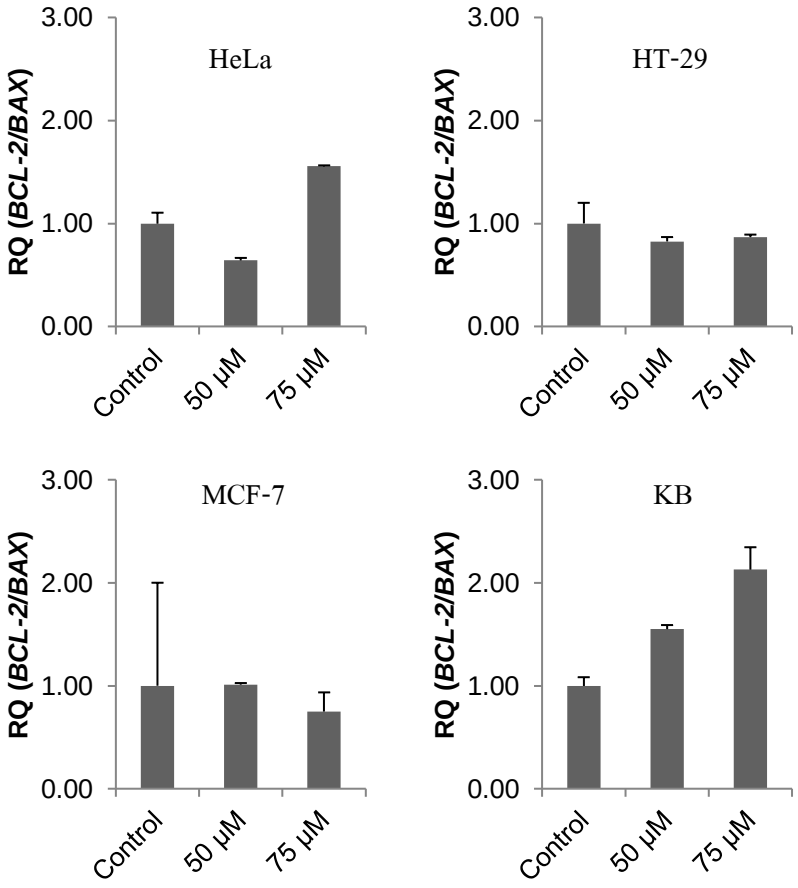

Figure 3.26 The *BCL-2/BAX* ratio of plaunol E treatment.

3.2.5 Effect of plaunol E on caspases activities

Apoptosis associates from the activation of caspases. These caspases normally function in cell disassembly (as effectors) and in initiating this disassembly in response to pro-apoptotic regulators (as initiators). Several caspases have been identified in mammals. In apoptosis, caspase-3 is triggered by caspase-8 (death receptor/ NF-κB signaling pathway) and caspase-9 (mitochondria dependent apoptotic pathway) and caspase-3 directly activates cellular targets such as cell structure, nuclear proteins and signaling proteins, resulting to the morphological and biochemical hallmark of apoptosis.

Plaunotol E exhibited on anti-proliferative activity, cell cycle analysis, apoptotic detection and transcription profiles of apoptotic related genes. To understanding apoptotic mechanism of plaunol E on translation level, caspase-3, -8 and caspase-9 were determined by colorimetric assay after plaunol E treatment. The plaunol E at 50 and 100 μM were prepared and were treated to MCF-7 cells for 48 h. Treated cells were harvested and were extracted to afford cytosol extract. The cytosol extract was determined the protein content using Bradford reaction. The cytosol extract equivalent to 100 μg protein was added into specific caspase substrates including caspase-3, -8 and caspase-9, and buffer solution. The caspase activities were considered by OD measurement at 405 nm and these results exhibited as fold of control treatment. According to this result as expressed in Fig. 3.27, the incubation of MCF-7 and plaunol E increased caspase-3 (2.67 fold), -8 (6.33 fold) and -9 (5.33 fold), when compared with untreated cells.

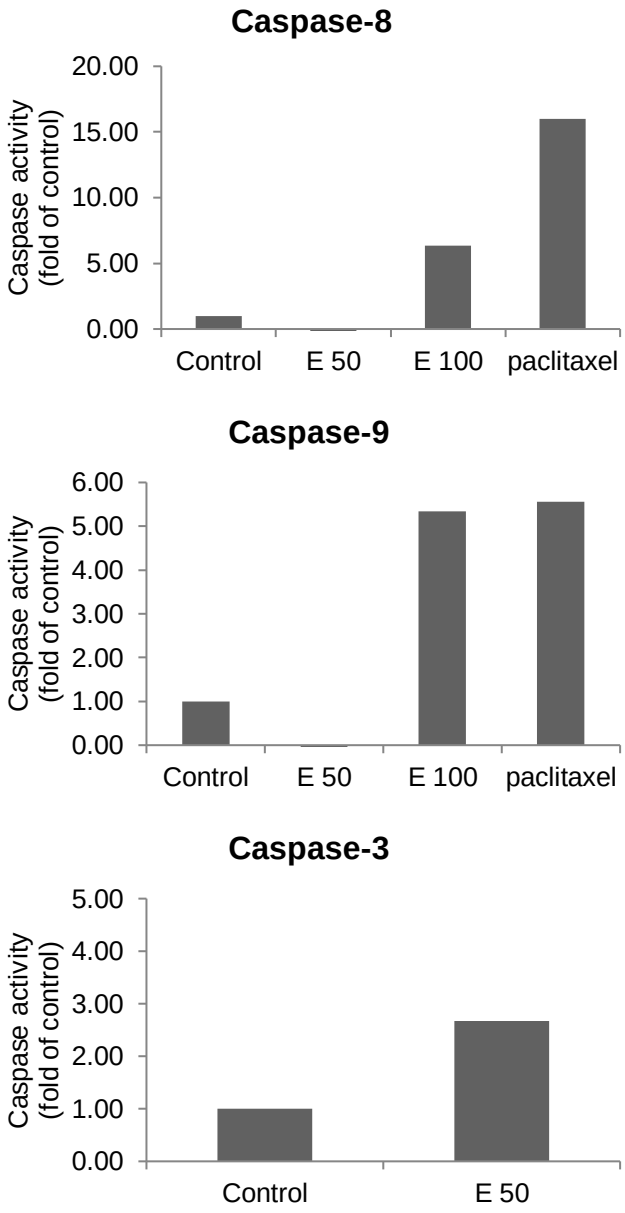

Figure 3.27 Caspases activities in MCF-7 after plaunol E treatment.

3.3 Anti-inflammatory activity of diterpene from *C. stellatopilosus*

Due to the proposed study, we aimed to investigate the effect of plaunol A on anti-inflammatory activity and to understand of its mechanisms. In this section, plaunol A, a furano clerodane type-diterpene isolated from *C. stellatopilosus* using chromatographic technique, was evaluated on anti-inflammatory using cell-based assay. A model of inhibitory of NO production in LPS-stimulated RAW 264.7 cells was used for evaluation. Furthermore, the effect on anti-inflammatory activity of plaunol A was also investigated by transcription profiles of *iNOS* and *COX-2* using qRT-PCR experiment. The plaunol A results obtained from these studies were described in the following sections.

3.3.1 Effects of plaunol A on nitric oxide (NO) production in RAW264.7 cells

The LPS-induced RAW264.7 cells affected the transcription and translation of iNOS, so the concentration of NO increased. Using Griess reaction to detect NO production in LPS-stimulated RAW264.7 macrophage cell line was carried out from the previous study (Premprasert *et al.,* 2013). Herein, cells were treated with plaunol A at various concentrations (0, 3, 10, 30 and 100 μM) for 24 h. The supernatant was reacted with Griess reagent and the mixed solution was determined by microplate reader at 570 nm. The inhibitory of NO production in RAW 264.7 cells after plaunol A treatment was shown in the Table 3.12. These results indicated that plaunol A significantly inhibited NO production when LPS-stimulated RAW 264.7 cells and it expressed with an IC_{50} value of 11.69 μM. The positive substances including caffeic acid phenethyl ester (CAPE), indomethacin (IDM), and L-nitro arginine (L-NA) also showed with an IC_{50} value of 5.17, 15.90, and 62.13 μM, respectively. In addition, the MTT assay was performed to check whether live cells or dead cells after treatment with plaunol A. The results suggested that plaunol A did not observe cytotoxicity.

Beside plaunol A study, three flavonoids from *C. stellatopilosus* including apigenin-8-C-β-D-glucoside (vitexin), luteolin-7-O-β-D-glucoside and luteolin-4′-O-β-D-glucoside were also

evaluated on inhibitory of NO production using RAW264.7 cells model, however these compounds did not observe their activities on anti-inflammatory activity as well as cytotoxicity (IC_{50}> 100 μM). These results related with previous reports.

According to the previous results, two furano clerodane-type diterpenes (plaunol E and plaunol F) were isolated and were purified from *C. stellatopilosus* as well as plaunol A. Two compounds also evaluated for anti-inflammatory activity using inhibitory of NO production on RAW 264.7 cell line. These NO results showed that plaunol E exhibited strong potency (an IC_{50} value less than 3 μM), whereas plaunol F showed high ability (an IC_{50} value = 17.02 μM). Furthermore, both compounds (plaunol E and plaunol F) were determined on *iNOS* and *COX-2* transcription profiles using qRT-PCR. However, the results were indicated that plaunol E and plaunol F different exhibited on transcription level, both compounds showed the anti-inflammatory effects (Premprasert *et al*., 2013). Corresponding to this study, plaunol A showed an IC_{50} better than plaunol F and it also showed an IC_{50} as same range with CAPE. Therefore, this compound also possessed anti-inflammatory activity. Moreover, the anti-inflammatory mechanism of plaunol A has not been evaluated yet. Due to iNOS and COX-2 are key enzymes on inflammatory pathways. Therefore to underlying inflammatory mechanisms of plaunol A, *iNOS* and *COX-2* mRNA transcription profiles were further determined using qRT-PCR.

Table 3.12 The % inhibition of NO production and IC_{50} of plaunol A.

Compound	[a] inhibitory activity (%) at various concentrations (μM)				IC_{50}
	3	10	30	100	(μM)
Plaunol A	2.06 ± 2.16	45.08 ± 6.99	94.35 ± 2.93	108.09 ± 1.12[b]	11.69
CAPE	28.87 ± 0.41	76.16 ± 0.48[b]	82.92 ± 0.32[b]	84.19 ± 0.45[b]	5.17
IDM	43.205 ±1.43	49.3 ± 1.22	52.45 ± 1.72	76.57 ± 1.22	15.90
L-NA	17.31 ± 1.77	20.45 ± 1.77	29.37 ± 1.31	67.13 ± 2.73	62.13

Untreated cell (cells maintained in RPMI with LPS) showed % inhibition of NO production with 0.00 ± 2.70 %.

[a]Each value represents mean ± S.E.M. of four determinations.

[b] Cytotoxicity was observed.

Table 3.13 The % inhibition of NO production and IC_{50} of three flavonoids.

Compound	[a] inhibitory activity (%) at various concentrations (μM)				IC_{50}
	3	10	30	100	(μM)
Apigenin-8-C-β-D-glucoside	2.48 ± 2.70	4.22 ± 1.93	6.45 ± 3.32	35.25 ± 3.31	> 100
Luteolin-7-O-β-D-glucoside	1.32 ± 1.17	4.63 ± 3.33	17.38 ± 3.11	46.69 ± 2.63	> 100
Luteolin-4′-O-β-D glucoside	8.94 ±0.84	10.92 ± 0.35	15.64 ± 1.19	41.95 ± 1.19	> 100
CAPE	21.68 ±1.76	57.96 ± 2.71	87.38 ± 0.67	94.21 ± 0.24[b]	7.62

Untreated cell (cells maintained in RPMI with LPS) showed % inhibition of NO production with 0.00 ± 4.22 %.

[a]Each value represents mean ± S.E.M. of four determinations.

[b] Cytotoxicity was observed.

3.3.2 *iNOS* and *COX-2* mRNA transcription profiles of plaunol A

iNOS and COX-2 are key enzymes in the inflammatory process. Considering to NF-κB signaling pathway, the increasing of iNOS and COX-2 directly affect on NO and PGE_2 production, respectively. NO is induced by iNOS, it is obtained from L-nitroarginine. For COX-2, it generates prostaglandins (PGEs) by alteration of phospholipid membrane. Both NO and PGE_2 are released from immunocytes and they are stimulated other immunocytes to produce pro-inflammatory mediators such as TNF-α, INF-γ, etc. Therefore, the inhibiting either iNOS or COX-2, the inflammation might be reduced. In the present study, plaunol A has been screened on inhibitory of NO production in RAW 264.7 and its result showed high anti-inflammatory potency (IC_{50} = 11.69 μM).

The plaunol A at 10 μM and 30 μM were selected and were treated to LPS-induced RAW 264.7 cells. After incubation for 20 h, the treated cells were harvested and were then investigated on mRNA level by qRT-PCR following ΔΔCq calculation. The relative expression level and % genes inhibition of *iNOS* and *COX-2* are summarized in Fig. 3.28. Each Cq value from each treated-cell was subtracted by Cq value of *GAPDH* (a housekeeping gene). The results were then normalized by control treated cells as a calibrator. The cells did not treat by LPS (normal group) showed a significant difference with LPS-induced group (control group), $p < 0.05$.

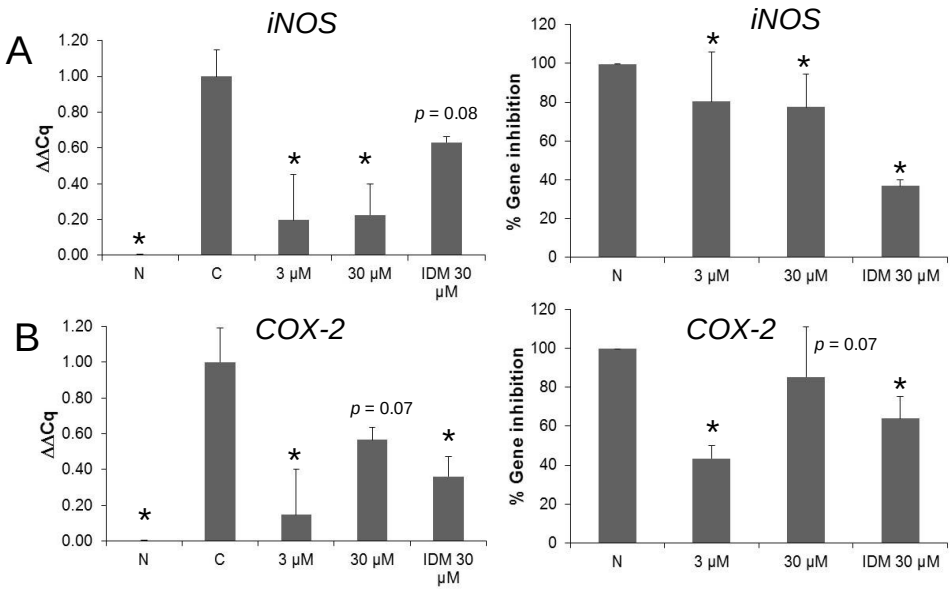

Figure 3.28 Relative expression ($2^{-\Delta\Delta Cq}$) and % gene inhibition of plaunol A. A. *iNOS* and B. *COX-2*. * indicates the significant $p<0.05$.

According to ΔΔCq results as shown in Fig. 3.28, the mean of ΔΔCq of plaunol A on *iNOS* and *COX-2* mRNA levels significantly decreased when compared with control group. The plaunol A at 3 μM and 30 μM also significantly suppressed % gene inhibition of *iNOS* expression with 80% and 77% and *COX-2* expression with 45% and 85%, respectively (Fig. 3.28). The indomethacin (IDM) as a reference drug was presented as well as plaunol A. The result concluded that *iNOS* and *COX-2* mRNA levels were inhibited with the % gene inhibition 37% and 64%, respectively.

The present study, plaunol A was isolated and purified by chromatography from *C. stellatopilosus* stem and this compound has not been evaluated on *iNOS* and *COX-2* mRNA expression before. This is the first time for report, plaunol A showed down regulation on *iNOS* and *COX-2* mRNA expression. In this study we found that plaunol A showed highly inhibitory effect on NO production and also inhibited a key enzyme on inflammatory pathway, especially NF-κB signaling pathway. From the previous report, plaunol E and F were also isolated from *C. stellatopilosus* and these compounds also exhibited anti-inflammatory effects via different

mechanisms. Furthermore, plaunol E showed the cytotoxic effect on tested concentration (< 10 μM). Plaunol E did not inhibit NO directly, but it also inhibited *COX-2*. In addition, plaunol A did not only affect on *iNOS*, but also on *COX-2*. Hence, this evident indicated that plaunol A did not directly inhibit on NO production, but it further linked to other anti-inflammatory signaling pathways as well as cancer pathways.

CHAPTER 4

DISCUSSION

Nowadays, the approved anti-cancer agents are derived from natural sources including taxol, camptothecin, podophyllotoxin and vincristine, for instance (Wilken *et al*., 2011; Newman and Cragg, 2016). The precise mechanism of action of anti-cancer derived natural products is involved on cell cycle, cell development and apoptosis. Taxol (paclitaxel) is one example and it shows a mode of action different from others. It binds to tubulin heterodimer of cellular microtubules resulting to induction cells arrest in cell development cycle at G2/M phase (Payne and Miles, 2008). The inhibition of cellular microtubules depolymerization leads to induce apoptosis and cell cycle signaling cascade (Wang *et al*., 2000). Additionally, anti-proliferative and cytotoxic effects of anti-cancer agents may be directly proposed on cell death signaling pathways or it may be triggered by several signaling cascade pathways including reactive oxygen species-mediated and oxidative effect, apoptosis, cell cycle arrest, autophagy effect and etc (Islam, 2017).

In the normal cell development, cell cycle and apoptosis are an important process. The cells use the cell cycle progression for cell dividing and cell regeneration, whereas the cells use apoptosis as a programmed cell death. In the case of cancer, the normal cells are abnormal development and these cells are lacking of apoptosis. Therefore, cancer cells are associated with a complex biological system.

Apoptosis or programmed cell death is a crucial process of cell death, which used for elimination of unwanted cells such as damage cells or cancer cells in order to tissue homeostasis, tissue remodeling, and normal development. Apoptosis is occurred in multi-cellular organism in daily life and the normal cells at 70-80 million cells were killed by this program. Regarding to a normal process of apoptosis, apoptosis is characterized by changes such as cell shrinkage,

mitochondrial cytochrome c release, fragmentation of cell DNA and the ultimate breakage of cells into small apoptotic bodies, which will be cleared through phagocytosis.

The damage DNA is detected using cell cycle analysis, and the apoptosis is detected from phosphatidylserine (PS) as a biomarker of apoptosis using annexin-V/7-AAD. Furthermore, the morphological and the biochemical changes during apoptosis are related to apoptotic genes including pro-apoptotic genes (*TNF-α, BAX* and *BAK*), and anti-apoptotic (*BCL-2*) genes and also associated with caspases activations, especially caspase-3, -8 and -9. The main initiators including caspase-8 and caspase-9, both caspases are served for active executioner caspases such as caspase-3. Considering to caspase-3 is triggered to nuclear DNA fragmentation and other morphological changes. Due to apoptotic pathway, the caspase-8 often associated in death receptor mediated signaling cascades. It is triggered by the ligand-receptor binding such as Fas ligand (FasL is transmembrane protein belonging to the tumor necrosis factor (TNF) family) and TNF-α. TNF-α, a pro-inflammatory cytokine normally plays an important role in inflammation process using NF-κB signaling pathway, and TNF-α also plays in apoptotic pathway using caspase-dependent signaling pathway. The high level of TNF-α induced cells undergoing to apoptosis and caspase-8 activation by the TNF-α to tumor necrotic factor receptor -1 (TNFR-1) binding, so the NF-κB signaling pathway is exhibited downstream. Caspase-9 activation is induced by the cytochrome C release in mitochondrial. The anti-apoptotic proteins such as BCL-2 block cytochrome C release, so the apoptosis is terminated. It contrasts to pro-apoptotic protein such as BAX and BAK (Cooper, 2000; Robertson *et al*., 2009).

As therapeutic strategies, the plant derived secondary metabolites have an important role nowadays. This evident was found on their published articles from researchers. The international databases including Pub Med, Science Direct, Scopus and Web of Sciences are many biological and pharmaceutical, and clinical trials resources. Focusing to anti-cancer, anti-proliferative, anti-apoptosis activities as keywords were found more than 20,000 articles, among of them, the molecule of their interest derived from natural products such as microorganism, plant, and marine,

etc. Furthermore, FDA also currently approved new anti-cancer drugs in 2015 (Newman and Cragg, 2016). Interestingly, among these drugs half of all are from natural sources. However, almost proposed anti-cancer compounds are derived from natural sources. Some of them were seen on journal and it showed the different mechanism or pathways (Newman and Cragg, 2016).

C. stellatopilosus (plaunoi), a traditional medicinal plant that found in Thailand, is a source of a major compound, namely plaunotol. The plaunotol is well known for anti-peptic ulcer drug (Kelnac®, Sankyo Company). To increasing the valuable of *C. stellatopilosus*, the plant derived compounds including plaunotol and plaunol derivatives such as plaunol A, plaunol B, plaunol C, plaunol D, plaunol E, and plaunol F, kauranes, labdanes, and esters of plaunotol derivatives have been isolated and purified since 30 years ago (Ogiso*et al*., 1978; Kitazawa *et al*., 1979; Kitazawa *et al*., 1980; Kitazawa and Ogiso, 1981; Kitazawa *et al*., 1982 Takahashi *et al*., 1983). About the biological and pharmacological activities, only plaunotol is mainly considered and it has been evaluated in a wide array of activity such as anti-peptic ulcer, anti-bacterial and anti-cancer activities. Moreover, plaunotol has been evaluated on toxicity and clinical trial and the results indicated that plaunotol was safe. However, the biological and pharmacological activities were rarely published on other compounds. For plaunol derivatives, plaunol A, plaunol B, plaunol C and plaunol E have been evaluated on anti-shay activity as an anti-gastric ulcer model. Other compounds such as plaunol F, kaurane and labdane have not been exhibited any activity so far.

In 2013, we studied the anti-inflammatory constituents from *C. stellatopilosus* leaves. The phytochemical investigation was carried out using chromatography. Using common chromatography, plaunotol, plaunol E and plaunol F were obtained. These compounds were evaluated on anti-inflammatory activity using cell based assay. The results indicated that all diterpenes exhibited anti-inflammatory effect on the inhibitory of NO production in RAW267.4 macrophage cells. Furthermore, these compounds also investigated on mRNA expression of *iNOS*, *COX-1* and *COX-2*. Following these results, diterpenes showed different mechanism. In parallel study, the plaunol E exhibited cytotoxicity (Premprasert *et al*., 2013).

According to cytotoxic effect in RAW 264.7 cells, we proposed that plaunol E might have potential for anti-cancer activity. Therefore, the investigation of plaunol E on the inhibitory effect in cancer cells is a topic of interest. Besides, there is not only plaunol E, but other diterpenes might be effect on cancer cells, plaunol derivatives for instance.

Focusing on cytotoxic or anti-proliferative activity as well as apoptotic activity of *C. stellatopilosus*, among these diterpenes only plaunol has been investigated for anti-cancer activity and apoptosis. Plaunotol has been shown an anti-proliferative effect in human umbilical vein endothelial cells (HUVECs) using anti-angiogenic properties as a model (Kawai *et al*., 2005). Furthermore, the effect of plaunotol on anti-cancer activity and apoptosis has recently been investigated by gastric and colon cancer cells (Yamada *et al*., 2007; Yoshikawa *et al*, 2009). It has been tested against three gastric cancer cell lines including MKN-45, MKN-74 and AZ-521, respectively (Yamada *et al*., 2007). These cancer cells were treated with plaunotol at 10, 20, 30 and 40 μM. The result indicated that plaunotol significantly inhibited the growth of cancer cells at dose-dependent manner and plaunotol also induced cells to apoptosis through caspase-3, -8, and caspase-9 activation. On translation level, plaunotol revealed that it induced BAX (pro-apoptotic protein), but it did not significantly affect on BCL-2. Due to these results, they suggested that plaunotol might be promised a new anti-tumor drug (Yamada *et al*., 2007). The apoptotic activity of plaunotol has been found in colon cancer (DLD1). It induced colon cancer to apoptosis by caspase activation and it also affected on cellular protein by cleavage poly (ADP-ribose) polymerase (PARP) (Yoshikawa *et al.*, 2009). Their studies about plaunotol indicated that plaunotol were quite clear on an anti-cancer and apoptotic effects. However, the furanoclerodane type diterpenes such as plaunol A, plaunol E and plaunol F have not been studied for anti-proliferative activity against cancer cells.

Conduct to our research, the phytochemical investigation from *C. stellatopilosus* leaves was firstly performed using chromatography. Following isolation and purification, plaunotol was first isolated from methanol extract from leaves by eluting with gradient solvent (hexane, hexane: CH_2Cl_2, CH_2Cl_2: EtOAc, and EtOAc: MeOH) according to ascending polarity. Plaunotol a major

compound and phytosterols were obtained, but other compounds could not isolate due to starting material. We further isolated and purified plaunol E and plaunol F from CH_2Cl_2 extract (LCS). Additionally, plaunol A was isolated and purified from CH_2Cl_2 extract from stems of plaunoi (SCS). In the present study, the plaunol A was isolated from stems. Subsequent separation by diaion HP-20 and Sephadex LH-20 afforded flavonoids from EtOAc extract. Herein, one acyclic diterpene (plaunotol), three cyclic diterpenes (plaunol A, plaunol E and plaunol F) were obtained and these compounds were further evaluated for anti-proliferative and anti-inflammatory activities.

In order to understand the characteristic of the cytotoxicity effect of plaunoi extracts on cancer cell lines, four human cancer cell lines were chosen; HeLa, HT-29, MCF-7 and KB cells and non-cancerous HGF cell line was used as the normal cells. In our study, we evaluated the cytotoxicity effect of diterpenes as the measurement percentage of either cell mortality or cell viability by MTT assay. After incubation for 48 h, the diterpenes in a dose dependent manner were able to inhibit the proliferation of cancer cells at ranging 60-80 μM and normal cells at > 100 μM. Therefore, the results from the present study showed slightly cytotoxic effect in cancer cells. However, all diterpenes did not have cytotoxic effect on normal cell.

Based on the our knowledge, eventhough plaunotol, plaunol A, and plaunol E showed less activity in cancer cells, these compounds also did not affect in human normal cells. These compounds exhibited their effects on cell cycle, morphological and biochemical changes, and transcription profiles. The results showed that plaunotol induced the cell cycle arrest in different phase and it also induced early apoptosis on HeLa, HT-29 and MCF-7. On the transcription profiles of *TNF-α*, *BCL-2*, *BAX* and *BAK* as apoptotic associated genes, plaunotol results indicated that its effect on both NF-κB death signaling and mitochondrial dependent pathways. These results of plaunotol corresponded to previously published report (Kawai *et al*., 2005; Yamada *et al*., 2007 and Yoshikawa *et al*., 2009).

Consideration on anti-cancer activity, plaunotol inhibited the growth of gastric ulcer and endothelial cells (Kawai *et al*., 2005 and Yamada *et al*., 2007) and plaunotol also triggered caspase-

mediated apoptosis including caspase-3, -8 and caspase-9 (Yoshikawa *et al*., 2009). For cyclic diterpenes, they have not been evaluated on several activities so far, except anti-peptic ulcer activity. In this study, we indicated that plaunol A showed the effects on different phases of cell cycle and induced early apoptosis as same as plaunol E, but plaunol A was less effective than plaunol E. Therefore, only plaunol E was selected to underlying apoptotic mechanism. On the transcription profiles of apoptotic related genes, plaunol E showed strong effect on *TNF-*α mRNA expression, but slightly on *BCL-2*, *BAX* and *BAK*. According to qRT-PCR and caspases activations, these results indicated that plaunol E has an apoptotic effect on NF-κB death signaling and mitochondrial dependent pathways, which was confirmed by caspase activity.

Anti-cancer activity of diterpenes derived from *Croton* species has been reported. Therefore the crude extract and pure compounds from *Croton* species such as *C. oblongifolius,* (Roengsumran *et al*., 1999; Roengsumran *et al*., 2001; Roengsumran *et al*., 2002; Sommit *et al*., 2003; Pudhom *et al*., 2007; Pudhom and Sommit *et al*., 2011), *C. cajucara* (Grynberg *et al*., 1999) and *C. argyrophylloides* (Santos *et al*., 2009), were assessed in several cancer cells. These results revealed that the bioactive diterpenes showed non-specific to type of cancer. Besides anti-cancer activity, many compounds exhibited high potent (2-10 μg/ml). However, the mode of action of their active compounds has less information. The mechanism of clerodane type diterpenes from previously reports are as following; clerodermic acid induced potent apoptosis against human leukemia HL60 cells (Efdi *et al*., 2007). Two compounds, which obtained from *C. cajacara* including *trans*-dehydrocrotonin (DCTN) and *trans*-crotonin (CTN), were established on anti-tumor activity against two murine tumors sarcoma 180 (S180) and Ehrlich ascites carcinoma (Grynberg *et al*., 1999). The anti-proliferative results of two compounds showed a significant on cytotoxicity with IC_{50} values of 166 μM (52.2 μg/ml) for DCTN and 164 μM (51.8 μg/ml) for CTN in Enrlich carcinoma cell line. Proliferation of cultured enrlich cells and TNF-α activity was investigated *In vivo* study, the 80 and 120 mg/kg of trans-dehydrocrotonin were treated on survival of mice bearing Sarcoma 180 and Ehrlich carcinoma ascitic tumors. During study, the cytotoxicity

was observed with 16 μM of trans-dehydrocrotonin and trans-crotonin, but no induction of apoptosis was observed by DNA fragmentation of nuclear DNA using gel electrophoresis after treatments. Following TNF-α activity, the trans-dehydrocrotonin significantly induced TNF-α level more than control treatment. These results concluded that the trans-dehydrocrotonin showed cytotoxic effect and also induced TNF-α, resulting to enhance immune function as well as other diterpenes such as paclitaxel, which enhance TNF-α production (Grymberg *et al*., 1999). The diosbulbin D from *Dioscorea bulbifera*, a furano norclerodane diterpene, has been studied on hepatotoxic activity of normal human liver L-02 cells. The effect on growth inhibition of this compound might be due to apoptosis induction (Ma *et al*., 2012). Additionally, plaunol A was also evaluated anti-inflammatory activity. The inhibitory effect of plaunol on NO production in RAW 264.7 cells was determined by Griess assay. The NO results indicated plaunol A showed strong activity with an IC_{50} 11.69 μM. According to qRT-PCR study results, the plaunol A also inhibited *iNOS* and *COX-2* mRNA expression. This result corresponds from our previous report on plaunotol, plaunol E and plaunol F (Premprasert *et al*., 2013). Herein, cyclic diterpenes isolated from *C. stellatopilosus* exhibited anti-inflammatory activity via *iNOS* and *COX-2* suppression.

To increasing value of *C. stellatopilosus*, we successfully demonstrated the anti-proliferative effect of diterpenes including plaunotol (as cyclic diterpenes), plaunol A, plaunol E and plaunol F (as cyclic diterpenes) isolated from *C. stellatopilosus* leaves and stems and these compounds were assessed on HeLa, HT-29, MCF-7 and KB cancer cell lines. Interestingly, anti-proliferative and apoptotic activities as well as cell cycle effect of plaunol A and plaunol E is reported for the first time. In the present study, our work highlights the mode of action of diterpenes on cell cycle progression and apoptosis.

Our finding the plaunol E on apoptotic related genes might be supported the chemopreventive potency of *C. stellatopilosus* as an alternative medicine.

CHAPTER 5

CONCLUSIONS

According to this research work in a title of anti-inflammatory and anti-proliferative constituents of diterpenes from *Croton stellatopilosus* Ohba; the following conclusions can be drawn:

(1) The phytochemical study in *Croton stellatopilosus* Ohba (Plau-noi) has been investigated, total of nine compounds including four diterpenes; plaunotol (1), plaunol A (2), plaunol E (3) and plaunol F (4), three flavonoids; apigenin-8-C-β-D-glucoside (5), luteolin-7-O-β-D-glucoside (6), luteolin-4′-O-β-D-glucoside (7), and two phytosterols; mixture of β-sitosterol and stigmasterol (8), β-sitosterol-D-glycoside (9), were obtained.

(2) Plaunol A showed the inhibitory effect on NO production in RAW264.7 cell by inhibiting the key enzymes in the inflammatory pathway.

(3) Plaunotol, plaunol A and plaunol E, but not plaunol F showed moderate activity against four cancer cells (HeLa, HT-29, MCF-7 and KB). These compounds have no toxic to the normal cells (HGF).

(4) Plaunol A induced the cell cycle arrest at S-phase (MCF-7) and G2/M phase (HeLa, HT-29, and KB). The plaunol E induced cell cycle arrest at G2/M in every cancer cells. The results indicated that these diterpenes induced the cell cycle arrest in the difference phase.

(5) Plaunotol, plaunol A and plaunol E induced apoptosis.

(6) The anti-proliferative effect of plaunotol and plaunol E could be caused by apoptosis through death receptor/NF-κB and mitochondrial dependent apoptotic pathways.

REFERENCES

Abbas, A.K., Lichtman, A.H. and Pober, J.S. 1997. Cytokines. Abbas, A.K., Lichtman, A.H. and Pober, J.S. (eds). *Cellular and molecular immunology*. (3rd ed.) Philadelphia, Saunders.

Abou-El-Wafa, G.S.E., Shaaban, M., Shaaban, K.A., El-Naggar, M.E.E., Maier, A., Fiebig, H.H. and Laatsch, H. 2013. Pachydictyols B and C: new diterpenes from *Dictyota dichotoma* Hudson. *Mar Drugs*. 11(9), 3109-3123.

Alberts, B., Johnson, A., Lewis, J., Raff, M., Roberts, K. and Walter, P. 2002. Chapter 10; Membrane proteins: Membrane structure. Alberts, B., Johnson, A., Lewis, J., Raff, M., Roberts, K. and Walter, P. (eds). *Molecular Biology of the Cell*. (4th ed), New York, Gerland Science.

Alcaraz, M., Achel, D.G., Olivares, A., Olmos, E., Alcaraz-Saura, M. and Castillo, J. 2013. Carnosol, radiation and melanoma: a translational possibility. *Clin Transl Oncol*. 15(9), 712-719.

Alenzi, F.Q.B. 2005. Links between apoptosis, proliferation and cell cycle. *Br J Biomed Sci*. 61(2), 99-102.

Al-Lihaibi, S.S., Alarif, W.M., Abdel-Lateff, A., Ayyad, SE.N., Abdel-Naim, A.B., El-Senduny, F.F. and Badria, F.A. 2014. Three new cembranoid-type diterpenes from Red Sea soft coral *Sarcophyton glaucum*: isolation and antiproliferative activity against HepG2 cells. *Eur J Med Chem*. 81, 314–322.

Almagro, M.C. and Vucic, D. 2012. The inhibitor of apoptosis (IAP) proteins are crucial regulators of signaling pathways and targets for anti-cancer therapy. *Exp Oncol*. 34(3), 200-211.

American Cancer Society. 2017. Cancer Facts & Figure. 2017. *Atlanta: American Cancer Society*.1-76.

Anh, H.L.T., Hien, N.T.T, Hang, D.T.T., Ha, T.M., Nhiem, N.X., Hien, T.T.T., Thu, V.K., Thao, D.T., Minh, C.V. and Kiem, P.V. 2014. *Ent*-Kaurane diterpenes from *Annona glabra* and their cytotoxic activities. *Nat Prod Commun*. 9(12), 1681-1682.

Ashkenazi, A. and Dixit, V.M. 1998. Death receptors: signaling and modulation. *Science.*281, 1305–1308.

Athikomkulchai, S., Prawat, H., Thasana, N., Ruangrungsi, N. and Ruchirawat, S. 2006. COX-1, COX-2 inhibitors and antifungal agents from *Croton hutchinsonianus*. *Chem Pharm Bull (Tokyo)*.54(2), 262-264.

Athikomkulchai. S., Tadtong, S., Ruangrungsi, N. and Hongratanaworakit, T. 2015. Chemical Composition of the essential oil from *Croton oblongifolius* and its antibacterial activity against *Propionibacterium acnes*. *Nat Prod Commun*. 10(8), 1459-1460.

Aviello, G., Borrelli, F., Guida, F., Romano, B., Lewellyn, K., Chiaro, M.D., Luongo, L., Zjawiony, J.K., Maione, S., Izzo, A.A. and Capasso, R. 2011. Ultrapotent effects of salvinorin A, a hallucinogenic compound from *Salvia divinorum*, on LPS-stimulated murine macrophages and its anti-inflammatory action *in vivo*. *J Mol Med*. 89, 891-902.

Baeuerle, PA. and Henkel, T. 1994. Function and activation of NF-kappa B in the immune system. *Annu Rev Immunol*. 12, 141-179.

Balkwill, F. 2009. Tumour necrosis factor and cancer. *Nat Rev Cancer*. 9, 361-371.

Barnum, K.J. and O'Connell, M.J. 2014. Cell Cycle Regulation by Checkpoints. *Methods Mol Biol*. 1170, 29-40.

Bar-Shavit, R., Maoz, M., Kancharla, A., Nag, J.K., Agranovich, D., Grisaru-Granovsky, S. and Uziely, B. 2016. G protein-coupled receptors in cancer. *Int J Mol Sci*. 17(8), 1320.

Bateman, A. and Carr, N. 2009. Cell death. Bateman, A. and Carr, N (eds). *Fresh and bone parthology*. Ediburgh, MOSBY Elsevier.

Bautista, E., Fragoso-Serrano, M., Ortiz-Pastrana, N., Toscano, RA. and Ortega, A. 2016. Structural elucidation and evaluation of multidrug-resistance modulatory capability of amarissinins A–C, diterpenes derived from *Salvia amarissima*. *Fitoterapia*. 114, 1-6.

Baychelier, F. and Vieillard, V. 2013. The Modulation of the Cell-Cycle: A Sentinel to Alert the NK Cells of Dangers. *Front Immuno*. 4, 235.

Benrezzouk, R., Terencio, M.C., Ferrándiz, M.L., San Feliciano, A., Gordaliza, M., Miguel del Corral, J.M., de la Puente, M.L., and Alcaraz, M.J. 1999. Inhibition of human $sPLA_2$ and 5-lipoxygenase activities by two *neo*-clerodane ditepenoids. *Life Sci*. 64 (19), 205-211.

Berg, J.M., Tymoczko, J.L. and Stryer, L. 2002. Chapter 15; Signal-transduction pathways: An introduction to information metabolism. Berg, J.M., Tymoczko, J.L. and Stryer, L. (eds). *Biochemistry*. (5^{th} ed.), New York, W H Freeman.

Bertoli, C., Skotheim, J.M. and Bruin, R.A.M. 2013. Control of cell cycle transcription during G1 and S phases. *Nat Rev Mol Cell Biol*. 14(8), 518-528.

Bhattacharyya, S., Dedeja, P.K. and Tobacman, J.K. 2010. Tumor necrosis factor alpha-induced inflammation is increased but apoptosis is inhibited by common food additive carrageenan. *J Biol Chem*. 285(50), 39511-39522.

Bhavana, J., Kalaivani, M.K. and Sumathy, A. 2016. Cytotoxic and pro-apoptotic activities of leaf extract of *Croton bonplandianus* Baill. against lung cancer cell line A549. *Indian J Exp Biol*. 54(6), 379-85.

Boonyarathanakornkit, L., Che, C., Fong, H.H.S. and Farnsworth, N.R. 1988. Constituents of *Croton crassifolius* Roots. *Planta Med*. 54(1), 61-63.

Bratton, D.L., Fadok, V.A., Richter, D.A., Kailey, J.M., Guthrie, L.A. and Henson, P.M. 1997. Appearance of phosphatidylserine on apoptotic cells requires calcium-mediated nonspecific flip-flop and is enhanced by loss of the aminophospholipid translocase. *J Biol Chem,* 272, 26159-26165.

Breitmaier, E. 2006. Diterpenes. Breitmaier, E (eds). *Terpenes: flavors, fragrances, pharmaca, pheromones*. Weinheim, Wiley-Vch verlag GmbH & Co. KGaA.

Brincks, E.L., Kucaba, T.A., James, B.R., Murphy, K.A., Schwertfeger, K.L., Sangwan, V., Banerjee, S., Saiuja, A.K. and Griffith, T.S. 2015. Triptolide enhances the tumoricidal activity of TRAIL against renal cell carcinoma. *FEBS J*. 282(24), 4747-4765.

Bunyapraphatsara, N. 1989. Plau-noi. *Med Plant Inform Cent Mahidol Univ*. 6, 1-6.

Castrillo, A. de Las Heras, B., Hortelano, S., Rodriguez, B., Villar, A. and Bosca, L. 2001. Inhibition of the nuclear factor kappa B (NF-kappa B) pathway by tetracyclic kaurane diterpenes in macrophage. Specific effects on NF-kappa B-inducting kinase activity and on the cooridinate activation of ERK and P38 MAPK. *J Biol Chem*. 276(19), 15854-15860.

Chang, CC., Kuan, CP., Lin, JY., Lai, JS. and Ho, TF. 2015. Tanshinone IIA facilitates TRAIL sensitization by up-regulating DR5 through the ROS-JNK-CHOP signaling axis in human ovarian carcinoma cell lines. *Chem Res Toxicol*. 28(8), 1574-1583.

Chang, FR., Huang, ST., Liaw, CC., Yen, MH., Hwang, TL., Chen, CY., Hou, MF., Yuan, SS., Cheng, YB. and Wu, YC. 2016. Diterpenes from *Grangea maderaspatana*. *Phytochemistry*. 131, 124-129.

Chang, FY., Hsu, FJ., Tai, CJ., Wei, WC., Yang, NS., Sheu, JH. 2014. Klymollins T-X, bioactive eunicellin-based diterpenoids from the soft coral *Klyxum molle*. *Mar Drugs*. 12(5), 3060-3071.

Chang, H.L., Chang, F.R., Chen, J.S., Wang, H.P., Wu, Y.H., Wang, C.C., Wu, Y.C. and Hwang, T.L. 2008. Inhibitory effects of 16-hydroxycleroda-3,13(14)E-dien-15-oic acid on superoxide anion and elastase release in human neutrophils through multiple mechanisms. *Eur J Pharmacol*. 586(1-3), 332-339.

Chao, D.L., Sanchez, C.A., Galipeau, P.C., Blount, P.L., Paulson, T.G., Cowan, D.S., Ayub, K., Odze, R.D., Rabinovitch, P.S. and Reid, B.J. 2008. Cell proliferation, cell cycle abnormalities, and cancer outcome in patients with Barrett's esophagus: a long-term prospective study. *Clin Cancer Res*. 14(21), 6988-6995

Chao, TH., Lam, T., Vong, BG., Través, PG., Hortelano, S., Chowdhury, C., Bahjat, FR., Lloyd, GK., Moldawer, LL., Palladino, MA. And Theodorakis, EA. 2005. A new family of synthetic diterpenes that regulates cytokine synthesis by inhibiting IkappaB alpha phosphorylation. *Chembiochem*. 6(1), 133-144.

Chaotham C., Chivapat, S., Chaikitwattana, A. and De-Eknamkul, W. 2013. Acute and chronic oral toxicity of a partially purified plaunotol extract from *Croton stellatopilosus* Ohba. *Biomed Res Inter.* 1-12.

Chen, M. and Wang, J. 2002. Initiator caspases in apoptosis signaling pathways. *Apoptosis*. 7(4), 313-319.

Chen, SR., Qiu, HC., Hu, Y., Wang, Y. and Wang, YT. 2016. Herbal medicine offered as an initiative therapeutic option for the management of hepatocellular carcinoma. *Phytother Res*. 30(6), 863-877.

Chen, TH., Chen, WF., Wen, ZH., Lu, MC., Wang, WH., Li, JJ., Wu, YC. And Sung, PJ. 2014. Cladieunicellins M-Q, new eunicellins from *Cladiella* sp. *Mar Drugs*. 12(4), 2144-2155.

Chen, WT., Li, Y. and Guo YW. 2012. Terpenoids of Sinularia soft corals chemistry and bioactivity. *Acta Pharm Sin B*. 2(3), 227-237.

Chen, Y., Wang, C., Hu, M., Pan, J., Chen, J., Duan, P., Zhai, T., Ding, J. and Xu, C. 2012. Effects of ginkgolide A on okadaic acid-induced tau hyperphosphorylation and the PI3K-Akt signaling pathway in N2a cells. *Planta Med*. 78(12), 1337-1341.

Chen, YY., Yang, KX., Yang, XW., Khan, A., Liu, L., Wang, B., Zhao, YL., Liu, YP., Li, Y. and Luo, XD. 2016. New cytotoxic tigliane diterpenoids from *Croton caudatus*. *Planta Med*. 82(8), 729-733.

Cheng, ZB., Liao, Q., Chen, Y., Fan, CQ., Huang, ZY., Xu, XJ. and Yin, S. 2014. Four new cembranoids from the soft coral *Sarcophyton* sp. *Magn Reson Chem*. 52(9), 515-520.

Cho, JG., Cha, BJ., Min, Lee S., Shrestha, S., Jeong, RH., Sung Lee, D., Kim, YC., Lee, DG., Kang, HC., Kim, J., Baek, NI. 2015. Diterpenes from the roots of *Oryza sativa* L. and their inhibition activity on NO production in LPS-stimulated RAW264.7 macrophages. *Chem Biodivers*. 12(9), 1356-1364.

Choi, Y., Moon, A. and Kim, YC. 2008. A pinusolide derivative, 15-methoxypinusolidic acid from Biota orientalis inhibits inducible nitric oxide synthase in microglial cells: implication for a potential anti-inflammatory effect. *Int Immunopharmacol.* 8(4), 548-555.

Christian, F., Smith, E. and Carmody, R. 2016. The regulation of NF-κB subunits by phosphorylation. *Cell*. 5(1), 12.

Cimmino, A., Mathieu, V., Masi, M., Baroncelli, R., Boari, A., Pescitelli, G., Ferderin, M., Lisy, R., Evidente, M., Tuzi, A., Zonno, MC., Kornieko, A., Kiss, R. and Evdente, A. 2016. Higginsianins A and B, two diterpenoid α-pyrones produced by *Colletotrichum higginsianum*, with in vitro cytostatic activity. *J Nat Prod*. 79(1), 116-125.

Coffman, J.A. 2004. Cell cycle development. *Dev Cell*. 6(3), 321-327.

Colotta, F., Allavena, P., Sica, A., Garlanda, C., Mantovani. 2009. Cancer-related inflammation, the seventh hallmark of cancer: links to genetic instability. *Carcinogenesis*. 30(7), 1073-1081.

Cooper, G.M. 2000. The development and causes of cancer. Cooper, G.M. (eds). *The cell: A molecular approach* (2nd ed). Sunderland (MA): Sinauer Associates.

Corea, G., Fattorusso, E., Lanzotti, V., Di Meglio, P., Maffia, P., Grassia, G., Ialenti, A. and Ianaro, A. 2005. Discovery and biological evaluation of the novel naturally occurring diterpene pepluanone as anti-inflammatory agent. *J Med Chem*. 48(22), 7055-7062.

Cory, S. and Adam, J.M. 2002. The Bcl2 family: regulators of the cellular life-or-death switch. *Nat Rev Cancer*. 2(9), 647-656.

Cuong, L.C.V., Trang, D.T., Cuc, N.T., Nhiem, N.X., Yen, P.H., Anh, H.L.T., Huong, L.M., Minh, C.V. and Kiem, P.V. 2015. Flavonoid glycosides from *Antidesma ghaesembilla*. *Vietnam Journal of Chemistry*. 53(2e), 94-97.

Dai, LP., Li, C., Yang, HZ., Lu, Y.Q., Yu, HY., Gao, HM. and Wang, ZM. 2015. Three new cytotoxic ent-kaurane diterpenes from *Isodon excisoides*. *Molecules*. 20(9), 17544-17556.

Dai, SJ., Zhang, L., Xiao, K. and Han, QT. 2016. New cytotoxic neoclerodane diterpenoids from *Scutellaria strigillosa*. *Bioorg Med Chem Lett*. 26(7), 1750-1753.

de las Heras, B. and Hortelano, S. 2009. Molecular basis of the anti-inflammatory effects of terpenoids. *Inflamm Allergy Drug Targets.* 8(1), 28-39.

de las Heras, B., Navarro, A., Díaz-Guerra, MJ., Bermejo, P., Castrillo, A., Boscá, L. and Villar, A. 1999. Inhibition of NOS-2 expression in macrophages through the inactivation of NF-kappaB by andalusol. *Br J Pharmcol*. 128(3), 605-612.

de Quesada, T., Rodríguez, T. and Valverde, S. 1972. Six new diterpenes from *Sideritis leucantha* Cav. and *Sideritis linearifolia* Lam. *Tetrahedron Lett*. 22, 2187-2190.

Dey, S., Mukherjee, D., Chakraborty, S., Mallick, S., Dutta, A., Ghosh, J., Swapana, N., Maiti, S., Ghorai, N, Singh, C.B. and Pal, C. 2015. Protective effect of *Croton caudatus* Geisel leaf extract against experimental visceral leishmaniasis induces proinflammatory cytokines in vitro and in vivo. *Exp Parasitol*. 151-152, 84-95.

Discovery and biological evaluation of the novel naturally occurring diterpene pepluanone as anti-inflammatory agent

Du, J., Chen, C., Sun, Y., Zheng, L. and Wang, W. 2015. Ponicidin suppresses HT29 cell growth via the induction of G1 cell cycle arrest and apoptosis. *Mol Med Rep*. 12(4), 5816-5820.

Duque, G.A. and Descoteaux, A. 2014. Macrophage cytokines: involvement in immunity and infectious diseases. *Front Immunol*, 5,491.

Duronio, R.J. and Xiong, Y. 2013. Signaling pathways that control cell proliferation. *Cold Spring Harb Perspect Biol*. 5 (3), a008904.

Eagle, H. 1955. Propagation in fluid medium of a human epidermoid carcinoma, strain KB. *Proc Soc Exp Biol Med.* 89, 362-364.

Eaton, A.L., Harinantenaina, L., Brodie, P.J., Cassera, M.B., Bowman, J.D., Callmander, M.W., Randrianaivo, R., Rakotondrajaona, R., Rakotobe, E., Rasamison, V.E. and Kingston, D.G.I. 2013. A new bioactive diterpene glycoside from *Molinaea retusa* from the Madagascar dry forest. *Nat Prod Commun*. 8(9), 1201-1203.

Efdi, M. Itoh, T., Akao, Y., Nozawa, Y., Koketsu, M., Ishihara, H. 2007. The isolation of secondary metabolites and in vitro potent anti-cancer activity of clerodermic acid from *Enicosanthum membranifolium*. *Bioorg Med Chem*. 15, 3667-3671.

El-Mekkawy, S., Meselhy, M.R., Nakamura, N., Hattori, M., Kawahata, T. and Otake, T. 1999. 12-O-acetylphorbol-13-decanoate potently inhibits cytopathic effects of human immunodeficiency virus type 1 (HIV-1), without activation of protein kinase C. *Chem Pharm Bull (Tokyo)*. 47(9), 1346-1347.

El-Mekkawy, S., Meselhy, M.R., Nakamura, N., Hattori, M., Kawahata, T. and Otake, T. 2000. Anti-HIV-1 phorbol esters from the seeds of *Croton tiglium*. *Phytochemistry*. 53(4), 457-464.

Elmore, S. 2007. Apoptosis: a review of programmed cell death. *Toxicol Pathol*. 35(4), 495-516.

Erharuyi O, Adhikari A, Falodun A, Jabeen, A., Imad, R., Ammad, M., Choudhary, M.I. and Goren, N. 2016. Cytotoxic, anti-inflammatory, and leishmanicidal activities of diterpenes isolated from the roots of *Caesalpinia pulcherrima*. *Planta Med*. 83(1-02), 104-110.

Esser, H. J., and Chayamarit, K. 2001. Two new species and a new name in Thai *Croton* (Euphorbiaceae). *Thai For Bull*. 29, 51-57.

Falodun, A., Kragl, U., Touem, S.M., Villinger, A., Fahrenwaldt, T. and Langer, P. 2012. A novel anticancer diterpenoid from *Jatropha gossypifolia*. *Nat Prod Commun*. 7(2), 151-152.

Fernandez-Medarde, A. and Santos, E. 2011. Ras in cancer and developmental diseases. *Genes Cancer*. 2(3), 344-358.

Fu, H., Yabe, Y., Asahi, K., Hayashi, Y., Murata, H., Eguchi, H., Tsujii, M., Tsuji, S. and Kawano, S. 2005. (2*E,*6*Z,*10*E*)-7-hydroxymethyl-3,11,15-trimethyl-2,6,10,14-hexadecatetraen-1-ol (Plaunotol) increases cyclooxygenase-2 expression via nuclear factor *kappa B* and cyclic AMP response element in rat gastric epithelial cells. *Eur J Pharmacol*. 7, 524(1-3), 38-43.

Fuentes, J.C., Castro, V., Jakupovic, J. and Murillo, R. 2004. Diterpenes and other components of *Croton hirtus* (Euphorbiaceae). *Rev Biol Trop*. 52(1), 269-285.

Fuentes, R.G, Toume, K., Arai, M.A., Sadhu, S.K., Ahmed, F., Ishibashi, M. 2015. Scopadulciol, isolated from Scoparia dulcis, induces β-catenin degradation and overcomes tumor necrosis factorrelated apoptosis ligand resistance in AGS human gastric adenocarcinoma cells. *J Nat Prod*. 78(4), 864-872.

Gao, Q., Liu, H., Yao, Y., Geng, L., Zhang, X., Jiang, L., Shi, B. and Yang, F. 2015. Carnosic acid induces autophagic cell death through inhibition of the Akt/mTOR pathway in human hepatoma cells. *J Appl Toxicol*. 35(5), 485-492.

Gao, SS., Li, XM., Williams, K., Proksch, P., Ji, NY. and Wang, BG. 2016. Rhizovarins A–F, indole-diterpenes from the mangrove-derived endophytic fungus *Mucor irregularis* QEN-189. *J Nat Prod*. 79(8), 2066-2074.

Garcia, P.A., Oliveira, A.B. and Batista, R. 2017. Occurrence, biological activities and synthesis of kaurane diterpenes and their glycosides. *Molecules*. 12, 455-483.

Gehringer, M. 2010. Signal transduction: Regulation of cell growth. Kirby, R., Downing, T.G. and Gohary, M.E. (eds.). *Fundamentals of biochemistry, cell biology and biophysics*. (volume II). United Kindom, Encyclopedia of Life Support Systems (EOLSS).

Gey G.O. Coffman, W.D. and Kubicek, M.T. 1952. Tissue culture studies of the proliferative capacity of cervical carcinosarcoma and normal epithelium. *Cancer Res*. 12, 264-265.

Ghanadian, M., Saeidi, H., Aghaei, M., Rahiminejad, M.R., Ahmadi, E., Ayatollahi, S.M., Choudhary, M.I. and Bahmani, B. 2015. New jatrophane diterpenes from *Euphorbia osyridea* with proapoptotic effects on ovarian cancer cells. *Phytochem Lett*. 12, 302-307.

Giang, PM., Jin, HZ., Son, PT., Lee, JH., Hong, YS. And Lee, JJ. 2003. *ent*-Kaurane diterpenoids from *Croton tonkinensis* inhibit LPS-induced NF-kappaB activation and NO production. *J Nat Prod*. 66(9), 1217-1220.

Girón, N., Través, PG., Rodríguez, B., López-Fontal, R., Boscá, L. Hortelano, S. and De las Heras, B. 2008. Suppression of inflammatory responses by labdane-type diterpenoids. *Toxical Appl Pharmacol.* 228(2), 179-189.

Gohari, A.R., Ebrahimi, H., Saeidnia, S., Foruzani, M., Ebrahimi, P. and Ajani, Y. 2011. Flavones and flavone glycosides from *Salvia macrosiphon* Boiss. *Iran J Pharm Res*. 10(2), 247-251.

Grynberg, N.F., Echevarria, A., Lima, J.E., Pamplona, S.S., Pinto, A.C. and Maciel, M.A. 1999. Anti-tumour activity of two 19-nor-clerodane diterpenes, *trans*-dehydrocrotonin and trans-crotonin, from *Croton cajucara*. *Planta Med*. 65(8), 687-689.

Gu, Z., Wang, X., Qi, R., Wei, L., Huo, Y., Ma, Y., Shi, L., Chang, Y., Li, G. and Zhou, L. 2015. Oridonin induces apoptosis in uveal melanoma cells by up regulation of Bim and down regulation of fatty acid synthase. *Biochem Biophys Res Commun*. 457(2), 187-193.

Guo, P., Li, Y., Jin, D-Q., Xu, J., He, Y., Zhang, L., Guo, Y. 2012. *neo*-Clerodane diterpenes from *Ajuga ciliata* and their inhibitory activities on LPS-induced NO production. *Phytochem. Lett*. 5, 563-566.

Gupta, M., Mazumder, U.K., Vamsi, M.L., Sivakumar, T. and Kandar, C.C. 2004. Anti-steroidogenic activity of the two Indian medicinal plants in mice. *J Ethnopharmacol*. 90(1):21-25.

Hacker, G. 2000. The morphology of apoptosis. *Cell Tissue Res*. 301(1), 5-17.

Han, Y., Di, XX., Li, HZ, Shen, T., Ren, DM., Lou, HX. and Wang, XN. 2014. Podoimbricatin A, a cytotoxic diterpenoid with an unprecedented 6/6/5/6-fused tetracyclic ring system from the twigs and leaves of *Podocarpus imbricatus*. *Bioorg Med Chem Lett*. 24(15), 3326–3328.

Hanna, A. and Shevde, L.A. 2016. Hedgehog signaling: modulation of cancer properties and tumor microenvironment. *Mol Cancer*. 15-24.

Harborne, J.B., Baxter, H. and Moss, G.P. 1999. Chapter 52 Diterpenoids. Harborne, J.B., Baxter, H. and Moss, G.P (eds). *Phytochemical Dictionary: A Handbook of Bioactive compounds from plants*. (2nd ed). London, Taylor & Francis Ltd.

Hardin, J. and Bertoni, G. 2015. The cell cycle and mitosis. Hardin, J. and Bertoni, G. (eds). Becker's World of the Cell. (9th ed). London, Pearson education.

Harinantenaina, L., Takahara, Y., Nishizawa, T., Kohchi, C., Soma, G-I. and Asakawa, Y. 2006. Chemical constituents of malagasy liverworts, part V: prenyl bibenzyls and clerodane diterpenoids with nitric oxide inhibitory activity from *Radula appressa* and *Thysananthus spathulistipus*. *Chem Pharm Bull*. 54(7), 1046–1049.

Hatai, H., Lepelley, A., Zeng, W., Hayden, M.S. and Ghosh, S. 2016. Toll-like receptor 11 (TLR11) interacts with flagellin and profilin through disparate mechanisms. *Plos one*. 11(2), e0148987.

Hayden, M.S. and Ghosh, S. 2008. Shared principles in NF-kappaB signaling. *Cell*. 132, 344-362.

He, L., Han, J., Li, B., Huang, L., Ma, K., Chen, Q., Liu, X., Bao, L. and Liu, H. 2016. Identification of a new cyathane diterpene that induces mitochondrial and autophagy dependent apoptosis and shows a potent in vivo anticolorectal cancer activity. *Eur J Med Chem*. 111, 183-192.

Hengartner, M.O. 2000. The biochemistry of apoptosis. *Nature*. 407, 770-776

Hill, M.M., Adrain, C., Duriez, P.J., Creagh, E.M., Martin, S.J. 2004. Analysis of the composition, assembly kinetics and activity of native Apaf-1 apoptosomes. *Embo J*. 23, 2134-2145.

Hoesel, B. and Schmid, J.A. 2013. The complexity of NF-κB signaling in inflammation and cancer. *Mol Cancer*. 12, 86.

Horgen, F.D., Edrada, R.A., de los Reyes, G., Agcaoili, F., Madulid, D.A., Wongpanich, V., Angerhofer, C.K., Pezzuto, J.M., Soejarto, D.D. and Farnsworth, N.R. 2001. Biological screening of rain forest plot trees from Palawan Island (Philippines). *Phytomedicine*, 8(1), 71-81.

Hosid, S. and Ioshikhes, I. 2014. Apoptotic Lymphocytes of *H. sapiens* Lose Nucleosomes in GC-Rich Promoters. *PLOS Comput Biol*.10(7), e1003760

Hou, P., Zeng, Y., Ma, B., Bi, K. and Chen, X. 2013. A new cytotoxic cembrane diterpene from the roots of *Euphorbia pekinensis* Rupr. *Fitoterapia*. 90, 10-13.

Hu, T., Wang, L., Zhang, L., Lu, L., Shen, J., Chan, R.L., Li, M., Wu, W.K., To, K.K. and Cho, C.H. 2015. Sensitivity of apoptosis resistant colon cancer cells to tanshinones is mediated by autophagic cell death and p53-independent cytotoxicity. *Phytomedicine*. 22(5), 536-544.

Hu, Y., Zhang, L., Wen, XQ., Zeng, XJ., Rui, W. and Cen, YZ. 2012. Two new diterpenoids from *Croton crassifolius*. *J Asian Nat Prod Res*. 14(8), 785-7888.

Huang, SC., Ho, CT., Lin-Shiau, SY. and Lin, JK. 2005. Carnosol inhibits the invasion of B16/F10 mouse melanoma cells by suppressing metalloproteinase-9 through down-regulating nuclear factor-kappa B and c-Jun. *Biochem Pharmacol*. 69(2), 221-232.

Huang, W., Wang, J., Liang, Y., Ge, W., Wang, G., Li, Y. and Chung, H.Y. 2015. Potent anti-angiogenic component in Croton crassifolius and its mechanism of action. *J Ethnopharmacol*. 175, 185-191.

Huang, W., Wang, J., Liang, Y., Li,Y., Wang, G. 2016. Pyran-2-one derivatives from the roots of *Croton crassifolius*. *Nat Prod Commun*. 11(6), 803-804.

Hwang, BY., Lee, JH., Koo, TH., Kim, HS., Hong, YS., Ro, JS., Lee, KS. And Lee, JJ. 2001. Kaurane diterpenes from *Isodon japonicas* inhibit nitric oxide and prostaglandin E2 production and NF-kappaB activation in LPS stimulated macrophage RAW264.7 cells. *Planta Med*. 67(5), 406-410.

Ikushima, H., Negishi, H. and Taniguchi, T. 2013. The IRF family transcription factors at the interface of innate and adaptive immune responses. *Cold Spring Harb Symp Quant Biol*.78, 105–116.

Imsamran, W., Chaiwarawattana, A., Wiangnon, S. and Pongnikorn, D (eds). 2015. *Cancer in Thailand* (Vol VIII, 2010-2012). National Cancer Institute, Thailand.

Islam, M.T. 2017. Diterpenes and their derivatives as potential anticancer agents. *Phytother Res*. 31(5), 691-712.

Iwannaszko, M. and Kimmel, M. 2015. NF-κB and IRF pathways: cross-regulation on target genes promoter level. *BMC Genomics*. 16(1), 307.

Jadranin, M., Pesic, M., Aliancic, I.S., Milosavijevic, S.M., Todorovic, N.M., Podolski-Renic, A., Bankovic, J., Tanic, N., Markovic, I. and Vajs, V. 2013. Jatrophane diterpenoids from the latex of *Euphorbia dendroides* and their anti-P-glycoprotein activity in human multi-drug resistant cancer cell lines. *Phytochemistry*. 86, 208-217.

Janar, J., Nugroho, A.E., Wong, C.P., Hirrasawa, Y., Kaneda, T., Shiroto, O. and Morita, H. 2012. Sabiperones A–F, new diterpenoids from *Juniperus sabina*. *Chem Pharm Bull(Tokyo).* 60(1), 154-159.

Janeway, C.A., Travers, J.R., Walport, M. and Shlomchik, M. 2001. Principles of innate and adaptive immunity. Janeway, C.A., Travers, J.R., Walport, M. and Shlomchik, M. (eds). *Immunobiology*. (5th ed). New York, Garland Science.

Janssens, S. and Beyaert, R. 2003. Role of Tool-like receptors in pathogen recognition. *Clin Microbiol Rev*. 16(4), 637-646.

Ji, L., Zheng, Z., Shi, L., Huang, Y., Lu, B. and Wang, Z. 2015. Andrographolide decreased VEGFD expression in hepatoma cancer cells by inducing ubiquitin/proteasome-mediated cFos protein degradation. *Biochim Biophys Acta*. 1850(4), 750-758.

Jiang, H., Zhao, L., Dong, X., He, A., Zheng, C., Johansson, M., Karlsson, A. and Zheng X. 2015. Tanshinone IIA enhances bystander cell killing of cancer cells expressing *Drosophila melanogaster* deoxyribonucleoside kinase in nuclei and mitochondria. *Oncol Rep*. 34(3), 1487-1493.

Jiang, L., Zhang, YB., Jiang, SQ., Zhou, YD., Luo, D., Niu, QW., Qian, YR., Li, YL. and Wang, GC. 2017. Phorbol ester-type diterpenoids from the twigs and leaves of *Croton tiglium*. *J Asian Nat Prod Res*. 4, 1-7.

Jiao, W., Wan, Z., Chen, S., Lu, R., Chen, X., Fang, D., Wang, J., Pu, S., Huang, X., Gao, H. and Shoa, H. 2015. Lathyrol diterpenes as modulators of P-glycoprotein dependent multidrug resistance structure-activity relationship studies on Euphorbia factor L3 derivatives. *J Med Chem*. 58(9), 3720-3738.

Joshi, R.K. 2014. Chemical composition of the essential oil of *Croton bonplandianus* from India. *Nat Prod Commun*. 9(2), 269-70.

Kang, HS., Kim, YH., Lee, CS., Lee, JJ., Choi, I. and Pyun, KH. 1996. Suppression of interleukin-1 and tumor necrosis factor-alpha production by acanthoic acid,(-)-pimara-9(11),15-dien-19-oic acid, and it antifibrotic effects in vivo. *Cell Immunol*. 170(2), 212-221.

Kang, N., Cao, SJ., Zhou, Y., He, H., Tashiro, SI., Onodera, S., Qiu, F. and Ikejima, T. 2015. Inhibition of caspase-9 by oridonin, a diterpenoid isolated from *Rabdosia rubescens*, augments apoptosis in human laryngeal cancer cells. *Int J Onco*l. 47(6), 2045-2056.

Kawai, K., Tsuno, N.H., Kitayama, J., Yazawa, K., AsakageM., Yamashita, H., Watanabe, T., Takahashi, K. and Nagawa, H. 2005. Anti-angigenic properties of plaunotol. *Anticancer Drugs*. 16(4), 401-407.

Kawai, K., Tsuno, N.H., Kitayama, J., Yazawa, K., AsakageM., Yamashita, H., Watanabe, T., Takahashi, K. and Nagawa, H. 2005. Anti-angigenic properties of plaunotol. *Anticancer Drugs* 16(4), 401-407.

Kawakami, S., Inagaki, M., Matsunami, K., Otsuka, H., Kawahata, M. and Yamaguchi, K. 2016. Crotofolane-type diterpenoids, crotocascarins L-Q, and a rearranged crotofolane-type diterpenoid, neocrotocascarin, from the stems of *Croton cascarilloides*. *Chem Pharm Bull (Tokyo)*. 64(10), 1492-1498.

Kawakami, S., Matsunami, K., Otsuka, H., Inagaki, M., Takeda, Y., Kawahata, M. and Yamaguchi, K. 2015. Crotocascarins I-K: crotofolane-type diterpenoids, crotocascarin γ, isocrotofolane glucoside and phenolic glycoside from the leaves of *Croton cascarilloides*. *Chem Pharm Bull (Tokyo)*. 63(12), 1047-1054.

Kawakami, S., Matsunami, K., Otsuka, H., Lhieochaiphant, D. and Lhieochaiphant, S. 2013. Two new cembranoids from the leaves of *Croton longissimus* Airy Shaw. *J Nat Med*. 67(2), 410-4.

Kawakami, S., Matsunami, K., Otsuka, H., Shinzato, T. and Takeda, Y. 2010. Crotonionosides A-G: megastigmane glycosides from leaves of *Croton cascarilloides* Räuschel. *Phytochemistry*. 72(1), 147-153.

Kawakami, S., Toyoda, H., Harinantenaina, L., Matsunami, K., Otsuka, H., Shinzato, T., Takeda, Y., Kawahata, M. and Yamaguchi, K. 2013. Eight new diterpenoids and two new nor-diterpenoids from the stems of *Croton cascarilloides*. *Chem Pharm Bull (Tokyo)*. 61(4), 411-418.

Kawasaki, T. and Kawai, T. 2014. Tool-like receptor signaling pathways. *Front Immunol*. 5(461), 1-8.

Kerr, J.F., Wyllie, A.H., Currie, A.R. 1972. Apoptosis: a basic biological phenomenon with wide-ranging implications in tissue kinetics. *Br J Cancer*. 26(4), 239-257.

Khiev, P., Oh, SR., Chae, HS., Kwon, OK., Ahn, KS., Chin, YW. and Lee, HK. 2011. Anti-inflammatory diterpene from *Thyrsanthera suborbicularis*. *Chem Pharm Bull (Tokyo)*. 59(3), 382-384.

Khovidhunkit S.O., Yingsaman N., Chairachvit K., Surarit R., Fuangtharnthip P. and Petsom A. 2011. In vitro study of the effects of plaunotol on oral proliferation and wound healing. *J Asain Nat Prod Res.* 13(2):149-159.

Khuankaew S, Srithi K, Tiansawat P, Jampeetong A, Inta A, Wangpakapattanawong P. 2014. Ethnobotanical study of medicinal plants used by Tai Yai in Northern Thailand. *J Ethnopharmacol*. 151(2), 829-38.

Kim, CW., Lee, H.J., Jung, J.H., Kim, Y.H., Jung, DB., Sohn, E.J., Lee, J.H., Woo, H.J., Baek, NI., Kim, Y.C. and Kim, SH. 2015. Activation of caspase-9/3 and inhibition of epithelial mesenchymal transition are critically involved in antitumor effect of phytol in hepatocellular carcinoma cells. *Phytother Res*. 29(7), 1026-1031.

Kim, JA., Kim, DK., Jin, T., Kang, OH., Choi, YA., Choi, SC., Kim, TH., Nah, YH., Choi, SJ., Kim, YH., Bae, KH. And Lee, YM. 2004. Acanthoic acid inhibits IL-8 production via MAPKs and NF-kappaB in a TNF-alpha-stimulated human intestinal epithelial cell line. *Clin Chim Acta.* 342(1-2), 193-202.

Kim, M.K., Park, G.H., Eo, H.J., Song, H.M., Lee, J.W., Kwon, M.J., Koo, J.S. and Jeong, J.B. 2015. Tanshinone I induces cyclin D1 proteasomal degradation in an ERK1/2 dependent way in human colorectal cancer cells. *Fitoterapia*. 101, 162-168.

Kitazawa, E. and Ogiso, A. 1981. Two diterpene alcohols from *Croton sublyratus*. *Phytochemistry*. 20(2), 287-289.

Kitazawa, E., Kurabayashi, M., Kasuga, S., Oda, O. and Ogiso, A. 1982. New esters of a diterpene alcohol from *Croton sublyratus*. *Ann. Rep. Sankyo Res. Lab*. 34, 39-41.

Kitazawa, E., Ogiso, A., Takahashi, S., Sato, A., Kurabayashi, M., Kuwano, H., Hata, T. and Tamura, C., 1979. Plaunol A and B, new anti-ulcer diterpene lactones from *Croton sublyratus*. *Tetrahedron Lett.* 20(13), 1117–1120.

Kitazawa, E., Sato, A. Takahashi, S. Kuwano, H. and Ogiso, A. 1980. Novel diterpenelactones with anti-peptic ulcer activity from *Croton sublyratus*. *Chem Pharm Bull.* 28(1), 227-234.

Koga, T., Watanabe, H., Kawada, H., Takahashi, K., Utsui, Y., Domon, H., Ishii, C., Narita, T. and Yasuda, H. 1998. Interactions of plaunotol with bacterial membranes. *J Antimicrob Chemother*. 42(2), 133-140.

Koga, T., Kawada, H., Utsui, Y., Domon, H., Ishii, C. and Yasuda, H. 1996b. Bactericidal effect of plaunotol, a cytoprotective antiulcer agent, against *Helicobacter pylori*. *J Antimicrob Chemother*. 38(3), 387-397.

Krenn, L., Miron, A., Pemp, E., Petr, U. and Kopp, B. 2003. Flavonoids from *Achillea nobilis* L. *Z. Naturforsch*. 58c, 11-16.

Kuang, X., Li, W., Kanno, Y., Yamashita, N., Nemoto, K., Asada, Y. and Koike, K. 2016. ent-Atisane diterpenoids from *Euphorbia fischeriana* inhibit mammosphere formation in MCF-7 cells. *J Nat Med*. 70(1), 120-126.

Kuo, CF., Su, JD., Chiu, CH., Peng, CC., Chang, CH., Sung, TH., Huang, SH., Lee, WC. And Chyau, CC. 2011. Anti-inflammatory effects of supercritical carbon dioxide extract and its isolated carnosic acid from *Rosmarinus officinalis* leaves. *J Agric Food Chem*. 59(8), 3674-3685.

Kupchan, S.M., Uchida, I., Branfman, A.R., Dailey, R.G., Jr, Fei, B.Y. 1976. Antileukemic principles isolated from euphorbiaceae plants. *Science*. 191(4227), 571-572.

Kurimoto, S., Pu, JX., Sun, HD., Shibata, H., Takaishi, Y. and Kashiwada, Y. 2016. Acylated neo-clerodane type diterpenoids from the aerial parts of *Scutellaria coleifolia* Levl. (Lamiaceae). *J Nat Med*. 70(2), 241-252

Lam, T., Ling, T., Chowdhury, C., Chao, TH., Bahjat, FR., Lloyd, GK., Moldawer, LL., Palladino, MA. And Theodorakis, EA. 2003. Synthesis of a novel family of diterpenes and their evaluation as anti-inflammatory agent. *Bioorg Med Chem Lett*. 13(19), 3217-3221.

Lanzotti, V., Barile, E., Scambia, G. and Ferlini, C. 2015. Cyparissins A and B, jatrophane diterpenes from *Euphorbia cyparissias* as Pgp inhibitors and cytotoxic agents against ovarian cancer cell lines. *Fitoterapia*.104, 75-79.

Lara-Gonzalez, P., Westhrpe, F. and Taylor, S.S. 2012. The spindle assembly checkpoint.*Curr Biol*. 22(22), R966-R980.

Lee, JH., Koo, TH., Hwang, BY. and Lee, JJ. 2002. Kaurane diterpene, kamebakuarin, inhibits NF-kappa B by directly targeting the DNA-binding activity of p50 and blocks the expression of antiapoptotic NF-kappa B target genes. *J Biol Chem*. 227(21), 18411-18420.

Lee, JW., Lee, MS., Kim, TH., Lee, HJ., Hong, SS., Noh, YH., Hwang, BY., Ro, JS. and Hong, JT. 2007. Inhibitory effect of inflexinol on nitric oxide generation and iNOS expression via inhibition of NF-kappa B activation. *Mediators Inflamm*. 2007, 93148.

Leung, CH., Grill, SP., Lam, W., Han, QB., Sun, HD. and Cheng, YC. 2005. Novel mechanism of inhibition of nuclear factor-kappa B DNA-binding activity by diterpenoids isolated from *Isodon rubescens*. *Mol Pharmacol*. 68(2), 286-297.

Li, CH., Wu, X., Sun, R., Zhao, P., Liu, F. and Zhang, CH. 2016. *Croton tiglium* extract induces apoptosis via Bax/Bcl-2 pathways in human lung cancer A549 cells. *Asian Pac J Cancer Prev*. 17(11), 4893-4898.

Li, D., Li, C., Li, L., Chen, S., Wang, L., Li, Q., Wang, X., Lei, X., Shen, Z. 2016. Natural product kongensin A is a non-canonical HSP90 inhibitor that blocks RIP3-dependent necroptosis. *Cell Chem Biol*. 23(2), 257-266.

Li, F., Sun, Q., Hong, L., Li, L., Wu, Y., Xia, M., Ikejima, T., Peng, Y. and Song, S. 2013. Daphnane-type diterpenes with inhibitory activities against human cancer cell lines from *Daphne genkwa*. *Bioorg Med Chem Lett*. 23(9), 2500-2504.

Li, L., Wu, L., Wang, M., Sun, J. and Liang, J. 2014. Abietane diterpenoids from *Clerodendrum trichotomum* and correction of NMR data of villosin C and B. *Nat Prod Commun*. 19(7), 907-910.

Li, L., Yue, G.G., Lau, C.B., Sun, H., Fung, K.P., Leung, P.C., Han, Q. and Leung, P.S. 2012. Eriocalyxin B induces apoptosis and cell cycle arrest in pancreatic adenocarcinoma cells through caspase- and p53-dependent pathways. *Toxicol Appl Pharmacol*. 262(1), 80-90.

Li, M. and Hong, L. 2015. Pseudolaric acid B exerts antitumor activity via suppression of the Akt signaling pathway in HeLa cervical cancer cells. *Mol Med Rep*.12(2), 2021–2026.

Li, R., Morris-Natschke, S.L. and Lee, KH. 2016. Clerodane diterpenes: sources, structures, and biological activities. *Nat Prod Rep*. 33, 1166-1226.

Li, WF., Wang, J., Zhang, JJ., Song, X., Ku, CF., Zou, J., Li, JX., Rong, LJ., Pan, LT. and Zhang, HJ. 2015. Henrin A: a new anti-HIV *ent*-kaurane diterpene from *Pteris henryi*. *Int J Mol Sci*. 16(11), 27978-27987.

Li, ZY., Li, QZ., Ma, GX., Chen, L., Zhang, C., Chen, BD., Yang, JS. and Li, WP. 2016. Cassane-type diterpenes from *Caesalpinia minax* induce apoptosis in pituitary adenoma: structure-activity relationship, ER stress and Wnt/β-catenin pathways. *J Asian Nat Prod Res*. 19(5), 423-435.

Li. W., Huang, C., Li, S., Ma, F., Li, Q., Asada, Y. and Koike, K. 2012. Clerodane diterpenoids from *Tinospora sagittata* (Oliv.) Gagnep. *Planta Med*. 78:82-85

Liang, Y., Zhang, Y., Wang, G., Li, Y., Huang, W. 2017. Penduliflaworosin, a diterpenoid from *Croton crassifolius*, exerts anti-angiogenic effect via VEGF receptor-2 signaling pathway. *Molecules*. 22(1), 126.

Lin, CZ., Zhao, W., Feng, XL., Liu, FL. and Zhu, CC. 2016. Cytotoxic diterpenoids from *Rabdosia lophanthoides* var. gerardianus. *Fitoterapia*. 109, 14-19.

Lin, CZ., Zhao, ZX., Xie, SM., Mao, JH., Zhu, CC., Li, XH., Bairi, ZD., Kangsa, SQ., Dun, Z., Xiong, T.Q. and Wu, A.Z. 2014. Diterpenoid alkaloids and flavonoids from *Delphinium trichophorum*. *Phytochemistry*. 97, 88–95.

Lin, H.C., Kuo, YL., Lee, WJ., Yap, HY. and Wang, SH. 2016. Antidermatophytic activity of ethanolic extract from *Croton tiglium*. *Biomed Res Int*. 2016, 3237586.

Lin, JY., Ke, YM., Lai, JS. and Ho, TF. 2015. Tanshinone IIA enhances the effects of TRAIL by downregulating survivin in human ovarian carcinoma cells. *Phytomedicine*. 22(10), 929-938.

Liu, Y., Wiedle Jr, C.H., Brodie, P.J., Callmander, M.W. Rakotondrajaona, R., Rakotobe, E., Rasamison, V.E. and Kingston, D.G.I. 2015. Antiproliferative diterpenes from a *Malleastrum* sp. from the Madagascar dry forest. *Nat Prod Commun*. 10(9), 1509-1512.

Liu, YN., Gu, JL., Ma, MS., Guo, H., Liu, L., Guo, LR., Wang, Y. and Li, Y. 2015. Diterpenoid B derived from *Plectranthus excisus* inhibits the melanoma cell cycle in the B16 melanoma cell line. *Mol Med Rep*. 12(3), 4578-4583.

Lo, AH., Liang, YC., Lin-shianu, SY., HO. CT. and Lin, JK. 2002. Carnosol, an antioxidant in rosemary, suppresses inducible nitric oxide synthase through down-regulating nuclear factor-kappaB in mouse macrophages. *Carcinogenesis*. 23(6), 983-991.

Lodish, H., Berk, A., Zipursky, S.L., Matsudaira, P., Baltimore, D. and Darnell, J. 2000. Overview of Extracellular Signaling: Cell-to-Cell Signaling: Hormones and Receptors. Lodish, H., Berk, A., Zipursky, S.L., Matsudaira, P., Baltimore, D. and Darnell, J (eds). *Molecular Cell Biology*. (4th ed). New York, W H Freeman.

Lu, D., Liu, Y. and Aisa, H.A. 2014. Jatrophane diterpenoid esters from *Euphorbia sororia* serving as multidrug resistance reversal agents. *Fitoterapia*. 92, 244-251.

Lucas, R., Casapullo, A., Ciasullo, L., Gomez-Paloma, L. and Paya, M. 2003. Cycloamphilectenes, a new type of potent marine diterpenes: inhibition of nitric oxide production in murine macrophages. *Life Sci*. 72(22), 2543-2552.

Ma, G., Wu, H., Chen, D., Zhu, N., Zhu, Y., Sun, Z., Li, P., Yuan, J. and Xu, X. 2015. Antimalarial and antiproliferative cassane diterpenes of *Caesalpinia sappan*. *J Nat Prod*. 78(10), 2364-2371.

Ma, GX,, Xu, N., Yuan, JQ., Wei, H., Zheng, QX., Sun, ZC., Yang, JS. and Xu, XD. 2012. Two new diterpenes, neocaesalpin MR and minaxin C, from *Caesalpinia minax*. *J Asian Nat Prod Res*. 14(12), 1156-1161.

Ma, GX., Xu, XD., Cao, L., Yuan, JQ., Yang, JS. and Ma, LY. 2012. Cassane type diterpenes from the seeds of *Caesalpinia minax* with their antineoplastic activity. *Planta Med*. 78, 1363-1369.

Ma, GX., Yuan, JQ., Cao, L., Yang, JS. and Xu, XD. 2013. Two new diterpenes from *Caesalpinia minax* Hance. *Nat Prod Res*. 27(9), 818–823.

Ma, M., Jiang, Z., Ruan, J., Tan, X., Liu, J., Wang, C., Zha, X.M. and Zhang, L. 2012. The furano norclerodane diterpenoid disobulbin-D induces apoptosis in normal human liver L-02 cells. *Exp Toxicol Pathol*. 64(6), 611-618.

Ma, YC., Ke, Y., Zi, X., Zhao, F., Yuan, L., Zhu, YL., Fan, XX., Zhao, NM., Li, QY., Qin, YH. and Liu, HM. 2016. Induction of the mitochondria mediated apoptosis in human esophageal cancer cells by DS2, a newly synthetic diterpenoid analog, is regulated by Bax and caused by generation of reactive oxygen species. *Oncotarget*. 7(52), 86211-86224.

Ma, YC., Su, N., Zhao, NM., Li, QY., Zhang, M., Zhao, HW., Liu, HM. and Qin, YH. 2016. Jaridonin, a new diterpenoid from *Isodon rubescens*, induces cell cycle arrest in gastric cancer cells through activating *ataxia telangiectasia* mutated kinase. *Zhonghua Zhong Liu Za Zhi*.38(4), 258-262.

Malumbres, M. and Barbacid, M. 2009. Cell cycle, CDKs and cancer: a changing paradigm. *Nat Rev Cancer*. 9(3), 153-166.

Man, S.M. and Kanneganti, TD.2016. Converging roles of caspases in inflammasome activation, cell death and innate immunity. *Nat Rev Immunol*.16(1), 7-21.

Mantaj, J., Rahman, S.M.A., Bokshi, B., Hasan, C.M., Jackson, P.J.M., Parsons, R.B. and Rahman, K.M. 2015. Crispene E, a *cis*-clerodane diterpene inhibits STAT3 dimerization in breast cancer cells. *Org Biomol Chem.* 13(13), 3882-3886.

Martin, G.S. 2003. Cell signaling and cancer. *Cancer Cell*. 4(3), 167-174.

Masters, J.R.W. (ed). 2000. Animal cell culture (3th ed). Oxford, Oxford University Press.

Mayer, I.A. and Arteaga, C.L. 2016. The PI3K/AKT pathway as a target of cancer treatment. *Annu Rev Med*. 67, 11-28.

Mcllwain, D.R., Berger, T. and Mak, T.W. 2013. Caspase functions in cell death and disease. *Cold Spring Harb Perspect Biol*. 5, a008656.

Miron-Lopez, G., Bazzocchi, I.L., Jimenez-Diaz, I.A., Moujir, L.M., Quijano-Quinones, R., Quijano, L. and Mena-Rejon, G.J. 2014. Cytotoxic diterpenes from roots of *Crossopetalum gaumeri*, a Celastraceae species from Yucatan Peninsula. *Bioorg Med Chem Lett.* 24(9), 2105-2109.

Mishra, S.K, Tripathi, S., Shukla, A., Oh, S.H. and Kim, H.M. 2015. Andrographolide and analogues in cancer prevention. *Front Biosci (Elite Ed)*. 7, 255-266.

Mittal, M., Siddiqui, M.R., Tran, K., Reddy, S.P. and Malik, A.B. 2014. Reactive oxygen species in inflammation and tissue injury. *Antioxid Redox Signal*. 20(7), 1126–1167.

Morgan, D.O. 2007. *The cell cycle: principles of control*. United Kingdom, New Science Press Ltd.

Morgan, M.J. and Liu, ZG. 2011. Crosstalk of reactive oxygen species and NF-κB. *Cell Res*. 21(1), 103-115.

Munagala, R., Aqil, F., Jeyabalan, J. and Gupta, R.C. 2015. Tanshinone IIA inhibits viral oncogene expression leading to apoptosis and inhibition of cervical cancer. *Cancer Lett*. 356(2), 536-546.

Murakami, K., Okajima, K., Harada, N., Isobe, H., Liu, W., Johno, M. and Okabe, H. 1999. Plaunotol prevents indomethacin-induced gastric mucosal injury in rats by inhibiting neutrophil activation. *Aliment Pharmacol Ther.* 13(4), 521-530.

Murphy, C.M. and Michael, W.M. 2013. Control of DNA replication by the nucleus/cytoplasm ratio in *Xenopus*. *J Biol Chem*. 288(41), 29382-29393.

Navarro, A., de las H eras, B. and Villar, A.M. 1997. Andalusol, a Diterpenoid with anti-inflammatory Activity from Siderits foetens Clemen A. *Z. Naturforsch*. 52c, 844-849.

Neuzillet, C., Tijeras-Raballand, A., Cohen, R., Cros, J., Faivre, S., Raymond, E., Gramont, A. 2015. Targeting the TGFβ pathway for cancer therapy. *Pharmacol Ther.* 147, 22-31.

Newman, D. and Cragg, G.M. 2016. Natural products as sources of new drugs from 1981 to 2014. *J Nat Prod*. 79(3), 629-661.

Ngamrojnavanich, N., Tonsiengsom, S., Lertpratchya, P., Roengsumran, S., Puthong, S. and Petsom, A. 2003. Diterpenoids from the stem barks of *Croton robustus*. *Arch Pharm Res*. 26(11), 898-901.

Nguyen, H.T., Truong, N.B., Doan, H.T., Liaudon, M., Retaileau, P., Do, T.T., Nguyen, H.V., Chau, M.V. and Pharm, C.V. 2015. Cytotoxic clerodane diterpenoids from the leaves of *Casearia grewiifolia*. *J Nat Prod*. 78(11), 2726-2730.

Nguyen, H.X., Nguyen, M.T.T., Nguyen, T.A., Nguyen, N.Y.T., Phan, D.A.T., Thi, P.H., Nguyen, T.H.P., Dang, P.H., Nguyen, N.T., Ueda, JY. And Awale, S. 2013. Cleistanthane diterpenes from the seed of *Caesalpinia sappan* and their antiausterity activity against PANC-1 human pancreatic cancer cell line. *Fitoterapia*. 91, 148-153.

Nguyen, HX., Nguyen, NT., Dang, PH., Ho, PT., Nguryen, MTT., Can, MV., Dibwe, DF., Ueda, J-Y. and Awale, S. 2016. Cassane diterpenes from the seed kernels of *Caesalpinia sappan*. *Phytochemistry*. 122, 286-293.

Nhiem, NX., Hien, NT., Tai, BH., Anh Hle, T., Hang, DT., Quang, TH., Kiem, PV., Minh, CV., Ko, W., Lee, S., Oh, H., Kim, SH. And Kim,YH. 2015. New ent-kauranes from the fruits of Annona glabra and their inhibitory nitric oxide production in LPS-stimulated RAW264.7 macrophages. *Bioorg Med Chem Lett*. 25(2), 254-258.

Noor Rain, A., Khozirah, S., Mohd Ridzuan, M.A.R., Ong, B.K., Rohaya, C., Rosilawati, M., Hamdino, I., Badrul Amin and Zakiah, I. 2007. Antiplasmodial properties of some Malaysian medicinal plants. *Trop Biomed.* 24(1), 29-35.

Nunez, G., Benedict, M.A., Hu, Y. and Inohara, N. 1998. Caspases: the proteases of the apoptotic pathway. *Oncogene*, 17, 3237-3245.

Oeckinghaus, A. and Ghosh, S. 2009. The NF-κB family of transcription factors and its regulation. *Cold Spring Harb Perspect Biol*. 1(4), a000034.

Ogiso A, Kitazawa E, Kobayashi S, Komai T, Matsunuma N, Kataumi S. 1985. Plaunotol (CS-684), a new anti-ulcer agent. *Sankyo Kenyusho Nempo*. 37, 1-39.

Ogiso, A., Kitazawa, E., Kurabayashi,M., Sato, A., Takahashi,M., Noguchi, H., Kuwano, H., Kobayashi, S., Mishima, H. 1978. Isolation and structure of antipeptic ulcer diterpene from Thai medicinal plant. *Chem Pharm Bull*. 26(10), 3117-3123.

Oh, DR., Kang, H.W., Kim, JR., Kim, S., Park, IK., Rhee, J.H., Oh, W.K. and Kim, Y.R. 2014. PMA induces vaccine adjuvant activity by the modulation of TLR signaling pathway. *Mediators Inflamm*. 2014(2014), 406514.

Ojo-Amaize, EA., Kapahi, P., Kakkanaiah, VN., Takahashi, T., Shalom-Barak, T., Cottam, HB., Adesomoju, AA., Nchekwube, EJ., Oyemade, OA., Karin, M. and Okogun, JI. 2001. Hypoestoxide, a novel anti-inflammatory natural diterpene, inhibits the activity of IkB kinase. *Cell Immunol.* 209(2), 149-157.

Oliveira, A., Beyer, G., Chugh, R., Skube, S.J., Majumder, K., Banerjee, S., Sangwan, V., Li, L., Dawra, R., Subramanian, S., Saluja, A. and Dudeja, V.2015. Triptolide abrogates growth of colon cancer and induces cell cycle arrest by inhibiting transcriptional activation of E2F. *Lab Invest*. 95(6), 648-659.

Ormerod, M. 2008. Flow cytometry-A basic introduction. 1st ed. [ebook]. Available at: http://flowbook.denovosoftware.com/ [30 Jan 2018].

Pan, ZH., Ning, DS., Liu, JL., Pan, B., Li, DP. 2014. A new triterpenoid saponin from the root of *Croton lachnocarpus* Benth. *Nat Prod Res*. 28(1), 48-51.

Panda, S.K., Dutta, S.K. and Bastia, A.K. 2010. Antibacterial activity of *Croton roxburghii* Balak. against the enteric pathogens. *J Adv Pharm Technol Res*. 1(4), 419-422.

Parfett, C.L. and Healy, C. 2006. Tandemly repeated DNA sequence instabilities induced by two promoters of morphological transformation *in vitro*: a short-term response to nonmutagenic agents in C3H/10T1/2 cells. *Mutat Res*. 604(1-2), 42-52.

Park, B.S. and Lee, J.O. 2013. Recognition of lipopolysaccharide pattern by TLR4 complexes. Exp Mol Med. 45(12), e66.

Park, HJ. Kim, IT., Won, JH., Jeong, SH., Park, EY., Nam, JH., Choi, J. and Lee, KT. 2007. Anti-inflammatory activities of ent-16 alphaH, 17-hydroxy-kauran-19-oic acid isolated from the root of *Siegesbeckia pubescens* are due to the inhibition of iNOS and COX-2 expression in RAW264.7 macrophage via NF-kappa B in activation. *Eur J Pharmacol*. 558(1-3), 185-193.

Parrish, A. B., Freeland, C.D. and Kornbluth, S. 2013. Cellular Mechanisms Controlling Caspase Activation and Function. *Cold Spring Harb Perspect Biol*. 5(6), a008672.

Payne, S. and Miles, D. 2008. Mechanisms of anticancer drugs. Gleeson, M., Browning, G.G., Burton, M.J., Clarke, R., Hibbert, J., Jones, N.S., Lund, V.J., Laxon, L.M., Watkinton, J.C. (eds). *Scott-Brown's Otorhinolaryngology*. New York, CRC press.

Pellegrini, M.P., Pinto, R.C.V. and Castilho, L.R. 2008. Mechanisms of cell proliferation and cell death in animal cell culture in vitro. Castilho, L.R., Moraes, A.M., Augusto, E.F. and Butler, M. (eds). *Animal cell technology: from Biopharmaceuticals to gene therapy*. New York, Taylor & Francis Group.

Peng, T., Hu, M., Wu, TT., Zhang, C., Chen, Z., Huang, S. and Zhou, XH. 2015. Andrographolide suppresses proliferation of nasopharyngeal carcinoma cells via attenuating NF-κB pathway. *Biomed Res Int.* 2015, 735056.

Perez-Rodriguez, R., Roncero, C., Olivan, A. M., Gonzalez, M. P. and Oset-Gasque, M. J. 2009. Signaling mechanisms of interferon gamma induced apoptosis in chromaffin cells: involvement of nNOS, iNOS, and NFkappaB. *J Neurochem*. 108, 1083-1096.

Pertino, M.W., Theoduloz, C., Butassi, E., Zacchino, S. and Schmeda-Hirschmann, G. 2015. Synthesis, antiproliferative and antifungal activities of 1,2,3-triazole-substituted carnosic acid and carnosol derivatives. *Molecules*. 20(5), 8666-8686.

Petiwala, S.M. and Johnson, J.J. 2015. Diterpenes from rosemary (*Rosmarinus officinalis*): defining their potential for anticancer activity. *Cancer Lett*. 367(2), 93-102.

Ponglux, D., Wongseripipatana, S., Phadungcharoen, T., Ruangrungsi, N. and Likhitwitayawuid, K. 1987. *Medicinal Plants*. The First Princess Chulabhorn Science Congress Bangkok, Thailand.

Pornpakakul, S., Liangsakul, J., Ngamrojanavanich, N., Roengsumran, S., Sihanonth, P., Piapukiew, J., Sangvichien, E., Puthong, S. and Petsom, A. 2006. Cytotoxic activity of four xanthones from *Emericella variecolor*, an endophytic fungus isolated from *Croton oblongifolius*. *Arch Pharm Res*. 29(2), 140-144.

Premprasert, C., Tewtrakul, S., Plubrukarn, A. and Wungsintaweekul, J. 2013. Anti-inflammatory activity of diterpenes from *Croton stellatopilosus* on LPS-induced RAW264.7 cells. *J Nat Med*. 67, 174-181.

Pucci, B., Kasten, M. and Giordano, A. 2000. Cell cycle and apoptosis. *Neoplasia*. 2(4), 291-299.

Pudhom, K., Vilaivan, T., Ngamrojanavanich, N., Dechangvipart, S., Sommit, D., Petsom, A. and Roengsumran, S. 2007. Furanocembranoids from the stem bark of *Croton oblongifolius*. *J Nat Prod*. 70(4), 659-661.

Qin, LH, Kong, L., Shi, GJ.,Wang, ZT. and Ge, BX. 2006. Andrographolide inhibits the production of TNF-alpha and interleukin-12 in lipopolysaccharide-stimulated macrophages: role of mitogen-activated protein kinases. *Biol Pharm Bull*. 29(2), 220-224.

Qiu, M., Cao, D., Gao, Y., Li, S., Zhu, J., Yang, B., Zhou, L., Zhou, Y., Jin, J. and Zhao, Z. 2016. New clerodane diterpenoids from *Croton crassifolius*. *Fitoterapia*. 108, 81-86.

Rath, S., Patra, J.K., Mohapatra, N., Mohanty, G., Dutta, S. and Thatoi, H. 2011. *In vitro* antibacterial and antioxidant studies of *Croton roxburghii* L., from similipal biosphere reserve. *Indian J Microbiol*. 51(3), 363-368.

Rédei, D., Boros, K., Forgo, P., Molnár., J., Kele, Z., Pálinkó, I., Pinke, G. and Hohmann, J. 2015. Diterpene constituents of *Euphorbia exigua* L. and multidrug resistance reversing activity of the isolated diterpenes. *Chem Biodivers*. 12(8), 1214-1221.

Reis, M.A., Paterna, A., Mónico, A., Molnar, J., Lage, H., Ferreira, MJ.U. 2014. Diterpenes from *Euphorbia piscatoria*: synergistic interaction of Lathyranes with doxorubicin on resistant cancer cells. *Planta Med*. 80(18), 1739-1745.

Reuter, S., Gupta, S.C., Chaturvedi, M.M. and Aggarwal, B.B. 2010. Oxidative stress, inflammation, and cancer: How are they linked?. *Free Radic Biol Med*. 49(11), 1603-1616.

Rivlin, N., Brosh, R., Oren, M. and Rotter, V. 2011. Mutations in the p53 Tumor Suppressor Gene Important Milestones at the Various Steps of Tumorigenesis. *Genes cancer*. 2(4), 466-474.

Robertson, G.S, Lacasse, E.C. and Holcik, M. 2009. Programmed cell death. Hacker, M., Messer, W. and Bachman, K. (eds). *Pharmacology*. California, Academic Press.

Rodriguez, J. and Lazebnik, Y. 1999. Caspase-9 and APAF-1 form an activie holoenzyme. *Gene Dev*. 13(24), 3179-3184.

Roengsumran, S., Achayindee, S., Petsom, A., Pudhom, K., Singtothong, P., Surachetapan, C. and Vilaivan, T. 1998. Two new cembranoids from *croton oblongifolius*. *J Nat Prod*. 61(5), 652-654.

Roengsumran, S., Musikul, K., Petsom, A., Vilaivan, T., Sangvanich, P., Pornpakakul, S., Puthong, S., Chaichantipyuth, C., Jaiboon, N. and Chaichit, N. 2002. Croblongifolin, a new anticancer clerodane from *Croton oblongifolius*. *Planta Med*. 68(3), 274-277.

Roengsumran, S., Petsom, A., Kuptiyanuwat, N., Vilaivan, T., Ngamrojnavanich, N., Chaichantipyuth, C. and Phuthong, S. 2001. Cytotoxic labdane diterpenoids from *Croton oblongifolius*. *Phytochemistry*. 56(1), 103-107.

Roengsumran, S., Pornpakakul, S., Muangsin, N., Sangvanich, P., Nhujak, T., Singtothong, P., Chaichit, N., Puthong, S. and Petsom, A. 2004. New halimane diterpenoids from *Croton oblongifolius*. *Planta Med*. 70(1), 87-89.

Roengsumran, S., Singtothong, P., Pudhom, K., Ngamrochanavanich, N., Petsom, A. and Chaichantipyuth, C. 1999. Neocrotovembranal from *Croton oblongifolius*. *J Nat Prod*. 62(8), 1163-1164.

Roengsumran, S., Singtothong, P., Pudhom, K., Ngamrochanavanich, N., Petsom, A. and Chaichantipyuth, C. 1999. Neocrotocembranal from *Croton oblongifolius*. *J Nat Prod*. 62(8), 1163-1164.

Rosenberg, H.F. and Gallin, J.I. 2003. Inflammation. Paul, W.E. (eds). *Fundamental immunity*. (5th ed). USA, Lippincott Williams & Wilkins.

Roy, P.K., Maarisit, W., Roy, M.C., Taira, J. and Ueda, K. 2012. Five new diterpenoids from an Okinawan soft coral, *Cespitularia* sp. *Mar Drugs*. 10(12), 2741-2748.

Salinas-Sánchez, DO., Zamilpa, A., Pérez, S., Herrera-Ruiz, M., Tortoriello, J., González-Cortazar, M. and Jiménez-Ferrer, E. 2015. Effect of hautriwaic acid isolated from *Dodonaea viscosa* in a model of kaolin/carrageenan-induced monoarthritis. *Planta Med*. 81(14), 1240-1247.

Santos, S.H., Barros, F.W.A., Albuquerque, M.R.J.R., Bandeira, P.N., Pessoa, C., Braz-Filho, R., Monte, F.J.Q., Henrique Leal-Cardoso, J. and Lemos, T.L.G. 2009. Cytotoxic diterpenoids from *Croton argyrophylloides*. *J Nat Prod*. 72(10), 1884-1887.

Sasaki, M., Mizoshita, T., Mizushima, T., Inoue, H., Kamiya, T., Kataoka, H., Ogaswara, N., Wada, T., Kubota, E., Mori, Y., Shimura, T., Hirata, H., Ando, K., Okamoto, Y., Ohara, H., Nakao, H. and Joh, T. 2007. Effect of plaunotol in combination with clarithromycin against clarithromycin-resistant *Helicobacter pylori in vitro* and *in vivo*. *J Antimicrob Chemother*. 60: 1060-1063.

Schmitt, J., Noble, A., Otsuka, M., Berry, P., Maitland, N.J. and Rumsby, M.G. 2014. Phorbol ester stimulates ethanolamine release from the metastatic basal prostate cancer cell line PC3 but not from prostate epithelial cell lines LNCaP and P4E6. *Br J Cancer*. 111(8), 1646-1656.

Schuler, M. and Green, D.R. 2001. Mechanisms of p53-dependent apoptosis. *Biochem Soc Trans*. 684-688.

Seshacharyulu, P., Ponnusamy, M., Haridas, D., Jain, M., Ganti., A. and Batra, S.K. 2012. Targeting the EGFR signaling pathway in cancer therapy. *Expert Opin Ther Targets*. 16(1), 15-31.

Shadi, S., Saeidi, H., Ghanadian, M., Rahimnejad, M.R., Aghaei, M., Ayatollahi, S.M. and Choudhary, M.I. 2015. New macrocyclic diterpenes from *Euphorbia connata* Boiss. with cytotoxic activities on human breast cancer cell lines. *Nat Prod Res*. 29(7), 607-614.

Shaulian, E. and Karin, M. 2001. AP-1 in cell proliferation and survival. *Oncogene*. 20, 2390-2400.

Shcheblyakov, D.V., Logunov, D.Y., Tukhvatulin, A.I., Shmarov, M.M., Naroditsky, B.S. and Gintsburg, A.L. 2010. Toll-Like Receptors (TLRs): The role in tumor progression. *Acta Naturae*. 2(3), 21-29.

Shih, FY., Chen, TH., Lu, MC., Chen, WF., Wen, ZH., Kuo, YH. and Sung, PJ. 2013. Cladieunicellins K and L, new eunicellin-based diterpenoids from an *Octocoral Cladiella sp*. *Int J Mol Sci*. 14(11), 21781–22179.

Shiratori, K., Watanabe, S. and Takeuchi, T. 1993. Role of endogenous prostaglandins in secretin- and plaunotol-induced inhibition of gastric acid secretion in rat. *Am J Gastroentrol*. 88(1), 84-89.

Siebenlist, U., Franzoso, G. and Brown, K.1994. Structure, regulation and function of NF-kappa B. *Annu Rev Cell Biol*.10, 405-55.

Sienko, A., Allen, T.C. and Cagle, P.T. 2008. Bcl-2. Zander, D.S., Popper, H., Jagirdar, J., Haque, A. and Barrios, R. (eds). *Molecular Pathology of Lung Diseases*. New York, Springer Science and Business Media LLC.

Silva, C.G., Santos Júnior, H.M., Barbosa, J.P., Costa, G.L., Rodrigues, F.A., Oliveira, D.F., Costa-Lotufo, L.V., Alves, R.J., Eleutherio, E.C. and Rezende, C.M. 2015. Structure Elucidation, Antimicrobial and cytotoxic activities of a halimane isolated *from Vellozia kolbekii* Alves (Velloziaceae). *Chem Biodivers*. 12(12), 1891-1901.

Simpson, BS., Luo, X., Costabile, M., Caughey, GE., Wang, J., Claudie, DJ., McKinnon, RA. and Semple, SJ. 2014. Polyandric acid A, a clerodane diterpenoid from the Australian medicinal plant *Dodonaea polyandra*, attenuates pro-inflammatory cytokine secretion *in vitro* and *in vivo*. *J Nat Prod*. 77(1), 85-91.

Sloan, E.J. and Ayer, D.E. 2010. Myc, Mondo, and metabolism. *Genes cancer*. 1(6), 587-596.

Sommit, D., Petsom, A., Ishikawa, T. and Roengsumran, S. 2003. Cytotoxic activity of natural labdanes and their semi-synthetic modified derivatives from *Croton oblongifolius*. *Planta Med*. 69(2), 167-170.

Song, JT., Han, Y., Wang, XL., Shen, T., Lou, HX., Wang, XN. 2015. Diterpenoids from the twigs and leaves of *Croton caudatus* var. tomentosus. *Fitoterapia*. 107, 54-59

Song, Y., Xin, Z., Wan, Y., Li, J., Ye, B. and Xue, X. 2015. Synthesis and anticancer activity of some novel indolo[3,2-β] andrographolide derivatives as apoptosis-inducing agents. *Eur J Med Chem*. 90, 695-706.

Sonnenshein, C. and Soto, A.M. 2013. The aging of the 2000 and 2011 Hallmarks of Cancer reviews: a critique. *J Bio Sci*. 38(3), 651-663.

Stewart, B.W. and Chistopher, P.W. 2014. Cancer worldwide. Stewart, B.W. and Chistopher, P.W (eds). *World Cancer Report 2014*. Lyon, International Agency for Research on Cancer (IARC).

Stirpe, F., Pession-Brizzi, A., Lorenzoni, E., Strocchi, P., Montanaro, L and Sperti, S. 1976. Studies on the proteins from the seeds of *Croton tiglium* and of *Jatropha curcas*. Toxic properties and inhibition of protein synthesis in vitro. *Biochem J*. 156(1), 1-6.

Sun, L., Meng, Z., Li, Z., Yang, B., Wang, Z., Ding, G., Xiao, W. 2014. Two new natural products from *Croton kongensis* Gagnep. *Nat Prod Res*. 28(8):563-567.

Sun, S.C. 2011. Non-canonical NF-κB signaling pathway. *Cell Res*. 21(1), 71-85.

Takagi, A., Koga, Y., Aiba, Y., Kabir, A.M., Watanabe, S., Ohta-Tada, U., Osaki, T. Kamiya, S. and Miwa, T. 2000. Plaunotol suppresses interleukin-8 secretion induced by *Helicobacter pylori:* therapeutic effect of plaunotol on *H. pylori* infection. *J Gastroenterol Hepatol*. 15(4), 374-380.

Takahashi, S., Kurabayashi, M., Kitazawa, E, Haruyama, H., and Ogiso, A. 1983. Plaunolide, a furanoid diterpene from *Croton sublyratus. Phytochemistry*. 22(1), 302-303.

Takeshige, Y., Kawakami, S., Matsunami, K., Otsuka, H., Lhieochaiphant, D. and Lhieochaiphant, S. 2012. Oblongionosides A-F, megastigmane glycosides from the leaves of *Croton oblongifolius* Roxburgh. *Phytochemistry*. 80, 132-136.

Talapatra, S.K. and Talapatra, B. 2015. A cyclic diterpenes: Occurrence, Biosynthesis. Talapatra, S.K. and Talapatra, B (eds). *Chemistry of plant natural products*. New York, Springer Heidelberg.

Tao, WW., Duan, JA., Tang, YP., Yang, NY., Li, JP. and Qian, YF. 2013. Casbane diterpenoids from the roots of *Euphorbia pekinensis*. *Phytochemistry*. 94, 249-253.

Thao, D.T, Phuong, D.T, Hanh, T.T.H., Thao, N.P., Cuoung, N.X., Nam, N.H. and Minh, C.V. 2014. Two new neoclerodane diterpenoids from *Scutellaria barbata* D. Don growing in Vietnam. *J Asian Nat Prod Res*. 16(4) 364–369.

Thongtan, J., Kittakoop, P., Ruangrungsi, N., Saenboonrueng, J. and Thebtaranonth, Y. 2003. New antimycobacterial and antimalarial 8, 9-secokaurane diterpenes from *Croton kongensis*. *J Nat Prod*. 66(6), 868-870.

Tian, JL., Yao, GD., Wang, YX., Gao, PY., Wang, D., Li, LZ., Lin, B., Huang, XX. and Song, SJ. 2017. Cytotoxic clerodane diterpenoids from *Croton crassifolius*. *Bioorg Med Chem Lett*. 27(5), 1237-1242.

Troutman, T.D., Bazan, J.F. and Pasare, C. 2012. Tool-like receptors, signaling adapters and regulation of the pro-inflammatory response by PI3K. *Cell Cycle*. 11(19), 3559-3567.

Tsai, TC., Wu, YJ., Su, JH., Lin, WT. and Lin, YS. 2013. A new spatane diterpenoid from the cultured soft coral *Sinularia leptoclados*. *Mar Drugs*. 11(1), 114-123.

Tseng, YJ., Yang, YC., Wang, SK. and Duh, CY. 2014. Numerosol A–D, new cembranoid diterpenes from the soft coral *Sinularia numerosa*. *Mar Drugs*. 12(6), 3371–3380.

Ur Rehman, T., Khan, AU., Abbas, A., Hussain, J., Khan, FU., Stieglitz, K. and Ali, S. 2018. Investigation of nepetolide as a novel lead compound: Antioxidant, antimicrobial, cytotoxic, anticancer, anti-inflammatory, analgesic activities and molecular docking evaluation. *Saudi Pharm J*. 26(3), 422-429.

Ushiyama, S., Matsuda, K., Asai, F. and Yamazaki, M. 1987. Stimulation of prostaglandin production by (2*E*, 6*Z*, 10*E*)-7-hydroxymethyl-3, 11, 15-trimethyl-2, 6, 10, 14-hexadecatetraen-1-ol (plaunotol), a new anti ulcer drug, *in vitro* and *in vivo*. *Biochem. Pharmacol*. 36(3), 369-375.

Valdés, A., García-Cañas, V., Artemenko, K.A., Simó, C., Bergquist, J. and Cifuentes, A. 2017. Nano-liquid chromatography-orbitrap MS based quantitative proteomics reveals differences between the mechanisms of action of carnosic acid and carnosol in colon cancer cells. *Mol Cell Proteomics*. 16, 8-22.

Vallabhapurapu, S. and Karin, M. 2009. Regulation and function of NF-kappaB transcription factors in the immune system. *Annu Rev Immunol*. 27, 693-733.

Vaughan, L., Glänzel, W., Korch, C. and Capes-Davis, A. 2017. Widespread use of misidentification cell line KB (HeLa): incorrect attribution and its impact revealed through mining the scientific literature. *Cancer Res*. 77 (11), 2784-2877.

Veseva, A.V. and Moll, U.M. 2009. The mitochondrial P53 pathway. *BBA-Bioenergics*. 1787(5), 414-420.

Vongsombath, C., Pålsson, K., Björk, L., Borg-Karlson, A.K. and Jaenson, T.G. 2012. Mosquito (*Diptera: Culicidae*) repellency field tests of essential oils from plants traditionally used in Laos. *J Med Entomol*. 49(6), 1398-1404.

Wang, C., Jiang, L., Wang, S., Shi, H., Wang, J., Wang, R., Li, R., Dou, Y., Liu, Y., Hou, G., Ke, Y. and Liu, H. 2015. The antitumor activity of the novel compound Jesridonin on human esophageal carcinoma cells. *PLoS One*. 10(6), e0130284.

Wang, GC., Li, JG., Li, GQ., Xu, JJ., Wu, X., Ye, WC. and Li, YL. 2012. Clerodane diterpenoids from *Croton crassifolius*. *J Nat Prod*. 75(12), 2188-2192.

Wang, JF., Yang, SH., Liu, YQ., Li, DX., He, WJ., Zhang, XX., Liu, YH., Zhou, XJ. 2015. Five new phorbol esters with cytotoxic and selective anti-inflammatory activities from *Croton tiglium*. *Bioorg Med Chem Lett*. 25(9), 1986-1989.

Wang, JJ., Chung, H.Y., Zhang, YB., Li, GQ., Li, YL., Huang, WH. and Wang, GC. 2016. Diterpenoids from the roots of *Croton crassifolius* and their anti-angiogenic activity. *Phytochemistry*. 122, 270-275.

Wang, K., Yu, H., Wu, H., Wang, X., Pan, Y., Chen, Y., Liu, L., Jin, Y. and Zhang, C. 2015. A new casbane diterpene from *Euphorbia pekinensis*. *Nat Prod Res*. 29(15), 1456-1460.

Wang, L., He, HS., Yu, HL., Zeng, Y., Han, H., He, N., Liu, ZG., Wang, ZY., Xu, SJ. and Xiong, M. 2015. Sclareol, a plant diterpene, exhibits potent antiproliferative effects via the induction of apoptosis and mitochondrial membrane potential loss in osteosarcoma cancer cells. *Mol Med Rep*. 11(6), 4273-4278.

Wang, SJ., Li, YX., Bao, L., Han, JJ., Yang, XL., Li, HR., Wang, YQ., Li, SJ. and Liu, HW. 2012. Eryngiolide A, a cytotoxic macrocyclic diterpenoid with an unusual cyclododecane core skeleton produced by the edible mushroom *Pleurotus eryngii*. *Org Lett*. 14(14), 3672-3675.

Wang, T.H., Wang, H.S. and Soong, Y.K. 2000. Paclitaxel-induced cell death: where the cell cycle and apoptosis come together. *Cancer*. 88(11), 2619-2628.

Wang, X., Zhang, L., Duan, W., Liu, B., Gong, P., Ding, Y. and Wu, X. 2014. Anti-inflammatory effects of triptolide by inhibiting the NF-κB signalling pathway in LPS-induced acute lung injury in a murine model. *Mol Med Rep*. 10(1), 447-452.

Wang, ZM., Kang, YH., Yang, X., Wang, JF., Zhang, Q., Yang, BX., Zhao, KL., Xu, LP., Yang, LP., Ma, JX., Huang, GH., Cai, J. and Sun, XC. 2016. Andrographolide radiosensitizes human esophageal cancer cell line ECA109 to radiation in vitro. *Dis Esophagus*. 29(1), 54-61.

White, E., Green, D.R. and Letai, A.G. 2015. Apoptosis, Necrosis and Autophagy. Mendelsohn, J., Howley, P.M., Israel, M.A., Gray, J.W. and Thompson, C.B. (eds). *The molecular basis of cancer*. Philadelphia, Elsevier Saunders.

Wilken, R., Veena, M.S., Wang, M.B. and Srivatsan, E.S. 2011. Curcumin: A review of anti-cancer properties and therapeutic activity in head and neck squamous cell carcinoma. *Mol Cancer*. 10, 12.

Win, N.N., Ito, T., Aimaiti, S., Imagawa, H., Ngwe, H., Abe, I. and Morita, H. 2015. Kaempulchraols A–H, diterpenoids from the rhizomes of *Kaempferia pulchra* collected in Myanmar. *J Nat Prod*. 78(5), 1113-1118.

Wisniewski, J., Wesolowska, O., Sroda-Pomianek, K., Paprocka, M., Bielawska-Pohl, A., Krawczenko, A., Duarte, N., Ferreira, M.J., Dus, D. and Michalak, K. 2016. Euphorbia species-derived diterpenes and coumarins as multidrug resistance modulators in human colon carcinoma cells. *Anticancer Res*. 36(5), 2259-2264.

Woo, SM., Min, KJ., Seo, BR., Nam, JO., Choi, KS., Yoo, YH. And Kwon, TK. 2014. Cafestol overcomes ABT-737 resistance in Mcl-1-overexpressed renal carcinoma Caki cells through downregulation of Mcl-1 expression and upregulation of Bim expression. *Cell Death Dis*. 5, e1514.

Wu, HF., Zhang, XP.,Wang, Y., Zhang, JY., Ma, GX., Tian, Y., Wu, LZ., Chen, SL., Yang, JS. and Xu, XD. 2013. Four new diterpenes from *Aphanamixis polystachya*. *Fitoterapia*. 90, 126–131.

Wu, SL., Su, JH., Huang, CY., Tai, CJ., Sung, PJ., Liaw, CC. and Sheu, JH. 2012. Simplexins P–S, eunicellin-based diterpenes from the soft coral *Klyxum simplex*. *Mar Drugs*. 10(6), 1203-1211.

Wu, XA., Zhao, YM. and Yu, NJ. 2007. A novel analgesic pyrazine derivative from the leaves of *Croton tiglium* L. *J Asian Nat Prod Res*. 9(3-5), 437-441.

Wu, XD., Zhang, LC., He, J., Li, GT., Ding, LF., Gao, X., Dong, LB., Song, LD., Li, Y. and Zhao, QS. 2013. Two new diterpenoids from *Excoecaria acerifolia*. *J Asian Nat Prod Res*. 15(2), 151-157.

Xia, Y., Shen, S. and Verma, I.M. 2014. NF-κB, an active player in human cancers. *Cancer Immunol Res*. 2(9), 823-830.

Xia, YF., Ye, BQ.,Li, YD., Wang, JG., He, XJ., Lin, X., Yao, X., Ma, D., Slungaard, A., Hebbel, RP., Key, NS. and Geng, JG. 2004. Andrographolide attenuates inflammation by inhibition of NF-kappa B activation through covalent modification of reduced cysteine 62 of p50. *J Immunol*. 173(6), 4207-4217.

Xu, M., Wang, S., Jia, O., Zhu, Q. and Shi, L. 2016. Bioactive diterpenoids from *Clerodendrum kiangsiense*. *Molecules*. 21(1), 86.

Xu, X., Yuan, J., Zhou, X., Li, W., Zhu, N., Wu, H., Li, P., Sun, Z., Yang, J. and Ma, G. 2016. Cassane diterpenes with oxygen bridge from the seeds of *Caesalpinia sappan*. *Fitoterapia*. 112, 205-210.

Xu, Y., Lang, JH., Jiao, WH., Wang, RP., Peng, Y., Song, SJ., Zhang, BH. and Lin, HW. 2012. Formamido-diterpenes from the South China Sea sponge *Acanthella cavernosa*. *Mar Drugs*. 10(7): 1445-1458.

Yadav, R.P. and Singh, A. 2010. Toxic effects of crotocaudin extracted from the medicinal plant *Croton tiglium*. *Z Naturforsch C*. 65(5-6), 327-336.

Yamada, J., Kawai, K., Tsuno, N.H., Kitayama, J., Tsuchiya, T., Yoneyama, S., Asakage, M., Okaji, Y., Takahashi, K. and Nagawa, H. 2007. Plaunotol induces apoptosis of gastric cancer cells. *Planta Med*. 73(10), 1068-1073.

Yamaoka, S., Courtois, G., Bessia, C., Whiteside, S.T., Weil, R., Agou, F., Kirk, H.E., Kay, R.J. and Israel, A. 1998. Complementation cloning of NEMO, a component of the IkappaB kinase complex essential for NF-kappaB activation. *Cell*. 93(7), 1231-1240.

Yang, B., Chen, GY., Song, XP., Yang, LQ., Wu, XY., Han, CR., Chen, WH., Zou, BY. And Li, HM. 2013. Five new degraded diterpenoids from *Trigonostemon xyphophylloides*. *Bioorg Med Chem Lett*. 23(20) 5748-5751.

Yang, J., Jiang, H.,Wang, C., Yang, B., Zhao, L., Hu, D., Qiu, G., Dong, X. and Xiao, B. 2015. Oridonin triggers apoptosis in colorectal carcinoma cells and suppression of microRNA-32 expression augments oridonin-mediated apoptotic effects. *Biomed Pharmacother*. 72, 125-134.

Yang, J.,Wang, WG.,Wu, HY., Du, X., Li, XN., Li, Y., Pu, JX. and Sun, HD. 2016. Bioactive enmein-type entkaurane diterpenoids from *Isodon phyllostachys*. *J Nat Prod*. 79(1), 132-140.

Yao, R., Chen, Z., Zhou, C., Luo, M., Shi, X., Li, J., Gao, Y., Zhou, F., Pu, J., Sun, H. and He, J. 2015. Xerophilusin B induces cell cycle arrest and apoptosis in esophageal squamous cell carcinoma cells and does not cause toxicity in nude mice. *J Nat Prod*. 78(1), 10-16.

Yao, Y., Li, HZ., Qian, BJ., Liu, CM., Zhang, JB. and Lin, MC. 2015. Crypotanshione reduces the expression of metadherin in DU145 prostate cancer cells. *Zhonghua Nan Ke Xue*. 21(9), 782-787.

Ye, Q., Yao, G., Zhang, M., Guo, G., Hu, Y., Jiang, J., Cheng, L., Shi, J., Li, H., Zhang, Y. and Liu, H. 2015. A novel ent-kaurane diterpenoid executes antitumor function in colorectal cancer cells by inhibiting Wnt/β-catenin signaling. *Carcinogenesis*. 36(3), 318-326.

Yoon, WJ., Ham Y.M., Yoon, H.S., Lee, W.J., Lee, N.H. and Hyun, C.G. 2013. Acanthoic acid inhibits melanogenesis through tyrosinase downregulation and melanogenic gene expression in B16 melanoma cells. *Nat Prod Commun*.18(10), 1359-1362.

Yoshikawa, N., Yamada, J., Tsuno, N.H., Okaji, Y., Kawai, K., Tsuchiya, T., Yoneyama, S., Tanaka, J., Shuno, Y., Nishikawa, T., Nakawa, H., Oshima, N. and Takahashi, K. 2009. Plaunotol and geranylgeraniol induce caspase-mediated apoptosis in colon cancer. *J. Surg. Res.* 153(2), 246-253.

Yoshikawa, N.Y., Tsuno, N.H., Okaji, Y., Kawai, K., Shuno, Y., Nagwa, H., Oshima, N. and Takahashi, K. 2010. Isoprenoid geranylgeranyacetone inhibits human colon cancer cells through induction of apoptosis and cell cycle arrest. *Anti-cancer Drugs*. 21, 850-860.

Youngsa-ad, W., Ngamrojanavanich, N., Mahidol, C., Ruchirawat, S., Prawat, H. and Kittakoop, P. 2007. Diterpenoids from the roots of *Croton oblongifolius*. *Planta Med*. 73(14), 1491-1494.

Yu, F., Li, K., Chen, S., Liu, Y. and Li, Y. 2015. Pseudolaric acid B circumvents multidrug resistance phenotype in human gastric cancer SGC7901/ADR cells by downregulating Cox-2 and Pgp expression. *Cell Biochem Biophys*. 71(1), 119-126.

Yuan, G., Wahlgvist, M.L. He, G., Yang, M. and Li, D. 2006. Natural products and anti-inflammatory activity. *Asia Pac J Clin Nutr.* 15(2), 143-152.

Yuan, QQ., Song, WB., Wang, WQ. and Xuan, LJ. 2017. A new patchoulane-type sesquiterpenoid glycoside from the roots of *Croton crassifolius*. *Nat Prod Res*. 31(3), 289-293.

Yuan, QQ., Tang, S., Song, WB., Wang, WQ., Huang, M. and Xuan, LJ. 2017. Crassins A-H, Diterpenoids from the Roots of *Croton crassifolius*. *J Nat Prod*. 80(2), 254-260.

Yuan, X., Wu, H., Xu, H., Xiong, H., Chu, Q., Yu, S., Wu, G.S. and Wu, K. 2015. Notch signaling: An emerging therapeutic target for cancer treatment. *Cancer Lett.* 369(1), 20-27.

Zandi, E., Rothwarf, D.M., Delhase, M., Hayakawa, M. and Karin, M. 1997. The IkappaB kinase complex (IKK) contains two kinase subunits, IKKalpha and IKKbeta, necessary for IkappaB phosphorylation and NF-kappaB activation. *Cell*. 91(2), 243-252.

Zhan, T., Rindtorft, N. and Boutros, M. 2017. Wnt signaling in cancer. *Oncogene*. 36(11), 1461-1473.

Zhang, G., Ma, H., Hu, S., Xu, H., Yang, B., Yang, Q., Xue, Y., Cheng, L., Jiang, J., Zhang, J., Wang, F. and Zhang, Y. 2016. Clerodane-type diterpenoids from tuberous roots of *Tinospora sagittata* (Oliv.) Gagnep. *Fitoterapia*. 110, 59-65.

Zhang, J., Li, Y., Zhu, R., Li, L., Wang, Y., Zhou, J., Qiao, Y., Zhang, Z. and Lou, H. 2015. Scapairrins A–Q, labdanetype diterpenoids from the Chinese liverwort *Scapania irrigua* and their cytotoxic activity. *J Nat Prod*. 78(8), 2087–2094.

Zhang, K., Li, J., Meng, W., Xing, H. and Yang, Y. 2016. Tanshinone IIA inhibits acute promyelocytic leukemia cell proliferation and induces their apoptosis in vivo. *Blood Cells Mol Dis*. 56(1), 46-52.

Zhang, X., Tan, Y., Li, Y., Jin, L., Wei, N., Wu, H., Ma, G., Zheng, Q., Tian, Y., Yang, J., Zhang, J. and Xu, X. 2014. Aphanamixins A–F, acyclic diterpenoids from the stem bark of *Aphanamixis polystachya*. *Chem Pharm Bull (Tokyo).* 62(5), 494-498.

Zhang, XL., Wang, L., Li, F., Yu, K. and Wang, MK. 2013. Cytotoxic phorbol esters of *Croton tiglium*. *J Nat Prod*. 76(5), 858-864.

Zhang, ZX., Li, HH., Fan, GX., Li, ZY., Dong, LL., Li, HY. and Fei, DQ. 2015. A novel norclerodane diterpenoid from the roots of *Croton crassifolius*. *Nat Prod Commun*. 10(11), 1917-1918.

Zhao, BQ., Peng, S., He, WJ., Liu, YH., Wang, JF. and Zhou, XJ. 2016. Antitubercular and cytotoxic tigliane-type diterpenoids from *Croton tiglium*. *Bioorg Med Chem Lett*. 26(20), 4996-4999.

Zhao, J., Fang, F., Yu, L., Wang, G. and Yang, L. 2012. Anti-nociceptive and anti-inflammatory effects of *Croton crassifolius* ethanol extract. *J Ethnopharmacol*. 142(2), 367-373.

Zhao, M., Guo, DL., Yuan, LY., Gu, YC., Chen, L., Ding, LS. and Zhou, Y. 2017. Three new labdane diterpenes from *Loxocalyx urticifolius*. *Phytochem Lett*. 19, 55-59.

Zhao, SM., Chou, GX., Yang, QS., Wang, W. and Zhou, JL. 2016. Abietane diterpenoids from *Caryopteris incana* (Thunb.) Miq. *Org Biomol Chem*. 14, 3510-3520.

Zheng, CJ., Zhu, JY., Yu, W., Ma, XQ., Rahman, K., Qin, LP. 2013. Labdane-type diterpenoids from the fruits of *Vitex trifolia*. *J Nat Prod*. 76(2), 287-291.

Zheng, Y., Zhang, SW., Cong, HJ., Huang, YJ. and Xuan, LJ. 2013. Caesalminaxins A–L, cassane diterpenoids from the seeds of *Caesalpinia minax*. *J Nat Prod.* 76(12), 2210-2218.

Zhivotosky, B. and Orrenius, S. 2010. Cell cycle and cell death in disease: past, present and future. *J Intern Med*. 268(5), 395-409.

Zhong, M., Wu, H., Zhang, X., Sun, G., Yu, S. and Xu, X. 2014. A new diterpene from *Clinopodium chinense*. *Nat Prod Res*. 28(7), 467-472.

Zilfou, J.T. and Lowe, S.W. 2009. Tumor suppressor functions of P53. *Cold Spring Harb Perspect Biol*. 1(5), a001883.

Zio, D.D., Cianfenelli, V. and Cecconi, F. 2013. New Insights into the link between DNA damage and apoptosis. *Antioxid Redox Signal*. 19(6), 559-571.

Zou, GA., Su, ZH., Zhang, HW., Wang, Y., Yang, JS. and Zou, ZM. 2010. Flavonoids from the stems of *Croton caudatus* Geisel. var. tomentosus Hook. *Molecules*. 15(3), 1097-10102.

Zou, QY., Wu, HF., Tang, YL. and Chen, DZ. 2016. A new labdane diterpene from the rhizomes of *Alpinia officinarum*. *Nat Prod Res*. 30(1), 1-6.

APPENDICES

KB (HeLa) misidentified cells

Cell-based assay is frequency used to evaluate on biological activities. However, the evidence from the widespread use of cell misidentification continue to be published in research articles (Vaughan *et al*., 2017). In a case of cancer cell line, one of the mostly used KB (HeLa) is made up from the continuous cell line developed from a patient, who died of cancer in the 1952 and HeLa is misidentified from cross-contamination at 1996. Therefore, the miss understanding of this KB (HeLa) cell line in the scientific research can be occurred. Since collecting 574 articles from 2000 to 2014, they found only 57 articles which provided in a correct ascription for KB, as cervical adenocarcinoma or HeLa cells. Whereas 171 articles provided an incorrect ascription for KB, associating with its miss identify as oral epidermoid carcinoma or oral cancer. Furthermore, they also indicated that the number of citations relating with an incorrected cell line are increased over time (Vaughan *et al*., 2017).

A historical perspective on cell line miss identification, HeLa cells have been identified since 1952 from **He**nrieta **La**cks (the patient with 31 years of age, she died from aggressive grandular cancer-adenocarcinoma of the cevix) and have established by Mury Kubrick in George Gey ‘s laboratory. KB cells have originally established by Harry Eagle in 1955. These cells were an epidermoid carcinoma (as known as squamous cell carcinoma (SCC), nowadays), from the larynx of male donor. At this time, Eagle also worked with HeLa cells. In 1966, the miss identification of KB was reported corresponding to HeLa by Gartle. The multiple times and multiple experiments have been proved Gartler ‘s finding, and the original KB cells were contributed to HeLa, supporting by Harry Eagle (www.atcc.org/Products/All/CCL-17. aspx#history).

There is still confusion in the literature. KB has not existed since at least 1962, when it was deposited at the ATCC. It was cross-contaminated when it originally established. KB is a subline of HeLa cells. Unfortunately, there is confusion by the term "contaminated" by

HeLa. Many articles published incorrect cell line, such as nasopharynx and oral cancer. All known samples of KB are HeLa by genetic testing, even though they may differ in phenotype. Different isolates of KB can also vary in phenotype. There are over 100 cell lines with different names and probably phenotypes, but they are all sublines of HeLa.

According to our thesis, we described the correctly cell line as KB cervical adenocarcinoma. This information may help to rises awareness of KB as misidentified cell lines. Recently, the authentication of human cell lines when use for any biological/biomedical research, should always be authenticated by either STR (Short tandem repeats; DNA profiling) or SNP (Single nucleotide polymorphism) genotyping, not only by phenotyping of these cell lines. These authentication analyses will be confirmed the intraspecies of cells.

Vaughan, L., Glänzel, W., Korch, C. and Capes-Davis, A. 2017. Widespread use of misidentification cell line KB (HeLa): incorrect attribution and its impact revealed through mining the scientific literature. *Cancer Res*. 77 (11), 2784-2877.

Table A1 The characteristic of HeLa and KB cell lines.

Characteristics	**HeLa**	**KB**
CLS order number	300194	300446
Organism	*Homo sapiens* (human)	*Homo sapiens* (human)
Tissue	Cervix	Cervix
Morphology	Epithelial	Epithelial
Cell type	Adenocarcinoma	Carcinoma, epimoid
Growth property	Monolayer, adherent	Monolayer, adherent
Description	HeLa cells have been reported to contain human papilloma virus 18 (HPV-18) sequence. P53 expression was reported to be low and normal levels of pRB (retinoblastoma suppressor) are found. The cells are positive for keratin by immunoperoxidase staining.	Cells of this line contain HeLa marker chromosomes were derived via HeLa contamination. The cells are positive for keratin by immunoperoxidase staining. KB cells have been reported to contain human papillomavirus 18 (HPV-18) sequences.
Reference	Gey G.O. Coffman, W.D. and Kubicek, M.T. 1952. Tissue culture studies of the proliferative capacity of cervical carcinosarcoma and normal epithelium. *Cancer Res*. 12, 264-265.	Eagle, H. 1955. Propagation in fluid medium of a human epidermoid carcinoma, strain KB. *Proc Soc Exp Biol Med.* 89, 362-364.

Table A1 (continued).

Characteristics	**HeLa**	**KB**
DNA profile (STR)	Amelogenin: X, X	Amelogenin: X, X
	CSF1PO: 9,10	CSF1PO: 9,10
	D13S317: 13, 13, 3	D13S317: **12**, 13, **2**
	D16S539: 9, 10	D16S539: 9, 10
	D5S818: 11, 12	D5S818: 11, 12
	D7S820: 8, 12	D7S820: 8, 12
	vWA: 16, 18	vWA: 16, 18
	D3S1358, 15, 18	D3S1358, 15, 18
	D21S11: 27	D21S11: 27, **28**
	D18S51: 16	D18S51: 16
	Penta E: 7, 17	Penta E: 7, 17
	Penta D: 8	Penta D: 8, **15**
	THO1: 7	THO1: 7
	TPOX: 8, 12	TPOX: 8, 12
	D8S1179: 12, 13	D8S1179: 12, 13
	FGA: **18**, 21	FGA: 21
Isoenzymes	G6PD, type A	G6PD, type A
Product	Keratin, Lysophosphatidylcholine (lyso-PC) induce AP-1 activity and c-jun N-terminal kinase activity (JNK1) by protein kinase C-independent pathway	Keratin

Source: CLS product information (CLS Cell lines service GmbH-Germany)

VITAE

List of Proceeding

Name Mr. Charoenwong Premprasert

Student ID 6010730015

Educational Attainment

Degree	Name of Institution	Year of Graduation
Bachelor of Sciences (Chemistry - Biology) (2^{nd} Class Honors)	Prince of Songkla University	2007
Master of Pharmacy (Pharmaceutical Sciences)	Prince of Songkla University	2011

Scholarship Awards during Enrolment

The Royal Golden Jubilee Ph.D. Program (Grant No. PHD/0171/2553)

List of Publication

Premprasert, C., Tewtrakul, S., Plubrukarn, A. and Wungsintaweekul, J. 2013. Anti-inflammatory activity of diterpenes from *Croton stellatopilosus* on LPS-induced RAW264.7 cells. *J. Nat. Med*. 67, 174-181.

Premprasert, C., Tewtrakul, S. and Wungsintaweekul, J. 2018. Plaunol A from *Croton stellatopilosus* inhibits inducible nitric oxide synthase and cyclooxygenase-2 in macrophage RAW264.7 cells. *Nat Prod Commun.* 13(7), 779-802.

Premprasert, C., Yoenyongsawad, S., Tewtrakul, S. and Wungsintaweekul, J. Plaunotol from *Croton stellatopilosus* Ohba inhibited cell growth and induced apoptosis in human cancer cell lines. *SJST.* (In press).

List of Proceeding

Pramprasert, J., Tewtakul, S. and Wungsintaweekul, J. 2008. The efficiency of *Croton stellatopilosus* leaves extracts on anti-inflammation and anti-bacterial activity. Proceeding of the 8th Joint Seminar NRCT-JSPS "Innovative Research in Natural Products for Sustainable Development". Faculty of Pharmaceutical Sciences, Chulalongkorn University, Bankok, Thailand. 189-190.

Pramprasert, C., Tewtrakul, S. and Wungsintaweekul, J. 2010.Anti-inflammatory activity of plaunotol isolated from *Croton stellatopilosus*in murine macrophage RAW264.7 cells. Abstracts of CDD 2010 The 1st Current Drug Development International Conference. Woraburi Phuket Resort & Spa, Phuket, Thailand. 73.

Premprasert, C., Tewtrakul, S. and Wungsintaweekul, J. 2014. Potential of *Croton oblongifolius* Leaf Extract on Nitric Oxide Inhibitory Activity in Murine Macrophage RAW 264.7 Cells. Abstracts of The 3rd Current Drug Development International Conference (CDD 2014). Pavilion Queen's Bay KrabiAo Nang Beach, Thailand. 170-180.

Premprasert, C., Yoenyongsawad, S., Tewtrakul, S. and Wungsintaweekul, J. 2016. Apoptotic Activity of Furanoditerpenes from *Croton stellatopilosus* Against Human Cervix Adenocarcinoma Cell line. Proceeding of The seventeenth RGJ-Ph.D. Congress (RGJ-Ph.D. Congress XVII). Jomtien Palm Beach Hotel & Resort, Pattaya, Chonburi, Thailand. 275.

Premprasert, C., Yoenyongsawad, S., Tewtrakul, S. and Wungsintaweekul, J. 2018. Anti-proliferative activity of diterpenes from *Croton stellatopilosus* in MCF-7 cells. Abstracts/Proceedings of The 5th Current Drug Development International Conferences & The 3th International Conference on Herbal and Traditional Medicine (CDD-HTM 2018). PSU Conference Hall, Songkhla, Thailand. 93-96.